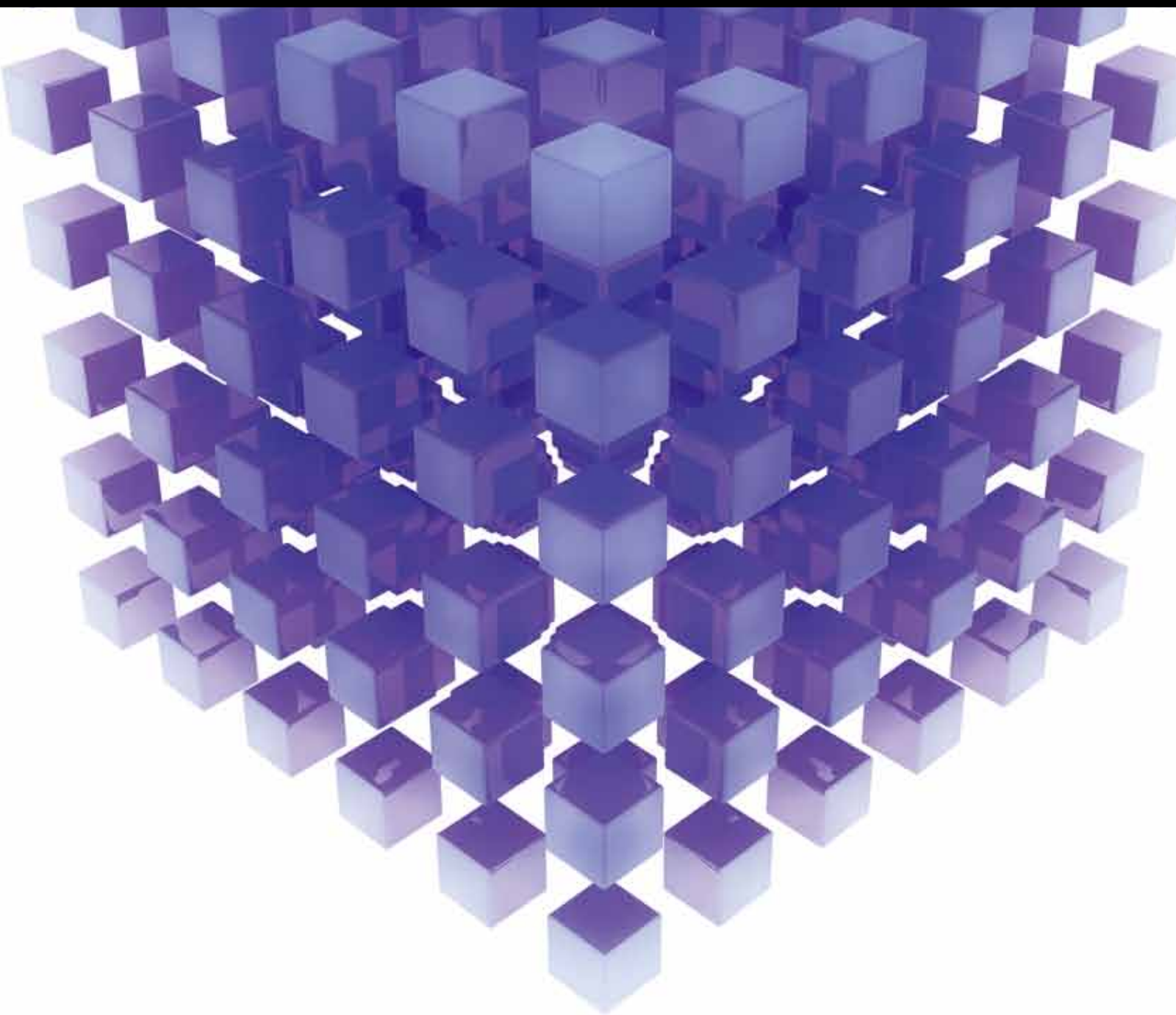


MATHEMATICAL PROBLEMS IN ENGINEERING

PROPAGATION PHENOMENA AND TRANSITIONS in Complex Systems 2013

GUEST EDITORS: EZZAT G. BAKHOUM, CRISTIAN TOMA, CARLO CATTANI, AND MING LI





Propagation Phenomena and Transitions in Complex Systems 2013

Mathematical Problems in Engineering

Propagation Phenomena and Transitions in Complex Systems 2013

Guest Editors: Ezzat G. Bakhoun, Cristian Toma,
Carlo Cattani, and Ming Li



Copyright © 2014 Hindawi Publishing Corporation. All rights reserved.

This is a special issue published in “Mathematical Problems in Engineering.” All articles are open access articles distributed under the Creative Commons Attribution License, which permits unrestricted use, distribution, and reproduction in any medium, provided the original work is properly cited.

Editorial Board

Mohamed Abd El Aziz, Egypt
Eihab M. Abdel-Rahman, Canada
Rashid K. Abu Al-Rub, USA
Sarp Adali, South Africa
Salvatore Alfonzetti, Italy
Igor Andrianov, Germany
Sebastian Anita, Romania
W. Assawinchaichote, Thailand
Er-wei Bai, USA
Ezzat G. Bakhoun, USA
José Manoel Balthazar, Brazil
Rasajit Kumar Bera, India
Jonathan N. Blakely, USA
Stefano Boccaletti, Spain
Stephane P. A. Bordas, USA
Daniela Boso, Italy
M. Boutayeb, France
Michael J. Brennan, UK
Salvatore Caddemi, Italy
Piermarco Cannarsa, Italy
Jose E. Capilla, Spain
Carlo Cattani, Italy
Marcelo Cavalcanti, Brazil
Diego J. Celentano, Chile
Mohammed Chadli, France
Arindam Chakraborty, USA
Yong-Kui Chang, China
Michael J. Chappell, UK
Kui Fu Chen, China
Kue-Hong Chen, Taiwan
Xinkai Chen, Japan
Jyh-Horng Chou, Taiwan
Slim Choura, Tunisia
Cesar Cruz-Hernandez, Mexico
Erik Cuevas, Mexico
Swagatam Das, India
Filippo de Monte, Italy
Yannis Dimakopoulos, Greece
Baocang Ding, China
Joao B. R. Do Val, Brazil
Daoyi Dong, Australia
B. Dubey, India
Horst Ecker, Austria
M. Onder Efe, Turkey
Elmetwally Elabbasy, Egypt

Alex Elías-Zúñga, Mexico
Anders Eriksson, Sweden
Vedat S. Erturk, Turkey
Moez Feki, Tunisia
Ricardo Femat, Mexico
Robertt Fontes Valente, Portugal
Claudio Fuerte-Esquivel, Mexico
Zoran Gajic, USA
Ugo Galvanetto, Italy
Xin-Lin Gao, USA
Furong Gao, Hong Kong
Behrouz Gatmiri, Iran
Oleg V. Gendelman, Israel
Paulo Batista Gonçalves, Brazil
Oded Gottlieb, Israel
Fabrizio Greco, Italy
Quang Phuc Ha, Australia
Tony Sheu Wen Hann, Taiwan
Thomas Hanne, Switzerland
Katica R. Hedrih, Serbia
M. I. Herreros, Spain
Wei-Chiang Hong, Taiwan
Jaromir Horacek, Czech Republic
Gordon Huang, Canada
Huabing Huang, China
Chuangxia Huang, China
Yi Feng Hung, Taiwan
Hai-Feng Huo, China
Asier Ibeas, Spain
Anuar Ishak, Malaysia
Reza Jazar, Australia
Zhijian Ji, China
Jun Jiang, China
J. J. Judice, Portugal
Tadeusz Kaczorek, Poland
Tamas Kalmar-Nagy, USA
Tomasz Kapitaniak, Poland
Hamid R. Karimi, Norway
Metin O. Kaya, Turkey
Farzad Khani, Iran
Ren-Jieh Kuo, Taiwan
Jurgen Kurths, Germany
Claude Lamarque, France
Usik Lee, Korea
Marek Lefik, Poland

Stefano Lenci, Italy
Roman Lewandowski, Poland
Shihua Li, China
Ming Li, China
S. Li, Canada
Jian Li, China
Teh-Lu Liao, Taiwan
Panos Liatsis, UK
Kim Meow Liew, Hong Kong
Yi-Kuei Lin, Taiwan
Shueei M. Lin, Taiwan
Jui-Sheng Lin, Taiwan
Wanquan Liu, Australia
Bin Liu, Australia
Yuji Liu, China
Paolo Lonetti, Italy
Vassilios C. Loukopoulos, Greece
Chien-Yu Lu, Taiwan
Junguo Lu, China
Alexei Mailybaev, Brazil
Manoranjan K. Maiti, India
Oluwole Daniel Makinde, South Africa
Rafael Martínez-Guerra, Mexico
Driss Mehdi, France
Roderick Melnik, Canada
Xinzhu Meng, China
Jose Merodio, Spain
Yuri Vladimirovich Mikhlin, Ukraine
Gradimir Milovanović, Serbia
Ebrahim Momoniat, South Africa
Trung Nguyen Thoi, Vietnam
Hung Nguyen-Xuan, Vietnam
Ben T. Nohara, Japan
Sotiris K. Ntouyas, Greece
Claudio Padra, Argentina
Bijaya Ketan Panigrahi, India
Francesco Pellicano, Italy
Matjaž Perc, Slovenia
Vu Ngoc Phat, Vietnam
Maria do Rosário Pinho, Portugal
Seppo Pohjolainen, Finland
Stanislav Potapenko, Canada
Sergio Preidikman, USA
Carsten Proppe, Germany
Hector Puebla, Mexico

Justo Puerto, Spain
Dane Quinn, USA
Kumbakonam Rajagopal, USA
Gianluca Ranzi, Australia
Sivaguru Ravindran, USA
G. Rega, Italy
Pedro Ribeiro, Portugal
J. Rodellar, Spain
Rosana Rodriguez-Lopez, Spain
Alejandro J. Rodriguez-Luis, Spain
Carla Roque, Portugal
Rubén Ruiz García, Spain
Manouchehr Salehi, Iran
Miguel A. F. Sanjuán, Spain
Ilmar Ferreira Santos, Denmark
Nickolas S. Sapidis, Greece
Evangelos J. Sapountzakis, Greece
Bozidar Sarler, Slovenia
Andrey V. Savkin, Australia
Massimo Scalia, Italy
Mohamed A. Seddeek, Egypt
Leonid Shaikhet, Ukraine
Cheng Shao, China
Bo Shen, Germany
Jian-Jun Shu, Singapore
Zhan Shu, UK
Dan Simon, USA
Luciano Simoni, Italy

Grigori M. Sisoiev, UK
Christos H. Skiadas, Greece
Davide Spinello, Canada
Sri Sridharan, USA
Hari M. Srivastava, Canada
Rolf Stenberg, Finland
Changyin Sun, China
Xi-Ming Sun, China
Jitao Sun, China
Andrzej Swierniak, Poland
Yang Tang, Germany
Allen Tannenbaum, USA
Cristian Toma, Romania
Gerard Olivar Tost, Colombia
Irina N. Trendafilova, UK
Alberto Trevisani, Italy
Jung-Fa Tsai, Taiwan
Kuppalapalle Vajravelu, USA
Victoria Vampa, Argentina
Josep Vehi, Spain
Stefano Vidoli, Italy
Yijing Wang, China
Cheng C. Wang, Taiwan
Dan Wang, China
Xiaojun Wang, China
Qing-Wen Wang, China
Yongqi Wang, Germany
Moran Wang, China

Youqing Wang, China
Gerhard-Wilhelm Weber, Turkey
Jeroen Witteveen, The Netherlands
Kwok-Wo Wong, Hong Kong
Ligang Wu, China
Zhengguang Wu, China
Gongnan Xie, China
Wang Xing-yuan, China
Xi Frank Xu, China
Xuping Xu, USA
Jun-Juh Yan, Taiwan
Xing-Gang Yan, UK
Suh-Yuh Yang, Taiwan
Mahmoud T. Yassen, Egypt
Mohammad I. Younis, USA
Bo Yu, China
Huang Yuan, Germany
S.P. Yung, Hong Kong
Ion Zaballa, Spain
Ashraf M. Zenkour, Saudi Arabia
Jianming Zhan, China
Yingwei Zhang, China
Xu Zhang, China
Lu Zhen, China
Liancun Zheng, China
Jian Guo Zhou, UK
Zexuan Zhu, China
Mustapha Zidi, France

Contents

Propagation Phenomena and Transitions in Complex Systems 2013, Ezzat G. Bakhoun, Cristian Toma, Carlo Cattani, and Ming Li
Volume 2014, Article ID 593591, 2 pages

Acoustic Response of a Sinusoidally Perturbed Hard-Walled Duct, Silvio Del Giudice and Giancarlo Bernasconi
Volume 2013, Article ID 267291, 6 pages

Nonholonomic Geometry of Viscoanelastic Media and Experimental Confirmation, Armando Ciancio and Carlo Cattani
Volume 2013, Article ID 524718, 7 pages

Identifying Vulnerable Nodes of Complex Networks in Cascading Failures Induced by Node-Based Attacks, Shudong Li, Lixiang Li, Yan Jia, Xinran Liu, and Yixian Yang
Volume 2013, Article ID 938398, 10 pages

Delay Bound: Fractal Traffic Passes through Network Servers, Ming Li, Wei Zhao, and Carlo Cattani
Volume 2013, Article ID 157636, 15 pages

Golden Ratio Phenomenon of Random Data Obeying von Karman Spectrum, Ming Li and Wei Zhao
Volume 2013, Article ID 130258, 6 pages

Legendre Wavelets Method for Solving Fractional Population Growth Model in a Closed System, M. H. Heydari, M. R. Hooshmandasl, C. Cattani, and Ming Li
Volume 2013, Article ID 161030, 8 pages


An Efficient Patch Dissemination Strategy for Mobile Networks, Dawei Zhao, Haipeng Peng, Lixiang Li, Yixian Yang, and Shudong Li
Volume 2013, Article ID 896187, 13 pages

Content-Based Image Retrieval Based on Hadoop, DongSheng Yin and DeBo Liu
Volume 2013, Article ID 684615, 7 pages

Attractor Transformation by Impulsive Control in Boolean Control Network, Bo Gao, Haipeng Peng, Dawei Zhao, Wenguang Zhang, and Yixian Yang
Volume 2013, Article ID 674571, 5 pages

Transient Aspects of Wave Propagation Connected with Spatial Coherence, Ezzat G. Bakhoun and Cristian Toma
Volume 2013, Article ID 691257, 5 pages

Smoothing the Sample Autocorrelation of Long-Range-Dependent Traffic, Ming Li and Wei Zhao
Volume 2013, Article ID 631498, 10 pages



Essay on Fractional Riemann-Liouville Integral Operator versus Mikusinski's, Ming Li and Wei Zhao
Volume 2013, Article ID 635412, 3 pages

A Class of Solutions for the Hybrid Kinetic Model in the Tumor-Immune System Competition,
Carlo Cattani and Armando Ciancio
Volume 2013, Article ID 430486, 11 pages

Editorial

Propagation Phenomena and Transitions in Complex Systems 2013

Ezzat G. Bakhoun,¹ Cristian Toma,² Carlo Cattani,³ and Ming Li⁴

¹ University of West Florida, Pensacola, FL 32514, USA

² Faculty of Applied Sciences, University Politehnica of Bucharest, 70709 Bucharest, Romania

³ University of Salerno, 84084 Fisciano, Italy

⁴ School of Information Science and Technology, East China Normal University, No. 500 Dong-Chuan Road, Shanghai 2002411, China

Correspondence should be addressed to Ezzat G. Bakhoun; ebakhoun@uwf.edu

Received 23 February 2014; Accepted 23 February 2014; Published 20 March 2014

Copyright © 2014 Ezzat G. Bakhoun et al. This is an open access article distributed under the Creative Commons Attribution License, which permits unrestricted use, distribution, and reproduction in any medium, provided the original work is properly cited.

The challenge in advanced engineering applications based on efficient mathematical models for propagation and transition phenomena can be noticed nowadays in many research fields. Fractal theory and special mathematical functions are used not only for the design of nanostructures but also for studying propagation in complex artificial networks. Differential geometry is adapted for solving nonlinear partial differential equations with very great number of variables for modelling propagation and transitions for different type of electromagnetic, acoustic, and optic waves. Commutative and/or additive consequences of quantum physics are used extensively in the design of long range transmission systems. Advanced mathematical tools connected to wavelets are recommended for biological phenomena. All these advanced engineering subjects require efficient mathematical models adapted for nonlinear propagation phenomena and for complex systems, when specific limitations are involved (very long distance propagation, fractal aspects and transitions in nanostructures, complex systems with great number of variables, and infinite spatiotemporal extension of material media). Using advanced mathematical tools for modeling propagation and transition phenomena, this special issue presents high qualitative and innovative developments for efficient mathematical approaches of Propagation Phenomena and Transitions in Complex Systems. Significant results were obtained for propagation of waves in advanced materials, dynamics of complex systems, efficient signal and image

analysis based on fundamental mathematical and physical laws, and transitions in complex networks.

This special issue involves 13 original papers selected by the editors so as to present the most significant results in the previously mentioned topics. These papers are organised as follows.

(a) Five papers are on advanced mathematical approach for propagation and transmission in complex artificial networks: “*Delay bound: fractal traffic passes through network servers*” by M. Li et al., “*Smoothing the sample autocorrelation of long-range-dependent traffic*” by M. Li and W. Zhao, “*An efficient patch dissemination strategy for mobile networks*” by D. Zhao et al., “*Attractor transformation by impulsive control in Boolean control network*” by B. Gao et al., and “*Identifying vulnerable nodes of complex networks in cascading failures induced by node-based attacks*” by S. Li et al.

(b) Three papers are on specific methods for the analysis of propagation phenomena in physics: “*Nonholonomic geometry of viscoelastic media and experimental confirmation*” by A. Ciancio and C. Cattani, “*Acoustic response of a sinusoidally perturbed hard-walled duct*” by S. D. Giudice and G. Bernasconi, and “*Transient aspects of wave propagation connected with spatial coherence*” by E. G. Bakhoun and C. Toma.

(c) Two papers are on accurate and efficient mathematical models for transition in biological systems: “*Legendre wavelets method for solving fractional population growth*

model in a closed system” by M. H. Heydari et al. and “*A class of solutions for the hybrid kinetic model in the tumor-immune system competition*” by C. Cattani and A. Ciancio.

(d) Three papers are on mathematical tools for analyzing mathematical complexity: “*Golden ratio phenomenon of random data obeying von Karman spectrum*” by M. Li and W. Zhao, “*Content-based image retrieval based on Hadoop*” by D. Yin and D. Liu, and “*Essay on fractional Riemann-Liouville integral operator versus Mikusinski’s*” by M. Li and W. Zhao.

Ezzat G. Bakhoun

Cristian Toma

Carlo Cattani

Ming Li

Research Article

Acoustic Response of a Sinusoidally Perturbed Hard-Walled Duct

Silvio Del Giudice and Giancarlo Bernasconi

Department of Electronics, Information and Bioengineering, Polytechnic University of Milan, Via Ponzio 34/5, 20133 Milan, Italy

Correspondence should be addressed to Silvio Del Giudice; delgiudice@elet.polimi.it

Received 2 August 2013; Revised 18 October 2013; Accepted 19 October 2013

Academic Editor: Carlo Cattani

Copyright © 2013 S. Del Giudice and G. Bernasconi. This is an open access article distributed under the Creative Commons Attribution License, which permits unrestricted use, distribution, and reproduction in any medium, provided the original work is properly cited.

Acoustic wave propagation in hard-walled ducts is of interest in many fields including vehicle design, musical instruments acoustics, and architectural and environmental noise-control. For the case of small sinusoidal perturbation of the cross-section, it is possible to derive simple though approximate analytical formulas of its plane wave acoustic reflection and transmission spectral response that resembles the optical situation of uniform Bragg gratings. The proof is given here, starting from the “horn equation” and then exploiting the coupled-modes theory. Examples of the results obtained with these analytical formulas are shown for some sinusoidally perturbed ducts and compared to results obtained through a numerical method, revealing a very good agreement.

1. Introduction

The propagation of waves in periodic media has received much attention in the past in different fields of physics: a comprehensive review can be found in Elachi [1], with references on the propagation of acoustic waves in ducts with sinusoidally perturbed walls [2–4]. An interesting feature of wave propagation in periodic media discussed in the review is the existence of stopbands and passbands related to the medium periodicities.

In the last decades much research effort was dedicated to the theoretical and experimental study of elastic wave propagation in periodic waveguides. For instance, Fokkema [5] dealt with periodic boundaries of elastic media; other authors studied waves propagating along periodically corrugated plates [6–10] and along ducts [11–15].

The purpose of this paper is not to advance the research work accomplished so far, but rather to provide an approximate simplification of the established theory, when proper hypotheses are satisfied. Attention is indeed limited to acoustic propagation in hard-walled ducts whose cross-section undergoes a small sinusoidal perturbation with respect to a reference mean value. The work holds for any filling fluid, typically air, provided that the hard-wall hypothesis is verified.

Like in Munday et al. [15], the analysis is restricted to one-dimensional (plane wave) propagation, where the waveguide geometry is defined simply by the cross-section along the axial coordinate. The starting point of the theoretical analysis is the Webster horn equation, as performed by Nagarkar and Finch [16], who studied sinusoidal horns, and by Griffiths and Steinke [17], who reviewed the theory of one-dimensional wave propagation in locally periodic media consisting of an arbitrary number of identical cells and showed the acoustic solution for some particular geometries. Lau and Campos [18] also solved the acoustic wave equation for one-dimensional propagation along a duct with a small wall sinusoidal perturbation: the exact solutions were obtained as power series expansions around the middle of the duct.

Recently, Hawwa [19] analyzed sound waves in a circular cylindrical duct having a geometric periodicity at its wall, by solving numerically the wave equations.

In optics, or more general in electromagnetics, a periodically perturbed medium is called a Bragg grating, or simply a multilayer medium: the transmission and reflection of a uniform grating can be expressed with simple closed-form formulas (Kogelnik [20]). The acoustic analog of the uniform Bragg grating is a duct whose cross-section sinusoidally varies but, to the authors' knowledge, a simple formula for

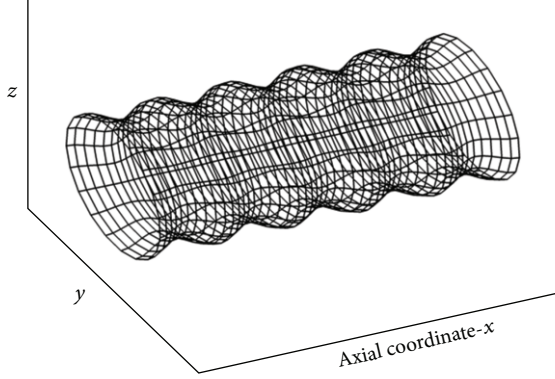


FIGURE 1: Duct with a periodic perturbation of the cross-section.

the acoustic response of such a waveguide is not available in literature.

This paper exploits thus the Bragg gratings theory to solve the acoustic “horn equation,” obtaining simple formulas for the reflection and transmission spectral response of the waveguide as a function of acoustic and geometric parameters, under the hypothesis of a small sinusoidal cross-section variation compared to the mean reference value.

Simple and closed-form solutions are advantageous in modeling/inversion procedures, as, for example, in bore reconstruction, design of noise-control devices (employed, e.g., for jet engines or HVAC systems), and even monitoring of transportation pipelines.

The following sections describe the scenario, the mathematical derivation, and the result for some example cases.

The solution provided can take into account also wave attenuation, typically hard-wall losses (boundary layer friction), whose terms are added a posteriori.

2. Theory

The scenario considered here is a circular hard-walled duct with a small periodic perturbation of the cross-section along the axial coordinate (Figure 1). Two similar though analytically different geometric cases are considered: one is when a sinusoidal function describes the variation of the cross-section; the other when a sinusoidal function describes the variation of the radius of the circular cross-section.

As in Lau and Campos [18], the acoustic wavelength is supposed to be larger than the transverse dimensions of the duct, so that only the fundamental longitudinal mode exists. Moreover, the changes in cross-section are supposed not to be too rapid with respect to the transverse dimension, so that the wavefronts remain approximately plane.

Under these hypotheses the governing geometrical parameters reduce to the cross-section area (the shape can be neglected), and the starting physical law is the one-dimensional “horn equation” [17]:

$$\frac{\partial^2 \Psi}{\partial t^2} = v^2 \left(\frac{\partial^2 \Psi}{\partial x^2} + \frac{1}{S} \frac{dS}{dx} \frac{d\Psi}{dx} \right). \quad (1)$$

The field variable Ψ is the pressure over ambient, S is the cross-section area, v is the phase velocity, x is the waveguide axial coordinate, and t is the time.

Let us consider harmonic waves:

$$\Psi = \psi(x) e^{-i\omega t}. \quad (2)$$

The substitution of (2) in the wave equation (1) yields

$$\frac{\partial^2 \psi}{\partial x^2} + \frac{1}{S} \frac{dS}{dx} \frac{d\psi}{dx} + \beta^2 \psi = 0, \quad (3)$$

where $\beta = \omega/v$ is the acoustic wavenumber.

From this point, the mathematical steps and the approximations introduced follow the computation of the transfer function for a uniform optical fiber Bragg grating (Erdogan [21] and Kogelnik [20]), with adaptation to the acoustic waveguide case.

The pressure field is expressed as a linear combination of the fundamental modes propagating in the opposite directions

$$\psi(x) = A(x) e^{-i\beta x} + B(x) e^{i\beta x}, \quad (4)$$

where, according to the adopted time convention, A and B are the amplitudes of the waves propagating in the $-x$ and $+x$ directions, respectively.

The first derivative of (4) is

$$\psi' = A' e^{-i\beta x} - i\beta A e^{-i\beta x} + B' e^{i\beta x} + i\beta B e^{i\beta x}, \quad (5)$$

with prime denoting derivative with respect to x .

In the hypothesis of weak coupling between the two modes, the second derivatives of A and B are neglected, because $A'' \ll \beta^2 A$ and $B'' \ll \beta^2 B$; therefore, the second derivative of (4) becomes

$$\psi'' \cong -2i\beta A' e^{-i\beta x} - \beta^2 A e^{-i\beta x} + 2i\beta B' e^{i\beta x} - \beta^2 B e^{i\beta x}. \quad (6)$$

Substituting the expressions for derivatives, and multiplying by $e^{i\beta x}$, the wave equation (3) yields

$$\frac{S'}{S} (A' - i\beta A + B' e^{2i\beta x} + i\beta B e^{2i\beta x}) - 2i\beta A' + 2i\beta B' e^{2i\beta x} = 0. \quad (7)$$

The solution of (7) requires a system of two differential equations for A and B . Therefore A' and B' are alternately isolated from (7), neglecting in each resulting equation the dependency on the derivative of the other coefficient. This is justified by the fact that S and so A and B are slowly variable functions of x [21].

The resulting system is

$$\begin{aligned} A' &= \frac{i\beta S'/S}{S'/S - 2i\beta} A + \frac{-i\beta S'/S}{S'/S - 2i\beta} B e^{2i\beta x}, \\ B' &= \frac{-i\beta S'/S}{S'/S + 2i\beta} B + \frac{i\beta S'/S}{S'/S + 2i\beta} A e^{-2i\beta x}, \end{aligned} \quad (8)$$

that can be expressed in this way:

$$\begin{aligned} A' &= -ic_{11}A - ic_{12}Be^{2i\beta x}, \\ B' &= -ic_{22}B - ic_{21}Ae^{-2i\beta x}. \end{aligned} \quad (9)$$

Under the hypothesis of slow section perturbations, and far from the null frequency, it is $|S'/S| \ll |2i\beta|$, and the coefficients c_{ij} in (9) become

$$\begin{aligned} c_{11} &= -\frac{\beta S'/S}{S'/S - 2i\beta} \cong \frac{S'}{2iS}, \\ c_{12} &= \frac{\beta S'/S}{S'/S - 2i\beta} \cong -\frac{S'}{2iS}, \\ c_{21} &= -\frac{\beta S'/S}{S'/S + 2i\beta} \cong -\frac{S'}{2iS}, \\ c_{22} &= \frac{\beta S'/S}{S'/S + 2i\beta} \cong \frac{S'}{2iS}. \end{aligned} \quad (10)$$

Now, the two aforementioned geometric cases are considered; first, when the cross-section is a cosine function of x ; that is,

$$S(x) = s \cos(\gamma x) + s_0, \quad (11)$$

and second, when the radius of the circular cross-section is a cosine function of x ; that is,

$$S(x) = \pi(s \cos(\gamma x) + s_0)^2. \quad (12)$$

γ is the perturbation wavenumber, s is the perturbation amplitude, and s_0 is the mean value.

The ratio between the derivative of the cross-section and the cross-section itself S'/S , for $s \ll s_0$, is approximately

$$\frac{S'(x)}{S(x)} \cong -4\kappa \sin(\gamma x) = 2i\kappa(e^{+i\gamma x} - e^{-i\gamma x}), \quad (13)$$

where $\kappa = s\gamma/4s_0$ for the cross-section sinusoidal perturbation and $\kappa = s\gamma/2s_0$ for the radius sinusoidal perturbation.

The system (9) becomes

$$\begin{aligned} A' &= -i\kappa(e^{+i\gamma x} - e^{-i\gamma x})A + i\kappa(e^{+i\gamma x} - e^{-i\gamma x})Be^{2i\beta x}, \\ B' &= -i\kappa(e^{+i\gamma x} - e^{-i\gamma x})B + i\kappa(e^{+i\gamma x} - e^{-i\gamma x})Ae^{-2i\beta x}. \end{aligned} \quad (14)$$

The terms that contain a rapidly oscillating dependence with x can be neglected: they correspond to the complex exponentials with high phase constant (in magnitude) compared to the others, that is, $e^{\pm i\gamma x}$, $e^{2i\beta x + i\gamma x}$, and $e^{-2i\beta x - i\gamma x}$ [21].

The result is

$$\begin{aligned} A' &= -i\kappa Be^{i(2\beta - \gamma)x}, \\ B' &= i\kappa Ae^{-i(2\beta - \gamma)x}. \end{aligned} \quad (15)$$

By performing in the system (15) the following substitutions:

$$\begin{aligned} a &= Ae^{-i(\beta - \gamma/2)x}, \\ b &= Be^{i(\beta - \gamma/2)x}, \end{aligned} \quad (16)$$

and calling $\sigma = \beta - \gamma/2$, one obtains

$$\begin{aligned} a' &= -i\sigma a - \kappa b \\ b' &= i\sigma b + \kappa a. \end{aligned} \quad (17)$$

The system (17) is a standard system of two coupled first-order ordinary differential equations with constant coefficients, for which closed-form solutions can be found, when appropriate boundary conditions are specified.

Since A corresponds to the backward propagating wave and B to the forward propagating one, the boundary conditions, for a forward propagating wave impinging the waveguide at $x = 0$, are

$$\begin{aligned} A(L) &= 0 \\ B(0) &= 1 \end{aligned} \implies \begin{aligned} a(L) &= 0 \\ b(0) &= 1, \end{aligned} \quad (18)$$

where L is the length of the sinusoidally perturbed duct.

The solution of system (17) with boundary conditions (18) is obtained by means of linear algebra:

$$\begin{aligned} a(x) &= \frac{i\kappa(e^{-\delta L}e^{\delta x} - e^{\delta L}e^{-\delta x})}{e^{\delta L}(i\sigma - \delta) - e^{-\delta L}(i\sigma + \delta)}, \\ b(x) &= \frac{e^{\delta L}e^{-\delta x}(i\sigma - \delta) - e^{-\delta L}e^{\delta x}(i\sigma + \delta)}{e^{\delta L}(i\sigma - \delta) - e^{-\delta L}(i\sigma + \delta)}. \end{aligned} \quad (19)$$

The reflection and transmission spectral responses $R(\omega)$ and $T(\omega)$ correspond, respectively, to $a(0)$ and $b(L)$. Hence, finally

$$\begin{aligned} R(\omega) &= \frac{iS \sinh \delta L}{\cosh \delta L - iP \sinh \delta L}, \\ T(\omega) &= \frac{1}{\cosh \delta L - iP \sinh \delta L}, \end{aligned} \quad (20)$$

where

$$\begin{aligned} \delta &= \sqrt{\kappa^2 - \sigma^2}, \\ S &= \frac{\kappa}{\delta}, \\ P &= \frac{\sigma}{\delta}. \end{aligned} \quad (21)$$

According to their definition, the spectral responses R and T refer to the acoustic pressure amplitude: the corresponding power spectral responses can be found by taking the square of their magnitude. In absence of attenuation, the sum of the power spectral responses is unitary, as expected.

Equations (20) are the acoustic analog of the optical formulas for the uniform Bragg grating in Kogelnik [20], and the parameters κ and σ are expressed here as a function of acoustic wave parameters and waveguide geometric parameters.

The reflection spectral response has a maximum for $\sigma = 0$, corresponding to the frequency $f_{\max} = \gamma v/4\pi$. For the same frequency the transmission response has a minimum.

Finally, even if the considered one-dimensional wave equation does not contain a loss term, one may add the

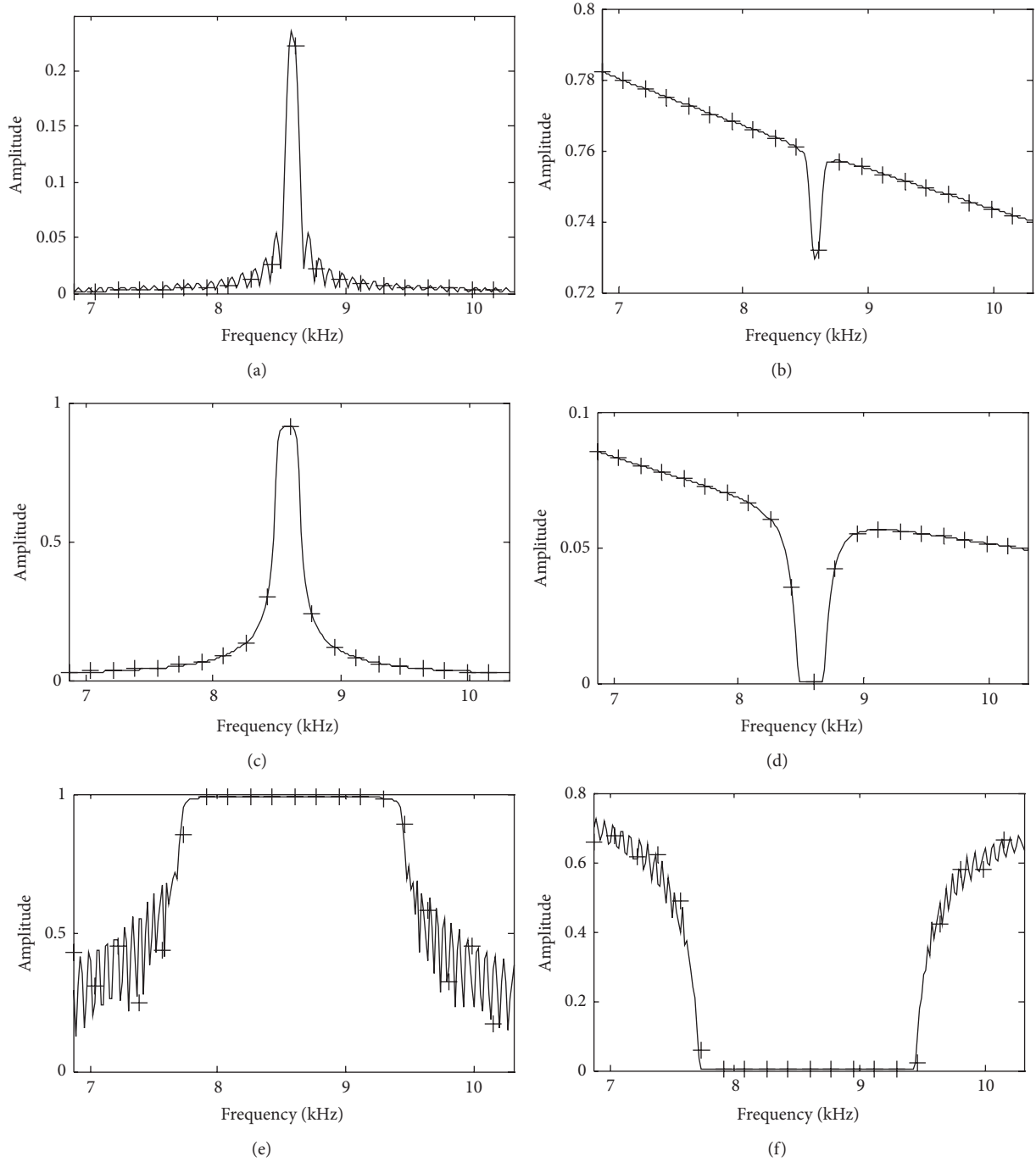


FIGURE 2: Reflection ((a), (c), (e)) and transmission ((b), (d), (f)) spectral responses, in magnitude, of a sinusoidally perturbed duct computed with (20) (solid line) and numerical results (crosses). ((a)-(b)) Case (i); ((c)-(d)) Case (ii); ((e)-(f)) Case (iii).

absorption phenomenon a posteriori, typically due to the duct walls, by redefining the acoustic wavenumber

$$\beta = \frac{\omega}{v} + i\alpha, \quad (22)$$

where $\alpha(\omega)$ is the absorption coefficient computed with mean cross-section parameters and $v(\omega)$ is the corresponding phase velocity.

3. Examples

Some examples of the acoustic behavior for a sinusoidally perturbed duct, filled with air at standard conditions (20°C, 1 atm), are presented here. They reveal the link between the passbands/stopbands response and the waveguide geometrical parameters, and they permit inferring the validity limit of the approximate formula.

Wave attenuation and dispersion are included too, using (22), and $\alpha(\omega)$ and $\nu(\omega)$ are computed according to the wide-tube approximation (well described by Tijdeman [22]). Closed-form solutions are compared with full waveform numerical methods.

We consider a sinusoidal duct with length L , parameterized by the radius of the circular cross-section r :

$$r(x) = s \cos(\gamma x) + s_0, \quad 0 < x < L. \quad (23)$$

The average radius s_0 is set to 2 cm, and the radius perturbation frequency $\gamma/2\pi$ is set to 50 m⁻¹.

The other parameters are set to the following values:

Case (i): $L = 2$ m, $s = 0.02$ mm;

Case (ii): $L = 20$ m, $s = 0.2$ mm;

Case (iii): $L = 2$ m, $s = 2$ mm.

Figure 2 shows the reflection and transmission responses, in magnitude, computed with (20), for the different cases, in a frequency interval centered at the frequency f_{\max} . The wavelength corresponding to f_{\max} is not much higher than the duct transverse dimension, as required.

The crosses in Figure 2 are computed with an “exact” one-dimensional simulator, based on the computation method described by Munday et al. [15], but with transmission coefficients included: the agreement between the approximate and the exact solution is very good.

The parameters values have been chosen to progressively increase the s/s_0 ratio, since a hypothesis for the approximation is $s \ll s_0$: the effect of increasing this ratio is to widen the stopband. Moreover, Case (ii) investigates the effect of extending the duct length L , which is the other geometric parameter of the periodic structure: a higher length results in a sharper transition of the stopband.

The difference between approximate and theoretical values is barely noticeable even when s/s_0 ratio is as large as 1/10, which may be considered the limit of validity of this approximation. Furthermore, the analytic formula is able to correctly simulate the attenuation phenomenon (this is apparent in the transmission response) which was not theoretically justified, but simply added a posteriori.

The phases are not shown here, but they have been verified as well.

4. Conclusion

The acoustic spectral response of a sinusoidally perturbed hard-wall duct has been derived and given in a simple formula, by following the optical analog of Bragg gratings. The formula is the same as in optics, with the electromagnetic parameters replaced by their equivalent acoustic parameters and periodic duct geometry.

Results are valid for small cross-section perturbations and in this case successful comparisons with a numerical method are shown, even in case of wave attenuation.

The availability of simple analytical formulas permits a direct analysis of the link between the acoustic response and the duct geometrical parameters and the design of efficient

modeling/inversion procedures in the fields of bore/pipe reconstruction, noise control, and so forth.

Finally it can be noticed that, even if the derivation strictly requires a sinusoidal perturbation, any cross-section deformation can be decomposed in sinusoidal functions and therefore the results can be applied, provided that the underlying hypotheses are satisfied, to a much broader range of scenarios.

Acknowledgment

The authors wish to thank professor Andrea Melloni for the profitable discussions on the Bragg gratings theory and for the comments and suggestions on the paper production.

References

- [1] C. Elachi, “Waves in active and passive periodic structures: a review,” *Proceedings of the IEEE*, vol. 64, no. 12, pp. 1666–1698, 1976.
- [2] R. F. Salant, “Acoustic propagation in waveguides with sinusoidal walls,” *Journal of the Acoustical Society of America*, vol. 53, no. 2, pp. 504–507, 1973.
- [3] A. H. Nayfeh, “Sound waves in two dimensional ducts with sinusoidal walls,” *Journal of the Acoustical Society of America*, vol. 56, no. 3, pp. 768–770, 1974.
- [4] O. R. Asfar and A. H. Nayfeh, “Circular Waveguide with Sinusoidally Perturbed Walls,” *IEEE Transactions on Microwave Theory and Techniques*, vol. 23, no. 9, pp. 728–734, 1975.
- [5] J. T. Fokkema, “Reflection and transmission of elastic waves by the spatially periodic interface between two solids (theory of integral-equation method),” *Wave Motion*, vol. 2, no. 4, pp. 375–393, 1980.
- [6] O. R. Asfar and A. H. Nayfeh, “Stopbands of the first-order Bragg interaction in a parallel-plate waveguide having multi-periodic wall corrugations,” *IEEE Transactions on Microwave Theory and Techniques*, vol. 28, no. 11, pp. 1187–1191, 1980.
- [7] A. El-Bahrawy, “Stopbands and passbands for symmetric rayleigh-lamb modes in a plate with corrugated surfaces,” *Journal of Sound and Vibration*, vol. 170, no. 2, pp. 145–160, 1994.
- [8] S. Banerjee and T. Kundu, “Elastic wave propagation in symmetrically periodic sinusoidal waveguide,” in *Health Monitoring and Smart Nondestructive Evaluation of Structural and Biological Systems III*, vol. 5394 of *Proceedings of SPIE*, pp. 89–98, March 2004.
- [9] S. Banerjee and T. Kundu, “Symmetric and anti-symmetric Rayleigh-Lamb modes in sinusoidally corrugated waveguides: an analytical approach,” *International Journal of Solids and Structures*, vol. 43, no. 21, pp. 6551–6567, 2006.
- [10] A. H. Nayfeh and O. R. Asfar, “Parallel-plate waveguide with sinusoidally perturbed boundaries,” *Journal of Applied Physics*, vol. 45, no. 11, pp. 4797–4800, 1974.
- [11] A. H. Nayfeh and O. A. Kandil, “Propagation of waves in cylindrical hard-walled ducts with generally weak undulations,” *AIAA Journal*, vol. 16, no. 10, pp. 1041–1045, 1978.
- [12] P. Latinopoulos and D. Tolikas, “Propagation of acoustic waves in ducts with varying cross sections and viscous mean flow,” *Computer Methods in Applied Mechanics and Engineering*, vol. 23, no. 2, pp. 215–224, 1980.

- [13] A. Boström, "Acoustic waves in a cylindrical duct with periodically varying cross section," *Wave Motion*, vol. 5, no. 1, pp. 59–67, 1983.
- [14] P. D. C. King and T. J. Cox, "Acoustic band gaps in periodically and quasiperiodically modulated waveguides," *Journal of Applied Physics*, vol. 102, no. 1, Article ID 014902, 2007.
- [15] J. N. Munday, C. B. Bennett, and W. M. Robertson, "Band gaps and defect modes in periodically structured waveguides," *Journal of the Acoustical Society of America*, vol. 112, no. 4, pp. 1353–1358, 2002.
- [16] B. N. Nagarkar and R. D. Finch, "Sinusoidal horns," *Journal of the Acoustical Society of America*, vol. 50, no. 1, pp. 23–31, 1971.
- [17] D. J. Griffiths and C. A. Steinke, "Waves in locally periodic media," *American Journal of Physics*, vol. 69, no. 2, pp. 137–154, 2001.
- [18] F. J. P. Lau and L. M. B. C. Campos, "On the effect of wall undulations on the acoustics of ducts with flow," *Journal of Sound and Vibration*, vol. 270, no. 1-2, pp. 361–378, 2004.
- [19] M. A. Hawwa, "Acoustic wave blocking in a duct with a chirped periodic wall," *Arabian Journal for Science and Engineering*, vol. 29, no. 1C, pp. 113–124, 2004.
- [20] H. Kogelnik, "Theory of optical waveguides," in *Guided-Wave Optoelectronics*, T. Tamir, Ed., pp. 60–65, Springer, 1988.
- [21] T. Erdogan, "Fiber grating spectra," *Journal of Lightwave Technology*, vol. 15, no. 8, pp. 1277–1294, 1997.
- [22] H. Tijdeman, "On the propagation of sound waves in cylindrical tubes," *Journal of Sound and Vibration*, vol. 39, no. 1, pp. 1–33, 1975.

Research Article

Nonholonomic Geometry of Viscoanelastic Media and Experimental Confirmation

Armando Ciancio¹ and Carlo Cattani²

¹ Department of Mathematics and Computer Science, University of Messina, Viale F. Stagno d'Alcontres 31, 98166 Messina, Italy

² Department of Mathematics, University of Salerno, Via Ponte Don Melillo, 84084 Fisciano, Italy

Correspondence should be addressed to Armando Ciancio; aciancio@unime.it

Received 16 July 2013; Accepted 9 August 2013

Academic Editor: Cristian Toma

Copyright © 2013 A. Ciancio and C. Cattani. This is an open access article distributed under the Creative Commons Attribution License, which permits unrestricted use, distribution, and reproduction in any medium, provided the original work is properly cited.

A thermodynamical model for viscoanelastic media is analyzed using the nonholonomic geometry. A 27-dimensional manifold is introduced, and the differential equations for the geodetics are determined and analytically solved. It is shown that, in this manifold, the best specific entropy is a harmonic function. In the linear case the propagation of transverse acoustic waves is studied, and the theoretical results are compared with some experimental data from a polymeric material (polyisobutylene).

1. Introduction

From macroscopic point of view the most popular mathematical approaches to nonequilibrium thermodynamics are based both on the Caratheodory theory [1–3] which involves Pfaff equations and on the contact structure of thermodynamic state space [4–6]. If these equations are completely integrable, then the thermodynamics is called *holonomic* otherwise *nonholonomic*.

The theory of nonequilibrium holonomic thermodynamics for mechanical phenomena in continuous media was developed in the 90s (see e.g., [7] and references therein). The phenomenological equations were derived [8, 9] by introducing the tensorial internal variables $\varepsilon_{\alpha\beta}^{(1)}$ ($\alpha, \beta = 1, 2, 3$) which occur in the entropy production.

In particular, if one linearizes this theory by neglecting the cross effects among the irreversible phenomena (heat flow, mechanical viscosity, and anelastic deformations), the following rheological equations for distortional phenomena are obtained [10]:

$$\frac{d\tilde{\tau}_{\alpha\beta}}{dt} + R_{(d)0}^{(\tau)} \tilde{\tau}_{\alpha\beta} = R_{(d)2}^{(\varepsilon)} \frac{d^2 \tilde{\varepsilon}_{\alpha\beta}}{dt^2} + R_{(d)1}^{(\varepsilon)} \frac{d\tilde{\varepsilon}_{\alpha\beta}}{dt} + R_{(d)0}^{(\varepsilon)} \tilde{\varepsilon}_{\alpha\beta}, \quad (1)$$

where $\tilde{\tau}_{\alpha\beta}$ and $\tilde{\varepsilon}_{\alpha\beta}$ are the deviators of the stress ($\tau_{\alpha\beta}$) and the strain ($\varepsilon_{\alpha\beta}$) tensors, respectively.

The quantities R are given by

$$\begin{aligned} R_{(d)0}^{(\tau)} &= a^{(1,1)} \eta_s^{(1,1)} = \frac{1}{\sigma} \geq 0, \\ R_{(d)0}^{(\varepsilon)} &= a^{(0,0)} (a^{(1,1)} - a^{(0,0)}) \eta_s^{(1,1)} \geq 0, \\ R_{(d)1}^{(\varepsilon)} &= a^{(0,0)} + a^{(1,1)} \eta_s^{(1,1)} \eta_s^{(0,0)} \geq 0, \\ R_{(d)2}^{(\varepsilon)} &= \eta_s^{(0,0)} \geq 0, \end{aligned} \quad (2)$$

in which σ is the relaxation time and $a^{(1,1)} \geq a^{(0,0)} \geq 0$ are the state coefficients, while $\eta_s^{(0,0)}$ and $\eta_s^{(1,1)}$ are the phenomenological coefficients related to the following physical phenomena:

$$\begin{aligned} a^{(0,0)} &\implies \text{elasticity}, \\ a^{(1,1)} &\implies \text{anelasticity}, \\ \eta_s^{(0,0)} &\implies \text{viscosity}, \\ \eta_s^{(1,1)} &\implies \text{fluidity}. \end{aligned} \quad (3)$$

In this paper we reconsider the theory from the point of view of the nonholonomic geometry.

In Sections 2 and 3 the analytic properties of the entropy are discussed, and in Section 4 the differential equations of geodetics in the space of state are obtained.

Finally, in Section 5 we study the transverse waves and we will show the connection between complex numbers and the shear complex modulus. By applying these results to a polymeric material, as polyisobutylene we will also show that the expected results of the theoretical model are in agreement with the experimental data.

2. Gibbs-Pfaff Equation of Viscoanelastic Media

Let us define the space of states

$$R^{27} = R^{2 \cdot 13 + 1} = \left\{ s, T, u, \tau_{\alpha\beta}^{(\text{eq})}, \varepsilon_{\alpha\beta}, \tau_{\alpha\beta}^{(1)}, \varepsilon_{\alpha\beta}^{(1)} \right\}, \quad (4)$$

where s is the specific entropy, T is the absolute temperature, u is the specific internal energy, $\tau_{\alpha\beta}^{(\text{eq})}$ is the symmetric equilibrium stress tensor, $\varepsilon_{\alpha\beta}$ is the total symmetric strain tensor, and $\tau_{\alpha\beta}^{(1)}$ is the symmetric affinity stress tensor conjugate to the anelastic tensor $\varepsilon_{\alpha\beta}^{(1)}$ (the symmetric tensorial thermodynamic internal variable).

Let ν be the specific volume related to the mass density $\varrho = \text{constant}$ (homogeneous media) by $\nu\varrho = 1$. The Gibbs-Pfaff equation of viscoanelastic media is

$$Tds = du - \nu\tau_{\alpha\beta}^{(\text{eq})} d\varepsilon_{\alpha\beta} + \nu\tau_{\alpha\beta}^{(1)} d\varepsilon_{\alpha\beta}^{(1)}. \quad (5)$$

This equation defines in R^{27} the nonholonomic contact distribution of dimension 26 so that the highest dimension of integral manifold is 13.

The C^∞ representation of this integral manifold (of maximum dimension) is usually given as follows:

$$\begin{aligned} s &= \Phi(u, \varepsilon_{\alpha\beta}, \varepsilon_{\alpha\beta}^{(1)}), \\ T^{-1} &= \frac{\partial \Phi}{\partial u}(u, \varepsilon_{\alpha\beta}, \varepsilon_{\alpha\beta}^{(1)}), \\ \tau_{\alpha\beta}^{(\text{eq})} &= -\varrho T \frac{\partial \Phi}{\partial \varepsilon_{\alpha\beta}}(u, \varepsilon_{\alpha\beta}, \varepsilon_{\alpha\beta}^{(1)}), \\ \tau_{\alpha\beta}^{(1)} &= \varrho T \frac{\partial \Phi}{\partial \varepsilon_{\alpha\beta}^{(1)}}(u, \varepsilon_{\alpha\beta}, \varepsilon_{\alpha\beta}^{(1)}). \end{aligned} \quad (6)$$

This parametrization is based on the arbitrary C^∞ -function Φ . So that we have a family of integral manifolds of dimension 13 indexed on the arbitrary function Φ .

The state parameters

$$T^{-1}, T^{-1}\varrho^{-1}\tau_{\alpha\beta}^{(\text{eq})}, T^{-1}\varrho^{-1}\tau_{\alpha\beta}^{(1)} \quad (7)$$

are related by the equations of motion and the equations of state [8, 9].

The C^∞ -representation is a generic element in the 1-jet space converted into

$$\left(u, \varepsilon_{\alpha\beta}, \varepsilon_{\alpha\beta}^{(1)}, s(u, \varepsilon_{\alpha\beta}, \varepsilon_{\alpha\beta}^{(1)}), \frac{\partial s}{\partial u}, -\frac{\partial s}{\partial \varepsilon_{\alpha\beta}}, \frac{\partial s}{\partial \varepsilon_{\alpha\beta}^{(1)}} \right). \quad (8)$$

In order to fix a representative for the specific entropy $s = \Phi(u, \varepsilon_{\alpha\beta}, \varepsilon_{\alpha\beta}^{(1)})$, we need a supplementary condition as follows.

Theorem 1. *If $s = \Phi(u, \varepsilon_{\alpha\beta}, \varepsilon_{\alpha\beta}^{(1)})$ is an homogeneous function of order one, then*

$$\Phi = \frac{u}{T} - \frac{1}{\varrho T} \tau_{\alpha\beta}^{(\text{eq})} \varepsilon_{\alpha\beta} + \frac{1}{\varrho T} \tau_{\alpha\beta}^{(1)} \varepsilon_{\alpha\beta}^{(1)}. \quad (9)$$

Proof. The condition of homogeneity of order one

$$\Phi(ku, k\varepsilon_{\alpha\beta}, k\varepsilon_{\alpha\beta}^{(1)}) = k\Phi(u, \varepsilon_{\alpha\beta}, \varepsilon_{\alpha\beta}^{(1)}) \quad (10)$$

gives the PDE

$$u \frac{\partial \Phi}{\partial u} + \varepsilon_{\alpha\beta} \frac{\partial \Phi}{\partial \varepsilon_{\alpha\beta}} + \varepsilon_{\alpha\beta}^{(1)} \frac{\partial \Phi}{\partial \varepsilon_{\alpha\beta}^{(1)}} = \Phi(u, \varepsilon_{\alpha\beta}, \varepsilon_{\alpha\beta}^{(1)}). \quad (11)$$

Then the entropy (solution of this PDE) appears as the potential (9). \square

Corollary 2. *If the specific entropy $s = \Phi(u, \varepsilon_{\alpha\beta}, \varepsilon_{\alpha\beta}^{(1)})$ is an homogeneous function of order one, then*

- (1) *the variables $s, u, \varepsilon_{\alpha\beta}, \varepsilon_{\alpha\beta}^{(1)}$ are conjugated to the intensive variables $T, \tau_{\alpha\beta}^{(\text{eq})}, \tau_{\alpha\beta}^{(1)}$;*
- (2) *the variables $s, u, \varepsilon_{\alpha\beta}, \varepsilon_{\alpha\beta}^{(1)}$ are not essential parameters (because they are not independent).*

Proof. From the expression (9) we find

$$\begin{aligned} Tds + sdT &= du - \frac{1}{\varrho} \left(\varepsilon_{\alpha\beta} d\tau_{\alpha\beta}^{(\text{eq})} + \tau_{\alpha\beta}^{(\text{eq})} d\varepsilon_{\alpha\beta} \right) \\ &\quad + \frac{1}{\varrho} \left(\varepsilon_{\alpha\beta}^{(1)} d\tau_{\alpha\beta}^{(1)} + \tau_{\alpha\beta}^{(1)} d\varepsilon_{\alpha\beta}^{(1)} \right). \end{aligned} \quad (12)$$

- (1) Replacing the relation (5), we get

$$sdT = -\frac{1}{\varrho} \varepsilon_{\alpha\beta} d\tau_{\alpha\beta}^{(\text{eq})} + \frac{1}{\varrho} \varepsilon_{\alpha\beta}^{(1)} d\tau_{\alpha\beta}^{(1)}, \quad (13)$$

and the first statement is true.

- (2) The foregoing relation shows that, for example,

$$\frac{\varepsilon_{\alpha\beta}}{s}, \quad \frac{\varepsilon_{\alpha\beta}^{(1)}}{s} \quad (14)$$

are essential parameters. \square

3. Specific Entropy via Least Squares Lagrangian

The most convenient way to fix a representative Φ of the specific entropy s is to look at (5) as a partial derivative

evolution equation and to build the least squares method Lagrangian L

$$2L = \left\| T^{-1} - \frac{\partial \Phi}{\partial u} \right\|^2 + \left\| \tau_{\alpha\beta}^{(\text{eq})} + \rho T \frac{\partial \Phi}{\partial \varepsilon_{\alpha\beta}} \right\|^2 + \left\| \tau_{\alpha\beta}^{(1)} - \rho T \frac{\partial \Phi}{\partial \varepsilon_{\alpha\beta}^{(1)}} \right\|^2 \quad (15)$$

and the functional

$$\int_{\Omega} L(u, \varepsilon_{\alpha\beta}, \varepsilon_{\alpha\beta}^{(1)}, \Phi, \Phi_u, \Phi_{\varepsilon_{\alpha\beta}}, \Phi_{\varepsilon_{\alpha\beta}^{(1)}}) d\Omega, \quad (16)$$

where $\Phi_u = \partial\Phi/\partial u$, $\Phi_{\varepsilon_{\alpha\beta}} = \partial\Phi/\partial \varepsilon_{\alpha\beta}$, and $\Phi_{\varepsilon_{\alpha\beta}^{(1)}} = \partial\Phi/\partial \varepsilon_{\alpha\beta}^{(1)}$.

The extremals are solutions of the Euler-Lagrange PDE

$$\frac{\partial L}{\partial \Phi} - \left(D_u \frac{\partial L}{\partial \Phi_u} + D_{\varepsilon_{\alpha\beta}} \frac{\partial L}{\partial \Phi_{\varepsilon_{\alpha\beta}}} + D_{\varepsilon_{\alpha\beta}^{(1)}} \frac{\partial L}{\partial \Phi_{\varepsilon_{\alpha\beta}^{(1)}}} \right) = 0, \quad (17)$$

where D_* is the total derivative with respect to the variable $*$.

In our case, we get

$$\begin{aligned} \frac{\partial L}{\partial \Phi} &= 0, & \frac{\partial L}{\partial \Phi_u} &= - \left(T^{-1} - \frac{\partial \Phi}{\partial u} \right), \\ \frac{\partial L}{\partial \Phi_{\varepsilon_{\alpha\beta}}} &= \rho T \left(\tau_{\alpha\beta}^{(\text{eq})} + \rho T \frac{\partial \Phi}{\partial \varepsilon_{\alpha\beta}} \right), & (18) \\ \frac{\partial L}{\partial \Phi_{\varepsilon_{\alpha\beta}^{(1)}}} &= -\rho T \left(\tau_{\alpha\beta}^{(1)} - \rho T \frac{\partial \Phi}{\partial \varepsilon_{\alpha\beta}^{(1)}} \right). \end{aligned}$$

So that, by replacing the partial derivatives of L in (17), there follows the Laplace equation for the entropy

$$\frac{\partial^2 \Phi}{\partial u^2} + \rho^2 T^2 \frac{\partial^2 \Phi}{\partial \varepsilon_{\alpha\beta}^2} + \rho^2 T^2 \frac{\partial^2 \Phi}{\partial \varepsilon_{\alpha\beta}^{(1)2}} = 0. \quad (19)$$

Consequently, we have the following.

Theorem 3. *The best entropy for the nonholonomic nonequilibrium thermodynamics is an harmonic function.*

4. Geodesics

Any curve in the distribution (5) is described by

$$T(t) \dot{s}(t) = \dot{u}(t) - \nu \tau_{\alpha\beta}^{(\text{eq})}(t) \dot{\varepsilon}_{\alpha\beta}(t) + \nu \tau_{\alpha\beta}^{(1)}(t) \dot{\varepsilon}_{\alpha\beta}^{(1)}(t). \quad (20)$$

In order to be a geodesic, this curve must minimize the energy functional

$$\begin{aligned} J &= \frac{1}{2} \int_{t_0}^{t_1} \left(\dot{T}^2(t) + \dot{s}^2(t) + \dot{u}^2(t) + \delta_{\alpha\gamma} \delta_{\beta\delta} \dot{\tau}_{\alpha\beta}^{(\text{eq})} \dot{\tau}_{\gamma\delta}^{(\text{eq})} \right. \\ &\quad + \delta_{\alpha\gamma} \delta_{\beta\delta} \dot{\tau}_{\alpha\beta}^{(1)} \dot{\tau}_{\gamma\delta}^{(1)} + \delta_{\alpha\gamma} \delta_{\beta\delta} \dot{\varepsilon}_{\alpha\beta} \dot{\varepsilon}_{\gamma\delta} \\ &\quad \left. + \delta_{\alpha\gamma} \delta_{\beta\delta} \dot{\varepsilon}_{\alpha\beta}^{(1)} \dot{\varepsilon}_{\gamma\delta}^{(1)} \right) dt. \end{aligned} \quad (21)$$

In short, we must solve the problem

$$\min J \text{ subject to (20)}. \quad (22)$$

To solve this problem, we use the method of Lagrange multipliers. For this we defined the constrained Lagrangian

$$\begin{aligned} L_1 &= \frac{1}{2} \left(\dot{T}^2(t) + \dot{s}^2(t) + \dot{u}^2(t) + \delta_{\alpha\gamma} \delta_{\beta\delta} \dot{\tau}_{\alpha\beta}^{(\text{eq})}(t) \dot{\tau}_{\gamma\delta}^{(\text{eq})}(t) \right. \\ &\quad + \delta_{\alpha\gamma} \delta_{\beta\delta} \dot{\tau}_{\alpha\beta}^{(1)}(t) \dot{\tau}_{\gamma\delta}^{(1)}(t) \\ &\quad + \delta_{\alpha\gamma} \delta_{\beta\delta} \dot{\varepsilon}_{\alpha\beta}(t) \dot{\varepsilon}_{\gamma\delta}(t) \\ &\quad \left. + \delta_{\alpha\gamma} \delta_{\beta\delta} \dot{\varepsilon}_{\alpha\beta}^{(1)}(t) \dot{\varepsilon}_{\gamma\delta}^{(1)}(t) \right) \\ &\quad + p \left(T(t) \dot{s}(t) - \dot{u}(t) + \nu \tau_{\alpha\beta}^{(\text{eq})}(t) \dot{\varepsilon}_{\alpha\beta}(t) \right. \\ &\quad \left. - \nu \tau_{\alpha\beta}^{(1)}(t) \dot{\varepsilon}_{\alpha\beta}^{(1)}(t) \right), \end{aligned} \quad (23)$$

where p is the Lagrangian multiplier.

Theorem 4. *The geodesics of the nonholonomic viscoanelastic distribution are solutions of the Euler-Lagrange ODEs for the Lagrangian (23)*

$$\frac{\partial L_1}{\partial x^i} - D_t \frac{\partial L_1}{\partial \dot{x}^i} = 0, \quad (24)$$

where x^i are the generalized coordinates:

$$\begin{aligned} x^1 &= T, & x^2 &= s, & x^3 &= u, \\ x_{\alpha\beta}^4 &= \tau_{\alpha\beta}^{(\text{eq})}, & x_{\alpha\beta}^5 &= \varepsilon_{\alpha\beta}, & x_{\alpha\beta}^6 &= \tau_{\alpha\beta}^{(1)}, \\ x_{\alpha\beta}^7 &= \varepsilon_{\alpha\beta}^{(1)}. \end{aligned} \quad (25)$$

So that explicitly from (23) and (24) we have

$$\begin{aligned} p\dot{s} - \ddot{T} &= 0, & \frac{d}{dt}(\dot{s} + pT) &= 0, & \frac{d}{dt}(\dot{u} - p) &= 0, \\ p\nu\dot{\varepsilon}_{\alpha\beta} - \frac{d}{dt}\dot{\tau}_{\alpha\beta}^{(\text{eq})} &= 0, & p\nu\dot{\varepsilon}_{\alpha\beta}^{(1)} + \frac{d}{dt}\dot{\tau}_{\alpha\beta}^{(1)} &= 0, \\ \frac{d}{dt}(\dot{\varepsilon}_{\alpha\beta}^{(1)} - p\nu\tau_{\alpha\beta}^{(1)}) &= 0, & \frac{d}{dt}(\dot{\varepsilon}_{\alpha\beta} + p\nu\tau_{\alpha\beta}^{(\text{eq})}) &= 0. \end{aligned} \quad (26)$$

The equations (26) with the condition (20) are the differential equations of geodesics.

Let

$$\begin{aligned} T_0 &= T(0), & \dot{T}_0 &= \dot{T}(0), & s_0 &= s(0), \\ \dot{s}_0 &= \dot{s}(0), & u_0 &= u(0), & \dot{u}_0 &= \dot{u}(0), \\ \tau_{\alpha\beta}^{(\text{eq})} &= \tau_{\alpha\beta}^{(\text{eq})}(0), & \dot{\tau}_{\alpha\beta}^{(\text{eq})} &= \dot{\tau}_{\alpha\beta}^{(\text{eq})}(0), \\ \tau_{\alpha\beta}^{(1)} &= \tau_{\alpha\beta}^{(1)}(0), & \dot{\tau}_{\alpha\beta}^{(1)} &= \dot{\tau}_{\alpha\beta}^{(1)}(0), \\ \varepsilon_{\alpha\beta} &= \varepsilon_{\alpha\beta}(0), & \dot{\varepsilon}_{\alpha\beta} &= \dot{\varepsilon}_{\alpha\beta}(0), \\ \varepsilon_{\alpha\beta}^{(1)} &= \varepsilon_{\alpha\beta}^{(1)}(0), & \dot{\varepsilon}_{\alpha\beta}^{(1)} &= \dot{\varepsilon}_{\alpha\beta}^{(1)}(0) \end{aligned} \quad (27)$$

be the given (constant) initial values.

By some explicit computation we can easily show that the following.

Theorem 5. *The geodesics of the nonholonomic viscoanelastic distribution, as solution of the Cauchy problem (26) and (27), are the family of curves:*

$$\begin{aligned}
 u(t) &= \dot{u}_0 t + u_0 \\
 s(t) &= \frac{\dot{T}_0}{p} \cos pt + \frac{\dot{s}_0}{p} \sin pt + \left(s_0 - \frac{\dot{T}_0}{p} \right) \\
 T(t) &= \frac{\dot{T}_0}{p} \sin pt - \frac{\dot{s}_0}{p} \cos pt + \left(T_0 + \frac{\dot{s}_0}{p} \right) \\
 \tau_{\alpha\beta}^{(eq)} &= \left[\tau_{0\alpha\beta}^{(eq)} - \frac{1}{\nu p} \left(\dot{\varepsilon}_{0\alpha\beta} + p\nu\tau_{0\alpha\beta}^{(eq)} \right) \right] \cos \nu pt \\
 &\quad + \frac{1}{\nu p} \dot{\tau}_{0\alpha\beta}^{(eq)} \sin \nu pt + \frac{1}{\nu p} \left(\dot{\varepsilon}_{0\alpha\beta} + p\nu\tau_{0\alpha\beta}^{(eq)} \right) \\
 \varepsilon_{\alpha\beta} &= - \left[\tau_{0\alpha\beta}^{(eq)} - \frac{1}{\nu p} \left(\dot{\varepsilon}_{0\alpha\beta} + p\nu\tau_{0\alpha\beta}^{(eq)} \right) \right] \sin \nu pt \\
 &\quad - \frac{1}{\nu p} \dot{\tau}_{0\alpha\beta}^{(eq)} \cos \nu pt + \left(\dot{\varepsilon}_{0\alpha\beta} + \frac{1}{\nu p} \dot{\tau}_{0\alpha\beta}^{(eq)} \right) \\
 \tau_{\alpha\beta}^{(1)} &= \left[\tau_{0\alpha\beta}^{(1)} + \frac{1}{\nu p} \left(\dot{\varepsilon}_{0\alpha\beta}^{(1)} + p\nu\tau_{0\alpha\beta}^{(1)} \right) \right] \cos \nu pt \\
 &\quad + \frac{1}{\nu p} \dot{\tau}_{0\alpha\beta}^{(1)} \sin \nu pt - \frac{1}{\nu p} \left(\dot{\varepsilon}_{0\alpha\beta}^{(1)} + p\nu\tau_{0\alpha\beta}^{(1)} \right) \\
 \varepsilon_{\alpha\beta}^{(1)} &= - \left[\tau_{0\alpha\beta}^{(1)} + \frac{1}{\nu p} \left(\dot{\varepsilon}_{0\alpha\beta}^{(1)} + p\nu\tau_{0\alpha\beta}^{(1)} \right) \right] \sin \nu pt \\
 &\quad - \frac{1}{\nu p} \dot{\tau}_{0\alpha\beta}^{(1)} \cos \nu pt - \left(\dot{\varepsilon}_{0\alpha\beta}^{(1)} + \frac{1}{\nu p} \dot{\tau}_{0\alpha\beta}^{(1)} \right).
 \end{aligned} \tag{28}$$

Proof. Let us first solve the simplest equation: from (26)₃ we have

$$\dot{u} - p = \dot{u}_0 \implies u = (\dot{u}_0 + p)t + u_0. \tag{29}$$

From (26)₁ it is

$$\frac{d}{dt} (ps - \dot{T}) = 0 \implies \dot{T} = p(s - s_0) + \dot{T}_0 \tag{30}$$

and deriving (26)₂

$$\ddot{s} + p\dot{T} = 0. \tag{31}$$

By replacing \dot{T} with the previous expression we get

$$\ddot{s} + p[p(s - s_0) + \dot{T}_0] = 0, \tag{32}$$

that is

$$\ddot{s} + p^2 s = (p^2 s_0 - p\dot{T}_0). \tag{33}$$

This is a linear nonhomogeneous second-order (harmonic) equation whose solution is

$$s(t) = \left(s_0 - \frac{\dot{T}_0}{p} \right) + \frac{\dot{T}_0}{p} \cos pt + \frac{\dot{s}_0}{p} \sin pt. \tag{34}$$

With this function, from the expression

$$\dot{T} = p(s - s_0) + \dot{T}_0, \tag{35}$$

we can compute also $T(t)$:

$$\dot{T} = p \left[\left(\left(s_0 - \frac{\dot{T}_0}{p} \right) + \frac{\dot{T}_0}{p} \cos pt + \frac{\dot{s}_0}{p} \sin pt \right) - s_0 \right] + \dot{T}_0; \tag{36}$$

that is,

$$\dot{T} = \dot{T}_0 \cos pt + \dot{s}_0 \sin pt. \tag{37}$$

The solution is

$$T(t) = \frac{\dot{T}_0}{p} \sin pt - \frac{\dot{s}_0}{p} \cos pt + \left(T_0 + \frac{\dot{s}_0}{p} \right). \tag{38}$$

Concerning (26)_{4,5,6,7} we can notice that it is enough to solve (26)_{4,7} since their solutions are formally equal to the solutions of (26)_{5,6} since these equations coincide with (26)_{4,7} apart from the substitutions:

$$\varepsilon_{\alpha\beta} \implies \varepsilon_{\alpha\beta}^{(1)}, \quad \tau_{\alpha\beta}^{(eq)} \implies -\tau_{\alpha\beta}^{(1)}. \tag{39}$$

Thus from (26)₇ it is

$$\dot{\varepsilon}_{\alpha\beta} + p\nu\tau_{\alpha\beta}^{(eq)} = \dot{\varepsilon}_{0\alpha\beta} + p\nu\tau_{0\alpha\beta}^{(eq)}; \tag{40}$$

that is,

$$\dot{\varepsilon}_{\alpha\beta} = -p\nu\tau_{\alpha\beta}^{(eq)} + \left(\dot{\varepsilon}_{0\alpha\beta} + p\nu\tau_{0\alpha\beta}^{(eq)} \right). \tag{41}$$

If we put this expression in (26)₄ we get

$$p\nu \left[-p\nu\tau_{\alpha\beta}^{(eq)} + \left(\dot{\varepsilon}_{0\alpha\beta} + p\nu\tau_{0\alpha\beta}^{(eq)} \right) \right] - \frac{d}{dt} \dot{\tau}_{\alpha\beta}^{(eq)} = 0, \tag{42}$$

and by some manipulation we get the (vectorial) linear second order harmonic equation for $\tau_{\alpha\beta}^{(eq)}$:

$$\frac{d}{dt} \dot{\tau}_{\alpha\beta}^{(eq)} + p^2 \nu^2 \tau_{\alpha\beta}^{(eq)} = p\nu \left(\dot{\varepsilon}_{0\alpha\beta} + p\nu\tau_{0\alpha\beta}^{(eq)} \right). \tag{43}$$

The solution is

$$\begin{aligned}
 \tau_{\alpha\beta}^{(eq)} &= \left[\tau_{0\alpha\beta}^{(eq)} - \frac{1}{\nu p} \left(\dot{\varepsilon}_{0\alpha\beta} + p\nu\tau_{0\alpha\beta}^{(eq)} \right) \right] \cos \nu pt \\
 &\quad + \frac{1}{\nu p} \dot{\tau}_{0\alpha\beta}^{(eq)} \sin \nu pt + \frac{1}{\nu p} \left(\dot{\varepsilon}_{0\alpha\beta} + p\nu\tau_{0\alpha\beta}^{(eq)} \right),
 \end{aligned} \tag{44}$$

so that by integrating (41) and using the previous equation, we can easily get the expression for $\varepsilon_{\alpha\beta}$

$$\varepsilon_{\alpha\beta} = - \left[\tau_{0\alpha\beta}^{(eq)} - \frac{1}{\nu p} \left(\dot{\varepsilon}_{0\alpha\beta} + p \nu \tau_{0\alpha\beta}^{(eq)} \right) \right] \sin \nu p t - \frac{1}{\nu p} \dot{\tau}_{0\alpha\beta}^{(eq)} \cos \nu p t + \left(\varepsilon_{0\alpha\beta} + \frac{1}{\nu p} \dot{\tau}_{0\alpha\beta}^{(eq)} \right). \quad (45)$$

With similar computations we get also the last two equations of (28). \square

The Lagrangian multiplier p is obtained by inserting the functions (28) and derivatives into (20).

It should be noticed that the the projection of the geodesics (28) into different planes gives rise to well known curves. For instance, in the plane $\langle T, s \rangle$ (28) are the parametric equations of a cycloid. Moreover, by assuming that all the initial values are positive, the asymptotic limits give

$$\lim_{t \rightarrow \infty} u(t) = +\infty, \quad \lim_{t \rightarrow \infty} |T(t)| \leq \left| T_0 - \frac{\dot{s}_0}{p} \right| + \left| \frac{\dot{T}_0}{p} \right| + \left| \frac{\dot{s}_0}{p} \right|, \quad (46)$$

$$\lim_{t \rightarrow \infty} |s(t)| \leq \left| s_0 - \frac{\dot{T}_0}{p} \right| + \left| \frac{\dot{T}_0}{p} \right| + \left| \frac{\dot{s}_0}{p} \right|,$$

which are in agreement with physical consideration especially for the entropy s which is upper bounded. Analogously we have similar bounded asymptotic limits for the vectorial functions.

5. Experimental Approach to the Linear Response Theory

In a previous paper [11] by the application of the linear response theory [12–15] numerical values of (1) were considered, and the results were compared with experimental data.

In this section we study another aspect of the transversal waves propagation in viscoelastic media, and we apply the theoretical results to a polymeric material as the polyisobutylene.

We consider, with respect to the Cartesian orthogonal axes (x_1, x_2, x_3) , the following displacement \mathbf{u}

$$u_3 = A e^{i(kx_1 - \omega t)}, \quad u_1 = u_2 = 0 \quad (47)$$

being $i^2 = -1$ and $k = k_1 + ik_2$ the complex wave number, so that

$$\nu_s = \frac{\omega}{k_1} \quad (48)$$

is the phase velocity and k_2 is connected with the attenuation of the waves.

As $\varepsilon_{\alpha\beta} = 1/2(\partial u_\alpha / \partial x_\beta + \partial u_\beta / \partial x_\alpha)$, from (1) one obtains

$$k_1 = \omega \sqrt{\varrho} \left\{ B(\omega) \left(\sqrt{1 + D(\omega)} + 1 \right) \right\}^{1/2}, \quad (49)$$

$$k_2 = \omega \sqrt{\varrho} \left\{ B(\omega) \left(\sqrt{1 + D(\omega)} - 1 \right) \right\}^{1/2},$$

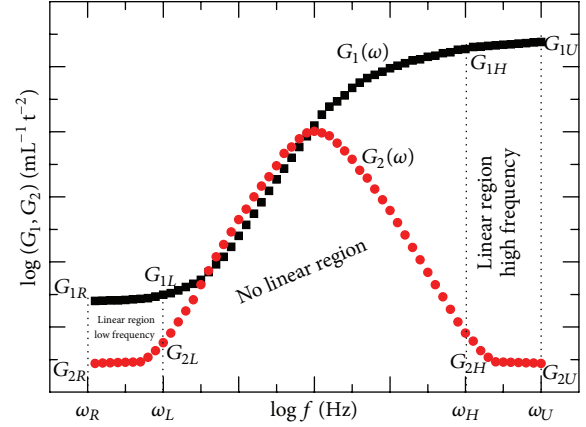


FIGURE 1: Generic storage and loss moduli.

where

$$B(\omega) = \frac{R_{(d)0}^{(\tau)} R_{(d)0}^{(\varepsilon)} + \omega^2 (R_{(d)1}^{(\varepsilon)} - R_{(d)0}^{(\tau)} R_{(d)2}^{(\varepsilon)})}{(R_{(d)0}^{(\varepsilon)} - \omega^2 R_{(d)2}^{(\varepsilon)})^2 + (\omega R_{(d)1}^{(\varepsilon)})^2}, \quad (50)$$

$$B(\omega) = \frac{\omega^2 (R_{(d)0}^{(\varepsilon)} - R_{(d)1}^{(\varepsilon)} R_{(d)0}^{(\tau)} - \omega^2 R_{(d)2}^{(\varepsilon)})^2}{\{R_{(d)0}^{(\tau)} R_{(d)0}^{(\varepsilon)} - \omega^2 (R_{(d)1}^{(\varepsilon)} - R_{(d)0}^{(\tau)} R_{(d)2}^{(\varepsilon)})\}^2}.$$

The complex shear velocity is [14]

$$\nu_c = \frac{1}{\nu_s} + \frac{k_2}{i\omega} = \frac{G_1(\omega) + iG_2(\omega)}{\varrho}, \quad (51)$$

where $0 \leq s \leq 257$, $G_1(\omega)$ (storage modulus), and $G_2(\omega)$ (loss modulus) are, respectively, linked with the nondissipative and dissipative phenomena, and their experimental curves are plotted in Figure 1.

From (47) to (50), the following relations are obtained:

$$k_1 = \frac{\omega \sqrt{(\varrho G_1/2) \left(\sqrt{1 + (G_2/G_1)^2} + 1 \right)}}{G_1 \sqrt{1 + (G_2/G_1)^2}}, \quad (52)$$

$$k_2 = \frac{\omega \sqrt{(\varrho G_1/2) \left(\sqrt{1 + (G_2/G_1)^2} - 1 \right)}}{G_1 \sqrt{1 + (G_2/G_1)^2}}.$$

Let us consider the range of high frequency $\omega_H \leq \omega \leq \omega_U$ and $\omega \tau \gg 1$ (of order 10^2) so that no relaxation phenomena occur (see Figure 1).

By putting

$$G_1 = G_{1H} 1,001^s$$

$$G_2 = G_{2H} 1,001^{-s}, \quad (53)$$

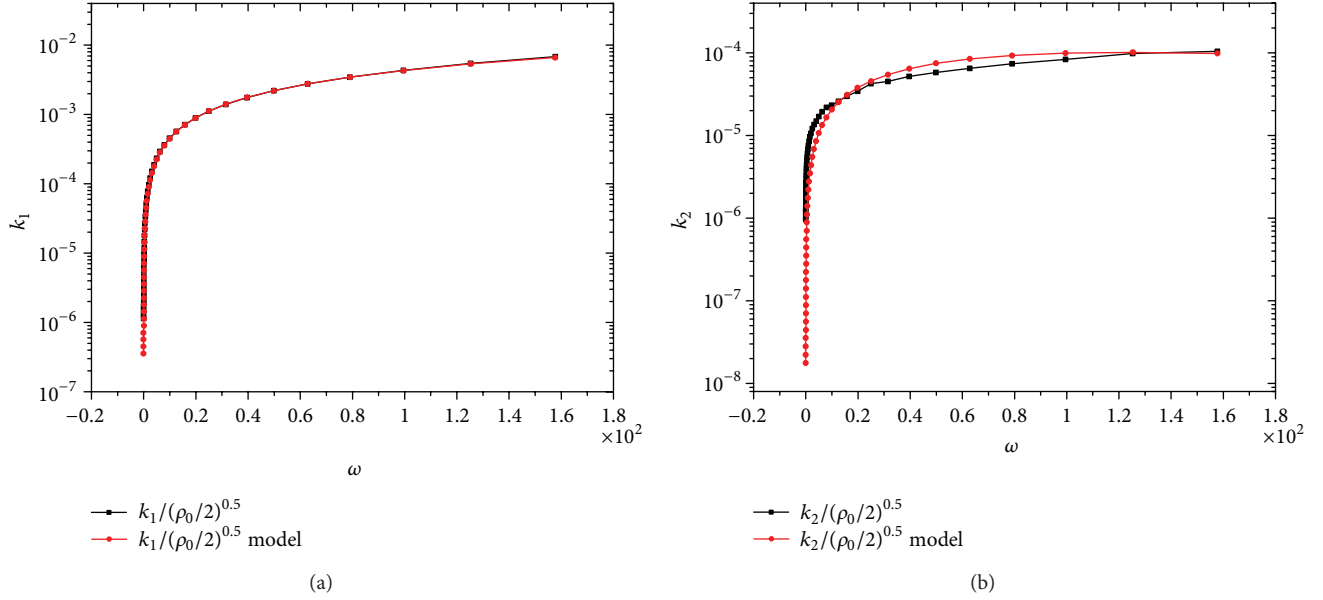


FIGURE 2: k_1 and k_2 for Polyisobutylene: (M.w. 10^6 g/mol; $T_0 = 273$ K) the experimental curves (in black) and the theoretical curves (in red) obtained by our model.

where $G_{1H} = G_1(\omega_H)$ and $G_{2H} = G_2(\omega_H)$, (52) becomes

$$k_1 = \omega \sqrt{\frac{\rho}{2}} \sqrt{\frac{\sqrt{(G_{1H})^2 1.001^{2s} + (G_{2H})^2} + G_{1H} 1.001^s}{(G_{1H})^2 1.001^{2s} + (G_{2H})^2}},$$

$$k_2 = \omega \sqrt{\frac{\rho}{2}} \sqrt{\frac{\sqrt{(G_{1H})^2 1.001^{2s} + (G_{2H})^2} - G_{1H} 1.001^s}{(G_{1H})^2 1.001^{2s} + (G_{2H})^2}}. \quad (54)$$

For the Polyisobutylene we have [15] the characteristic values which are

$$\sigma = 10^{-7} \text{ sec.}, \quad \omega_H = 3.2 \cdot 10^{14} \text{ Hz},$$

$$\omega_U = 6 \cdot 10^{14} \text{ Hz}, \quad (55)$$

$$G_{1U} = 2.4 \cdot 10^9 \text{ Pa}, \quad G_{2U} = 2.75 \cdot 10^4 \text{ Pa},$$

and the graphics confirm (see Figure 2) with experimental data the validity of the model proposed for viscoelastic phenomena in continuous media.

6. Conclusions

From the viewpoint of nonholonomic irreversible thermodynamics, it is shown that the best specific entropy is an harmonic function in a 27-dimensional manifold. The differential equations of geodetics are obtained and the corresponding curves are explicitly computed. In the linearized theory it is shown that the theoretical results are in agreement with the experimental data in the case of polymeric material (Polyisobutylene) (Figure 2).

Conflict of Interests

The authors declare that there is no conflicts of interests regarding the publication of this paper.

References

- [1] C. Caratheodory, *Untersuchungen über die Grundlagen der Thermodynamik*, vol. 2, Gesammelte Mathematische Werke, Munich, Germany, 1995.
- [2] R. Hermann, *Geometry, Physics, and Systems*, vol. 18, Marcel Dekker, New York, NY, USA, 1973.
- [3] R. Mrugała, "Submanifolds in the thermodynamic phase space," *Reports on Mathematical Physics*, vol. 21, no. 2, pp. 197–203, 1985.
- [4] C. Udriște, O. Dogaru, and I. Țevy, *Extrema with Nonholonomic Constraints: Selected Papers*, vol. 4 of *Monographs and Textbooks*, Geometry Balkan Press, Bucharest, Romania, 2002, Selected papers.
- [5] C. Stamin and C. Udriște, "Nonholonomic geometry of gibbs contact structure," *UPB Scientific Bulletin A*, vol. 72, no. 1, pp. 153–170, 2010.
- [6] J. Merker and M. Krüger, "On a variational principle in thermodynamics," *Continuum Mechanics and Thermodynamics*, 2012.
- [7] G. D. C. Kuiken, *Thermodynamics of Irreversible to Diffusion and Rheology*, Wiley Tutorial Series in Theoretical Chemistry, John Wiley & Sons, Chichester, UK, 1994.
- [8] G. A. Kluitenberg and V. Ciancio, "On linear dynamical equations of state for isotropic media—I: general formalism," *Physica A*, vol. 93, no. 1-2, pp. 273–286, 1978.
- [9] V. Ciancio and G. A. Kluitenberg, "On linear dynamical equations of state for isotropic media—II. Some cases of special interest," *Physica A*, vol. 99, no. 3, pp. 592–600, 1979.
- [10] V. Ciancio, *An Introduction to Thermomechanical of Continuous Media. Rheology*, vol. 10 of *Monographs and Textbooks*, Geometry Balkan Press, Bucharest, Romania, 2009.

- [11] A. Ciancio, "An approximate evaluation of the phenomenological and state coefficients for visco-anelastic media with memory," *UPB Scientific Bulletin A*, vol. 73, no. 4, pp. 3–14, 2011.
- [12] N. G. McCrum, B. F. Read, and G. Williams, *Anelastic and Dielectric Effects in Polymeric Solids*, John Wiley & Sons, London, UK, 1967.
- [13] P. Hedvig, *Dielectric Spectroscopy of Polymers*, Adam Hilger, Bristol, UK, 1977.
- [14] W. Graham, *Comprehensive Polymer Science: the Synthesis, Characterization, Reactions & Applications of Polymers*, vol. 2, chapter 16, edited by G. Allen and J.C. Bevington, Pergamon Press, 1989.
- [15] I. M. Ward and D. W. Hadley, *Mechanical Properties of Solid Polymers*, John Wiley & Sons, 1993.

Research Article

Identifying Vulnerable Nodes of Complex Networks in Cascading Failures Induced by Node-Based Attacks

Shudong Li,^{1,2} Lixiang Li,³ Yan Jia,² Xinran Liu,⁴ and Yixian Yang³

¹ College of Mathematics and Information Science, Shandong Institute of Business and Technology, Shandong, Yantai 264005, China

² School of Computer Science, National University of Defense Technology, Hunan, Changsha 410073, China

³ Information Security Center, Beijing University of Posts and Telecommunications, P.O. Box 145, Beijing 100876, China

⁴ National Computer Network Emergency Response Technical Team/Coordination Center, Beijing 100029, China

Correspondence should be addressed to Lixiang Li; li.lixiang2006@163.com

Received 18 July 2013; Accepted 7 August 2013

Academic Editor: Ming Li

Copyright © 2013 Shudong Li et al. This is an open access article distributed under the Creative Commons Attribution License, which permits unrestricted use, distribution, and reproduction in any medium, provided the original work is properly cited.

In the research on network security, distinguishing the vulnerable components of networks is very important for protecting infrastructures systems. Here, we probe how to identify the vulnerable nodes of complex networks in cascading failures, which was ignored before. Concerned with random attack (RA) and highest load attack (HL) on nodes, we model cascading dynamics of complex networks. Then, we introduce four kinds of weighting methods to characterize the nodes of networks including Barabási-Albert scale-free networks (SF), Watts-Strogatz small-world networks (WS), Erdos-Renyi random networks (ER), and two real-world networks. The simulations show that, for SF networks under HL attack, the nodes with small value of the fourth kind of weight are the most vulnerable and the ones with small value of the third weight are also vulnerable. Also, the real-world autonomous system with power-law distribution verifies these findings. Moreover, for WS and ER networks under both RA and HL attack, when the nodes have low tolerant ability, the ones with small value of the fourth kind of weight are more vulnerable and also the ones with high degree are easier to break down. The results give us important theoretical basis for digging the potential safety loophole and making protection strategy.

1. Introduction

In modern society, people's life depends on the infrastructure networks more and more, such as the power grid, Internet, transportation networks and the financial networks, and so forth. The overall efficiency of these network systems is being increased, while the internal connections and the dynamical characteristics within the networks are becoming more close and complex, respectively. These behaviours make the networks more vulnerable and increase the possibility of system crash. Especially, with the improvement of network-based degree, a small incident, through a cascade of reaction, can lead to the collapse of the whole network systems and a great number of economic loss. The typical example is the accident that emerged in the power grid of North America in 2003 [1]. The fault of three extra-high voltage transmission

lines leads to a chain reaction in power system, spreads to the eight states in the northeast U.S., affects about 50 million people, and finally results in the economic loss of 4 billion to 10 billion. Another example is the electrical collapse that occurred in Italy [2], which has seriously influenced the operation of the Internet.

These large-scale accidents have threatened the network safety and attracted considerable attentions of scientific researchers [3]. On the one hand, The robustness and vulnerability of topological structure of complex networks are investigated carefully. Some indexes are proposed to measure how robust or vulnerable the complex networks are under different attacks [4–6]. The structural vulnerability of the important real-world networks is also probed, including Italian electrical network [7], the US power grid [8], the European grid [9], and other electrical systems [10] and

the robustness of computer networks under attacks [11], the stability analysis for the uncertain systems [12–14], and the cyber-physical networking systems [15].

On the other hand, there exist the physical flows (also defined as load) in real-world networks, such as the electric stream in power grids, the data transmitted in communication networks, and the cars in transportation networks. Also, the physical load is dynamical. The fault of some local components (nodes or edges) always leads to the redistribution of load over the whole networks. Then, the overloaded components will fail as the new load on them exceeds their capacity (the maximum load). Therefore, the new redistribution of load over the whole networks will begin and lead to the cascade over the networks. This evolving procedure is called “cascading failure” which emerged locally and always resulted in the whole collapse of networks. Therefore, the cascading failures of complex networks have been one of the hottest topics in network safety. Induced by random breakdown and intentional attack, Motter explored the condition of cascading failures occurring in complex networks [16]. The similar procedure of load redistribution included the works [17–20]. For the local redistribution of load on nodes or edges, the cascading dynamics due to node overloaded breakdown in US power grid [21] and the edge overloaded breakdown in scale-free networks [22] are investigated, respectively. Also, the condition of cascading failures in weighted networks under edge-based attack is analyzed carefully [23], where the redistribution of load on edges is similar to the process [22]. Then, the influence of different definitions of load on cascading failures in weighted complex networks is probed to reduce the possibility of cascading failures [24]. The features and time characteristics shown in cascading failures are revealed [25]. In addition, recently, considering that the networks in real world are interdependent and internally connected, the cascading propagation in the interdependent networks is investigated [26–29] and the robustness and critical effect of networks are also explored carefully [30, 31].

All the previous researches mainly focus on the structural vulnerability or the cascading dynamics of the integral complex networks. However, in the cascading failures caused by overloaded breakdown, the following important problems have not been considered. What features do the nodes easy to break down or crash have? How should we describe the characteristics of the congested node in complex networks? These problems are the correlations between the vulnerability of nodes and the cascading failures in complex networks. We argue that, by exploring this problem, we are able to identify the vulnerable nodes, analyze the potential safety hazard in networks, and find the bottlenecks in the dynamical change of network “flows”. Finally, it can provide the important theoretical basis for protecting complex networks and improving the robustness of real-world networks.

Here, this paper explores the correlations between the vulnerability of nodes and the cascading failures in complex networks. Firstly, by assigning the load on nodes, we model the cascading dynamics of complex networks induced by random attack and intentional attack on nodes. Secondly, we introduce four kinds of weighting methods to describe the characteristics of the nodes in complex networks including

BA scale-free networks (SF), WS small-world networks (WS), ER random networks (ER), and two real-world networks (autonomous system network and US airport network). Finally, in order to identify the features of the vulnerable nodes in complex networks, we numerically computed the ratio of the failed nodes with four kinds of weights less than their respective average weights to the total failed ones in networks. As a result, we find that, for SF network under intentional attack, the ratio of the failed nodes with small value of the fourth kind of weight defined here is the highest. The autonomous system network with power-law distribution also shows similarity to SF network. It reveals that the nodes with small value of the fourth kind of weight defined in this work are more vulnerable. Moreover, for the WS small-world network and ER random network, under both random and intentional attack, when the tolerance ability of nodes is low, the ratio of the failed nodes with small value of the fourth kind of weight is higher, and, at the same time, the ratio of the failed ones with high degree is also higher. It means that the nodes with smaller value of the fourth kind of weight and large degree are vulnerable and the nodes with large degree are also vulnerable.

The rest of this paper is organized as follows. Section 2 develops the model of cascading dynamics of complex networks induced by random attack (RA) and highest load attack (HL) on node. In Section 3, we introduce four kinds of weighting methods to characterize the nodes in complex networks in order to distinguish them. In Section 4, we describe the studied complex networks including BA scale-free network, WS small-world networks, ER random network, and two real-world networks. In Section 5, we simulate and analyze the characteristics of the failed nodes of complex networks in cascading failures. Section 6 summarizes the most important contribution of this paper and points out the meaning of this work.

2. Modelling the Cascading Failures in Complex Networks

In this section, we will model the cascading dynamics of complex networks under node-based attacks. For a general undirected network comprising of N nodes, its adjacent matrix is defined as $A = (a_{ij})_{N \times N}$, where $a_{ij} = 1$ if the node i links to node j ; otherwise, $a_{ij} = 0$. Usually, modelling cascading dynamics of complex networks is based on the following three key points [19–23]: the definition of load on node, the relationship between the load and the capacity, and the evolving procedure of cascading failures.

- (1) The definition of load on node: usually, the physical flows (data packets, energy, etc.) are transmitted in many networks according to the shortest path routing strategy [1, 3, 16, 17]. For a given pair of nodes (a, b) , the physical flows are exchanged and transmitted along the shortest paths connecting them; maybe there exist some shortest paths through node i . In this case, it is natural to regard the total number of shortest paths passing through the node i between any pair of nodes in a network as the load on node i . Therefore,

we define $L_i(t)$ as the load on node i , where $L_i(t)$ is the number of the shortest paths passing through node i at some time t after attacks ($t = 0$ means the initial load $L_i(0)$ before attack).

- (2) The relationship between the load and the capacity: usually, there is some maximum load (the maximum capacity) that node i can handle. So, we assume that the maximum load C_i on node i is proportional to its initial load $L_i(0)$; namely,

$$C_i = (1 + \alpha) L_i(0), \quad \forall i, \quad (1)$$

where the constant $0 \leq \alpha \leq 1$ is the tolerance parameter. The bigger α means the higher capacity of node i and then the higher ability against failures. It is a rational definition in the design of real-world networks including power grids and Internet because the capacity of the components (nodes or links) in these networks is always limited by the cost.

- (3) The evolving procedure of cascading failures: beginning with the removal of some nodes in networks, the load on other nodes will change and be redistributed over the whole networks. At some time t , the node j will fail if the new load $L_j(t)$ on j exceeds its capacity C_j . This will cause the new redistribution of load over the networks. This process is iterated until there is no node exceeding their capacity. At this time, the iterative process can be regarded as being completed. This iterative process is called “cascading failures” in complex networks, which is described in Figure 1.

Here, we consider two kinds of attack strategies.

- (1) Random attack (RA): we choose some proportion of nodes randomly and then remove them from the networks; here we assume the proportion $\rho = 0.01$. This attack mainly simulates the case of complex networks subject to some random breakdown, such as the natural disasters, misoperations and random disturbances, and so forth.
- (2) Highest load attack (HL): first, we descend the order of nodes according to the initial load $L_i(0)$ and then remove some proportion of nodes with the highest initial load; here, the proportion $\rho = 0.01$. This attack simulates the case of the intentional attack.

3. The Weighting Methods of Nodes in Complex Networks

In order to identify the vulnerable nodes of complex networks in cascading failures, in this paper, we introduce four kinds of weighting methods $w_i^{(1)}$, $w_i^{(2)}$, $w_i^{(3)}$, and $w_i^{(4)}$ to describe the characteristics of nodes in complex networks. These quantities can distinguish the failed nodes in cascading failures.

(1) *The Weighting Method $w_i^{(1)}$* . Considering that we assume the load (physical flows) is transmitted according to the shortest path strategy, while the initial load $L_i(0)$ of node i

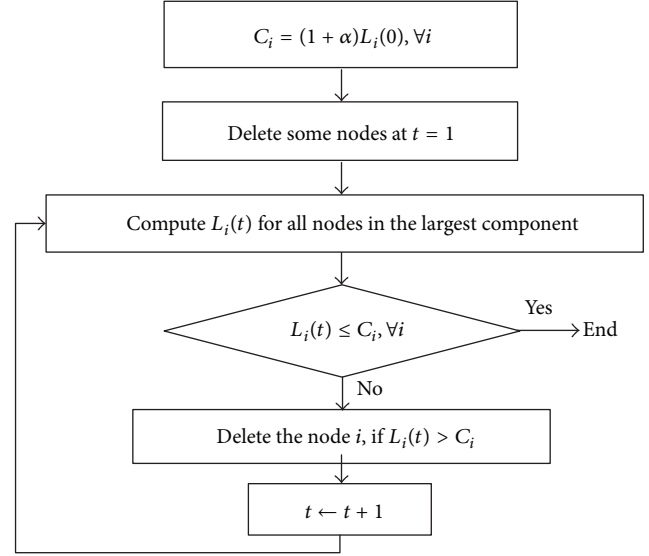


FIGURE 1: The iterative process of cascading failures in complex networks.

is the number of the shortest paths, thus the initial load can describe the characteristic of node. Here, we define the first weighting method $w_i^{(1)}$ as

$$w_i^{(1)} = L_i(0). \quad (2)$$

(2) *The Weighting Method $w_i^{(2)}$* . In the research of complex networks, the degree k_i of node i is always used to describe its feature, which can measure the importance of node in complex networks. Usually, the node with higher degree means higher importance, and it will become the hubs in networks. Thus, we use it to describe the characteristic of node i ; namely,

$$w_i^{(2)} = k_i = \sum_{j \in \Gamma_i} a_{ij}, \quad (3)$$

where Γ_i is the set of the neighbors of node i .

(3) *The Weighting Method $w_i^{(3)}$* . In the investigation of cascading dynamics, the product $(k_i k_j)^\theta$ of the degrees k_i and k_j of the two end nodes of an edge e_{ij} can measure the weight of an edge e_{ij} . Wang shows that the networks with $\theta = 1$ have the strongest robustness against cascading failures [23]. Thus, in this paper, we define the third weighting method as:

$$w_i^{(3)} = \sum_{j \in \Gamma_i} (k_i k_j)^\theta = k_i^\theta \sum_{j \in \Gamma_i} k_j^\theta, \quad (4)$$

where Γ_i is the set of the neighbors of node i , and here we assume the parameter $\theta = 1$.

Furthermore, according to the theory of the degree of networks and probability [32], as $\theta = 1$, the second term on the right hand side of (4) will become

$$\sum_{j \in \Gamma_i} k_j = k_i \sum_{k'=k_{\min}}^{k_{\max}} P(k' | k_i) k', \quad (5)$$

where k_{\min} and k_{\max} are the minimum degree and the maximum degree in a network, respectively. $P(k' | k_i)$ is the conditional probability that the node with degree k_i links to a neighbouring node with degree k' , and this conditional probability satisfies the normalized and equilibrium conditions:

$$\sum_{k'} P(k' | k_i) = 1, \quad (6)$$

$$k_i P(k' | k_i) P(k_i) = k' P(k_i | k') P(k').$$

Since the BA scale-free networks, WS small-world networks, and ER random networks have no degree-degree correlation [33], according to the conditions in (6), one can get

$$P(k' | k_i) = \frac{k' P(k')}{\langle k \rangle}, \quad (7)$$

where $\langle k \rangle$ is the average degree of networks. Therefore, inserting (7) back into (5), we get

$$\sum_{j \in \Gamma_i} k_j = k_i \sum_{k'=k_{\min}}^{k_{\max}} \frac{k' P(k')}{\langle k \rangle} = \frac{k_i \langle k^2 \rangle}{\langle k \rangle}. \quad (8)$$

Now, finally (4) is simplified as

$$w_i^{(3)} = \frac{k_i^2 \langle k^2 \rangle}{\langle k \rangle}. \quad (9)$$

One can see that the weighting method $w_i^{(3)}$ is different with $w_i^{(2)}$ obviously.

(4) *The Weighing Method $w_i^{(4)}$* . Here, we introduce the fourth kind of weighting method based on node centrality betweenness. The link is always important as the two nodes of its end are important in many real-world networks. For example, the packet has always been transmitted along the links with the important chosen nodes, while the node betweenness centrality is used to describe the importance of nodes in networks [34]. Considering this intuition, usually, the product $(B_i B_j)^\theta$ is used to measure the weight of the edge e_{ij} [24], where B_i and B_j are the node betweenness of node i and j , respectively. The node betweenness of node i is defined as

$$B_i = \sum_{a \neq b} \frac{\sigma_{ab}(i)}{\sigma_{ab}}, \quad (10)$$

where σ_{ab} is the number of the shortest paths between node a and b . $\sigma_{ab}(i)$ is the number of the shortest paths passing through the node i in the shortest paths σ_{ab} .

Therefore, we define the fourth kind of weighting method $w_i^{(4)}$ as the follows:

$$w_i^{(4)} = \sum_{j \in \Gamma_i} (B_i B_j)^\theta = B_i^\theta \sum_{j \in \Gamma_i} B_j^\theta, \quad (11)$$

where Γ_i is the set of the neighbors of node i , and here we assume the parameter $\theta = 1$.

Using Bayes' rules [32], (11) can become

$$w_i^{(4)} = B_i \sum_{B'=B_{\min}}^{B_{\max}} k_i P(B' | B_i) B', \quad (12)$$

where B_{\min} and B_{\max} are the minimum and the maximum node betweenness in networks, respectively. $P(B' | B_i)$ is the conditional probability that a node with node betweenness centrality B_i links to the node with node betweenness centrality B' .

Considering that it has been shown that small-world networks do not show betweenness-betweenness correlations [24], therefore, we can assume $P(B' | B_i) = P(B')$. Then, (12) can be simplified as

$$w_i^{(4)} = B_i k_i \sum_{B'=B_{\min}}^{B_{\max}} P(B') B' = B_i k_i \langle B \rangle, \quad (13)$$

where $\langle B \rangle$ is the average node betweenness in networks.

Now, it is obvious that the four kinds of weighting methods of node introduced here can describe the characteristics of nodes and distinguish the nodes in network.

4. The Studied Complex Networks

In this paper, to investigate the vulnerable nodes in networks subject to cascading failures, we mainly take the following typical complex networks into account: Barabasi-Albert scale-free networks (SF), Watts-Strogatz small-world networks (WS), and ER random networks (ER).

- (1) Scale-free networks (SF): SF network model in this paper is generated according to the two rules: growth and preferential attachment [35]. The degree distribution of the generated SF network obeys the power law distribution $P(k) \sim k^{-\gamma}$ ($\gamma = 3$) and the mean degree $\langle k \rangle \approx 4$.
- (2) WS small-world networks (WS): here, according to Watts-Strogatz model [36], we generate the small-world network by changing the rewiring probability p . We mainly consider the two cases with the rewiring probability $P = 0.1$ and $P = 0.5$. It should be noticed that the rewiring probability $P = 1$ means that the WS network will become a completely random network.
- (3) ER random networks (ER): the random network model studied is generated according to the rules in [37], where we control the average degree $\langle k \rangle \approx 4$.

Also, in order to compare with the network models, we consider two real-world networks: the autonomous system network (AS) and US airport network (US airport).

- (4) The autonomous system network (AS): from the AS level topology of Internet, the Internet can be seen as a network comprising of routers. Usually, the data is transmitted between routers according

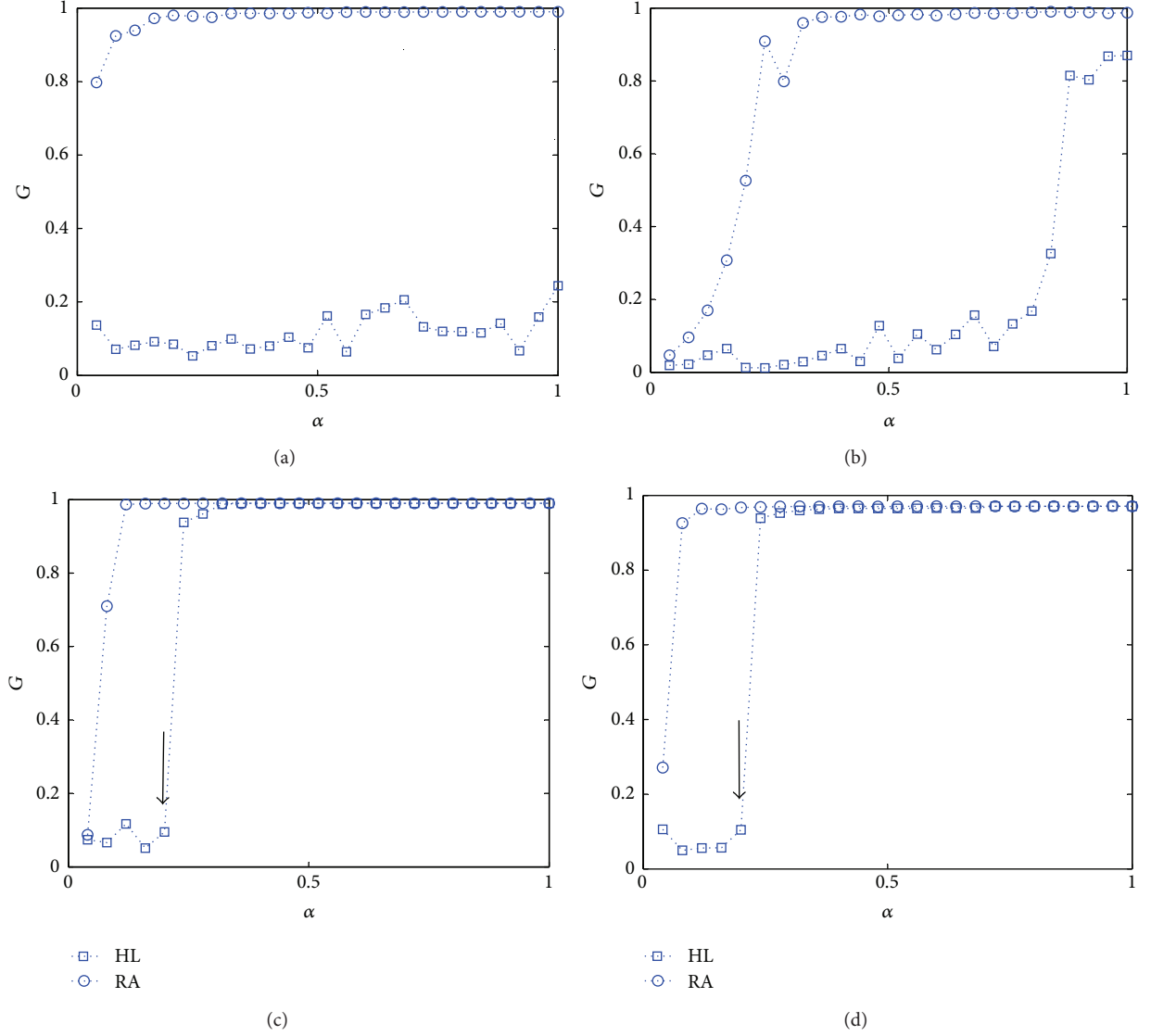


FIGURE 2: Under RA and HL attacks, the relative size of nodes in the largest component G as a function of α for (a) SF network, (b) WS small-world network with the rewiring probability $P = 0.1$, (c) WS network with $P = 0.5$, and (d) ER random network. The simulations under RA attack are averaged over 20 times.

to BGP protocols. Thus, the routers (as nodes) and links construct the autonomous system network (AS) [38]. Here, we take the AS network with 1470 nodes, for example, and the mean degree $\langle k \rangle \approx 4.3$. By computation, we find that the degree of distribution of AS network clearly obeys power-law distribution: $P(k) \sim k^{-\gamma}$, where the index $\gamma \approx 0.005$.

- (5) US airport network: as an example of transportation networks, we study the famous USA airport network with 500 airports and 2980 links [39]. The mean degree $\langle k \rangle \approx 11.9$.

5. The Simulation and Analysis

Now, in this section, concerned with two kinds of node-based attacks, we will investigate how to identify the vulnerable

nodes of complex networks subject to cascading failures. The studied networks include SF, WS, and ER complex networks models and two real-world networks.

Firstly, we use the relative size of nodes in the largest component of network (G) to quantify the integral robustness of complex networks under cascading failures. The metric G is defined as

$$G = \frac{N'}{N}, \quad (14)$$

where N' and N are the number of nodes in the largest component after attacks and the total number of nodes in network, respectively.

Obviously, the metric G can be seen as a function of the tolerance parameter α and $0 \leq G \leq 1$. Also, it should be noticed that, with the higher G , the network maintains higher

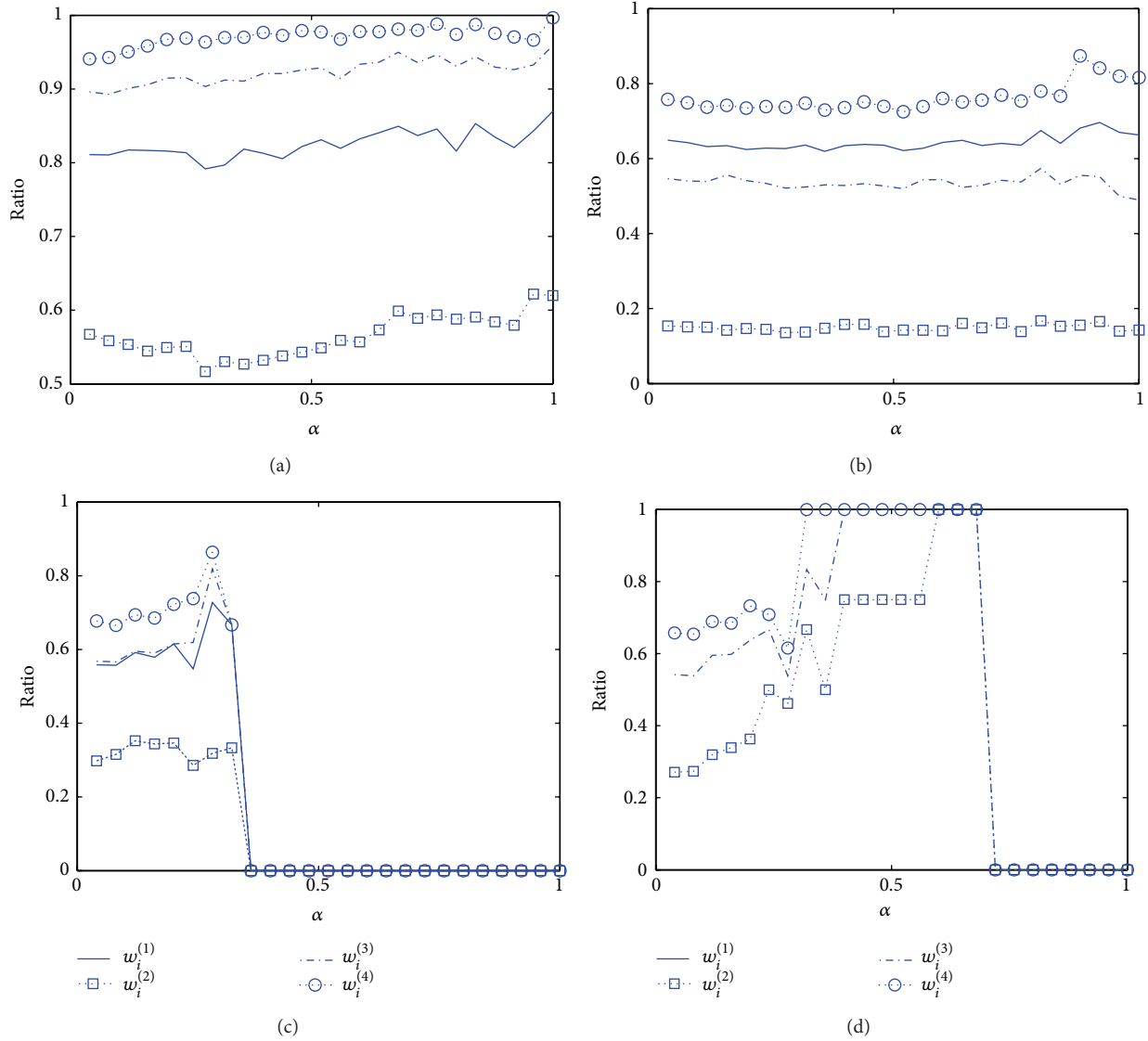


FIGURE 3: Under HL attack, the ratio for different weighting methods as a function of α for (a) SF network, (b) WS small-world network with the rewiring probability $P = 0.1$, (c) WS network with $P = 0.5$, and (d) ER random network.

connectivity and shows higher robustness against cascading failures.

Secondly, to identify the features of the vulnerable nodes in complex networks, we numerically computed the ratio of the failed nodes with four kinds of weights less than their respective average weights to the total of the failed ones in networks when the iterative process of complex networks in Figure 1 is stopped (at this time, the cascading failures are completed); namely,

$$\text{ratio} = \frac{\sum_{t: w_i^{(n)} < \overline{w^{(n)}}} as(t)}{\sum_t as(t)}, \quad n = 1, 2, 3, 4, \quad (15)$$

where $\overline{w^{(n)}}$ is the average value of the n th kind of weight defined in Section 3 in network ($n = 1, 2, 3, 4$). $as(t)$ is the number of failed nodes at time step t after attacks in network.

One can see that the ratio in (15) can mainly distinguish the characteristics of the failed nodes in complex networks.

5.1. The Analysis of Complex Networks Models. In this part, induced by random attack (RA) and the highest-load attack (HL), we mainly focus on analyzing the integral robustness and identifying the vulnerable nodes of three kinds of typical complex networks models: scale-free networks (SF), WS small-world networks (WS), and ER random networks (ER).

- (1) From the relative size of nodes in the largest component G , as shown in Figure 2, being subject to intentional attack (HL), SF network and WS small-world network with $P = 0.1$ are more vulnerable, while WS network with $P = 0.5$ and ER random network are more robust. being subject to random attack (RA), SF network model is more robust. It means that SF

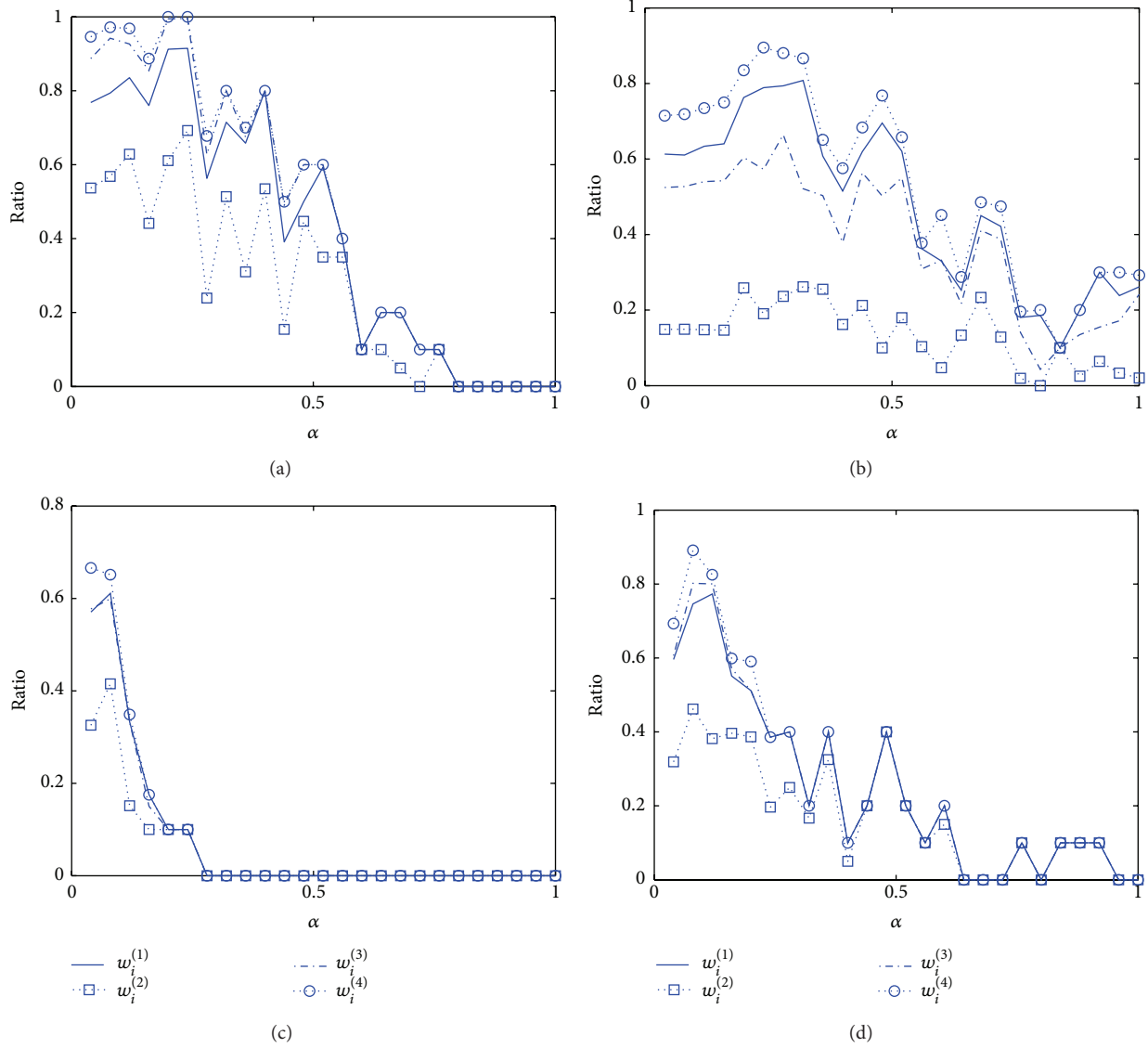


FIGURE 4: Under RA attack, the ratio for different weighting methods as a function of α for (a) SF network, (b) WS small-world network with the rewiring probability $P = 0.1$, (c) WS network with $P = 0.5$, and (d) ER random network. The simulations under RA attack are averaged over 20 times.

network models show the dual characteristics of both robustness and vulnerability.

- (2) From the ratio in (15), under HL attack, as shown in Figure 3, for SF network models, the ratio of the failed nodes with small weighting value to the total failed ones is always more than 50%. Especially, we should notice that the highest ratio is the one of the failed nodes with small $w_i^{(4)}$ ($w_i^{(4)} < \overline{w^{(4)}}$) and it is always more than 90%. In addition, the second highest is the ratio of the failed ones with small $w_i^{(3)}$. These results reveal that, under intentional attack, the nodes with small $w_i^{(4)}$ are more vulnerable.

For WS small-world network, from Figure 3(b), under HL attack, as the rewiring probability $P = 0.1$, the ratio of the failed nodes with small $w_i^{(4)}$ is almost

more than 80% and also the ratio of the failed nodes with small $w_i^{(2)}$ is less than 20% (it implies that the ratio of the failed nodes with big $w_i^{(2)}$ is more than 80%). At the same time, for $P = 0.5$, since $\alpha = 0.2$ is the transition point of the connectivity of WS network from low to high (see the arrow in Figure 2(c)) and there are few failed nodes when $\alpha > 0.2$, here, we mainly focus on the case of $\alpha < 0.2$. As shown in Figure 3(c), for $\alpha < 0.2$, the ratio of the failed nodes with small $w_i^{(4)}$ is more than 70%. Also, the ratio of the failed nodes with small $w_i^{(2)}$ is less than 40%. Now, obviously, we can see that, under intentional attack, for WS small-world network, the nodes with small $w_i^{(4)}$ are more vulnerable and also the ones with big $w_i^{(2)}$ (namely, the nodes with high degree) are easy to break down.

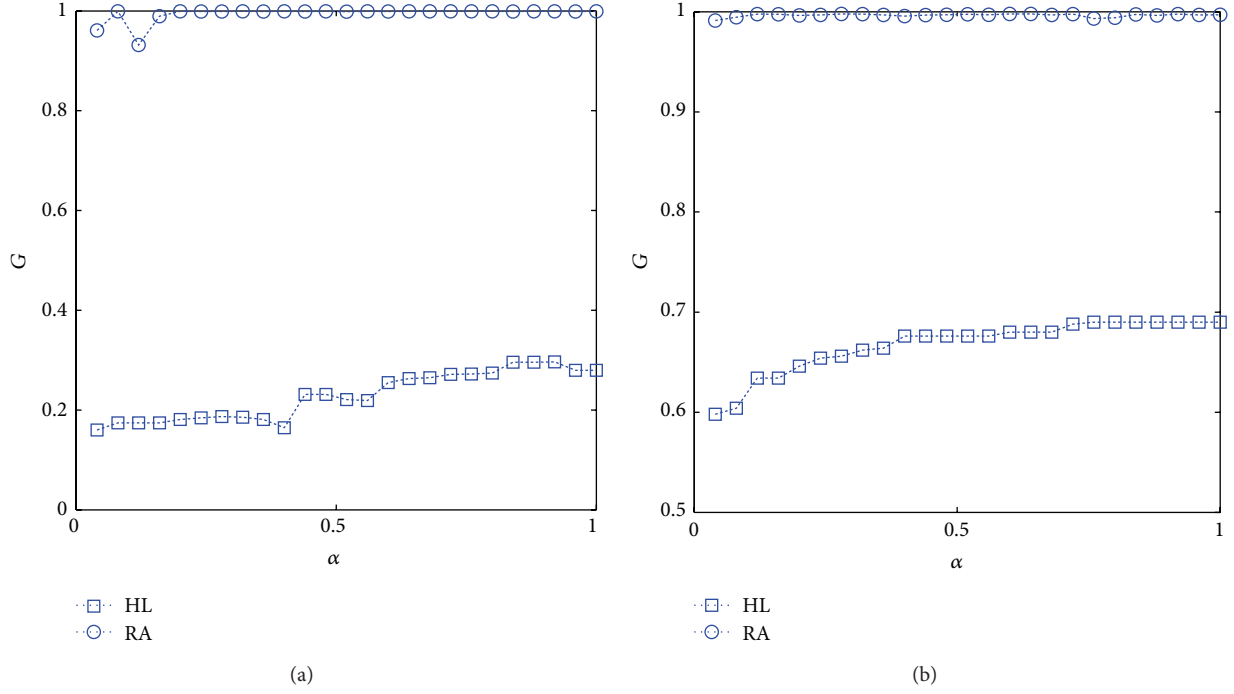


FIGURE 5: Under RA and HL attacks, the relative size of nodes in the largest component G as a function of α for (a) the autonomous system network (AS) and (b) US airport network. The simulations under RA attack are averaged over 20 times.

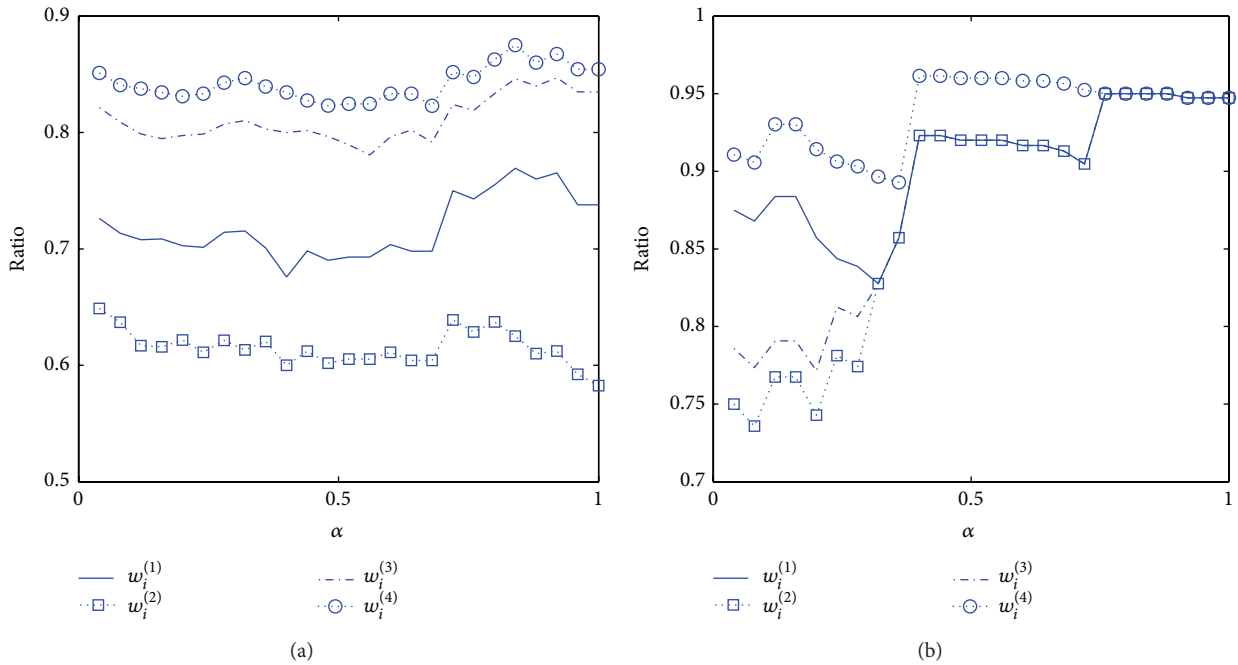


FIGURE 6: Under HL attack, the ratio for different weighting methods as a function of α for (a) the autonomous system network (AS) and (b) US airport network.

For ER random network under HL attack, as $\alpha < 0.2$ ($\alpha = 0.2$ is the turning point of the connectivity from low to high; see the arrow in Figure 2(d)), ER random network shows similarity to WS small-world network; namely, the nodes with small $w_i^{(4)}$ are more vulnerable and also the ones with big $w_i^{(2)}$ are easy to break down.

(3) Under RA attack, there are the failed nodes only for small α (see the curves in Figure 2); thus, we only consider the case of small α . Figure 4 shows that most of the failed nodes in SF network are still the ones with small $w_i^{(4)}$. While WS small-world network and ER random network show similarity to their case under

HL attack; namely, the nodes with small $w_i^{(4)}$ are more vulnerable and also the ones with big $w_i^{(2)}$ (the nodes with high degree) are easy to break down.

5.2. The Analysis of Real-World Networks. In order to compare with the simulations of the network models, we also analyze two real-world networks: the autonomous system network (AS) and US airport network.

As shown in Figure 5, both AS network and US airport network are very robust under RA attack and vulnerable under HL attack. Especially, AS network is more vulnerable under HL attack. Then, in the following discussion of this part, we only consider the case under HL attack because of their strong robustness against random disturbance.

From Figure 6(a), it is obvious that AS network with scale-free characteristics shows similarity to SF network model, and also the ratio of the failed nodes with small weighting values to the total failed ones is always more than 50%. Especially, the ratio of the failed nodes with small $w_i^{(4)}$ ($w_i^{(4)} < \overline{w}^{(4)}$) is highest and always more than 80%. The second highest is the ratio of the failed ones with small $w_i^{(3)}$. It reveals that, for SF networks under intentional attack, the nodes with small $w_i^{(4)}$ are more vulnerable than other nodes and these nodes are easy to break down.

For US airport network, as shown in Figure 6(b), similarly, this ratio of the failed nodes with small $w_i^{(4)}$ is highest and it is more than 90%. Also, the nodes with small $w_i^{(4)}$ are more vulnerable under intentional attack.

6. Conclusions

In the research on cascading dynamics, finding and distinguishing the vulnerable nodes of networks are very important for the protection of infrastructures systems, but the traditional research on the vulnerability of complex networks has not considered this. This paper mainly probes the question of how to identify the vulnerable nodes of complex networks in cascading failures caused by the overload on nodes. We model the cascading dynamics of complex networks induced by deleting some proportion of nodes that are chosen randomly or intentionally. Then, four kinds of weighting methods of node are introduced to distinguish the failed nodes of complex networks, including BA scale-free networks, WS small-world networks, ER random networks, and two real-world networks. The main contributions of this paper are as follows.

- (1) For SF networks, under HL attack, the nodes with small $w_i^{(4)}$ are most vulnerable and the ones with small $w_i^{(3)}$ are also easy to break down. The simulation of the autonomous system network (AS) with power-law distribution also verifies our findings. However, the weight $w_i^{(4)}$ involved in computing the node betweenness needs to know the whole structure of networks. In fact, The complexity of computing node betweenness is high, especially for large-scale networks. While, computing the weight $w_i^{(3)}$ only needs

to know the local structure of networks. Therefore, we should pay attention to the nodes with small $w_i^{(3)}$ in distinguishing the vulnerable components of large networks. It should be pointed out that the recent research of Ercsey demonstrates that the local information can be used to approximately calculate the node betweenness of large-scale networks in order to reduce the complexity [40].

- (2) For WS small-world networks and ER random network, when the tolerance ability of node is low, no matter under RA attack or HL attack, the nodes with small $w_i^{(4)}$ are more vulnerable and also the ones with big $w_i^{(2)}$ are easier to break down.

The findings of this paper provide important theory basis for analyzing network security, mining the hidden potential risk of networks, and protecting various real-world networks with load assigned to nodes.

Acknowledgments

This work is supported by the National Natural Science Foundation of China (Grant nos. 61202362, 61121061, 61262057, 61372191, and 91124002), the 863 programs (Grant nos. 2012AA01A401, 2010AA-012505, and 2011AA010702), the State Key Development Program of Basic Research of China 973 (Grant nos. 2013CB329601 and 2011CB302600), the China Postdoctoral Science Foundation Programs (BS2013SF009, 2012m520114, and 2013T60037), and the Beijing Higher Education Young Elite Teacher Project.

References

- [1] A. E. Motter and Y.-C. Lai, "Cascade-based attacks on complex networks," *Physical Review E*, vol. 66, no. 6, Article ID 065102, 4 pages, 2002.
- [2] V. Rosato, L. Issacharoff, F. Tiriticco, S. Meloni, S. de Porcellinis, and R. Setola, "Modelling interdependent infrastructures using interacting dynamical models," *International Journal of Critical Infrastructures*, vol. 4, no. 1-2, pp. 63-79, 2008.
- [3] S. Boccaletti, V. Latora, Y. Moreno, M. Chavez, and D.-U. Hwang, "Complex networks: structure and dynamics," *Physics Reports*, vol. 424, no. 4-5, pp. 175-308, 2006.
- [4] S. Boccaletti, J. Buldú, R. Criado et al., "Multiscale vulnerability of complex networks," *Chaos*, vol. 17, no. 4, Article ID 043110, 2007.
- [5] I. Mishkovski, M. Biey, and L. Kocarev, "Vulnerability of complex networks," *Communications in Nonlinear Science and Numerical Simulation*, vol. 16, no. 1, pp. 341-349, 2011.
- [6] I. Petreska, I. Tomovski, E. Gutierrez, L. Kocarev, F. Bono, and K. Poljansek, "Application of modal analysis in assessing attack vulnerability of complex networks," *Communications in Nonlinear Science and Numerical Simulation*, vol. 15, no. 4, pp. 1008-1018, 2010.
- [7] P. Crucitti, V. Latora, and M. Marchiori, "A topological analysis of the Italian electric power grid," *Physica A*, vol. 338, no. 1-2, pp. 92-97, 2004.
- [8] E. Bompard, M. Masera, R. Napoli, and F. Xue, "Assessment of structural vulnerability for power grids by network performance

- based on complex networks,” in *Critical Information Infrastructure Security*, vol. 5508 of *Lecture Notes in Computer Science*, pp. 144–154, 2009.
- [9] R. V. Solé, M. Rosas-Casals, B. Corominas-Murtra, and S. Valverde, “Robustness of the European power grids under intentional attack,” *Physical Review E*, vol. 77, no. 2, Article ID 026102, 2008.
 - [10] E. Bompard, D. Wu, and F. Xue, “Structural vulnerability of power systems: a topological approach,” *Electric Power Systems Research*, vol. 81, no. 7, pp. 1334–1340, 2011.
 - [11] B. K. Mishra and A. K. Singh, “Two quarantine models on the attack of malicious objects in computer network,” *Mathematical Problems in Engineering*, vol. 2012, Article ID 407064, 13 pages, 2012.
 - [12] M. Hua, P. Cheng, J. Fei, J. Zhang, and J. Chen, “Network-based robust H_∞ filtering for the uncertain systems with sensor failures and noise disturbance,” *Mathematical Problems in Engineering*, vol. 2012, Article ID 945271, 19 pages, 2012.
 - [13] M. Li and W. Zhao, “On $1/f$ noise,” *Mathematical Problems in Engineering*, vol. 2012, Article ID 673648, 23 pages, 2012.
 - [14] M. Li, “Fractal time series—a tutorial review,” *Mathematical Problems in Engineering*, vol. 2010, Article ID 157264, 26 pages, 2010.
 - [15] M. Li and W. Zhao, “Visiting power laws in cyber-physical networking systems,” *Mathematical Problems in Engineering*, vol. 2012, Article ID 302786, 13 pages, 2012.
 - [16] A. E. Motter and Y.-C. Lai, “Cascade-based attacks on complex networks,” *Physical Review E*, vol. 66, no. 6, Article ID 065102, 4 pages, 2002.
 - [17] P. Crucitti, V. Latora, and M. Marchiori, “Model for cascading failures in complex networks,” *Physical Review E*, vol. 69, no. 4, Article ID 045104, 4 pages, 2004.
 - [18] H. J. Sun, H. Zhao, and J. J. Wu, “A robust matching model of capacity to defense cascading failure on complex networks,” *Physica A*, vol. 387, no. 25, pp. 6431–6435, 2008.
 - [19] Y. Xia, J. Fan, and D. Hill, “Cascading failure in Watts-Strogatz small-world networks,” *Physica A*, vol. 389, no. 6, pp. 1281–1285, 2010.
 - [20] M. Babaei, H. Ghassemieh, and M. Jalili, “Cascading failure tolerance of modular small-world networks,” *IEEE Transactions on Circuits and Systems II*, vol. 58, no. 8, pp. 527–531, 2011.
 - [21] J.-W. Wang and L.-L. Rong, “Cascade-based attack vulnerability on the US power grid,” *Safety Science*, vol. 47, no. 10, pp. 1332–1336, 2009.
 - [22] J.-W. Wang and L.-L. Rong, “Edge-based-attack induced cascading failures on scale-free networks,” *Physica A*, vol. 388, no. 8, pp. 1731–1737, 2009.
 - [23] W.-X. Wang and G. Chen, “Universal robustness characteristic of weighted networks against cascading failure,” *Physical Review E*, vol. 77, no. 2, Article ID 026101, 5 pages, 2008.
 - [24] B. Mirzasoleiman, M. Babaei, M. Jalili, and M. Safari, “Cascaded failures in weighted networks,” *Physical Review E*, vol. 84, no. 4, Article ID 046114, 8 pages, 2011.
 - [25] S. Li, L. Li, Y. Yang, and Q. Luo, “Revealing the process of edge-based-attack cascading failures,” *Nonlinear Dynamics*, vol. 69, no. 3, pp. 837–845, 2012.
 - [26] S. V. Buldyrev, R. Parshani, G. Paul, H. E. Stanley, and S. Havlin, “Catastrophic cascade of failures in interdependent networks,” *Nature*, vol. 464, no. 7291, pp. 1025–1028, 2010.
 - [27] X. Huang, J. Gao, S. V. Buldyrev, S. Havlin, and H. E. Stanley, “Robustness of interdependent networks under targeted attack,” *Physical Review E*, vol. 83, no. 6, Article ID 065101, 4 pages, 2011.
 - [28] J. Gao, S. V. Buldyrev, H. E. Stanley, and S. Havlin, “Networks formed from interdependent networks,” *Nature Physics*, vol. 8, no. 1, pp. 40–48, 2012.
 - [29] W. Li, A. Bashan, S. V. Buldyrev, H. E. Stanley, and S. Havlin, “Cascading failures in interdependent lattice networks: the critical role of the length of dependency links,” *Physical Review Letters*, vol. 108, no. 22, Article ID 228702, 5 pages, 2012.
 - [30] J. Gao, S. V. Buldyrev, S. Havlin, and H. E. Stanley, “Robustness of a network of networks,” *Physical Review Letters*, vol. 107, no. 19, Article ID 195701, 5 pages, 2011.
 - [31] R. Parshani, S. V. Buldyrev, and S. Havlin, “Critical effect of dependency groups on the function of networks,” *Proceedings of the National Academy of Sciences of the United States of America*, vol. 108, no. 3, pp. 1007–1010, 2011.
 - [32] C. Howson and P. Urbach, *Scientific Reasoning: The Bayesian Approach*, Open Court, La Salle, Ill, USA, 1993.
 - [33] Z. Nikoloski, N. Deo, and L. Kucera, “Degree-correlation of a scale-free random Graph process,” in *Proceedings of the European conference on combinatorics, Graph Theory and Applications*, pp. 239–244, Berlin, Germany, September 2005.
 - [34] T. B. Hashimoto, M. Nagasaki, K. Kojima, and S. Miyano, “BFL: a node and edge betweenness based fast layout algorithm for large scale networks,” *BMC Bioinformatics*, vol. 10, article 19, 2009.
 - [35] A.-L. Barabási and R. Albert, “Emergence of scaling in random networks,” *Science*, vol. 286, no. 5439, pp. 509–512, 1999.
 - [36] D. J. Watts and S. H. Strogatz, “Collective dynamics of “small-world” networks,” *Nature*, vol. 393, no. 6684, pp. 440–442, 1998.
 - [37] P. Erdős and A. Rényi, “On the evolution of random graphs,” in *Publication of the Mathematical Institute of the Hungarian Academy of Sciences*, vol. 5, pp. 17–61, 1960.
 - [38] J. Leskovec, J. Kleinberg, and C. Faloutsos, “Graphs over time: densification laws, shrinking diameters and possible explanations,” in *Proceedings of the 11th ACM SIGKDD International Conference on Knowledge Discovery and Data Mining (KDD ’05)*, pp. 177–187, New York, NY, USA, August 2005.
 - [39] V. Colizza, R. Pastor-Satorras, and A. Vespignani, “Reaction-diffusion processes and metapopulation models in heterogeneous networks,” *Nature Physics*, vol. 3, no. 4, pp. 276–282, 2007.
 - [40] M. Ercsey-Ravasz and Z. Toroczkai, “Centrality scaling in large networks,” *Physical Review Letters*, vol. 105, no. 3, Article ID 038701, 4 pages, 2010.

Research Article

Delay Bound: Fractal Traffic Passes through Network Servers

Ming Li,¹ Wei Zhao,² and Carlo Cattani³

¹ School of Information Science & Technology, East China Normal University, No. 500 Dongchuan Road, Shanghai 200241, China

² Department of Computer and Information Science, University of Macau, Avenida Padre Tomas Pereira, Taipa 1356, Macau

³ Department of Mathematics, University of Salerno, Via Ponte Don Melillo, 84084 Fisciano, Italy

Correspondence should be addressed to Ming Li; ming_lihk@yahoo.com

Received 25 August 2013; Accepted 5 September 2013

Academic Editor: Ezzat G. Bakhoum

Copyright © 2013 Ming Li et al. This is an open access article distributed under the Creative Commons Attribution License, which permits unrestricted use, distribution, and reproduction in any medium, provided the original work is properly cited.

Delay analysis plays a role in real-time systems in computer communication networks. This paper gives our results in the aspect of delay analysis of fractal traffic passing through servers. There are three contributions presented in this paper. First, we will explain the reasons why conventional theory of queuing systems ceases in the general sense when arrival traffic is fractal. Then, we will propose a concise method of delay computation for hard real-time systems as shown in this paper. Finally, the delay computation of fractal traffic passing through servers is presented.

1. Introduction

There are two categories of communications to perform the delivery of a message M from the source A to the destination B . One is in the sense of best effort. By best effort, one means that the computer communication system, which is denoted by S , does not guarantee the connection of sending M from A to B , and accordingly, the quantity of the time delay D that M suffers from S may not be guaranteed, generally. User Datagram Protocol (UDP) is used for communications by best effort (Tanenbaum [1], Postel [2]). The other is in the sense of Transmission Control Protocol (TCP), which is connection oriented, implying that the connection for sending M from A to B is guaranteed ([1], Postel [3]). Guaranteed connection is the premise for guaranteeing the quantity of the time delay D that M suffers from S from A to B . This is particularly the case when mission critical applications are required (Zhao and Ramamritham [4], Zhao et al. [5], Zhao and Stankovic [6], Mahapatra and Zhao [7], Rader [8], and Mahmoodi et al. [9]).

In the case of guaranteed connections, there are two types of communication systems. One is in the type of real-time systems. The other is in the type of nonreal-time ones. By real-time system, one implies that the predetermined time delay should be guaranteed (Natarajan and Zhao [10], Chakraborty and Eberspacher [11]). If the delay, which M

suffers from S , exceeds the predetermined deadline of delay, one will consider that the message M is meaningless, and communication of M from A to B is taken to be a failure from a view of real-time systems.

In the field of computer communications, there are two categories of real-time systems. One is for hard real-time systems, and the other is for soft ones. By hard real-time systems, we mean that the time constraint, more precisely, the predetermined time delay, has to be assured. Otherwise, the communication is regarded as a failure ([4, 5, 10, 11], Buttazzo [12], Raha et al. [13], Malcolm and Zhao [14], Malcolm et al. [15], Budka et al. [16], and Liem and Mendiratta [17]). By soft real-time systems, on the other side, we imply that the predetermined time constraint may be statistically violated with a predetermined probability ([10], Zhao and Chong [18], and Wang et al. [19]).

Recall that the time constraint mentioned above is the message delay suffering from S from A to B (Sandmann [20], Rodríguez-Pérez et al. [21], Anjum et al. [22], Papastergiou et al. [23], Panshenskoy and Vakhitov [24], Kumar et al. [25], Ferrandiz et al. [26], Pin et al. [27], Florens et al. [28], Lenzini et al. [29], and Tu et al. [30]). More precisely, in the case of the Internet, this term specifically means the delay of data packets. Unless otherwise stated, this paper uses the term packet delay or delay for short.

While we mentioned above that delay serves as a key parameter in the aspect of traffic passing through servers in the field of computer networks, one may say that the delay denoted by d is actually queuing time denoted by t_q in terms of queuing system as illustrated in Figure 1. Queuing theory may appear complex mathematically. From the point of view of applications, however, it may be quite easy to do the performance analysis of a queuing system with the basic knowledge of statistical means and standard deviations together with a pen and a piece of paper or with a few lines of code of simple computer program (Cooper [31], Reich [32], Kendall [33], Luchak [34], Little [35], Whitt [36, 37], and Li et al. [38]). Indeed, we said so if arrival traffic $X(t)$ is Markovian as those discussed in [33–38], Jagerman [39], Doshi [40], McKenna and Mitra [41], Li and Chen [42], Brandão and Nova [43], Reiman and Simon [44], Ancker Jr. and Gafarian [45, 46], Daley [47], and Casale et al. [48].

Note that traffic of the Markovian type implies that it is light tailed. By light tail, we mean that its autocorrelation function (ACF) is exponentially decayed and so are its power spectrum density (PSD) function and probability density function (PDF) (Li and Zhao [49, 50], Li [51]). Nevertheless, traffic is heavy tailed (Loiseau et al. [52], Hernández-Campos et al. [53], Resnick [54], Takayasu et al. [55], Willinger et al. [56], Leland et al. [57], Paxson and Floyd [58], Willinger and Paxson [59], and Beran et al. [60]), which implies that the ACF of traffic is hyperbolically decayed, that is, slowly decayed (Tsybakov and Georganas [61]). To be precise, the ACF of traffic decays slowly such that it is nonintegrable, which implies long memory or long-range dependence (LRD) (Csabai [62], Adas [63], Terdik and Gyires [64], Callado et al. [65], Owczarczuk [66], Scherrer et al. [67], Devetskiotis and da Fonseca [68], Smith [69], Tadaki [70], Erramilli et al. [71], Karasaridis and Hatzinakos [72], Stathis and Maglaris [73], López-Ardao et al. [74], and Beran [75]). The LRD of traffic may be so strong that the variance of traffic may not exist or may be infinite ([54], Willinger et al. [76], Resnick et al. [77], López-Oliveros and Resnick [78], D'Auria and Resnick [79], and Fishman and Adan [80]). Consequently, conventional queuing theory may stop being used for analyzing queuing time or delay when arrival traffic is fractal with heavy tails or LRD such that it is of infinite variance.

Possible applications of conventional queuing theory to delay analysis are in the case of fractal traffic models with finite variance, such as fractional Brownian motion (fBm), fractional Gaussian noise (fGn); see, for example, Norros [81], Jin and Min [82], Iftikhar et al. [83], Dahl and Willemain [84], Chevalier and Wein [85], Ou and Wein [86], Wein [87, 88], Harrison and Wein [89], Murata et al. [90], Boxma and Cohen [91], Haddad and Mazumdar [92], Ghosh and Weerasinghe [93], Duncan et al. [94], Li and Zhao [95], and Yue et al. [96]. However, overlarge buffer size may be required even when arrival fractal traffic is of finite variance (Albin and Samorodnitsky [97], Massoulie and Simonian [98], Heath et al. [99], Simonian and Guibert [100], Tsybakov and Georganas [101, 102], Willinger et al. [103], Kozachenko et al. [104], Carpio [105], Juneja [106], Shah and Wischik [107], and Vieira et al. [108]). The required buffer size may

be so large that the value of the delay time obtained with conventional queuing theory may be impractically large for real-time systems.

The previous discussions imply that the key reason that makes the conventional queuing theory very difficult, if not impossible, to be used in the delay analysis of communication systems with fractal arrivals is the fractal properties of traffic, namely, self-similarity and LRD. Thus, fractal arrival traffic substantially challenges queuing theory of real-time systems.

As known, performance analysis of conventional queuing systems has to assume that statistical means and variances of arrival traffic exist (Cooper et al. [31–47], Pitts and Schormans [109], Stalling [110, 111], and Gibson [112]). However, generally speaking, it is inappropriate to assume that the variance of fractal traffic exists ([76–78], Li and Zhao [113], and Doukhan et al. [114]). Thus, new methodology *that does not rely on statistical means and variances of arrival traffic* is desired in the field of computer communication networks and real-time systems in particular.

Note that variance analysis of random functions or time series plays a key role in statistics (Bendat and Piersol [115], Gelman [116], Freedman [117], Sheskin [118], Meyer [119], Lindgren and McElrath [120], and Fuller [121]) as well as conventional queuing theory [31–47], which is actually a branch of statistics (Papoulis [122], Bhat [123]). Therefore, one may see how it is significant for us to turn away from variance analysis of arrival traffic and queuing systems to treat delay analysis of fractal traffic passing through servers. Network calculus may be a promising theory to deal with delay analysis of queuing systems, irrelevant to means and variances of arrival traffic, exhibiting remarkable advances in the aspect of queuing theory.

There are two categories with respect to the theory of network calculus. One is for deterministic delay analysis of queuing systems (Le Boudec and Thiran [124], Firoiu et al. [125], Le Boudec [126], and Cruz [127]). The other is stochastic network calculus (Jiang and Liu [128], Wang et al. [129], Burchard et al. [130], Ciucu et al. [131], and Li and Knightly [132]). We should keep in mind that the theory of stochastic network calculus substantially differs from conventional queuing theory in methodology because it follows the criterion of being irrelevant to means and variances of arrival traffic.

This paper aims at presenting novel computation methods of delay of fractal traffic passing through servers without relating to the concepts of means and variances of arrival traffic.

The rest of the paper is organized as follows. We will give the brief of fractal traffic in Section 2. In Section 3, we will exhibit the result for the delay analysis of deterministic queuing theory. Section 4 presents our delay analysis of fractal traffic passing through servers. Finally, Section 5 concludes the paper.

2. Brief of Fractal Traffic

Denote by $x(t_i)$ the arrival traffic time series (traffic for short), where t_i is the timestamp of the i th packet, where i is a natural

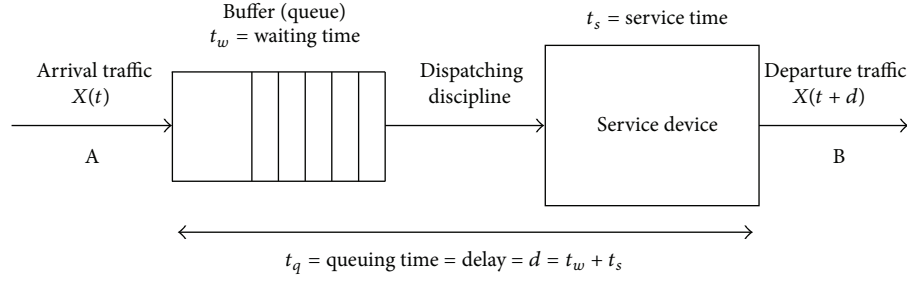


FIGURE 1: Queuing system for single server.

number (Li et al. [133]). Then, $x(t_i)$ implies the data size of the i th packet. Since statistics of $x(t_i)$ is consistent with that of $x(i)$, we use $x(i)$ to indicate traffic for simplicity.

2.1. Non-Markovian Property and LRD. Denote by $r_{xx}(k) = E[x(i)x(i+k)]$ the ACF of $x(i)$, where k is the time lag. The ACF $r_{xx}(k)$ indicates how the size of the i th packet correlates to that of another packet $(i+k)$ apart. If an ACF $R(k)$ is exponentially decayed, $R(k)$ may be neglected even for small k . For instance, suppose the ACF of a time series $B(i)$ that follows the Poisson distribution. It is given by (Bendat and Piersol [115])

$$R_{BB}(k) = \exp(-2\lambda|k|) \quad (\lambda > 0). \quad (1)$$

Then, in the case of $\lambda = 1$, we have

$$R_{BB}(1) \approx 0.135; \quad R_{BB}(2) \approx 0.018. \quad (2)$$

Equation (2) implies that $R_{BB}(1)$ can be neglected in engineering because $x(i)$ is almost orthogonal to $x(i+1)$, letting along $R_{BB}(k)$ for $k > 1$. Therefore, $R_{BB}(k) \approx 0$ for $k > 0$. That means that $B(i)$ is memoryless. Accordingly, it is Markovian ([121, 122], Bunin [134], and Benes [135]). However, traffic $x(i)$ is non-Markovian, which is a property that distinguishes it from conventional time series, because $r_{xx}(k)$ is hyperbolically decayed in the form

$$r_{xx}(k) \sim k^{-\beta}, \quad 0 < \beta < 1, \quad k \rightarrow \infty. \quad (3)$$

The above implies that

$$\sum_0^{\infty} r_{xx}(k) = \infty. \quad (4)$$

Thus, $x(i)$ is LRD or of long memory. Consequently, it is non-Markovian (Yulmetyev et al. [136], Asgari et al. [137], van Kampen [138], Mura et al. [139], and Luczka [140]).

2.2. Property of $1/f$ Noise. Let $S_{xx}(\omega)$ be the PSD of $x(i)$, where ω is angular frequency. According to the Wiener theorem, which is also known as the Wiener-Khintchine theorem and sometimes as the Khinchin-Kolmogorov theorem (Robinson [141], Wiener [142, 143], Khintchine [144], and Yaglom [145]), $S_{xx}(\omega)$ is the Fourier transform of $r_{xx}(k)$. Since

$$\sum_0^{\infty} r_{xx}(k) = S_{xx}(\omega)|_{\omega=0} = \infty, \quad (5)$$

it is easy to infer that $S_{xx}(\omega)$ is in the form

$$S_{xx}(\omega) \sim \frac{1}{\omega}. \quad (6)$$

Therefore, $x(i)$ follows $1/f$ noise (Mandelbrot [146, 147], Ruseckas et al. [148], Lenoir [149], Aquino et al. [150], Amir et al. [151], Carlini et al. [152, 153], Beran [154, 155], Lim and Teo [156], Eab and Lim [157], Muniandy and Lim [158], Muniandy et al. [159], Muniandy and Stanslas [160], Pinchas [161, 162], Wang and Yan [163], Bakhoum and Toma [164, 165], Yang et al. [166], Wang [167], Wornell [168], Barnes and Allan [169], Kasdin [170], and Corsini and Saletti [171]).

2.3. Self-Similarity. Traffic $x(i)$ approximately satisfies the definition of self-similarity given by

$$x(ai) \equiv a^H x(i), \quad a > 0, \quad (7)$$

where \equiv denotes equality in the sense of probability distribution and $0 < H < 1$ stands for the Hurst parameter [58, 61]. In general, H varies with time. Hence, traffic has the property of multifractals ([108], Vieira et al. [172], Vieira and Lee [173], Masugi and Takuma [174], Masugi [175], Veitch et al. [176], Salvador et al. [177], Nogueira et al. [178], Krishna et al. [179], Feldmann et al. [180], Ayache et al. [181], Ayache [182], Liao et al. [183], Liao [184], Carbone et al. [185, 186], Stanley and Meakin [187], Yang et al. [188], Song and Shang [189], Shang et al. [190], Kantelhardt et al. [191], Ostrowsky et al. [192], Sastry et al. [193], and Min et al. [194]).

2.4. The Hurst Parameter and Fractal Dimension. Expressing β in (3) by H yields

$$\beta = 2 - 2H. \quad (8)$$

The parameter β is the index of LRD, and H is the measure of LRD ([52, 60, 75, 76, 154], Roughan et al. [195], Abry et al. [196], and Hall and Hart [197]). In the fields, people usually use H instead of β to characterize LRD of time series for dedicating the famous hydrologist Hurst [198].

We consider the local behavior of traffic $x(i)$ using its ACF $r_{xx}(k)$. For $k \rightarrow 0$, if $r_{xx}(k)$ is sufficiently smooth on $(0, \infty)$ and if

$$[r_{xx}(0) - r_{xx}(k)] \sim c_1 |k|^\alpha, \quad 0 < \alpha \leq 2, \quad (9)$$

where c_1 is a constant and α is the fractal index of $x(i)$ (Adler [199], Chan et al. [200], Davies and Hall [201], Constantine and Hall [202], Hall and Roy [203], Kent and Wood [204], Gneiting and Schlather [205], Gneiting [206], and Lim and Teo [207]), then the fractal dimension, denoted by D_f , of $x(i)$ is given by

$$D_f = 2 - \frac{\alpha}{2}. \quad (10)$$

Under the constraint of $0 < \alpha \leq 2$, one has

$$1 \leq D_f < 2. \quad (11)$$

2.5. Power Laws and Heavy Tails. Taqqu's law says that the PDF of a random function $x(t)$ is in the form of a power function if it is LRD (Loiseau et al. [52], Doukhan et al. [114], Abry et al. [196], and Samorodnitsky and Taqqu [208]). Therefore, the PDF, ACF, and PSD of traffic are all in the form of power functions as can be seen from (3) and (6). When the PDF of a random function follows power laws, one says that it is heavy tailed (Adler et al. [209], Podobnik et al. [210, 211], Chen et al. [212], Xu et al. [213], Buraczewski et al. [214], Kulik and Soulier [215], Pisarenko and Rodkin [216], Resnick [217], Stanley [218], Bowers et al. [219], Eliazar and Klafter [220], Jakšić [221], Bansal et al. [222], Milojević [223], and Pareto [224]).

Denote by $p(x)$ the PDF of $x(t)$. Then, the tail of $p(x)$ may be so heavy that its mean and variance, expressed, respectively, by (12) and (13), may not exist:

$$E[x(t)] = \int_{-\infty}^{\infty} xp(x) dx, \quad (12)$$

$$\text{Var}(x) = \int_{-\infty}^{\infty} (x - \mu)^2 p(x) dx. \quad (13)$$

2.6. Remarks. Previous discussions imply the following remarks.

Remark 1. Traffic follows power laws.

Remark 2. It is LRD.

Remark 3. It is approximately self-similar.

Remark 4. It is a type of $1/f$ noise.

Remark 5. It is heavy tailed.

Remark 6. LRD is a global property of traffic, which is measured by H .

Remark 7. Fractal dimension D_f characterizes the local self-similarity or local roughness or local smoothness of traffic.

In general, we do not talk about means and variances of traffic. Instead, we are interested in other two, namely, local self-similarity and LRD in the theory of fractal traffic.

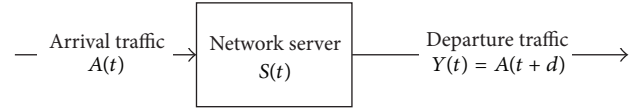


FIGURE 2: Traffic passing through single server.

3. Delay of Deterministic Queuing Systems

Network calculus may be applied to the delay analysis with respect to quality of service (QoS) in computer communication networks ([124–132], Cruz [225]). The issue of traffic passing through a server with respect to traffic delay can be described by Figure 2. The essential questions about it are stated as follows.

Question 1: how to model arrival traffic $A(t)$ towards assuring a predetermined delay, which is denoted by D , such that $d \leq D$?

Question 2: how to design a service scheme, which is denoted by $S(t)$, towards assuring a predetermined delay D , such that $d \leq D$?

Question 3: in order to guarantee the predetermined delay when $A(t)$ passes through $S(t)$, what is the operation among $A(t)$, $Y(t)$, and $S(t)$ such that $d \leq D$?

The answer to question 1 is about traffic modeling. The one to question 2 is about system modeling. That to the third is the relationship among the arrival $A(t)$, the server $S(t)$, and the departure traffic $Y(t) = A(t + d)$. Three answers constitute the basic of network calculus described in [124–127, 225].

3.1. Deterministic Envelope of Traffic. In order to assure a predetermined delay D such that $d \leq D$, one may utilize an envelope, which is denoted by $A(t)$, of arrival traffic $x(t)$. There are two categories of envelopes of random functions. One is in the sense of statistical envelopes, and the other is in the sense of deterministic ones.

The literature regarding statistical envelopes of light-tailed random functions is rich, as they are needed in many fields of sciences and technologies, ranging from electronics engineering to ocean one; see, for example, Rice [226, 227], Veltcheva et al. [228], Fang and Xie [229], Tayfun and Lo [230], Ochi and Sahinoglou [231, 232], Longuet-Higgins [233], Nigam [234], and Yang [235], just mentioning a few. Nonetheless, they cannot be taken as candidates of traffic envelopes because means and variances are essential to them [226–235].

In the society of computer science, people are interested in a type of envelopes of traffic, called bounding models of traffic (Michiel and Laevens [236]). Considering that arrival traffic has the property of $x(t) \geq 0$ (Li and Zhao [237]), following Cruz [127], and supposing that $x(t)$ is continuous for $t \geq 0$, a possible envelope in the time interval $[0, t]$ may be given by the inequality in the form

$$A(t) = \int_0^t x(t) dt \leq \sigma + pt. \quad (14)$$

There are two parameters in the above expression. One is σ that characterizes the local property of $A(t)$ called the

burtiness in the field of computer networks ([124–127], [225], McDysan [238], Kouvatso et al. [239], and Anantharam and Konstantopoulos [240, 241]). The other is ρ that captures the property of long-term rate of $A(t)$, citing two nice survey papers by Mao and Panwar [242] and Fidler [243], respectively, about (14).

As a matter of fact, on one hand, we have

$$\lim_{t \rightarrow 0} A(t) = \lim_{t \rightarrow 0} \int_0^t x(t) dt \leq \sigma. \quad (15)$$

Thus, σ characterizes the burtiness of $A(t)$. On the other hand, one has

$$\lim_{t \rightarrow \infty} \frac{A(t)}{t} = \lim_{t \rightarrow \infty} \frac{\int_0^t x(t) dt}{t} \leq \rho. \quad (16)$$

Therefore, ρ represents the long-term rate of $A(t)$. This model of traffic is denoted by

$$A(t) \sim (\sigma, \rho), \quad (17)$$

with the special term “Leaky Bucket” [124–127, 225, 238, 242, 243].

The deterministic envelop of traffic, namely, $A(t)$, has the properties remarked as follows.

Remark 8. $A(t)$ is increasing in the wide sense, implying that $A(t_2) \geq A(t_1)$ if $t_2 \geq t_1$.

Remark 9. $A(t)$ expressed by (14) is irrelevant of statistics of $x(t)$. Consequently, we do not need the concepts of statistical means and variances for modeling traffic $x(t)$ by using (σ, ρ) .

Remark 10. Remark 9 is consistent in philosophy with fractal models of traffic.

3.2. Service Curves. Denote a service curve of a server by $S(t)$; see Figure 2. It represents a scheme of the server to allocate enough resources, such as bandwidth, to arrival traffic $A(t)$ such that the delay d does not exceed the predetermined D . Mathematically, $S(t)$ has the same properties of $A(t)$ as described in Remarks 8–10. Thus, a function $S(t) \geq A(t)$ may be a candidate of service curve (Yin and Poo [244], Pyun et al. [245], Khanjari et al. [246], Chu et al. [247], Fulton and Li [248], Li and Hwang [249], Lau and Li [250], Li and Pruneski [251], Jamin et al. [252], Wu et al. [253], Chen et al. [254], Agrawal et al. [255], Feng et al. [256], Raha et al. [257], and Zhao and Chen [258]). Skills behind the idea of service curves appear simple, but it is significant in the development of linearizing nonlinear systems in general (Houssin et al. [259], Okumura et al. [260], and Shinzawa [261]) and queuing theory in particular [124].

3.3. Relationship among Arrival $A(t)$, Service $S(t)$, and Departure $A(t + d)$. As previously mentioned, $S(t)$ has the same properties as those of $A(t)$. Thus, we denote by \mathbb{S} the set of increasing functions in the wide sense. That is, $A(t), S(t) \in \mathbb{S}$.

Let $X_1(t), X_2(t) \in \mathbb{S}$. Then, the operation expressed by (18) is called min-plus convolution [126, 262]

$$X_1(t) \otimes X_2(t) = \inf_{0 \leq u \leq t} \{X_1(u) + X_2(t - u)\}. \quad (18)$$

With the tool of min-plus convolution, referring to [124–127], one has the relationship among $A(t)$, $S(t)$, and $A(t + d)$ given by

$$A(t) \otimes S(t) \leq Y(t) = A(t + d). \quad (19)$$

3.4. Delay Computation of Single Server. The reports regarding delay computation are rich; see, for example, [124–132, 225, 244–258, 262], Raha et al. [263, 264], Ng et al. [265], Jia et al. [266, 267], Amigo et al. [268], Lenzini et al. [269], Boggia et al. [270], Karam and Tobagi [271], Fuks et al. [272], Wrege et al. [273], Liebeherr et al. [274], and Golestani [275]. In this research, we present a novel way of delay computation, which is stated below.

Theorem 11. Denote by $Y_{AS}(t) = A(t) \otimes S(t)$. Then, the delay $d(t)$ that $A(t)$ suffers from $S(t)$ at time t is given by

$$d(t) \geq \frac{Y_{AS}(t) - \sigma - \rho t}{\rho}. \quad (20)$$

Proof. According to (14) and (19), we have

$$Y_{AS}(t) \leq A(t + d(t)) \leq \sigma + \rho(t + d(t)). \quad (21)$$

Thus,

$$Y_{AS}(t) \leq \sigma + \rho(t + d(t)). \quad (22)$$

Solving $d(t)$ from the above yields (20). Thus, the theorem results. \square

3.5. Guaranteed Delay of Single Server. Suppose that D is the predetermined deadline of delay. Then, the constraint of guaranteed delay is expressed by

$$d(t) \leq D \quad (t > 0). \quad (23)$$

In order to achieve (23), we let

$$\frac{Y_{AS}(t) - \sigma - \rho t}{\rho} \leq d(t) \leq D. \quad (24)$$

Note that $Y_{AS}(t) = A(t) \otimes S(t)$. Therefore, we may design either proper $S(t)$ or $A(t)$ or both such that (24) is satisfied. For given $A(t)$, the following theorem gives the constraint of $S(t)$ to assure (24).

Theorem 12. Denote the inverse of \otimes by \oplus . Let D be a given deadline of delay. Then, (24) is satisfied if

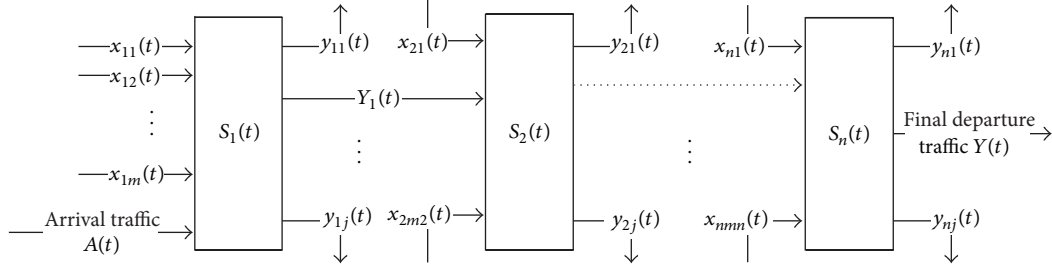
$$S(t) \geq A(t) \oplus [\rho(D - t) - \sigma]. \quad (25)$$

Proof. Let (24) be satisfied. Then, we have

$$\frac{Y_{AS}(t) - \sigma - \rho t}{\rho} \leq D. \quad (26)$$

Changing the sign on the left side in the above expression produces

$$\frac{\sigma + \rho t - Y_{AS}(t)}{\rho} \geq D. \quad (27)$$

FIGURE 3: Arrival traffic $A(t)$ passing through n servers in series.

Therefore, one has

$$Y_{AS}(t) = A(t) \otimes S(t) \geq \rho(D - t) - \sigma. \quad (28)$$

From the above, using the inverse of min-plus convolution, we have $S(t) \geq A(t) \oplus [\rho(D - t) - \sigma]$. This completes the proof. \square

3.6. End-to-End Delay in Tandem Network. Consider arrival traffic $A(t)$ that passes through n servers in series as indicated in Figure 3. In practice, there are a number of arrival traffic that concurrently join each server at its input port and there are some traffic that may leave at the output port of that server (Coulouris et al. [276]). Either the number of traffic joining a server or leaving it is uncertain. For instance, for the first server that is denoted by $S_1(t)$, there are $m + 1$ arrival traffic and $j + 1$ departure ones at time t . We are only interested in the arrival denoted by $A(t)$ and the departure denoted by $Y(t)$.

One way to find the end-to-end delay of $A(t)$ passing through n servers in series is to find delay $d_i(t)$ that $A(t)$ suffers from the i th server using Theorem 11 with the constraint stated in Theorem 12. Then, the end-to-end delay at time t is given by

$$d(t) = \sum_{i=1}^n d_i(t). \quad (29)$$

Denote $S(t)$ the service curve of n servers in series. Then [124],

$$S(t) = S_1(t) \otimes S_2(t) \otimes \cdots \otimes S_n(t). \quad (30)$$

Therefore, when $S(t)$ is designed following Theorem 12 and it is decomposed into n servers in series, (23) is guaranteed.

The discussions in the previous subsections produce the following remarks.

Remark 13. The above delay analysis and its computations do not need any information of the statistics of arrival traffic $A(t)$.

Remark 14. The delay can be deterministically guaranteed. Hence, the deterministic queuing systems as Le Boudec and Thiran stated in [124].

The advantage described by Remarks 13 and 14 is at cost that more resources are required (Zhao [277], Davaril et al.

[278]). In order to reduce the resource requirements that deterministic queuing analysis demands, stochastic network calculus is considered by computer scientists ([19, 95, 128, 130, 131, 243], Jiang et al. [279], Starobinski and Sidi [280], Ng et al. [281], Borst et al. [282], Liu et al. [283], Li et al. [284], Jiang [285], and Baccarelli et al. [286]). In what follows, we present a novel method of stochastic calculus for computing delay of fractal traffic passing through servers.

4. Novel Delay Analysis of Fractal Traffic Passing through Servers

We previously reported our bound of arrival traffic by taking into account its fractal dimension D_f and the Hurst parameter H [287]. It is in the form

$$A(t) = \int_0^t x(u) du \leq r^{2D_f-5} \sigma + a^{-H} \rho t, \quad (31)$$

where $r > 0$, $a > 0$. Applying (31) to Theorem 11 immediately yields a novel delay computation as stated below.

Theorem 15. Denote by $Y_{AS}(t) = A(t) \otimes S(t)$. Then, the delay $d(t)$, which $A(t)$ suffers from $S(t)$ at time t , is given by

$$d(t) \geq \frac{Y_{AS}(t) - r^{2D_f-5} \sigma - a^{-H} \rho t}{a^{-H} \rho}. \quad (32)$$

Proof. According to (14) and (19), we obtain

$$Y_{AS}(t) \leq A(t + d(t)) \leq r^{2D_f-5} \sigma + a^{-H} \rho(t + d(t)). \quad (33)$$

Solving $d(t)$ from the above yields (32), which completes the proof. \square

Remark 16. The bandwidth regarding $d(t)$ expressed by (34) may be generally less than that expressed by (21).

Remark 16 is true because we take into account two parameters of fractal traffic, namely, fractal dimension and the Hurst parameter. As a matter of fact,

$$\begin{aligned} & (\sigma + \rho t) - (r^{2D_f-5} \sigma + a^{-H} \rho t) \\ &= (1 - r^{2D_f-5}) \sigma + (1 - a^{-H}) \rho \geq 0. \end{aligned} \quad (34)$$

The above expression implies that, for a given $d(t)$, the bandwidth required based on Theorem 15 is less than that based on Theorem 11.

Remark 17. Theorem 15 does not relate to statistical means and variances of arrival traffic.

Note that (31) represents a statistical bound of $A(t)$ because D_f is a fractal parameter [199–207] and so is H [198, 205–207]. D_f expressed by (10) is with probability one and so is H expressed by (8).

We previously mentioned several times that we are studying queuing systems irrelevant to statistical means and variances of arrival traffic because variances and or means of traffic may not exist [54, 76–80]. A common case that means and variances do not exist is for random functions that follow the Cauchy distribution (G. A. Korn and T. M. Korn [288], Rice [289], and Meyer [290]). Two papers by Field et al. [291, 292] utilized the Cauchy distribution for modeling traffic. A concise explanation of random functions without mean and variance is given by Bassingthwaite [293]. The point, namely, irrelevant to statistical means and variances of arrival traffic, makes the queuing theory based on network calculus substantially differ from the conventional one. Considering large queue size based on conventional queuing theory when arrival is fractal, network calculus may yet be an attractive theory for guaranteeing queue size in a queuing system.

5. Conclusions

We have explained the reasons why conventional theory of queuing systems is inappropriate to be used in the delay analysis of queuing systems when arrival traffic is fractal. Then, we have given concise method of delay computation of deterministic queuing systems. Finally, we have derived the computation method of delay when arrival traffic is fractal.

Acknowledgments

This work was supported in part by the National Natural Science Foundation of China under the project Grant nos. 61272402, 61070214, and 60873264 and by the 973 Plan under the project Grant nos. 2011CB302800.

References

- [1] A. S. Tanenbaum, *Computer Networks*, Pearson Education, 4th edition, 2003.
- [2] J. Postel, User Datagram Protocol, IETF RFC 768, 1980, <http://www.ietf.org/rfc/rfc768.txt>.
- [3] J. Postel, Transmission Control Protocol, IETF RFC 793, 1981, <http://www.ietf.org/rfc/rfc793.txt>.
- [4] W. Zhao and K. Ramamritham, "Virtual time CSMA protocols for hard real-time communications," *IEEE Transactions on Software Engineering*, vol. 13, no. 8, pp. 938–952, 1987.
- [5] W. Zhao, K. Ramamritham, and J. A. Stankovic, "Scheduling tasks with resource requirements in hard real-time systems," *IEEE Transactions on Software Engineering*, vol. 13, no. 5, pp. 564–577, 1987.
- [6] W. Zhao and J. A. Stankovic, "Performance analysis of FCFS and improved FCFS scheduling algorithms for dynamic real-time computer systems," in *Proceedings of the Real-Time Systems Symposium (RTSS '89)*, pp. 156–165, Santa Monica, Calif, USA, December 1989.
- [7] R. N. Mahapatra and W. Zhao, "An energy-efficient slack distribution technique for multimode distributed real-time embedded systems," *IEEE Transactions on Parallel and Distributed Systems*, vol. 16, no. 7, pp. 650–662, 2005.
- [8] R. Rader, "Operations support systems for mission critical public safety communication networks," *Bell Labs Technical Journal*, vol. 16, no. 3, pp. 151–162, 2011.
- [9] T. Mahmoodi, V. Friderikos, and H. Aghvami, "Using traffic asymmetry to enhance TCP performance," *Computer Networks*, vol. 57, no. 1, pp. 317–329, 2013.
- [10] S. Natarajan and W. Zhao, "Issues in building dynamic real-time systems," *IEEE Software*, vol. 9, no. 5, pp. 16–21, 1992.
- [11] S. Chakraborty and J. Eberspacher, *Advances in Real-Time Systems*, Springer, New York, NY, USA, 2012.
- [12] G. C. Buttazzo, *Hard Real-Time Computing Systems*, Springer, New York, NY, USA, 2011.
- [13] A. Raha, S. Kamat, W. Zhao, and W. Jia, "Admission control for hard real-time connections in ATM LANs," *IEEE Proceedings: Communications*, vol. 148, no. 4, pp. 217–228, 2001.
- [14] N. Malcolm and W. Zhao, "Hard real-time communication in multiple-access networks," *Real-Time Systems*, vol. 8, no. 1, pp. 35–77, 1995.
- [15] N. Malcolm, W. Zhao, and C. Barter, "Performance comparison of guarantee communication protocols for transmission of hard real-time messages," *Australian Computer Science Communications*, vol. 12, no. 1, pp. 256–265, 1990.
- [16] K. C. Budka, T. Chu, T. L. Doumi, W. Brouwer, P. Lamoureux, and M. E. Palamara, "Public safety mission critical voice services over LTE," *Bell Labs Technical Journal*, vol. 16, no. 3, pp. 133–149, 2011.
- [17] M. Liem and V. B. Mendiratta, "Mission critical communication networks for railways," *Bell Labs Technical Journal*, vol. 16, no. 3, pp. 29–46, 2011.
- [18] W. Zhao and E. Chong, "Performance evaluation of scheduling algorithms for dynamic imprecise soft real-time computer systems," *Australian Computer Science Communications*, vol. 11, no. 1, pp. 329–340, 1989.
- [19] S. Wang, D. Xuan, R. Bettati, and W. Zhao, "Toward statistical QoS guarantees in a differentiated services network," *Telecommunication Systems*, vol. 43, no. 3–4, pp. 253–263, 2010.
- [20] W. Sandmann, "Delays in a series of queues with correlated service times," *Journal of Network and Computer Applications*, vol. 35, no. 5, pp. 1415–1423, 2012.
- [21] M. Rodríguez-Pérez, S. Herrería-Alonso, M. Fernández-Veiga, and C. López-García, "Common problems in delay-based congestion control algorithms: a gallery of solutions," *European Transactions on Telecommunications*, vol. 22, no. 4, pp. 168–179, 2011.
- [22] B. Anjum, H. Perros, X. Mountrouidou, and K. Kontovasilis, "Bandwidth allocation under end-to-end percentile delay bounds," *International Journal of Network Management*, vol. 21, no. 6, pp. 536–547, 2011.
- [23] G. Papastergiou, C. Georgiou, L. Mamatas, and V. Tsaoussidis, "A delay-oriented prioritization policy based on non-congestive queuing," *International Journal of Communication Systems*, vol. 24, no. 8, pp. 1065–1086, 2011.
- [24] M. A. Panshenskov and A. T. Vakhitov, "General method for network providers to choose applications with guaranteed QoS," *Bell Labs Technical Journal*, vol. 16, no. 2, pp. 57–61, 2011.

- [25] N. Kumar, N. Chilamkurti, and J. Lee, "A novel minimum delay maximum flow multicast algorithm to construct a multicast tree in wireless mesh networks," *Computers and Mathematics with Applications*, vol. 63, no. 2, pp. 481–491, 2012.
- [26] T. Ferrandiz, F. Frances, and C. Fraboul, "Worst-case end-to-end delays evaluation for SpaceWire networks," *Discrete Event Dynamic Systems*, vol. 21, no. 3, pp. 339–357, 2011.
- [27] F. Pin, D. Veitch, and B. Kauffmann, "Statistical estimation of delays in a multicast tree using accelerated EM," *Queueing Systems*, vol. 66, no. 4, pp. 369–412, 2010.
- [28] C. Florens, M. Sharif, and R. J. McEliece, "Random sensory networks: a delay analysis," *IEEE Transactions on Information Theory*, vol. 55, no. 4, pp. 1650–1664, 2009.
- [29] L. Lenzini, E. Mingozzi, and G. Stea, "A methodology for computing end-to-end delay bounds in FIFO-multiplexing tandems," *Performance Evaluation*, vol. 65, no. 11–12, pp. 922–943, 2008.
- [30] W. Q. Tu, C. J. Sreenan, and W. J. Jia, "Worst-case delay control in multigroup overlay networks," *IEEE Transactions on Parallel and Distributed Systems*, vol. 18, no. 10, pp. 1407–1419, 2007.
- [31] R. B. Cooper, *Introduction to Queueing Theory*, Elsevier, New York, NY, USA, 2nd edition, 1981.
- [32] E. Reich, "Waiting times when queues are in tandem," *Annals of Mathematical Statistics*, vol. 28, pp. 768–773, 1957.
- [33] D. G. Kendall, "Some problems in the theory of queues," *Journal of the Royal Statistical Society B*, vol. 13, no. 2, pp. 151–185, 1951.
- [34] G. Luchak, "The continuous time solution of the equations of the single channel queue with a general class of service-time distributions by the method of generating functions," *Journal of the Royal Statistical Society B*, vol. 20, no. 1, pp. 176–181, 1958.
- [35] J. D. C. Little, "A proof for the queueing formula: $L = \lambda W$," *Operations Research*, vol. 9, pp. 383–387, 1961.
- [36] W. Whitt, "The queueing network analyzer," *The Bell System Technical Journal*, vol. 62, no. 9, pp. 2779–2815, 1983.
- [37] W. Whitt, "Performance of the queueing network analyzer," *The Bell System Technical Journal*, vol. 62, no. 9, pp. 2817–2843, 1983.
- [38] M. Li, L. Longpre, and P. Vitanyi, "Power of the queue," *SIAM Journal on Computing*, vol. 21, no. 4, pp. 697–712, 1992.
- [39] D. L. Jagerman, "Approximate mean waiting times in transient GI/G/1 queues," *The Bell System Technical Journal*, vol. 61, no. 8, pp. 2003–2022, 1982.
- [40] B. T. Doshi, "An M/G/1 queue with a hybrid discipline," *The Bell System Technical Journal*, vol. 62, no. 5, pp. 1251–1271, 1983.
- [41] J. McKenna and D. Mitra, "Integral representations and asymptotic expansions for closed Markovian queueing networks: normal usage," *The Bell System Technical Journal*, vol. 61, no. 5, pp. 661–683, 1982.
- [42] J. Li and A. Chen, "The decay parameter and invariant measures for Markovian bulk-arrival queues with control at idle time," *Methodology and Computing in Applied Probability*, vol. 15, no. 2, pp. 467–484, 2013.
- [43] R. M. Brandão and A. M. O. P. Nova, "Analysis of event-based, single-server nonstationary simulation responses using classical time-series models," *European Journal of Operational Research*, vol. 218, no. 3, pp. 676–686, 2012.
- [44] M. I. Reiman and B. Simon, "Open queueing systems in light traffic," *Mathematics of Operations Research*, vol. 14, no. 1, pp. 26–59, 1989.
- [45] C. J. Ancker Jr. and A. V. Gafarian, "Some queueing problems with balking and reneging. I," *Operations Research*, vol. 11, no. 1, pp. 88–100, 1963.
- [46] C. J. Ancker Jr. and A. V. Gafarian, "Some queueing problems with balking and reneging. II," *Operations Research*, vol. 11, no. 6, pp. 928–937, 1963.
- [47] D. J. Daley, "Revisiting queueing output processes: a point process viewpoint," *Queueing Systems*, vol. 68, no. 3, pp. 395–405, 2011.
- [48] G. Casale, E. Z. Zhang, and E. Smirni, "Trace data characterization and fitting for Markov modeling," *Performance Evaluation*, vol. 67, no. 2, pp. 61–79, 2010.
- [49] M. Li and W. Zhao, "On $1/f$ noise," *Mathematical Problems in Engineering*, vol. 2012, Article ID 673648, 23 pages, 2012.
- [50] M. Li and W. Zhao, "Visiting power laws in cyber-physical networking systems," *Mathematical Problems in Engineering*, vol. 2012, Article ID 302786, 13 pages, 2012.
- [51] M. Li, "Fractal time series—a tutorial review," *Mathematical Problems in Engineering*, vol. 2010, Article ID 157264, 26 pages, 2010.
- [52] P. Loiseau, P. Gonçalves, G. Dewaele, P. Borgnat, P. Abry, and P. V. B. Primet, "Investigating self-similarity and heavy-tailed distributions on a large-scale experimental facility," *IEEE/ACM Transactions on Networking*, vol. 18, no. 4, pp. 1261–1274, 2010.
- [53] F. Hernández-Campos, J. S. Marron, G. Samorodnitsky, and F. D. Smith, "Variable heavy tails in Internet traffic," *Performance Evaluation*, vol. 58, no. 2–3, pp. 261–284, 2004.
- [54] S. I. Resnick, "Heavy tail modeling and teletraffic data," *Annals of Statistics*, vol. 25, no. 5, pp. 1805–1869, 1997.
- [55] M. Takayasu, H. Takayasu, and T. Sato, "Critical behaviors and $1/f$ noise in information traffic," *Physica A*, vol. 233, no. 3–4, pp. 824–834, 1996.
- [56] W. Willinger, M. S. Taqqu, W. E. Leland, and D. V. Wilson, "Self-similarity in high-speed packet traffic: analysis and modeling of ethernet traffic measurements," *Statistical Science*, vol. 10, no. 1, pp. 67–85, 1995.
- [57] W. E. Leland, M. S. Taqqu, W. Willinger, and D. V. Wilson, "On the self-similar nature of ethernet traffic (extended version)," *IEEE/ACM Transactions on Networking*, vol. 2, no. 1, pp. 1–15, 1994.
- [58] V. Paxson and S. Floyd, "Wide area traffic: the failure of Poisson modeling," *IEEE/ACM Transactions on Networking*, vol. 3, no. 3, pp. 226–244, 1995.
- [59] W. Willinger and V. Paxson, "Where mathematics meets the internet," *Notices of the American Mathematical Society*, vol. 45, no. 8, pp. 961–970, 1998.
- [60] J. Beran, R. Sherman, M. S. Taqqu, and W. Willinger, "Long-range dependence in variable-bit-rate video traffic," *IEEE Transactions on Communications*, vol. 43, no. 2, pp. 1566–1579, 1995.
- [61] B. Tsybakov and N. D. Georganas, "Self-similar processes in communications networks," *IEEE Transactions on Information Theory*, vol. 44, no. 5, pp. 1713–1725, 1998.
- [62] I. Csabai, " $1/f$ noise in computer network traffic," *Journal of Physics A*, vol. 27, no. 12, pp. L417–L421, 1994.
- [63] A. Adas, "Traffic models in broadband networks," *IEEE Communications Magazine*, vol. 35, no. 7, pp. 82–89, 1997.
- [64] G. Terdik and T. Gyires, "Lévy flights and fractal modeling of internet traffic," *IEEE/ACM Transactions on Networking*, vol. 17, no. 1, pp. 120–129, 2009.

- [65] A. Callado, C. Kamiński, G. Szabó et al., "A survey on internet traffic identification," *IEEE Communications Surveys and Tutorials*, vol. 11, no. 3, pp. 37–52, 2009.
- [66] M. Owczarczuk, "Long memory in patterns of mobile phone usage," *Physica A*, vol. 391, no. 4, pp. 1428–1433, 2012.
- [67] A. Scherrer, N. Larrieu, P. Owezarski, P. Borgnat, and P. Abry, "Non-Gaussian and long memory statistical characterizations for Internet traffic with anomalies," *IEEE Transactions on Dependable and Secure Computing*, vol. 4, no. 1, pp. 56–70, 2007.
- [68] M. Devetsikiotis and N. L. S. da Fonseca, "Modeling network traffic with long range dependence: characterization, visualization and tools," *Computer Networks*, vol. 48, no. 3, pp. 289–291, 2005.
- [69] R. D. Smith, "The dynamics of internet traffic: self-similarity, self-organization, and complex phenomena," *Advances in Complex Systems*, vol. 14, no. 6, pp. 905–949, 2011.
- [70] S. Tadaki, "Long-term power-law fluctuation in Internet traffic," *Journal of the Physical Society of Japan*, vol. 76, no. 4, Article ID 044001, 5 pages, 2007.
- [71] A. Erramilli, M. Roughan, D. Veitch, and W. Willinger, "Self-similar traffic and network dynamics," *Proceedings of the IEEE*, vol. 90, no. 5, pp. 800–819, 2002.
- [72] A. Karasaridis and D. Hatzinakos, "Network heavy traffic modeling using α -stable self-similar processes," *IEEE Transactions on Communications*, vol. 49, no. 7, pp. 1203–1214, 2001.
- [73] C. Stathis and B. Maglaris, "Modelling the self-similar behaviour of network traffic," *Computer Networks*, vol. 34, no. 1, pp. 37–47, 2000.
- [74] J. C. López-Ardao, C. López-García, A. Suárez-González, M. Fernández-Veiga, and R. Rodríguez-Rubio, "On the use of self-similar processes in network simulation," *ACM Transactions on Modeling and Computer Simulation*, vol. 10, no. 2, pp. 125–151, 2000.
- [75] J. Beran, "Statistical methods for data with long-range dependence," *Statistical Science*, vol. 7, no. 4, pp. 404–416, 1992.
- [76] W. Willinger, V. Paxson, R. H. Riedi, and M. S. Taqqu, "Long-range dependence and data network traffic," in *Theory and Applications of Long-Range Dependence*, P. Doukhan, G. Oppenheim, and M. S. Taqqu, Eds., pp. 373–407, Birkhäuser Boston, Boston, Mass, USA, 2002.
- [77] S. Resnick, G. Samorodnitsky, and F. Xue, "How misleading can sample ACFs of stable MAs be? (very!)," *Annals of Applied Probability*, vol. 9, no. 3, pp. 797–817, 1999.
- [78] L. López-Oliveros and S. I. Resnick, "Extremal dependence analysis of network sessions," *Extremes*, vol. 14, no. 1, pp. 1–28, 2011.
- [79] B. D'Auria and S. I. Resnick, "The influence of dependence on data network models," *Advances in Applied Probability*, vol. 40, no. 1, pp. 60–94, 2008.
- [80] G. S. Fishman and I. J. B. F. Adan, "How heavy-tailed distributions affect simulation-generated time averages," *ACM Transactions on Modeling and Computer Simulation*, vol. 16, no. 2, pp. 152–173, 2006.
- [81] I. Norros, "On the use of fractional Brownian motion in the theory of connectionless networks," *IEEE Journal on Selected Areas in Communications*, vol. 13, no. 6, pp. 953–962, 1995.
- [82] X. L. Jin and G. Y. Min, "Modelling and analysis of priority queueing systems with multi-class self-similar network traffic: a novel and efficient queue-decomposition approach," *IEEE Transactions on Communications*, vol. 57, no. 5, pp. 1444–1452, 2009.
- [83] M. Iftikhar, T. Singh, B. Landfeldt, and M. Caglar, "Multi-class G/M/1 queueing system with self-similar input and non-preemptive priority," *Computer Communications*, vol. 31, no. 5, pp. 1012–1027, 2008.
- [84] T. A. Dahl and T. R. Willemain, "The effect of long-memory arrivals on queue performance," *Operations Research Letters*, vol. 29, no. 3, pp. 123–127, 2001.
- [85] P. B. Chevalier and L. M. Wein, "Scheduling networks of queues. Heavy traffic analysis of a multistation closed network," *Operations Research*, vol. 41, no. 4, pp. 743–758, 1993.
- [86] J. Ou and L. M. Wein, "On the improvement from scheduling a two-station queueing network in heavy traffic," *Operations Research Letters*, vol. 11, no. 4, pp. 225–232, 1992.
- [87] L. M. Wein, "Scheduling networks of queues. Heavy traffic analysis of a multistation network with controllable inputs," *Operations Research*, vol. 40, no. 2, pp. S312–S334, 1992.
- [88] L. M. Wein, "Scheduling networks of queues. Heavy traffic analysis of a two-station network with controllable inputs," *Operations Research*, vol. 38, no. 6, pp. 1065–1078, 1990.
- [89] J. M. Harrison and L. M. Wein, "Scheduling networks of queues. Heavy traffic analysis of a two-station closed network," *Operations Research*, vol. 38, no. 6, pp. 1052–1064, 1990.
- [90] M. Murata, Y. Oie, T. Suda, and H. Miyahara, "Analysis of a discrete-time single-server queue with bursty inputs for traffic control in ATM networks," *IEEE Journal on Selected Areas in Communications*, vol. 8, no. 3, pp. 447–458, 1990.
- [91] O. J. Boxma and J. W. Cohen, "The M/G/1 queue with heavy-tailed service time distribution," *IEEE Journal on Selected Areas in Communications*, vol. 16, no. 5, pp. 749–763, 1998.
- [92] J. P. Haddad and R. R. Mazumdar, "Heavy traffic approximation for the stationary distribution of stochastic fluid networks," *Queueing Systems*, vol. 70, no. 1, pp. 3–21, 2012.
- [93] A. P. Ghosh and A. P. Weerasinghe, "Optimal buffer size and dynamic rate control for a queueing system with impatient customers in heavy traffic," *Stochastic Processes and Their Applications*, vol. 120, no. 11, pp. 2103–2141, 2010.
- [94] T. E. Duncan, Y. Yan, and P. Yan, "Exact asymptotics for a queue with fractional Brownian input and applications in ATM networks," *Journal of Applied Probability*, vol. 38, no. 4, pp. 932–945, 2001.
- [95] C. Li and W. Zhao, "Stochastic performance analysis of non-feedforward networks," *Telecommunication Systems*, vol. 43, no. 3–4, pp. 237–252, 2010.
- [96] W. Yue, H. Takagi, and Y. Takahashi, *Advances in Queueing Theory and Network Applications*, Springer, New York, NY, USA, 2009.
- [97] J. M. P. Albin and G. Samorodnitsky, "On overload in a storage model, with a self-similar and infinitely divisible input," *Annals of Applied Probability*, vol. 14, no. 2, pp. 820–844, 2004.
- [98] L. Massoulié and A. Simonian, "Large buffer asymptotics for the queue with fractional Brownian input," *Journal of Applied Probability*, vol. 36, no. 3, pp. 894–906, 1999.
- [99] D. Heath, S. Resnick, and G. Samorodnitsky, "Patterns of buffer overflow in a class of queues with long memory in the input stream," *Annals of Applied Probability*, vol. 7, no. 4, pp. 1021–1057, 1997.
- [100] A. Simonian and J. Guibert, "Large deviations approximation for fluid queues fed by a large number of on/off sources," *IEEE Journal on Selected Areas in Communications*, vol. 13, no. 6, pp. 1017–1027, 1995.

- [101] B. Tsybakov and N. D. Georganas, "On self-similar traffic in atm queues: definitions, overflow probability bound, and cell delay distribution," *IEEE/ACM Transactions on Networking*, vol. 5, no. 3, pp. 397–409, 1997.
- [102] B. Tsybakov and N. D. Georganas, "Self-similar traffic and upper bounds to buffer-overflow probability in an ATM queue," *Performance Evaluation*, vol. 32, no. 1, pp. 57–80, 1998.
- [103] W. Willinger, M. S. Taqqu, R. Sherman, and D. V. Wilson, "Self-similarity through high-variability: statistical analysis of Ethernet LAN traffic at the source level," *IEEE/ACM Transactions on Networking*, vol. 5, no. 1, pp. 71–86, 1997.
- [104] Y. Kozachenko, O. Vasylyk, and T. Sottinen, "Path space large deviations of a large buffer with Gaussian input traffic," *Queueing Systems*, vol. 42, no. 2, pp. 113–129, 2002.
- [105] K. J. E. Carpio, "Long-range dependence of stationary processes in single-server queues," *Queueing Systems*, vol. 55, no. 2, pp. 123–130, 2007.
- [106] S. Juneja, "Estimating tail probabilities of heavy tailed distributions with asymptotically zero relative error," *Queueing Systems*, vol. 57, no. 2-3, pp. 115–127, 2007.
- [107] D. Shah and D. Wischik, "Fluid models of congestion collapse in overloaded switched networks," *Queueing Systems*, vol. 69, no. 2, pp. 121–143, 2011.
- [108] F. H. T. Vieira, F. G. C. Rocha, and J. A. dos Santos Jr., "Loss probability estimation and control for OFDM/TDMA wireless systems considering multifractal traffic characteristics," *Computer Communications*, vol. 35, no. 2, pp. 263–271, 2012.
- [109] J. M. Pitts and J. A. Schormans, *Introduction to IP and ATM Design and Performance: With Applications and Analysis Software*, John Wiley & Sons, New York, NY, USA, 2000.
- [110] W. Stallings, *Data and Computer Communications*, Macmillan, New York, NY, USA, 4th edition, 1994.
- [111] W. Stallings, *High-Speed Networks: TCP/IP and ATM Design Principles*, Prentice Hall, New York, NY, USA, 1998.
- [112] J. D. Gibson, *The Communications Handbook*, IEEE Press, 1997.
- [113] M. Li and W. Zhao, "Wild fluctuations of random functions with the Pareto distribution," *Mathematical Problems in Engineering*, vol. 2013, Article ID 767502, 3 pages, 2013.
- [114] P. Doukhan, G. Oppenheim, and M. S. Taqqu, *Theory and Applications of Long-Range Dependence*, Birkhäuser, Boston, Mass, USA, 2003.
- [115] J. S. Bendat and A. G. Piersol, *Random Data: Analysis and Measurement Procedure*, Wiley Series in Probability and Statistics, John Wiley & Sons, Hoboken, NJ, USA, 3rd edition, 2000.
- [116] A. Gelman, "Discussion paper analysis of variance—why it is more important than ever," *Annals of Statistics*, vol. 33, no. 1, pp. 1–53, 2005.
- [117] D. A. Freedman, *Statistical Models: Theory and Practice*, Cambridge University Press, Cambridge, UK, 2005.
- [118] D. Sheskin, *Statistical Tests and Experimental Design: A Guidebook*, Gardner Press, New York, NY, USA, 1984.
- [119] S. L. Meyer, *Data Analysis for Scientists and Engineers*, John Wiley & Sons, New York, NY, USA, 1975.
- [120] B. W. Lindgren and G. W. McElrath, *Introduction to Probability and Statistics*, Macmillan, New York, NY, USA, 1959.
- [121] W. A. Fuller, *Introduction to Statistical Time Series*, Wiley Series in Probability and Statistics: Probability and Statistics, John Wiley & Sons, New York, NY, USA, 2nd edition, 1996.
- [122] A. Papoulis, *Probability, Random Variables, and Stochastic Processes*, McGraw-Hill, New York, NY, USA, 2nd edition, 1984.
- [123] U. N. Bhat, "Sixty years of queueing theory," *Management Science*, vol. 15, pp. 280–294, 1968/1969.
- [124] J. Y. Le Boudec and P. Thiran, *Network Calculus: A Theory of Deterministic Queueing Systems for the Internet*, vol. 2050 of *Lecture Notes in Computer Science*, Springer, Berlin, Germany, 2001.
- [125] V. Firoiu, J. Y. Le Boudec, D. Towsley, and Z. L. Zhang, "Theories and models for internet quality of service," *Proceedings of the IEEE*, vol. 90, no. 9, pp. 1565–1591, 2002.
- [126] J. Y. Le Boudec, "Application of network calculus to guaranteed service networks," *IEEE Transactions on Information Theory*, vol. 44, no. 3, pp. 1087–1096, 1998.
- [127] R. L. Cruz, "A calculus for network delay—I: network elements in isolation," *IEEE Transactions on Information Theory*, vol. 37, no. 1, pp. 114–131, 1991.
- [128] Y. M. Jiang and Y. Liu, *Stochastic Network Calculus*, Springer, New York, NY, USA, 2008.
- [129] S. Wang, Z. Mai, D. Xuan, and W. Zhao, "Design and implementation of QoS-provisioning system for voice over IP," *IEEE Transactions on Parallel and Distributed Systems*, vol. 17, no. 3, pp. 276–288, 2006.
- [130] A. Burchard, J. Liebeherr, and S. D. Patek, "A min-plus calculus for end-to-end statistical service guarantees," *IEEE Transactions on Information Theory*, vol. 52, no. 9, pp. 4105–4114, 2006.
- [131] F. Ciucu, A. Burchard, and J. Liebeherr, "Scaling properties of statistical end-to-end bounds in the network calculus," *IEEE Transactions on Information Theory*, vol. 52, no. 6, pp. 2300–2312, 2006.
- [132] C. Li and E. W. Knightly, "Schedulability criterion and performance analysis of coordinated schedulers," *IEEE/ACM Transactions on Networking*, vol. 13, no. 2, pp. 276–287, 2005.
- [133] M. Li, W. Jia, and W. Zhao, "Correlation form of timestamp increment sequences of self-similar traffic on Ethernet," *Electronics Letters*, vol. 36, no. 19, pp. 1668–1669, 2000.
- [134] B. J. Bunin, "Rate-distortion function for Gaussian Markov processes," *The Bell System Technical Journal*, vol. 48, no. 9, pp. 3059–3074, 1969.
- [135] V. E. Beneš, "Markov processes representing traffic in connecting networks," *The Bell System Technical Journal*, vol. 42, pp. 2795–2837, 1963.
- [136] R. M. Yulmetyev, N. Emelyanova, P. Hänggi, F. Gafarov, and A. Prokhorov, "Long-range memory and non-Markov statistical effects in human sensorimotor coordination," *Physica A*, vol. 316, no. 1–4, pp. 671–687, 2002.
- [137] H. Asgari, S. V. Muniandy, and C. S. Wong, "Stochastic dynamics of charge fluctuations in dusty plasma: a non-Markovian approach," *Physics of Plasmas*, vol. 18, no. 8, Article ID 083709, 2011.
- [138] N. G. van Kampen, "Remarks on non-Markov processes," *Brazilian Journal of Physics*, vol. 28, no. 2, pp. 90–96, 1998.
- [139] A. Mura, M. S. Taqqu, and F. Mainardi, "Non-Markovian diffusion equations and processes: analysis and simulations," *Physica A*, vol. 387, no. 21, pp. 5033–5064, 2008.
- [140] J. Łuczka, "Non-Markovian stochastic processes," *Chaos*, vol. 15, no. 2, Article ID 026107, 13 pages, 2005.
- [141] E. A. Robinson, "A historical perspective of spectrum estimation," *Proceedings of the IEEE*, vol. 70, no. 9, pp. 885–907, 1982.
- [142] N. Wiener, *Time Series*, MIT Press, Cambridge, Mass, USA, 1964.

- [143] N. Wiener, *Extrapolation, Interpolation, and Smoothing of Stationary Time Series*, MIT Press, Cambridge, Mass, USA, 1949.
- [144] A. Khintchine, "Korrelationstheorie der stationären stochastischen Prozesse," *Mathematische Annalen*, vol. 109, no. 1, pp. 604–615, 1934.
- [145] A. M. Yaglom, *Correlation Theory of Stationary and Related Random Functions, Volume I: Basic Results*, Springer Series in Statistics, Springer, New York, NY, USA, 1987.
- [146] B. B. Mandelbrot, *Multifractals and 1/f noise*, Springer, New York, NY, USA, 1998.
- [147] B. B. Mandelbrot, "Some noises with 1/f spectrum, a bridge between direct current and white noise," *IEEE Transactions on Information Theory*, vol. 13, no. 2, pp. 289–298, 1967.
- [148] J. Ruseckas, B. Kaulakys, and V. Gontis, "Herding model and 1/f noise," *Europhysics Letters*, vol. 96, no. 6, Article ID 60007, 2011.
- [149] B. Lenoir, "Predicting the variance of a measurement with 1/f noise," *Fluctuation and Noise Letters*, vol. 12, no. 1, Article ID 1350006, 6 pages, 2013.
- [150] G. Aquino, M. Bologna, P. Grigolini, and B. J. West, "Beyond the death of linear response: 1/f optimal information transport," *Physical Review Letters*, vol. 105, no. 6, Article ID 040601, 4 pages, 2010.
- [151] A. Amir, Y. Oreg, and Y. Imry, "1/f noise and slow relaxations in glasses," *Annalen der Physik*, vol. 18, no. 12, pp. 836–843, 2010.
- [152] M. Carlini, T. Honorati, and S. Castellucci, "Photovoltaic greenhouses: comparison of optical and thermal behaviour for energy savings," *Mathematical Problems in Engineering*, vol. 2012, Article ID 743764, 10 pages, 2012.
- [153] M. Carlini, S. Castellucci, E. Allegrini, and A. Tucci, "Down-hole heat exchangers: modelling of a low-enthalpy geothermal system for district heating," *Mathematical Problems in Engineering*, vol. 2012, Article ID 845192, 11 pages, 2012.
- [154] J. Beran, *Statistics for Long-Memory Processes*, vol. 61 of *Mono-graphs on Statistics and Applied Probability*, Chapman & Hall, New York, NY, USA, 1994.
- [155] J. Beran, "Discussion: heavy tail modeling and teletraffic data," *Annals of Statistics*, vol. 25, no. 5, pp. 1852–1856, 1997.
- [156] S. C. Lim and L. P. Teo, "The fractional oscillator process with two indices," *Journal of Physics A*, vol. 42, no. 6, Article ID 065208, 2009.
- [157] C. H. Eab and S. C. Lim, "Accelerating and retarding anomalous diffusion," *Journal of Physics A*, vol. 45, no. 14, Article ID 145001, 17 pages, 2012.
- [158] S. V. Muniandy and S. C. Lim, "Modeling of locally self-similar processes using multifractional Brownian motion of Riemann-Liouville type," *Physical Review E*, vol. 63, no. 4, Article ID 046104, 2001.
- [159] S. V. Muniandy, W. X. Chew, and C. S. Wong, "Fractional dynamics in the light scattering intensity fluctuation in dusty plasma," *Physics of Plasmas*, vol. 18, no. 1, Article ID 013701, 2011.
- [160] S. V. Muniandy and J. Stanslas, "Modelling of chromatin morphologies in breast cancer cells undergoing apoptosis using generalized Cauchy field," *Computerized Medical Imaging and Graphics*, vol. 32, no. 7, pp. 631–637, 2008.
- [161] M. Pinchas, "Symbol error rate as a function of the residual ISI obtained by blind adaptive equalizers for the SIMO and fractional Gaussian noise case," *Mathematical Problems in Engineering*, vol. 2013, Article ID 860389, 9 pages, 2013.
- [162] M. Pinchas, "Residual ISI obtained by blind adaptive equalizers and fractional noise," *Mathematical Problems in Engineering*, vol. 2013, Article ID 972174, 11 pages, 2013.
- [163] Z. Wang and L. Yan, "The S-transform of sub-fBm and an application to a class of linear sub-fractional BSDEs," *Advances in Mathematical Physics*, vol. 2013, Article ID 827192, 11 pages, 2013.
- [164] E. G. Bakhoum and C. Toma, "Specific mathematical aspects of dynamics generated by coherence functions," *Mathematical Problems in Engineering*, vol. 2011, Article ID 436198, 10 pages, 2011.
- [165] E. G. Bakhoum and C. Toma, "Modeling transitions in complex systems by multiplicative effect of temporal patterns extracted from signal flows," *Mathematical Problems in Engineering*, vol. 2012, Article ID 409856, 11 pages, 2012.
- [166] J. W. Yang, Y. J. Chen, and M. Scalia, "Construction of affine invariant functions in spatial domain," *Mathematical Problems in Engineering*, vol. 2012, Article ID 690262, 11 pages, 2012.
- [167] Y. M. Wang, "Maximum norm error estimates of ADI methods for a two-dimensional fractional subdiffusion equation," *Advances in Mathematical Physics*, vol. 2013, Article ID 293706, 10 pages, 2013.
- [168] G. W. Wornell, "Wavelet-based representations for the 1/f family of fractal processes," *Proceedings of the IEEE*, vol. 81, no. 10, pp. 1428–1450, 1993.
- [169] J. A. Barnes and D. W. Allan, "A statistical model of flicker noise," *Proceedings of the IEEE*, vol. 54, no. 2, pp. 176–178, 1966.
- [170] N. J. Kasdin, "Discrete simulation of colored noise and stochastic processes and 1/f^α power law noise generation," *Proceedings of the IEEE*, vol. 83, no. 5, pp. 802–827, 1995.
- [171] G. Corsini and R. Saletti, "1/f^γ power spectrum noise sequence generator," *IEEE Transactions on Instrumentation and Measurement*, vol. 37, no. 4, pp. 615–619, 1988.
- [172] F. H. T. Vieira, G. R. Bianchi, and L. L. Lee, "A network traffic prediction approach based on multifractal modeling," *Journal of High Speed Networks*, vol. 17, no. 2, pp. 83–96, 2008.
- [173] F. H. T. Vieira and L. L. Lee, "Adaptive wavelet-based multifractal model applied to the effective bandwidth estimation of network traffic flows," *IET Communications*, vol. 3, no. 6, pp. 906–919, 2009.
- [174] M. Masugi and T. Takuma, "Multi-fractal analysis of IP-network traffic for assessing time variations in scaling properties," *Physica D*, vol. 225, no. 2, pp. 119–126, 2007.
- [175] M. Masugi, "Multi-fractal analysis of IP-network traffic based on a hierarchical clustering approach," *Communications in Nonlinear Science and Numerical Simulation*, vol. 12, no. 7, pp. 1316–1325, 2007.
- [176] D. Veitch, N. Hohn, and P. Abry, "Multifractality in TCP/IP traffic: the case against," *Computer Networks*, vol. 48, no. 3, pp. 293–313, 2005.
- [177] P. Salvador, A. Nogueira, and R. Valadas, "Framework based on stochastic L-Systems for modeling IP traffic with multifractal behavior," *Computer Communications*, vol. 27, no. 18, pp. 1799–1811, 2004.
- [178] A. Nogueira, P. Salvador, R. Valadas, and A. Pacheco, "Modeling network traffic with multifractal behavior," *Telecommunication Systems*, vol. 24, no. 2–4, pp. 339–362, 2003.
- [179] P. M. Krishna, V. M. Gadre, and U. B. Desai, "Modelling and control of broad band traffic using multiplicative multifractal cascades," *Sadhana*, vol. 27, no. 6, pp. 699–723, 2002.
- [180] A. Feldmann, A. C. Gilbert, W. Willinger, and T. G. Kurtz, "The changing nature of network traffic: scaling phenomena," *ACM SIGCOMM Computer Communication Review*, vol. 28, no. 2, pp. 5–29, 1998.

- [181] A. Ayache, S. Cohen, and J. L. Vehel, "Covariance structure of multifractional Brownian motion, with application to long range dependence," in *Proceedings of the IEEE International Conference on Acoustics, Speech, and Signal Processing (ICASSP '00)*, vol. 6, pp. 3810–3813, June 2000.
- [182] A. Ayache, "Continuous Gaussian multifractional processes with random pointwise Hölder regularity," *Journal of Theoretical Probability*, vol. 26, no. 1, pp. 72–93, 2013.
- [183] Z. W. Liao, S. X. Hu, D. Sun, and W. F. Chen, "Enclosed laplacian operator of nonlinear anisotropic diffusion to preserve singularities and delete isolated points in image smoothing," *Mathematical Problems in Engineering*, vol. 2011, Article ID 749456, 15 pages, 2011.
- [184] Z. W. Liao, "Regularization multi directions and multi scales anisotropic diffusion for sinogram restoration of low-dosed computed tomography," *Mathematical Problems in Engineering*. In press.
- [185] A. Carbone, G. Castelli, and H. E. Stanley, "Analysis of clusters formed by the moving average of a long-range correlated time series," *Physical Review E*, vol. 69, no. 2, Article ID 026105, 4 pages, 2004.
- [186] A. Carbone, G. Castelli, and H. E. Stanley, "Time-dependent Hurst exponent in financial time series," *Physica A*, vol. 344, no. 1-2, pp. 267–271, 2004.
- [187] H. E. Stanley and P. Meakin, "Multifractal phenomena in physics and chemistry," *Nature*, vol. 335, no. 6189, pp. 405–409, 1988.
- [188] J. W. Yang, Z. Chen, W. S. Chen, and Y. J. Chen, "Robust affine invariant descriptors," *Mathematical Problems in Engineering*, vol. 2011, Article ID 185303, 15 pages, 2011.
- [189] J. Song and P. J. Shang, "Effect of linear and nonlinear filters on multifractal detrended cross-correlation analysis," *Fractals*, vol. 19, no. 4, pp. 443–453, 2011.
- [190] P. J. Shang, Y. Lu, and S. Kama, "The application of Hölder exponent to traffic congestion warning," *Physica A*, vol. 370, no. 2, pp. 769–776, 2006.
- [191] J. W. Kantelhardt, S. A. Zschiegner, E. Koscielny-Bunde, S. Havlin, A. Bunde, and H. E. Stanley, "Multifractal detrended fluctuation analysis of nonstationary time series," *Physica A*, vol. 316, no. 1-4, pp. 87–114, 2002.
- [192] L. O. Ostrowsky, N. L. S. da Fonseca, and C. A. V. Melo, "A multiscaling traffic model for UDP streams," *Simulation Modelling Practice and Theory*, vol. 26, pp. 32–48, 2012.
- [193] C. S. Sastry, S. Rawat, A. K. Pujari, and V. P. Gulati, "Network traffic analysis using singular value decomposition and multiscale transforms," *Information Sciences*, vol. 177, no. 23, pp. 5275–5291, 2007.
- [194] G. Min, M. Ould-Khaoua, S. Loucif, and H. Yin, "An analytical model for hypercubes in the presence of multiple time-scale bursty traffic," *Journal of Systems Architecture*, vol. 52, no. 7, pp. 423–431, 2006.
- [195] M. Roughan, D. Veitch, and P. Abry, "Real-time estimation of the parameters of long-range dependence," *IEEE/ACM Transactions on Networking*, vol. 8, no. 4, pp. 467–478, 2000.
- [196] P. Abry, P. Borgnat, F. Ricciato, A. Scherrer, and D. Veitch, "Revisiting an old friend: on the observability of the relation between long range dependence and heavy tail," *Telecommunication Systems*, vol. 43, no. 3-4, pp. 147–165, 2010.
- [197] P. Hall and J. D. Hart, "Nonparametric regression with long-range dependence," *Stochastic Processes and Their Applications*, vol. 36, no. 2, pp. 339–351, 1990.
- [198] H. E. Hurst, "Long term storage capacity of reservoirs," *Transactions of the American Society of Civil Engineers*, vol. 116, pp. 770–799, 1951.
- [199] R. J. Adler, *The Geometry of Random Fields*, John Wiley & Sons, New York, NY, USA, 1981.
- [200] G. Chan, P. Hall, and D. S. Poskitt, "Periodogram-based estimators of fractal properties," *Annals of Statistics*, vol. 23, no. 5, pp. 1684–1711, 1995.
- [201] S. Davies and P. Hall, "Fractal analysis of surface roughness by using spatial data," *Journal of the Royal Statistical Society B*, vol. 61, no. 1, pp. 3–37, 1999.
- [202] A. G. Constantine and P. Hall, "Characterizing surface smoothness via estimation of effective fractal dimension," *Journal of the Royal Statistical Society B*, vol. 56, no. 1, pp. 97–113, 1994.
- [203] P. Hall and R. Roy, "On the relationship between fractal dimension and fractal index for stationary stochastic processes," *The Annals of Applied Probability*, vol. 4, no. 1, pp. 241–253, 1994.
- [204] J. T. Kent and A. T. A. Wood, "Estimating the fractal dimension of a locally self-similar Gaussian process by using increments," *Journal of the Royal Statistical Society B*, vol. 59, no. 3, pp. 679–699, 1997.
- [205] T. Gneiting and M. Schlather, "Stochastic models that separate fractal dimension and the hurst effect," *SIAM Review*, vol. 46, no. 2, pp. 269–282, 2004.
- [206] T. Gneiting, "Power-law correlations, related models for long-range dependence and their simulation," *Journal of Applied Probability*, vol. 37, no. 4, pp. 1104–1109, 2000.
- [207] S. C. Lim and L. P. Teo, "Gaussian fields and Gaussian sheets with generalized Cauchy covariance structure," *Stochastic Processes and Their Applications*, vol. 119, no. 4, pp. 1325–1356, 2009.
- [208] G. Samorodnitsky and M. S. Taqqu, *Stable Non-Gaussian Random Processes*, Chapman & Hall, New York, NY, USA, 1994.
- [209] R. J. Adler, R. Feldman, and M. S. Taqqu, *A Practical Guide to Heavy Tails: Statistical Techniques and Applications*, Birkhäuser, Boston, Mass, USA, 1998.
- [210] B. Podobnik, P. C. Ivanov, K. Biljakovic, D. Horvatic, H. E. Stanley, and I. Grosse, "Fractionally integrated process with power-law correlations in variables and magnitudes," *Physical Review E*, vol. 72, no. 2, Article ID 026121, 7 pages, 2005.
- [211] B. Podobnik, P. C. Ivanov, V. Jazbinsek, Z. Trontelj, H. E. Stanley, and I. Grosse, "Power-law correlated processes with asymmetric distributions," *Physical Review E*, vol. 71, no. 2, Article ID 025104, 4 pages, 2005.
- [212] Z. Chen, P. C. Ivanov, K. Hu, and H. E. Stanley, "Effect of nonstationarities on detrended fluctuation analysis," *Physical Review E*, vol. 65, no. 4, Article ID 041107, 15 pages, 2002.
- [213] L. Xu, P. C. Ivanov, K. Hu, Z. Chen, A. Carbone, and H. E. Stanley, "Quantifying signals with power-law correlations: a comparative study of detrended fluctuation analysis and detrended moving average techniques," *Physical Review E*, vol. 71, no. 5, Article ID 051101, 14 pages, 2005.
- [214] D. Buraczewski, E. Damek, S. Mentemeier, and M. Mirek, "Heavy tailed solutions of multivariate smoothing transforms," *Stochastic Processes and Their Applications*, vol. 123, no. 6, pp. 1947–1986, 2013.
- [215] R. Kulik and P. Soulier, "Estimation of limiting conditional distributions for the heavy tailed long memory stochastic volatility process," *Extremes*, vol. 16, no. 2, pp. 203–239, 2013.
- [216] V. Pisarenko and M. Rodkin, *Heavy-Tailed Distributions in Disaster Analysis*, Springer, New York, NY, USA, 2010.

- [217] S. I. Resnick, *Heavy-Tail Phenomena: Probabilistic and Statistical Modeling*, Springer Series in Operations Research and Financial Engineering, Springer, New York, NY, USA, 2007.
- [218] H. E. Stanley, "Power laws and universality," *Nature*, vol. 378, no. 6557, p. 554, 1995.
- [219] M. C. Bowers, W. W. Tung, and J. B. Gao, "On the distributions of seasonal river flows: lognormal or power law?" *Water Resources Research*, vol. 48, Article ID W05536, 12 pages, 2012.
- [220] I. Eliazar and J. Klafter, "A probabilistic walk up power laws," *Physics Reports*, vol. 511, no. 3, pp. 143–175, 2012.
- [221] N. Jakšić, "Power law damping parameter identification," *Journal of Sound and Vibration*, vol. 330, no. 24, pp. 5878–5893, 2011.
- [222] A. R. Bansal, G. Gabriel, and V. P. Dimri, "Power law distribution of susceptibility and density and its relation to seismic properties: an example from the German continental deep drilling program (KTB)," *Journal of Applied Geophysics*, vol. 72, no. 2, pp. 123–128, 2010.
- [223] S. Milojević, "Power law distributions in information science: making the case for logarithmic binning," *Journal of the American Society for Information Science and Technology*, vol. 61, no. 12, pp. 2417–2425, 2010.
- [224] V. Pareto, "La legge della domanda," *Giornale degli Economisti*, vol. 10, pp. 59–68, 1895, English translation in *Rivista di Politica Economica*, vol. 87, pp. 691–700, 1997.
- [225] R. L. Cruz, "Quality of service guarantees in virtual circuit switched networks," *IEEE Journal on Selected Areas in Communications*, vol. 13, no. 6, pp. 1048–1056, 1995.
- [226] S. O. Rice, "Mathematical analysis of random noise, parts III and IV," *The Bell System Technical Journal*, vol. 24, pp. 46–156, 1945.
- [227] S. O. Rice, "Mathematical analysis of random noise," *The Bell System Technical Journal*, vol. 23, pp. 282–332, 1944.
- [228] A. Velcheva, P. Cavaco, and C. G. Soares, "Comparison of methods for calculation of the wave envelope," *Ocean Engineering*, vol. 30, no. 7, pp. 937–948, 2003.
- [229] Z. S. Fang and N. Xie, "An analysis of various methods for computing the envelope of a random signal," *Applied Ocean Research*, vol. 17, no. 1, pp. 9–19, 1995.
- [230] M. A. Tayfun and J. M. Lo, "Wave envelope and related spectra," *Journal of Waterway, Port, Coastal and Ocean Engineering*, vol. 115, no. 4, pp. 515–533, 1989.
- [231] M. K. Ochi and I. I. Sahinoglou, "Stochastic characteristics of wave groups in random seas: part 1—time duration of and number of waves in a wave group," *Applied Ocean Research*, vol. 11, no. 1, pp. 39–50, 1989.
- [232] M. K. Ochi and I. I. Sahinoglou, "Stochastic characteristics of wave groups in random seas: part 2—Frequency of occurrence of wave groups," *Applied Ocean Research*, vol. 11, no. 2, pp. 89–99, 1989.
- [233] M. S. Longuet-Higgins, "Statistical properties of wave groups in a random sea state," *Philosophical Transactions of the Royal Society of London A*, vol. 312, no. 1521, pp. 219–250, 1984.
- [234] N. C. Nigam, *Introduction to Random Vibrations*, MIT Press, Cambridge, Mass, USA, 1983.
- [235] J. N. Yang, "Simulation of random envelope processes," *Journal of Sound and Vibration*, vol. 21, no. 1, pp. 73–85, 1972.
- [236] H. Michiel and K. Laevens, "Teletraffic engineering in a broadband era," *Proceedings of the IEEE*, vol. 85, no. 12, pp. 2007–2033, 1997.
- [237] M. Li and W. Zhao, "Asymptotic identity in min-plus algebra: a report on CPNS," *Computational and Mathematical Methods in Medicine*, vol. 2012, Article ID 154038, 11 pages, 2012.
- [238] D. McDysan, *QoS & Traffic Management in IP & ATM Networks*, McGraw-Hill, New York, NY, USA, 2000.
- [239] D. D. Kouvasos, I. Awan, and K. Al-Begain, "Performance modelling of GPRS with bursty multiclass traffic," *IEEE Proceedings: Computers and Digital Techniques*, vol. 150, no. 2, pp. 75–85, 2003.
- [240] V. Anantharam and T. Konstantopoulos, "Burst reduction properties of the leaky bucket flow control scheme in ATM networks," *IEEE Transactions on Communications*, vol. 42, no. 12, pp. 3085–3089, 1994.
- [241] V. Anantharam and T. Konstantopoulos, "A methodology for the design of optimal traffic shapers in communication networks," *IEEE Transactions on Automatic Control*, vol. 44, no. 3, pp. 583–586, 1999.
- [242] S. W. Mao and S. S. Panwar, "A survey of envelope processes and their applications in quality of service provisioning," *IEEE Communications Surveys & Tutorials*, vol. 8, no. 3, pp. 2–20, 2006.
- [243] M. Fidler, "A survey of deterministic and stochastic service curve models in the network calculus," *IEEE Communications Surveys and Tutorials*, vol. 12, no. 1, pp. 59–86, 2010.
- [244] Y. Yin and G. S. Poo, "End-to-end QoS guarantees for a network based on Latency-Rate Max-Min service curve," *Computer Communications*, vol. 29, no. 18, pp. 3833–3843, 2006.
- [245] K. Pyun, J. Song, and H. K. Lee, "The service curve service discipline for the rate-controlled EDF service discipline in variable-sized packet networks," *Computer Communications*, vol. 29, no. 18, pp. 3886–3899, 2006.
- [246] S. A. Khanjari, B. Arafeh, K. Day, and N. Alzeidi, "Bandwidth borrowing-based QoS approach for adaptive call admission control in multiclass traffic wireless cellular networks," *International Journal of Communication Systems*, vol. 26, no. 7, pp. 811–831, 2013.
- [247] W. Chu, X. Guan, Z. Cai, and L. Gao, "Real-time volume control for interactive network traffic replay," *Computer Networks*, vol. 57, no. 7, pp. 1611–1629, 2013.
- [248] C. A. Fulton and S. Q. Li, "Delay jitter first-order and second-order statistical functions of general traffic on high-speed multimedia networks," *IEEE/ACM Transactions on Networking*, vol. 6, no. 2, pp. 150–163, 1998.
- [249] S. Q. Li and C. L. Hwang, "On the convergence of traffic measurement and queueing analysis: a statistical-matching and queueing (SMAQ) tool," *IEEE/ACM Transactions on Networking*, vol. 5, no. 1, pp. 95–110, 1997.
- [250] W. C. Lau and S. Q. Li, "Statistical multiplexing and buffer sharing in multimedia high-speed networks: a frequency-domain perspective," *IEEE/ACM Transactions on Networking*, vol. 5, no. 3, pp. 382–396, 1997.
- [251] S. Q. Li and J. D. Pruneski, "The linearity of low frequency traffic flow: an intrinsic I/O property in queueing systems," *IEEE/ACM Transactions on Networking*, vol. 5, no. 3, pp. 429–443, 1997.
- [252] S. Jamin, P. B. Danzig, S. J. Shenker, and L. X. Zhang, "A measurement-based admission control algorithm for integrated service packet networks," *IEEE/ACM Transactions on Networking*, vol. 5, no. 1, pp. 56–70, 1997.
- [253] J. J. Wu, J. C. Liu, and W. Zhao, "A general framework for parameterized schedulability bound analysis of real-time

- systems," *IEEE Transactions on Computers*, vol. 59, no. 6, pp. 776–783, 2010.
- [254] B. Chen, S. Kamat, and W. Zhao, "Fault-tolerant, real-time communication in FDDI-based networks," *Computer*, vol. 30, no. 4, pp. 83–90, 1997.
- [255] G. Agrawal, B. Chen, and S. Davari, "Guaranteeing synchronous message deadlines with the timed token medium access control protocol," *IEEE Transactions on Computers*, vol. 43, no. 3, pp. 327–339, 1994.
- [256] F. Feng, W. Zhao, and A. Kumar, "Bounding application-to-application delays for multimedia traffic in FDDI-based communication systems," in *Multimedia Computing and Networking*, vol. 2667 of *Proceedings of the SPIE*, pp. 174–185, San Jose, Calif, USA, January 1996.
- [257] A. Raha, S. Kamat, and W. Zhao, "Admission control for hard real-time connections in ATM LANs," in *Proceedings of the 15th Annual Joint Conference of the IEEE Computer and Communications Societies (INFOCOM '96)*, vol. 1, pp. 180–188, San Francisco, Calif, USA, March 1996.
- [258] W. Zhao and B. Chen, "On guaranteeing message deadlines in ATM-based heterogeneous networks," in *Proceedings of the International Conference of Computing Science*, pp. 186–195, Minneapolis, Minn, USA, October 1996.
- [259] L. Houssin, S. Lahaye, and J. L. Boimond, "Control of (max, +)-linear systems minimizing delays," *Discrete Event Dynamic Systems*, vol. 23, no. 3, pp. 261–276, 2013.
- [260] T. Okumura, J. Matsukidaira, and D. Takahashi, "Max-min-plus expressions for one-dimensional particle cellular automata obtained from a fundamental diagram," *Journal of Physics A*, vol. 46, no. 29, Article ID 295101, 2013.
- [261] N. Shinzawa, "Elimination of variables and the determinant of the max plus algebra," *Journal of Physics A*, vol. 45, no. 10, Article ID 105202, 27 pages, 2012.
- [262] M. Li and W. Zhao, *Analysis of Min-Plus Algebra*, Nova Science Publishers, 2011.
- [263] A. Raha, S. Kamat, and W. Zhao, "Guaranteeing end-to-end deadlines in ATM networks," in *Proceedings of the International Conference on Distributed Computing Systems (ICDCS '95)*, pp. 60–68, Vancouver, Canada, June 1995.
- [264] A. Raha, S. Kamat, X. Jia, and W. Zhao, "Using traffic regulation to meet end-to-end deadlines in ATM networks," *IEEE Transactions on Computers*, vol. 48, no. 9, pp. 917–935, 1999.
- [265] J. K. Ng, S. Song, and W. Zhao, "Integrated end-to-end delay analysis for regulated ATM networks," *Real-Time Systems*, vol. 25, no. 1, pp. 93–124, 2003.
- [266] X. Jia, W. Zhao, and J. Li, "An integrated routing and admission control mechanism for real-time multicast connections in ATM networks," *IEEE Transactions on Communications*, vol. 49, no. 9, pp. 1515–1519, 2001.
- [267] W. Jia and W. Zhao, "Efficient connection admission control algorithms for adaptive QoS real-time connections over ATM networks," *European Transactions on Telecommunications*, vol. 10, no. 2, pp. 135–151, 1999.
- [268] I. Amigo, S. Vaton, T. Chonavel, and F. Larroca, "Maximum delay computation for interdomain path selection," *International Journal of Network Management*, vol. 22, no. 2, pp. 162–179, 2012.
- [269] L. Lenzi, E. Mingozzi, and G. Stea, "Delay bounds for FIFO aggregates: a case study," *Computer Communications*, vol. 28, no. 3, pp. 287–299, 2005.
- [270] G. Boggia, P. Camarda, L. A. Grieco, and S. Mascolo, "Feedback-based bandwidth allocation with call admission control for providing delay guarantees in IEEE 802.11e networks," *Computer Communications*, vol. 28, no. 3, pp. 325–337, 2005.
- [271] M. J. Karam and F. A. Tobagi, "Analysis of delay and delay jitter of voice traffic in the Internet," *Computer Networks*, vol. 40, no. 6, pp. 711–726, 2002.
- [272] H. Fekki, A. T. Lawniczak, and S. Volkov, "Packet Delay in Models of Data Networks," *ACM Transactions on Modeling and Computer Simulation*, vol. 11, no. 3, pp. 233–250, 2001.
- [273] D. E. Wrege, E. W. Knightly, H. Zhang, and J. Liebeherr, "Deterministic delay bounds for VBR video in packet-switching networks: fundamental limits and practical trade-offs," *IEEE/ACM Transactions on Networking*, vol. 4, no. 3, pp. 352–362, 1996.
- [274] J. Liebeherr, D. E. Wrege, and D. Ferrari, "Exact admission control for networks with a bounded delay service," *IEEE/ACM Transactions on Networking*, vol. 4, no. 6, pp. 885–901, 1996.
- [275] S. J. Golestani, "Network delay analysis of a class of fair queueing algorithms," *IEEE Journal on Selected Areas in Communications*, vol. 13, no. 6, pp. 1057–1070, 1995.
- [276] G. Coulouris, J. Dollimore, and T. Kindberg, *Distributed Systems: Concepts and Design*, Addison-Wesley, New York, NY, USA, 3rd edition, 2001.
- [277] W. Zhao, "Challenges in design and implementation of middlewares for real-time systems," *Real-Time Systems*, vol. 20, no. 2, pp. 115–116, 2001.
- [278] S. Davari, T. Leibfried Jr., S. Natarajan, D. Pruett, L. Sha, and W. Zhao, "Real-time issues in the design of the data management system for space station freedom," in *Proceedings of the IEEE Workshop on Real-Time Applications*, pp. 161–165, New York, NY, USA, May 1993.
- [279] Y. Jiang, Q. Yin, Y. Liu, and S. Jiang, "Fundamental calculus on generalized stochastically bounded bursty traffic for communication networks," *Computer Networks*, vol. 53, no. 12, pp. 2011–2021, 2009.
- [280] D. Starobinski and M. Sidi, "Stochastically bounded burstiness for communication networks," *IEEE Transactions on Information Theory*, vol. 46, no. 1, pp. 206–212, 2000.
- [281] J. K. Ng, S. Song, and W. Zhao, "Statistical delay analysis on an ATM switch with self-similar input traffic," *Information Processing Letters*, vol. 74, no. 3, pp. 163–173, 2000.
- [282] S. Borst, M. Mandjes, and M. van Uiter, "Generalized processor sharing with light-tailed and heavy-tailed input," *IEEE/ACM Transactions on Networking*, vol. 11, no. 5, pp. 821–834, 2003.
- [283] Y. Liu, C. K. Tham, and Y. Jiang, "A calculus for stochastic QoS analysis," *Performance Evaluation*, vol. 64, no. 6, pp. 547–572, 2007.
- [284] C. Li, A. Burchard, and J. Liebeherr, "A network calculus with effective bandwidth," *IEEE/ACM Transactions on Networking*, vol. 15, no. 6, pp. 1442–1453, 2007.
- [285] Y. Jiang, "A basic stochastic network calculus," *ACM SIGCOMM Computer Communication Review*, vol. 36, no. 4, pp. 123–134, 2006.
- [286] E. Baccarelli, N. Cordeschi, and T. Patriarca, "QoS Stochastic Traffic Engineering for the wireless support of real-time streaming applications," *Computer Networks*, vol. 56, no. 1, pp. 287–302, 2012.
- [287] M. Li and W. Zhao, "Representation of a stochastic traffic bound," *IEEE Transactions on Parallel and Distributed Systems*, vol. 21, no. 9, pp. 1368–1372, 2010.

- [288] G. A. Korn and T. M. Korn, *Mathematical Handbook for Scientists and Engineers*, McGraw-Hill, New York, NY, USA.
- [289] J. A. Rice, *Mathematical Statistics and Data Analysis*, Wadsworth Inc., 2nd edition, 1995.
- [290] A. A. Borovkov, *Probability Theory*, Springer, New York, NY, USA, 2013.
- [291] T. Field, U. Harder, and P. Harrison, "Network traffic behaviour in switched Ethernet systems," *Performance Evaluation*, vol. 58, no. 2-3, pp. 243–260, 2004.
- [292] A. J. Field, U. Harder, and P. G. Harrison, "Measurement and modelling of self-similar traffic in computer networks," *IEE Proceedings: Communications*, vol. 151, no. 4, pp. 355–363, 2004.
- [293] J. B. Bassingthwaighe, *Fractal Physiology*, Oxford University Press, New York, NY, USA, 1994.

Research Article

Golden Ratio Phenomenon of Random Data Obeying von Karman Spectrum

Ming Li¹ and Wei Zhao²

¹ School of Information Science & Technology, East China Normal University, No. 500, Dong-Chuan Road, Shanghai 200241, China

² Department of Computer and Information Science, University of Macau, Avenue Padre Tomas Pereira, Taipa 1356, Macau

Correspondence should be addressed to Ming Li; ming_lihk@yahoo.com

Received 9 July 2013; Accepted 26 July 2013

Academic Editor: Ezzat G. Bakhoum

Copyright © 2013 M. Li and W. Zhao. This is an open access article distributed under the Creative Commons Attribution License, which permits unrestricted use, distribution, and reproduction in any medium, provided the original work is properly cited.

von Karman originally deduced his spectrum of wind speed fluctuation based on the Stokes-Navier equation. Taking into account, the practical issues of measurement and/or computation errors, we suggest that the spectrum can be described from the point of view of the golden ratio. We call it the golden ratio phenomenon of the von Karman spectrum. To depict that phenomenon, we derive the von Karman spectrum based on fractional differential equations, which bridges the golden ratio to the von Karman spectrum and consequently provides a new outlook of random data following the von Karman spectrum in turbulence. In addition, we express the fractal dimension, which is a measure of local self-similarity, using the golden ratio, of random data governed by the von Karman spectrum.

1. Instruction

The golden ratio, denoted by φ , is an irrational number given by $\varphi = (1 + \sqrt{5})/2$ [1]. The paper by Ackermann [2] may likely be the earliest literature on the golden ratio in a mathematics journal in English in 1895, but it attracted and has attracted the interest of scientists and engineers in various fields of sciences and engineering, ranging from chemistry to computer science; see, for example, [1], Benassi [3], Putz [4], Orita et al. [5], Perez [6], Hassaballah et al. [7], Kellerhals [8], Henein et al. [9], Hurtle [10], Coldea et al. [11], Affleck [12], Jones et al. [13], Kaygn et al. [14], Cervantes et al. [15], Chebotarev [16], Benavoli et al. [17], Manikantan et al. [18], Assimakis et al. [19], Good [20], Davis and Jahnke [21], Totland [22], Moufarrège [23], Boeyens [24], Iñiguez et al. [25], Andrews and Zhang [26], Hofri and Rosberg [27], Itai and Rosberg [28], Cassandras and Julka [29], and Tanackov et al. [30], just to mention a few.

In the field of random functions, more precisely, turbulence in fluid mechanics, a kind of power spectra density (PSD) function introduced by von Karman [31], known as the von Karman spectra (VKS), has been widely used in the diverse fields, ranging from turbulence to acoustic wave propagation in random media; see, for example, Goedecke

et al. [32] and the references therein. Among the von Karman spectra, the spectrum (VKSW for short) expressed in (1) is particularly useful in the field of wind engineering for the modeling of wind speed fluctuation; see, for example, [33–41]. That PSD is in the form

$$S_{\text{von}}(f) = \frac{4u_f^2 b_v w}{f(1 + 70.8w^2)^{5/6}}, \quad w = \frac{fL_u^x}{U}, \quad (1)$$

where f is frequency (Hz), L_u^x is turbulence integral scale, U is mean speed, u_f is friction velocity (ms^{-1}), and b_v is friction velocity coefficient such that the variance of wind speed $\sigma_u^2 = b_v u_f^2$.

Note that (1) was conventionally deduced based on the Stokes-Navier equation ([31], Bauer and Zeibig [42], Tropea [43], Monin and Yaglom [44], Xiushu [45]). It does not originally relate to the concept of either the golden ratio or fractal dimension. As a matter of fact, reports regarding turbulence's fractal dimension derived directly based on the Stokes-Navier equation are rarely seen as Gaoan stated in [46, page 55], letting alone the golden ratio.

This paper aims at contributing the following three results. First, we will propose a rigorous but concise derivation of (1). Then, we will generalize (1) such that the generalization may be described from the point of view of the golden ratio. Finally, we will explain the golden ratio phenomenon of the VKSW from the point of view of fractal dimension or local self-similarity. As a result, we achieve the goal of bridging the golden ratio to the VKSW as well as self-similarity of random data, establishing a new outlook of data following the VKSW.

The rest of the paper is organized as follows. The preliminaries are briefed in Section 2. The results are given in Section 3, which is followed by conclusions.

2. Preliminaries

2.1. Golden Ratio. One of the conventional ways to deduce the golden ratio φ is to solve the difference equation that produces the Fibonacci sequences. The equation is given by (see, e.g., [1], Jamieson [46], Ranum [47], and Eggar [48])

$$F(n) = F(n-1) + F(n-2), \quad (2)$$

$n \in \mathbf{N}$ (the set of natural numbers).

Denote by $Z_F(z)$ the z -transform of $F(n)$. Then, doing the z -transform on both sides of (2) yields

$$Z_F(z) = Z_F(z)(z^{-1} + z^{-2}). \quad (3)$$

The above expression can be rewritten as

$$z^2 - z - 1 = 0. \quad (4)$$

The solutions to (4) are expressed by

$$z_{1,2} = \begin{cases} \frac{1 + \sqrt{5}}{2} \\ \frac{1 - \sqrt{5}}{2} \end{cases}. \quad (5)$$

The golden ratio equals z_1 ; that is,

$$\varphi = z_1 = \frac{1 + \sqrt{5}}{2} \approx 1.618. \quad (6)$$

In addition,

$$z_2 = \frac{1 - \sqrt{5}}{2} = -\frac{1}{\varphi} \approx -0.618. \quad (7)$$

2.2. Fractional Oscillators. There are three types of fractional oscillators. The conventional type, see, for example, Achar et al. [49, 50], is given by

$$\frac{d^{2-\varepsilon} x(t)}{dt^{2-\varepsilon}} + \omega_0^2 x(t) = e(t), \quad 0 < \varepsilon < 1. \quad (8)$$

The second type was introduced by Lim and Muniandy [51]. It is in the form

$$\left(\frac{d^2}{dt^2} + \lambda \right)^\beta x(t) = e(t), \quad \beta > 0. \quad (9)$$

The third type introduced by Lim and Teo [52] is expressed by

$$({}_a D_t^\alpha + \lambda)^\beta x_{\alpha,\beta}(t) = e(t), \quad 0 < \alpha < 1, \beta > 0. \quad (10)$$

The symbol ${}_a D_t^\alpha$ is a fractional differential operator; see, for example, Eab and Lim [53, 54], Lim et al. [55], Klafter et al. [56], Machado et al. [57], and Cattani [58]. In what follows, we use (10) in the general sense.

We now consider the fractional differential equation with the coefficient A in the form

$$A \left(\frac{d}{dt} + \lambda \right)^\beta y_{\text{fOU}}(t) = \eta(t), \quad \beta > 0, \quad (11)$$

where $\eta(t)$ is a white noise. Then, the solution to (11) is the fractional Ornstein-Uhlenbeck (OU) process [59], referring to Coffey et al. [60] for the meaning of OU process.

3. Results

Denote that $g_{\text{fOU}}(t)$ is the impulse response function of (11). Then, it is the solution to the following equation with zero initial conditions

$$A \left(\frac{d}{dt} + \lambda \right)^\beta g_{\text{fOU}}(t) = \delta(t), \quad (12)$$

where $\delta(t)$ is the Dirac- δ function. Doing the Fourier transforms on both sides of the above equation yields

$$G_{\text{fOU}}(f) = \frac{A}{(\lambda - j2\pi f)^\beta}, \quad (13)$$

where $G_{\text{fOU}}(f)$ is the Fourier transform of $g_{\text{fOU}}(t)$.

Let $S_{y_{\text{fOU}}}(f)$ be the PSD of $y_{\text{fOU}}(t)$. Then, $S_{y_{\text{fOU}}}(f)$ is given by

$$S_{y_{\text{fOU}}}(f) = |G_{\text{fOU}}(f)|^2 = \frac{A^2}{[\lambda^2 + (2\pi f)^2]^\beta}. \quad (14)$$

Thus, we have the theorem below.

Theorem 1. Let $X_{vk}(t)$ be the random function that obeys (1). Then, $X_{vk}(t)$ is governed by the fractional differential equation that is in the form

$$\sqrt{A_{vk}} \left(\frac{d}{dt} + B_{vk} \right)^{5/6} X_{vk}(t) = \eta(t). \quad (15)$$

Its solution in frequency domain is given by

$$S_{vk}(f) = \frac{A_{vk}}{[(B_{vk})^2 + (2\pi f)^2]^{5/6}}. \quad (16)$$

Proof. Replacing A , λ , and β in (11) with $\sqrt{A_{vk}}$, B_{vk} , and $5/6$, respectively, yields (15). Substituting A , λ , and β in (14) with $\sqrt{A_{vk}}$, B_{vk} , and $5/6$, respectively, produces (16). Thus, Theorem 1 results. \square

From Theorem 1, we obtain the following corollary.

Corollary 2 (modified VKSW). Let $X_{vk\varphi}(t)$ be the random function that is governed by the fractional differential equation given by

$$\sqrt{A_{vk}} \left(\frac{d}{dt} + B_{vk} \right)^{\varphi/2} X_{vk\varphi}(t) = \eta(t). \quad (17)$$

Then, its solution in frequency domain is in the form

$$S_{vk\varphi}(f) = \frac{A_{vk}}{[(B_{vk})^2 + (2\pi f)^2]^{\varphi/2}}. \quad (18)$$

The proof is straightforward and omitted consequently.

From Theorem 1 and Corollary 2, we immediately have the remark below.

Remark 3. The VKSW may be approximately expressed by the golden ratio.

As a matter of fact,

$$\frac{\varphi}{2} \approx \frac{5}{6}. \quad (19)$$

Thus, (16) approximately equals (18). This may not be a simple approximation but substantially develops the implication of the VKSW from the point of view of the golden ratio.

Note that there are errors in measuring real random data [61–63] and computation errors [64–66]. Thus, from a view of practice, the power of the VKSW may not exactly be the value of 5/6 in most cases in engineering. Rather, it may be in the form

$$\left(\frac{5}{6} \right) + e, \quad (20)$$

where e is error. Thus, by using the golden ratio, (18) is quite reasonable to characterize random functions that obey the VKSW.

For the purpose of exhibiting the results in time domain, we denote by F and F^{-1} the operator of the Fourier transform and its inverse, respectively. Then, we get the theorem below.

Theorem 4. The inverse Fourier transform of $1/[1 + (2\pi f)^2]^{\varphi/2}$ is given by

$$\begin{aligned} F^{-1} \left\{ \frac{1}{[1 + (2\pi f)^2]^{\varphi/2}} \right\} \\ = \frac{2\sqrt{\pi}}{\Gamma(\varphi/2)} \left(\frac{|\tau|}{2} \right)^{(\varphi-1)/2} K_{(\varphi-1)/2}(|\tau|), \end{aligned} \quad (21)$$

where $K_v(z)$ is the modified Bessel function of second kind or the MacDonald function and τ is the time lag.

Proof. Because $(\varphi-1)/2 > 1/2$, according to the computation formula in Gelfand and Vilenkin [67, page 188, in Section 2, Chapter 2], (21) holds. \square

Recall that the Fourier transform of $|t|^\alpha$ is expressed by [68]

$$F(|t|^\alpha) = -2 \sin\left(\frac{\alpha\pi}{2}\right) \Gamma(\alpha+1) |\omega|^{-\alpha-1}, \quad (22)$$

where $\alpha \neq 1, 3, \dots$

Note that

$$S_{vk\varphi}(f) \sim \frac{1}{f^{\varphi/2}} \quad \text{for } f \rightarrow \infty. \quad (23)$$

Then, denoting $r_{vk\varphi}(\tau)$ is the inverse Fourier transform of $S_{vk\varphi}(f)$, one has

$$r_{vk\varphi}(\tau) \sim |\tau|^{(\varphi-1)/2} \quad \text{for } \tau \rightarrow 0. \quad (24)$$

The fractal dimension of a process can be determined by its autocorrelation function (ACF) for $\tau \rightarrow 0$ [69]. Thus,

$$r_{vk}(0) - r_{vk}(\tau) \sim |\tau|^{(\varphi-1)/2} \quad \text{for } \tau \rightarrow 0. \quad (25)$$

Therefore, with the probability one [69], the fractal dimension of the modified von Karman process based on the golden ratio is given by

$$D_{vk\varphi} = \left(2 - \frac{\varphi-1}{4} \right) = \frac{7-\varphi}{4}. \quad (26)$$

Approximately, it is expressed by

$$D_{vk\varphi} \approx 1.346. \quad (27)$$

Note that fractal dimension is a measure of local self-similarity, irregularity, or roughness [70]. High value of fractal dimension of a sample path implies high irregularity of that path. Thus, (26) means that the modified von Karman process with the golden ratio has considerable local irregularity.

We would like to call out the work described above as the golden ratio phenomenon of the von Karman process. From the point of view of our work in data science or big data, this research may not be enough. The future work will investigate possible golden ratio phenomena in other topics of data such as those discussed in [71–82], exploring laws associating with the golden ratio in the universe.

4. Conclusions

We have given the derivation of the von Karman spectrum based on the fractional differential equation (10). The results suggest that the process obeying VKSW is in the class of fractional OU processes. Moreover, we have explained the reasons why the VKSW may be described from the point of view of the golden ratio. The fractal dimension of random data obeying the VKSW by using the golden ratio has also been discussed.

Acknowledgments

This work was supported in part by the National Natural Science Foundation of China under the Project Grant nos. 61272402, 61070214, and 60873264 and by the 973 Plan under the Project Grant no. 2011CB302800.

References

- [1] M. Livio, *The Golden Ratio*, Random House, Inc., 2003.
- [2] E. C. Ackermann, "The golden section," *The American Mathematical Monthly*, vol. 2, no. 9-10, pp. 260-264, 1895.
- [3] E. Benassi, "What do the azobenzene oligomer helices have to do with the golden ratio?" *Computational and Theoretical Chemistry*, vol. 1014, pp. 13-23, 2013.
- [4] M. V. Putz, "Valence atom with bohmian quantum potential: the golden ratio approach," *Chemistry Central Journal*, vol. 6, article 135, 2012.
- [5] M. Orita, K. Ohno, and T. Niimi, "Two "golden ratio" indices in fragment-based drug discovery," *Drug Discovery Today*, vol. 14, no. 5-6, pp. 321-328, 2009.
- [6] J. C. Perez, "Codon populations in single-stranded whole human genome DNA Are fractal and fine-tuned by the golden ratio 1.618," *Interdisciplinary Sciences, Computational Life Sciences*, vol. 2, no. 3, pp. 228-240, 2010.
- [7] M. Hassaballah, K. Murakami, and S. Ido, "Face detection evaluation: a new approach based on the golden ratio Φ ," *Signal, Image and Video Processing*, vol. 7, no. 2, pp. 307-316, 2013.
- [8] R. Kellerhals, "Scissors congruence, the golden ratio and volumes in hyperbolic 5-space," *Discrete and Computational Geometry*, vol. 47, no. 3, pp. 629-658, 2012.
- [9] M. Y. Henein, Y. Zhao, R. Nicoll et al., "The human heart: application of the golden ratio and angle," *International Journal of Cardiology*, vol. 150, no. 3, pp. 239-242, 2011.
- [10] S. Hurtley, "Hidden symmetry revealed," *Science*, vol. 327, no. 5962, p. 123, 2010.
- [11] R. Coldea, D. A. Tennant, E. M. Wheeler et al., "Quantum criticality in an ising chain: experimental evidence for emergent e8 symmetry," *Science*, vol. 327, no. 5962, pp. 177-180, 2010.
- [12] I. Affleck, "Solid-state physics: golden ratio seen in a magnet," *Nature*, vol. 464, no. 7287, pp. 362-363, 2010.
- [13] P. W. Jones, M. Maggioni, and R. Schul, "Manifold parametrizations by eigenfunctions of the Laplacian and heat kernels," *Proceedings of the National Academy of Sciences of the United States of America*, vol. 105, no. 6, pp. 1803-1808, 2008.
- [14] B. Kaygn, B. Balçın, C. Yildiz, and S. Arslan, "The effect of teaching the subject of Fibonacci numbers and golden ratio through the history of mathematics," *Procedia—Social and Behavioral Sciences*, vol. 15, pp. 961-965, 2011.
- [15] E. Cervantes, J. J. Martín, R. Ardanuy, J. G. de Diego, and Á. Tocino, "Modeling the Arabidopsis seed shape by a cardioid: efficacy of the adjustment with a scale change with factor equal to the golden ratio and analysis of seed shape in ethylene mutants," *Journal of Plant Physiology*, vol. 167, no. 5, pp. 408-410, 2010.
- [16] P. Chebotarev, "Spanning forests and the golden ratio," *Discrete Applied Mathematics*, vol. 156, no. 5, pp. 813-821, 2008.
- [17] A. Benavoli, L. Chisci, and A. Farina, "Fibonacci sequence, golden section, Kalman filter and optimal control," *Signal Processing*, vol. 89, no. 8, pp. 1483-1488, 2009.
- [18] K. Manikantan, B. V. Arun, and D. K. S. Yaradoni, "Optimal multilevel thresholds based on Tsallis entropy method using golden ratio particle swarm optimization for improved image segmentation," *Procedia Engineering*, vol. 30, pp. 364-371, 2012.
- [19] N. Assimakis, M. Adam, and C. Triantafyllou, "Lainiotis filter, golden section and Fibonacci sequence," *Signal Processing*, vol. 93, no. 4, pp. 721-730, 2013.
- [20] I. J. Good, "Complex Fibonacci and Lucas numbers, continued fractions, and the square root of the golden ratio (condensed version)," *The Journal of the Operational Research Society*, vol. 43, no. 8, pp. 837-842, 1992.
- [21] S. T. Davis and J. C. Jahnke, "Unity and the golden section: rules for aesthetic choice?" *The American Journal of Psychology*, vol. 104, no. 2, pp. 257-277, 1991.
- [22] H. Totland, "Quartic polynomials and the golden ratio," *Mathematics Magazine*, vol. 82, no. 3, pp. 197-201, 2009.
- [23] R. Moufarrège, "The golden ratios of the breast," in *Breast Augmentation, Principles and Practice*, chapter 13, Springer, New York, NY, USA, 2009.
- [24] J. C. A. Boeyens, "Covalent interaction," in *Electronic Structure and Number Theory, Structure and Bonding*, J. C. A. Boeyens and P. Comba, Eds., vol. 148, Springer, New York, NY, USA, 2013.
- [25] J. Iñiguez, A. Hansen, I. Pérez et al., "On division in extreme and mean ratio and its connection to a particular re-expression of the golden quadratic equation $x^2 - x - 1 = 0$," *Nexus Network Journal*, vol. 8, no. 2, pp. 93-100, 2006.
- [26] M. Andrews and L. Zhang, "Creating templates to achieve low delay in multi-carrier frame-based wireless data systems," *Wireless Networks*, vol. 16, no. 6, pp. 1765-1776, 2010.
- [27] M. Hofri and Z. Rosberg, "Packet delay under the golden ratio weighted TDM policy in a multiple-access channel," *IEEE Transactions on Information Theory*, vol. 33, no. 3, pp. 341-349, 1987.
- [28] A. Itai and Z. Rosberg, "A golden ratio control policy for a multiple-access channel," *IEEE Transactions on Automatic Control*, vol. 29, no. 8, pp. 712-718, 1984.
- [29] C. G. Cassandras and V. Julka, "Scheduling policies using marked/phantom slot algorithms," *Queueing Systems*, vol. 20, no. 1-2, pp. 207-254, 1995.
- [30] I. Tanackov, G. Stojić, J. Tepić, M. Kostelac, F. Sinani, and S. Sremac, "Golden ratio (section aurea) in Markovian ants AI hybrid," in *Adaptive and Intelligent Systems*, vol. 6943 of *Lecture Notes in Computer Science*, pp. 356-367, Springer, New York, NY, USA, 2011.
- [31] T. von Karman, "Progress in the statistical theory of turbulence," *Proceedings of the National Academy of Sciences of the United States of America*, vol. 34, no. 11, pp. 530-539, 1948.
- [32] G. H. Goedecke, V. E. Ostashev, D. K. Wilson, and H. J. Auvermann, "Quasi-wavelet model of von Kármán spectrum of turbulent velocity fluctuations," *Boundary-Layer Meteorology*, vol. 112, no. 1, pp. 33-56, 2004.
- [33] E. E. Morfiadakis, G. L. Glinou, and M. J. Koulouvari, "The suitability of the von Karman spectrum for the structure of turbulence in a complex terrain wind farm," *Journal of Wind Engineering and Industrial Aerodynamics*, vol. 62, no. 2-3, pp. 237-257, 1996.
- [34] M. C. H. Hui, A. Larsen, and H. F. Xiang, "Wind turbulence characteristics study at the Stonecutters Bridge site: part II: wind power spectra, integral length scales and coherences," *Journal of Wind Engineering and Industrial Aerodynamics*, vol. 97, no. 1, pp. 48-59, 2009.
- [35] G. Huang and X. Chen, "Wavelets-based estimation of multivariate evolutionary spectra and its application to nonstationary downburst winds," *Engineering Structures*, vol. 31, no. 4, pp. 976-989, 2009.
- [36] D. K. Wilson, V. E. Ostashev, and G. H. Goedecke, "Quasi-wavelet formulations of turbulence and other random fields with correlated properties," *Probabilistic Engineering Mechanics*, vol. 24, no. 3, pp. 343-357, 2009.

- [37] G. Li and Q. Li, *Theory of Time-Varying Reliability for Engineering Structures and Its Applications*, Science Press, Beijing, China, 2001, (Chinese).
- [38] J. Pang, Z. Lin, and Y. Lu, "Discussion on the simulation of atmospheric boundary layer with spires and roughness elements in wind tunnels," *Experiments and Measurements in Fluid Mechanics*, vol. 18, no. 2, pp. 32–37, 2004 (Chinese).
- [39] Y. Q. Xiao, J. C. Sun, and Q. Li, "Turbulence integral scale and fluctuation wind speed spectrum of typhoon: an analysis based on field measurements," *Journal of Natural Disasters*, vol. 15, no. 5, pp. 45–53, 2006 (Chinese).
- [40] J. C. Kaimal, J. C. Wyngaard, Y. Yzumi, and O. R. Cote, "Spectral characteristics of surface layer turbulence," *Quarterly Journal of the Royal Meteorological Society*, vol. 98, no. 417, pp. 563–589, 1972.
- [41] H. A. Panofsky, D. Larko, R. Lipschutz et al., "Spectra of velocity components over complex terrain," *Quarterly Journal, Royal Meteorological Society*, vol. 108, no. 455, pp. 215–230, 1982.
- [42] M. Bauer and A. Zeibig, "Towards the applicability of the modified von Kármán spectrum to predict trailing edge noise," *Notes on Numerical Fluid Mechanics*, vol. 92, pp. 381–388, 2006.
- [43] C. C. Tropea, A. L. Yarin, and J. F. Foss, Eds., *Springer Handbook of Experimental Fluid Mechanics*, Springer, New York, NY, USA, 2007.
- [44] A. S. Monin and A. M. Yaglom, *Statistical Fluid Mechanics: Mechanics of Turbulence*, vol. 2, The MIT Press, Cambridge, Mass, USA, 1971, edited by J. L. Lumley.
- [45] H. M. Hastings and G. Sugihara, *Fractals, a User's Guide for the Natural Sciences*, Oxford University Press, Oxford, UK, 1993.
- [46] M. J. Jamieson, "Fibonacci numbers and Aitken sequences revisited," *The American Mathematical Monthly*, vol. 97, no. 9, pp. 829–831, 1990.
- [47] D. L. Ranum, "On some applications of Fibonacci numbers," *The American Mathematical Monthly*, vol. 102, no. 7, pp. 640–645, 1995.
- [48] M. H. Eggar, "Applications of Fibonacci numbers," *The Mathematical Gazette*, vol. 63, no. 423, pp. 36–39, 1979.
- [49] B. N. N. Achar, J. W. Hanneken, and T. Clarke, "Damping characteristics of a fractional oscillator," *Physica A*, vol. 339, no. 3–4, pp. 311–319, 2004.
- [50] B. N. N. Achar, J. W. Hanneken, and T. Clarke, "Response characteristics of a fractional oscillator," *Physica A*, vol. 309, no. 3–4, pp. 275–288, 2002.
- [51] S. C. Lim and S. V. Muniandy, "Self-similar Gaussian processes for modeling anomalous diffusion," *Physical Review E*, vol. 66, no. 2, Article ID 021114, 14 pages, 2002.
- [52] S. C. Lim and L. P. Teo, "The fractional oscillator process with two indices," *Journal of Physics A*, vol. 42, no. 6, Article ID 065208, 34 pages, 2009.
- [53] C. H. Eab and S. C. Lim, "Fractional generalized Langevin equation approach to single-file diffusion," *Physica A*, vol. 389, no. 13, pp. 2510–2521, 2010.
- [54] C. H. Eab and S. C. Lim, "Path integral representation of fractional harmonic oscillator," *Physica A*, vol. 371, no. 2, pp. 303–316, 2006.
- [55] S. C. Lim, M. Li, and L. P. Teo, "Langevin equation with two fractional orders," *Physics Letters A*, vol. 372, no. 42, pp. 6309–6320, 2008.
- [56] J. Klafter, S. C. Lim, and R. Metzler, *Fractional Dynamics: Recent Advances*, World Scientific Publishing, Singapore, 2012.
- [57] J. A. T. Machado, M. F. Silva, R. S. Barbosa et al., "Some applications of fractional calculus in engineering," *Mathematical Problems in Engineering*, vol. 2010, Article ID 639801, 34 pages, 2010.
- [58] C. Cattani, "Fractional calculus and Shannon wavelet," *Mathematical Problems in Engineering*, vol. 2012, Article ID 502812, 26 pages, 2012.
- [59] S. C. Lim and S. V. Muniandy, "Generalized Ornstein-Uhlenbeck processes and associated self-similar processes," *Journal of Physics A*, vol. 36, no. 14, pp. 3961–3982, 2003.
- [60] W. T. Coffey, Y. P. Kalmykov, and J. T. Waldron, *The Langevin Equation*, vol. 14 of *World Scientific Series in Contemporary Chemical Physics*, World Scientific Publishing, Singapore, 2nd edition, 2004.
- [61] J. S. Bendat and A. G. Piersol, *Random Data: Analysis and Measurement Procedure*, Wiley Series in Probability and Statistics, John Wiley & Sons, New York, NY, USA, 3rd edition, 2000.
- [62] C. M. Harris, *Shock and Vibration Handbook*, McGraw-Hill, New York, NY, USA, 4th edition, 1995.
- [63] S. V. Gupta, *Measurement Uncertainties*, Springer, New York, NY, USA, 2012.
- [64] W. Gautschi, *Numerical Analysis*, Springer, New York, NY, USA, 2nd edition, 2012.
- [65] S. K. Mitra and J. F. Kaiser, *Handbook for Digital Signal Processing*, John Wiley & Sons, New York, NY, USA, 1993.
- [66] M. Drosig, *Dealing with Uncertainties: A Guide to Error Analysis*, Springer, New York, NY, USA, 2nd edition, 2009.
- [67] I. M. Gelfand and K. Vilenkin, *Generalized Functions*, vol. 1, Academic Press, New York, NY, USA, 1964.
- [68] M. Li and S. C. Lim, "A rigorous derivation of power spectrum of fractional Gaussian noise," *Fluctuation and Noise Letters*, vol. 6, no. 4, pp. C33–C36, 2006.
- [69] P. Hall and R. Roy, "On the relationship between fractal dimension and fractal index for stationary stochastic processes," *The Annals of Applied Probability*, vol. 4, no. 1, pp. 241–253, 1994.
- [70] B. B. Mandelbrot, *Gaussian Self-Affinity and Fractals*, Springer, New York, NY, USA, 2001.
- [71] C. Cattani, G. Pierro, and G. Altieri, "Entropy and multifractality for the myeloma multiple TET 2 gene," *Mathematical Problems in Engineering*, vol. 2012, Article ID 193761, 14 pages, 2012.
- [72] E. G. Bakhoun and M. H. M. Cheng, "Miniature carbon monoxide detector based on nanotechnology," *IEEE Transactions on Instrumentation and Measurement*, vol. 62, no. 1, pp. 240–245, 2013.
- [73] E. G. Bakhoun, "High-sensitivity miniature smoke detector," *IEEE Sensors Journal*, vol. 12, no. 10, pp. 3031–3035, 2012.
- [74] C. Toma, "Advanced signal processing and command synthesis for memory-limited complex systems," *Mathematical Problems in Engineering*, vol. 2012, Article ID 927821, 13 pages, 2012.
- [75] E. G. Bakhoun and C. Toma, "Modeling transitions in complex systems by multiplicative effect of temporal patterns extracted from signal flows," *Mathematical Problems in Engineering*, vol. 2012, Article ID 409856, 11 pages, 2012.
- [76] M. Pinchas, "Symbol error rate as a function of the residual ISI obtained by blind adaptive equalizers for the SIMO and fractional Gaussian noise case," *Mathematical Problems in Engineering*, vol. 2013, Article ID 860389, 9 pages, 2013.
- [77] L. X. Li, C. Yang, S. L. Hui et al., "A reconfigurable logic cell based on a simple dynamical system," *Mathematical Problems in Engineering*. In press.

- [78] Y. M. Wang, "Maximum-norm error estimates of ADI methods for a two-dimensional fractional sub-diffusion equation," *Advances in Mathematical Physics*. In press.
- [79] Z. Wang and L. T. Yan, "The S-transform of sub-fBm and an application to a class of linear sub-fractional BSDEs," *Advances in Mathematical Physics*, vol. 2013, Article ID 827192, 11 pages, 2013.
- [80] H. P. Peng, G. Hu, L. X. Li, Y. X. Yang, and J. H. Xiao, "Constructing dynamic multiple-input multiple-output logic gates," *Mathematical Problems in Engineering*, vol. 2011, Article ID 380345, 12 pages, 2011.
- [81] H. P. Peng, L. X. Li, Y. X. Yang, and F. Sun, "Conditions of parameter identification from time series," *Physical Review E*, vol. 83, no. 3, Article ID 036202, 8 pages, 2011.
- [82] L. X. Li, J. H. Xiao, H. P. Peng, Y. X. Yang, and Y. H. Chen, "Improving synchronous ability between complex networks," *Nonlinear Dynamics*, vol. 69, no. 3, pp. 1105–1110, 2012.

Research Article

Legendre Wavelets Method for Solving Fractional Population Growth Model in a Closed System

M. H. Heydari,¹ M. R. Hooshmandasl,¹ C. Cattani,² and Ming Li³

¹ Faculty of Mathematics, Yazd University, Yazd 89195741, Iran

² Department of Mathematics, University of Salerno, Via Ponte Don Melillo, 84084 Fisciano, Italy

³ School of Information Science & Technology, East China Normal University, Shanghai 200241, China

Correspondence should be addressed to M. R. Hooshmandasl; hooshmandasl@yazduni.ac.ir

Received 7 August 2013; Accepted 17 August 2013

Academic Editor: Cristian Toma

Copyright © 2013 M. H. Heydari et al. This is an open access article distributed under the Creative Commons Attribution License, which permits unrestricted use, distribution, and reproduction in any medium, provided the original work is properly cited.

A new operational matrix of fractional order integration for Legendre wavelets is derived. Block pulse functions and collocation method are employed to derive a general procedure for forming this matrix. Moreover, a computational method based on wavelet expansion together with this operational matrix is proposed to obtain approximate solution of the fractional population growth model of a species within a closed system. The main characteristic of the new approach is to convert the problem under study to a nonlinear algebraic equation.

1. Introduction

In recent years, fractional calculus and differential equations have found enormous applications in mathematics, physics, chemistry, and engineering because of the fact that a realistic modeling of a physical phenomenon having dependence not only at the time instant but also on the previous time history can be successfully achieved by using fractional calculus. The applications of the fractional calculus have been demonstrated by many authors. For examples, it has been applied to model the nonlinear oscillation of earthquakes, fluid-dynamic traffic, frequency dependent damping behavior of many viscoelastic materials, continuum and statistical mechanics, colored noise, solid mechanics, economics, signal processing, and control theory [1–5]. However, during the last decade fractional calculus has attracted much more attention of physicists and mathematicians. Due to the increasing applications, some schemes have been proposed to solve fractional differential equations. The most frequently used methods are Adomian decomposition method (ADM) [6, 7], homotopy perturbation method [8], homotopy analysis method [9], variational iteration method (VIM) [10], fractional differential transform method (FDTM) [11, 12], fractional difference method (FDM) [13], power series method [14], generalized block pulse operational matrix method [15],

and Laplace transform method [16]. Also, recently the Haar wavelets [17], Legendre wavelets [18, 19], and the Chebyshev wavelets of first kind [20–23] and second kind [24] have been developed to solve the fractional differential equations. It is worth noting that wavelets are localized functions, which are the basis for energy-bounded functions and in particular for $L^2(R)$, so that localized pulse problems can be easily approached and analyzed [25–28].

Approximation by orthogonal family of basis functions has found wide applications in science and engineering. The most commonly used orthogonal families of functions in recent years are sine-cosine functions, block pulse functions, Legendre, Chebyshev, and Laguerre polynomials and also orthogonal wavelets, for example Haar, Legendre, Chebyshev, and CAS wavelets. The main advantages of using an orthogonal basis is that the problem under consideration reduces to a system of linear or nonlinear algebraic system equations [18]; thus this act not only simplifies the problem enormously but also speeds up the computation work during the implementation. This work can be done by truncating the series expansion in orthogonal basis function for the unknown solution of the problem and using the operational matrices [29]. There are two main approaches for numerical solution of fractional differential equations.

One approach is based on using the operational matrix of fractional derivative to reduce the problem under consideration into a system of algebraic equations and solving this system to obtain the numerical solution of the problem. Another useful approach is based on converting the underlying fractional differential equations into fractional integral equations, and using the operational matrix of fractional integration, to eliminate the integral operations and reducing the problem into solving a system of algebraic equations. The operational matrix of fractional Riemann-Liouville integration is given by

$$I^\alpha \Psi(x) \approx P^\alpha \Psi(x), \quad (1)$$

where $\Psi(x) = [\psi_1(x), \psi_2(x), \dots, \psi_{\widehat{m}}(x)]^T$, in which $\psi_i(x)$ ($i = 1, 2, \dots, \widehat{m}$) are orthogonal basis functions which are orthogonal with respect to a specific weight function on a certain interval $[a, b]$ and P^α is the operational matrix of fractional integration of $\Psi(x)$. Notice that P^α is a constant $\widehat{m} \times \widehat{m}$ matrix and α is an arbitrary positive constant.

In view of successful application of wavelet operational matrices in numerical solution of integral and differential equations, together with the characteristics of wavelet functions, we believe that they can be applicable in solving fractional population growth model. In this paper, the operational matrix of fractional order integrations for Legendre wavelets is derived, and a general procedure based on collocation method and block Pulse functions (BPFs) for forming this matrix is presented. Then, by using this matrix a computational method for solving fractional population growth model in a closed system is proposed. This paper is organized as follows. In Section 2, some necessary definitions of the fractional calculus are reviewed. In Section 3, the Legendre wavelets with some of their properties are presented. In Section 4, the proposed method for solving fractional population growth model in a closed system is described. Finally a conclusion is drawn in Section 5.

2. Preliminaries

In this section, we present some notations, definitions, and preliminary facts that will be used further in this paper.

The Riemann-Liouville fractional integral operator I^α of order $\alpha \geq 0$ on the usual Lebesgue space $L^1[0, b]$ is given by [30]

$$(I^\alpha u)(x) = \begin{cases} \frac{1}{\Gamma(\alpha)} \int_0^x (x-s)^{\alpha-1} u(s) ds, & \alpha > 0, \\ u(x), & \alpha = 0. \end{cases} \quad (2)$$

The Riemann-Liouville fractional derivative of order $\alpha > 0$ is normally defined as

$$D^\alpha u(x) = \left(\frac{d}{dx} \right)^m I^{m-\alpha} u(x), \quad (m-1 < \alpha \leq m), \quad (3)$$

where m is an integer.

The fractional derivative of order $\alpha > 0$ in the Caputo sense is given by [30]

$$D_*^\alpha u(x) = \frac{1}{\Gamma(m-\alpha)} \int_0^x (x-s)^{m-\alpha-1} u^{(m)}(s) ds, \quad (m-1 < \alpha \leq m), \quad (4)$$

where m is an integer, $x > 0$, and $u^{(m)} \in L^1[0, b]$.

The useful relation between the Riemann-Liouville operator and Caputo operator is given by the following expression:

$$I^\alpha D_*^\alpha u(x) = u(x) - \sum_{k=0}^{m-1} u^{(k)}(0^+) \frac{x^k}{k!}, \quad (m-1 < \alpha \leq m), \quad (5)$$

where m is an integer, $x > 0$, and $u^{(m)} \in L^1[0, b]$.

3. The Legendre Wavelets

In this section, we briefly present some properties of Legendre wavelets.

3.1. Constructing the Legendre Wavelets. Here we introduce a process to construct the Legendre wavelets on the unit interval $[0, 1]$, using recursive wavelet construction which has been proposed in [31, 32] for piecewise polynomials on $[0, 1]$. For this purpose, we first introduce some notations. Throughout this work, \mathbb{N} denotes the set of all natural numbers, $\mathbb{N}_0 = \mathbb{N} \cup \{0\}$ and $\mathbb{Z}_\mu = \{0, 1, \dots, \mu-1\}$, for a positive integer μ .

For an integer $\mu > 1$, we consider the following contractive mappings on the interval $I = [0, 1]$:

$$\psi_\epsilon(t) = \frac{t+\epsilon}{\mu}, \quad t \in [0, 1], \quad \epsilon \in \mathbb{Z}_\mu. \quad (6)$$

It is obvious that the mappings $\{\psi_\epsilon\}$ satisfy the following properties:

$$\begin{aligned} \psi_\epsilon(I) &\subset I, \quad \forall \epsilon \in \mathbb{Z}_\mu, \\ \bigcup_{\epsilon \in \mathbb{Z}_\mu} \psi_\epsilon(I) &= I. \end{aligned} \quad (7)$$

Now, let F_0 denote the finite dimensional linear space on $[0, 1]$ that is spanned by the Legendre polynomials $P_0(2x-1), P_1(2x-1), \dots$, and $P_{M-1}(2x-1)$, where $M \in \mathbb{N}$ and P_m are the Legendre polynomials of degree m , namely,

$$F_0 = \text{span} \{P_m(2x-1) \mid x \in [0, 1], m \in \mathbb{Z}_\mu\}. \quad (8)$$

It is well known that the Legendre polynomials P_m are orthogonal with respect to the weight function $w(x) = 1$ on the interval $[-1, 1]$.

In order to construct an orthonormal basis for $L^2[0, 1]$, for each $\epsilon \in \mathbb{Z}_\mu$ we define an isometry T_ϵ on $L^2[0, 1]$ as follows:

$$(T_\epsilon f)(x) = \begin{cases} \sqrt{\mu} f(\psi_\epsilon^{-1}(x)), & x \in \psi_\epsilon(I), \\ 0, & x \notin \psi_\epsilon(I). \end{cases} \quad (9)$$

Starting from the space F_0 , we define a sequence of spaces $\{F_k \mid k \in \mathbb{N}_0\}$ using the recurrence formula

$$F_{k+1} = \bigoplus_{\epsilon \in \mathbb{Z}_\mu} T_\epsilon F_k, \quad k \in \mathbb{N}_0, \quad (10)$$

where \oplus denotes the direct sum; that is, if A and B are two subspaces of $L^2[0, 1]$ with $A \cap B = \{0\}$, then

$$A \oplus B = \{f + g : f \in A, g \in B\}. \quad (11)$$

The sequence of spaces $\{F_k \mid k \in \mathbb{N}_0\}$ is nested, that is, [32]:

$$\begin{aligned} F_0 \subset F_1 \subset \cdots \subset F_k \subset F_{k+1} \subset \cdots, \\ \dim F_k = M\mu^k, \quad k \in \mathbb{N}_0. \end{aligned} \quad (12)$$

Moreover, similar to Theorem 2.4 in [33], it can be proved that

$$\overline{\bigcup_{k=0}^{\infty} F_k} = L^2[0, 1]. \quad (13)$$

Now, we construct an orthonormal basis for each of the spaces F_k . We first notice that

$$G_0 = \{\sqrt{2m+1}P_m(2x-1) \mid x \in [0, 1], m \in \mathbb{Z}_\mu\} \quad (14)$$

is an orthonormal basis for F_0 , and moreover for $f(x) \in L^2[0, 1]$ with compact support and for $\epsilon \neq \epsilon'$ we have

$$\text{supp}\{T_\epsilon f\} \cap \text{supp}\{T_{\epsilon'} f\} = \emptyset, \quad \epsilon \neq \epsilon', \quad (15)$$

where $\text{supp}(f)$ denotes the support of the function f . It can be simply seen that [31]

$$\begin{aligned} G_k = \{T_{\epsilon_0} \circ \cdots \circ T_{\epsilon_{k-1}} (\sqrt{2m+1}P_m(2x-1)) \mid \\ m \in \mathbb{Z}_M, \epsilon_\ell \in \mathbb{Z}_\mu, \ell \in \mathbb{Z}_k\} \end{aligned} \quad (16)$$

is an orthonormal basis for F_k , where “ \circ ” denotes composition of functions. In other words, if for $n = 1, 2, \dots, \mu^k$, $k \in \mathbb{N}$, we set

$$\begin{aligned} \psi_{nm}(x) &= \psi(k, m, n, x) \\ &= \begin{cases} \sqrt{2m+1}\mu^{k/2}P_m(2\mu^k x - 2n+1), & x \in \left[\frac{n-1}{\mu^k}, \frac{n}{\mu^k}\right), \\ 0, & \text{otherwise,} \end{cases} \end{aligned} \quad (17)$$

then $\{\psi_{nm}(x) \mid n = 1, 2, \dots, \mu^k, m \in \mathbb{Z}_M\}$ forms an orthonormal basis for F_k .

3.2. Function Approximation. A function $f(x)$ defined over $[0, 1]$ may be expanded by the Legendre wavelets as

$$u(x) = \sum_{n=1}^{\infty} \sum_{m=0}^{\infty} c_{nm} \psi_{nm}(x), \quad (18)$$

where $c_{nm} = (u(x), \psi_{nm}(x))$, and (\cdot, \cdot) denotes the inner product. If the infinite series in (18) is truncated, then it can be written as

$$u(x) \approx \sum_{n=1}^{\mu^k} \sum_{m=0}^{M-1} c_{nm} \psi_{nm}(x) = C^T \Psi(x), \quad (19)$$

where T indicates transposition, C and $\Psi(x)$ are $\widehat{m} = \mu^k M$ column vectors which are given by

$$\begin{aligned} C &= [c_{10}, \dots, c_{1M-1} \mid c_{20}, \dots, c_{2M-1} \mid \cdots \mid c_{\mu^k 0}, \dots, c_{\mu^k M-1}]^T, \\ \Psi(x) &= [\psi_{10}(x), \dots, \psi_{1M-1}(x) \mid \psi_{20}(x), \dots, \\ &\quad \psi_{2M-1}(x) \mid \cdots \mid \psi_{\mu^k 0}(x), \dots, \psi_{\mu^k M-1}(x)]^T. \end{aligned} \quad (20)$$

Taking the collocation points

$$t_i = \frac{(2i-1)}{2\widehat{m}}, \quad i = 1, 2, \dots, \widehat{m}, \quad (21)$$

we define the wavelet matrix $\Phi_{\widehat{m} \times \widehat{m}}$ as

$$\Phi_{\widehat{m} \times \widehat{m}} = \left[\Psi\left(\frac{1}{2\widehat{m}}\right), \Psi\left(\frac{3}{2\widehat{m}}\right), \dots, \Psi\left(\frac{2\widehat{m}-1}{2\widehat{m}}\right) \right]. \quad (22)$$

Indeed $\Phi_{\widehat{m} \times \widehat{m}}$ has the following form:

$$\Phi_{\widehat{m} \times \widehat{m}} = \begin{pmatrix} A & 0 & 0 & \cdots & 0 \\ 0 & A & 0 & \cdots & 0 \\ 0 & 0 & A & \cdots & 0 \\ \vdots & \vdots & \vdots & \ddots & \vdots \\ 0 & 0 & \cdots & 0 & A \end{pmatrix}, \quad (23)$$

where A is an $M \times M$ matrix given by

$$A = \begin{pmatrix} \psi_{10}\left(\frac{1}{2\widehat{m}}\right) & \psi_{10}\left(\frac{3}{2\widehat{m}}\right) & \cdots & \psi_{10}\left(\frac{2\widehat{m}-1}{2\widehat{m}}\right) \\ \psi_{11}\left(\frac{1}{2\widehat{m}}\right) & \psi_{11}\left(\frac{3}{2\widehat{m}}\right) & \cdots & \psi_{11}\left(\frac{2\widehat{m}-1}{2\widehat{m}}\right) \\ \vdots & \vdots & \vdots & \vdots \\ \psi_{\mu^k M-1}\left(\frac{1}{2\widehat{m}}\right) & \psi_{\mu^k M-1}\left(\frac{3}{2\widehat{m}}\right) & \cdots & \psi_{\mu^k M-1}\left(\frac{2\widehat{m}-1}{2\widehat{m}}\right) \end{pmatrix}. \quad (24)$$

For example, for $\mu = 3$, $k = 1$, $M = 2$, the Legendre matrix can be expressed as:

$$\Phi_{6 \times 6} = \begin{pmatrix} 1.7321 & 1.7321 & 0.0 & 0.0 & 0.0 & 0.0 \\ -1.5000 & 1.5000 & 0.0 & 0.0 & 0.0 & 0.0 \\ 0.0 & 0.0 & 1.7321 & 1.7321 & 0.0 & 0.0 \\ 0.0 & 0.0 & -1.5000 & 1.5000 & 0.0 & 0.0 \\ 0.0 & 0.0 & 0.0 & 0.0 & 1.7321 & 1.7321 \\ 0.0 & 0.0 & 0.0 & 0.0 & -1.5000 & 1.5000 \end{pmatrix}. \quad (25)$$

3.3. Operational Matrix of Fractional Order Integration. The fractional integration of order α of the vector function $\Psi(x)$ can be expressed as

$$(I^\alpha \Psi)(x) \simeq P^\alpha \Psi(x), \quad (26)$$

where P^α is the $\widehat{m} \times \widehat{m}$ operational matrix of fractional integration of order α . In the following we obtain an explicit form of the matrix P . For this purpose, we need to introduce a new family of basis functions, namely, block pulse functions (BPFs).

We define a \widehat{m} -set of BPFs as [34, 35]

$$b_i(x) = \begin{cases} 1, & \frac{i}{\widehat{m}} \leq x < \frac{(i+1)}{\widehat{m}}, \\ 0, & \text{otherwise,} \end{cases} \quad (27)$$

where $i = 0, 1, 2, \dots, (\widehat{m} - 1)$.

The functions $b_i(x)$ are disjoint and orthogonal.

The Legendre wavelets may be expanded into a \widehat{m} -set of BPFs as

$$\Psi(x) \simeq \Phi_{\widehat{m} \times \widehat{m}} B_{\widehat{m}}(x), \quad (28)$$

where $B_{\widehat{m}}(x) = [b_0(x), b_1(x), \dots, b_i(x), \dots, b_{\widehat{m}-1}(x)]^T$.

In [34], Kilicman et al. have given the block pulse operational matrix of fractional integration P_B^α as

$$(I^\alpha B_{\widehat{m}})(x) \simeq P_B^\alpha B_{\widehat{m}}(x), \quad (29)$$

where

$$P_B^\alpha = \frac{1}{\widehat{m}^\alpha} \frac{1}{\Gamma(\alpha + 2)} \begin{pmatrix} 1 & \xi_1 & \xi_2 & \cdots & \xi_{\widehat{m}-1} \\ 0 & 1 & \xi_1 & \cdots & \xi_{\widehat{m}-2} \\ 0 & 0 & 1 & \cdots & \xi_{\widehat{m}-3} \\ 0 & 0 & 0 & \ddots & \vdots \\ 0 & 0 & 0 & 0 & 1 \end{pmatrix}, \quad (30)$$

and $\xi_i = (i+1)^{\alpha+1} - 2i^{\alpha+1} + (i-1)^{\alpha+1}$.

Next, we derive the Legendre wavelets operational matrix of fractional integration. By considering (26) and using (28), and (29) we have

$$\begin{aligned} (I^\alpha \Psi)(x) &\simeq (I^\alpha \Phi_{\widehat{m} \times \widehat{m}} B_{\widehat{m}})(x) = \Phi_{\widehat{m} \times \widehat{m}} (I^\alpha B_{\widehat{m}})(x) \\ &\simeq \Phi_{\widehat{m} \times \widehat{m}} P_B^\alpha B_{\widehat{m}}(x). \end{aligned} \quad (31)$$

Thus, by considering (28) and (31), we obtain the Legendre wavelets operational matrix of fractional integration as

$$(I^\alpha \Psi)(x) \simeq \Phi_{\widehat{m} \times \widehat{m}} P_B^\alpha \Phi_{\widehat{m} \times \widehat{m}}^{-1}. \quad (32)$$

To illustrate the calculation procedure we choose $\mu = 3$, $k = 1$, $M = 2$, and $\alpha = 1/2$; thus we have:

$$P^{(1/2)} = \begin{pmatrix} 0.43433 & 0.14689 & 0.35988 & -0.069510 & 0.23430 & -0.017626 \\ -0.11016 & 0.17991 & 0.052129 & -0.028562 & 0.013219 & -0.0032248 \\ 0.0 & 0.0 & 0.43433 & 0.14689 & 0.35988 & -0.069510 \\ 0.0 & 0.0 & -0.11016 & 0.17991 & 0.052129 & -0.028562 \\ 0.0 & 0.0 & 0.0 & 0.0 & 0.43433 & 0.14689 \\ 0.0 & 0.0 & 0.0 & 0.0 & -0.11016 & 0.17991 \end{pmatrix}. \quad (33)$$

4. Application for Fractional Population Growth Model

As we have already mentioned, the fractional order models are more accurate than integer order models; that is, there are more degrees of freedom in the fractional order models. In this section, we will apply Legendre wavelets for solving a fractional population growth model. The model is characterized by the nonlinear fractional Volterra integrodifferential equation [36] as follows:

$$D_*^\alpha p(\bar{t}) - \bar{a}p(\bar{t}) + \bar{b}[p(\bar{t})]^2 + \bar{c}p(\bar{t}) \int_0^{\bar{t}} p(\tau) d\tau = 0, \quad (34)$$

$$p(0) = p_0, \quad 0 < \alpha \leq 1,$$

where α is a constant parameter describing the order of the time fractional derivative, $\bar{a} > 0$ is the birth rate coefficient, $\bar{b} > 0$ is the crowding coefficient, $\bar{c} > 0$ is the toxicity coefficient, p_0 is the initial population, and $p(\bar{t})$ is the population of identical individuals at time \bar{t} which exhibits crowding and sensitivity to the amount of toxins produced [37]. The coefficient \bar{c} indicates the essential behavior of the population evolution before its level falls to zero in the long run. It is worth mentioning that when the toxicity coefficient is zero, (34) reduces to the well-known logistic equation [37, 38]. The last term contains the integral which indicates the total metabolism or total amount of toxins produced since time zero. The individual death rate is proportional to this integral, and also the population death rate due to toxicity must include a factor p . Due to the fact that the system is closed, the presence of the toxic term always causes the population level falling to zero in the long run, as it will be seen later. The relative size of the sensitivity to toxins, \bar{c} , determines the manner in which the population evolves before its extinction. It is worth noting that in case $\alpha = 1$, the fractional equation reduces to a classical logistic growth model, so the proposed method can be also applied in this situation. Here we apply the scale time and population by introducing the non-dimensional variables $t = \bar{c}\bar{t}/\bar{b}$ and $u = \bar{b}p/\bar{a}$, to obtain the following non-dimensional problem:

$$\kappa D_*^\alpha u(t) - u(t) + [u(t)]^2 + u(t) \int_0^t u(\tau) d\tau = 0, \quad (35)$$

$$u(0) = u_0, \quad 0 < \alpha \leq 1,$$

where $u(t)$ is the scaled population of identical individuals at time t and $\kappa = \bar{c}/\bar{a}\bar{b}$ is a prescribed non-dimensional

parameter. The only equilibrium solution of (35) is the trivial solution $u(t) = 0$, and the analytical solution for $\alpha = 1$ is [39]

$$u(t) = u_0 \exp\left(\frac{1}{\kappa} \int_0^t \left(1 - u(\tau) - \int_0^\tau u(s) ds\right) d\tau\right). \quad (36)$$

In recent years, several numerical methods have been proposed to solve the classical and fractional population growth model, for instance, the reader is advised to see [36–43] and references therein. Here we use the operational matrix of fractional integration for solving nonlinear fractional integrodifferential population model (35). For this purpose, we first approximate $D_*^\alpha u(t)$ as

$$D_*^\alpha u(t) \approx U^T \Psi(t), \quad (37)$$

where U is an unknown vector which should be found and $\Psi(t)$ is the vector which is defined in (20).

By using initial condition and (5), we have

$$u(t) \approx U^T P^\alpha \Psi(t) + u_0. \quad (38)$$

Since $\Psi(t) \approx \Phi_{\bar{m} \times \bar{m}} B_{\bar{m}}(t)$, from (38), we have:

$$u(t) \approx U^T P^\alpha \Phi_{\bar{m} \times \bar{m}} B_{\bar{m}}(t) + u_0 [1, 1, \dots, 1] B_{\bar{m}}(t). \quad (39)$$

Define

$$A^T = [a_1, a_2, \dots, a_{\bar{m}}] = U^T P^\alpha \Phi_{\bar{m} \times \bar{m}} + u_0 [1, 1, \dots, 1]. \quad (40)$$

By using (38) and (39), we have $u(t) \approx A^T B_{\bar{m}}(t)$. From (27), we have

$$[u(t)]^2 \approx [a_1^2, a_2^2, \dots, a_{\bar{m}}^2] B_{\bar{m}}(t) = \tilde{A}^T B_{\bar{m}}(t). \quad (41)$$

Also, we have

$$\int_0^t u(\tau) d\tau \approx A^T P_B B_{\bar{m}}(t) = C^T B_{\bar{m}}(t), \quad (42)$$

where $C^T = A^T P_B$. Now using (27), (39), and (42), we have

$$u(t) \int_0^t u(\tau) d\tau \approx \tilde{U}^T B_{\bar{m}}(t), \quad (43)$$

where

$$\tilde{U}^T = [a_1 c_1, a_2 c_2, \dots, a_{\bar{m}} c_{\bar{m}}]. \quad (44)$$

Now by substituting (37), (39), (41) and (43), into (35), we obtain

$$(\bar{\kappa} U^T \Phi_{\bar{m} \times \bar{m}} - A^T + \tilde{A}^T + \tilde{U}^T) B_{\bar{m}}(t) \approx 0, \quad (45)$$

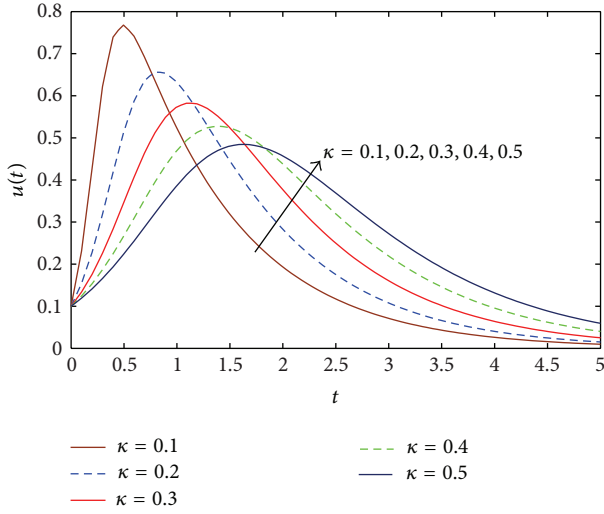


FIGURE 1: Numerical solutions of the classical population growth model for different values of κ .

and by replacing \approx by $=$, we obtain the following system of nonlinear algebraic equations:

$$\kappa U^T \Phi_{\widehat{m} \times \widehat{m}} - A^T + \widetilde{A}^T + \widetilde{U}^T = 0. \quad (46)$$

Finally by solving this system and determining A , we obtain the approximate solution of the problem as $u(t) = A^T \Psi(t)$.

As a numerical example, we consider the nonlinear fractional integrodifferential equation (35) with the initial condition $u(0) = 0.1$, which is investigated in several papers, for instance see [36–43]. Here our purpose is to study the mathematical behavior of the solution of this fractional population growth model as the order of the fractional derivative changes. In particular, we seek to study the rapid growth along the logistic curve that will reach a peak then slow exponential decay for different values of α . To see the behavior solution of this problem for different values of α , we will take advantage of the proposed method and consider the following two special cases.

Case 1. We investigate the classical population growth model ($\alpha = 1$) for some different small values κ . The behavior of the numerical solutions for $\widehat{m} = 162$ ($\mu = 3$, $k = 3$, and $M = 6$) is shown in Figure 1. From Figure 1 it can be seen that as κ increases, the amplitude of $u(t)$ decreases, whereas the exponential decay increases.

Case 2. In this case we investigate the fractional population growth model (35) for different values of α and κ .

From Figures 2, 3, and 4 it can be simply seen that as the order of the fractional derivative decreases, the amplitude of $u(t)$ decreases, whereas the exponential decay increases and also it can be concluded that as κ increases, the maximum of $u(t^*)$ of $u(t)$ decreases. This tendency is similar to the case $\alpha = 1$, which we have already mentioned.

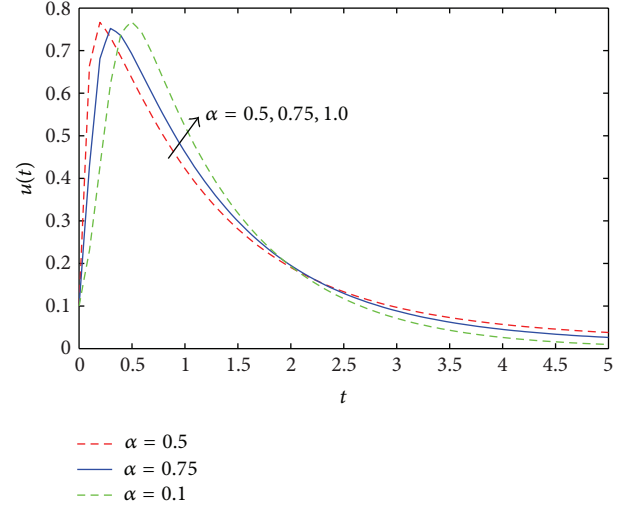


FIGURE 2: Numerical solutions of the fractional population growth model for $\kappa = 0.1$.

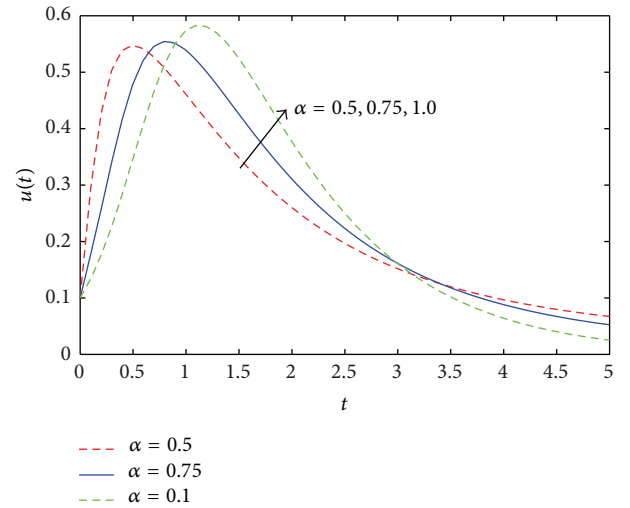


FIGURE 3: Numerical solutions of the fractional population growth model for $\kappa = 0.3$.

5. Conclusion

In this paper, the operational matrix of fractional order integration for Legendre wavelets was derived. Block pulse functions and collocation method were employed to derive a general procedure for forming this matrix. Moreover, a wavelet expansion together with this operational matrix was used to obtain approximate solution of the fractional population growth model of a species within a closed system. The main characteristic of the new approach is to convert the problem under study to a system of nonlinear algebraic equations by introducing the operational matrix of fractional integration for these basis functions. Analysis of the behavior of the model showed that it increases rapidly along the logistic curve followed by a slow exponential decay after reaching a maximum point, and also when the order of

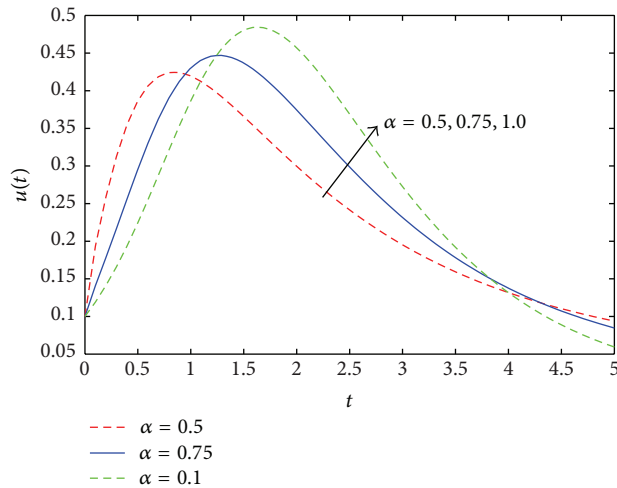


FIGURE 4: Numerical solutions of the fractional population growth model for $\kappa = 0.5$.

the fractional derivative α decreases, the amplitude of the solution decreases, whereas the exponential decay increases.

Acknowledgment

This work was supported in part by the National Natural Science Foundation of China under the project Grant nos. 61272402, 61070214, and 60873264.

References

- [1] J. H. He, "Nonlinear oscillation with fractional derivative and its applications," in *Proceedings of the International Conference on Vibrating Engineering*, vol. 98, pp. 288–291, Dalian, China, 1998.
- [2] R. L. Bagley and P. J. Torvik, "A theoretical basis for the application of fractional calculus to viscoelasticity," *Journal of Rheology*, vol. 27, no. 3, pp. 201–210, 1983.
- [3] F. Mainardi, "Fractional calculus: some basic problems in continuum and statistical mechanics," in *Fractals and Fractional Calculus in Continuum Mechanics*, A. Carpinteri and F. Mainardi, Eds., vol. 378, pp. 291–348, Springer, New York, NY, USA, 1997.
- [4] Y. A. Rossikhin and M. V. Shitikova, "Applications of fractional calculus to dynamic problems of linear and nonlinear hereditary mechanics of solids," *Applied Mechanics Reviews*, vol. 50, pp. 15–67, 1997.
- [5] R. T. Baillie, "Long memory processes and fractional integration in econometrics," *Journal of Econometrics*, vol. 73, no. 1, pp. 5–59, 1996.
- [6] S. Momani and Z. Odibat, "Numerical approach to differential equations of fractional order," *Journal of Computational and Applied Mathematics*, vol. 207, no. 1, pp. 96–110, 2007.
- [7] S. A. El-Wakil, A. Elhanbaly, and M. A. Abdou, "Adomian decomposition method for solving fractional nonlinear differential equations," *Applied Mathematics and Computation*, vol. 182, no. 1, pp. 313–324, 2006.
- [8] N. H. Sweilam, M. M. Khader, and R. F. Al-Bar, "Numerical studies for a multi-order fractional differential equation," *Physics Letters A*, vol. 371, no. 1-2, pp. 26–33, 2007.
- [9] I. Hashim, O. Abdulaziz, and S. Momani, "Homotopy analysis method for fractional IVPs," *Communications in Nonlinear Science and Numerical Simulation*, vol. 14, no. 3, pp. 674–684, 2009.
- [10] S. Das, "Analytical solution of a fractional diffusion equation by variational iteration method," *Computers & Mathematics with Applications*, vol. 57, no. 3, pp. 483–487, 2009.
- [11] A. Arikoglu and I. Ozkol, "Solution of fractional integro-differential equations by using fractional differential transform method," *Chaos, Solitons and Fractals*, vol. 40, no. 2, pp. 521–529, 2009.
- [12] V. S. Ertürk and S. Momani, "Solving systems of fractional differential equations using differential transform method," *Journal of Computational and Applied Mathematics*, vol. 215, no. 1, pp. 142–151, 2008.
- [13] M. M. Meerschaert and C. Tadjeran, "Finite difference approximations for two-sided space-fractional partial differential equations," *Applied Numerical Mathematics*, vol. 56, no. 1, pp. 80–90, 2006.
- [14] Z. M. Odibat and N. T. Shawagfeh, "Generalized Taylor's formula," *Applied Mathematics and Computation*, vol. 186, no. 1, pp. 286–293, 2007.
- [15] Y. Li and N. Sun, "Numerical solution of fractional differential equations using the generalized block pulse operational matrix," *Computers & Mathematics with Applications*, vol. 62, no. 3, pp. 1046–1054, 2011.
- [16] I. Podlubny, "The Laplace transform method for linear differential equations of the fractional order," UEF-02-94, Institute of Experimental Physics, Slovak Academy of Sciences, Kosice, Slovakia, 1994.
- [17] Y. Li and W. Zhao, "Haar wavelet operational matrix of fractional order integration and its applications in solving the fractional order differential equations," *Applied Mathematics and Computation*, vol. 216, no. 8, pp. 2276–2285, 2010.
- [18] M. Rehman and R. Ali Khan, "The Legendre wavelet method for solving fractional differential equations," *Communications in Nonlinear Science and Numerical Simulation*, vol. 16, no. 11, pp. 4163–4173, 2011.
- [19] M. H. Heydari, M. R. Hooshmandasl, F. M. M. Ghaini, and F. Fereidouni, "Two-dimensional legendre wavelets for solving fractional poisson equation with dirichlet boundary conditions," *Engineering Analysis With Boundary Elements*, vol. 37, pp. 1331–1338, 2013.
- [20] Y. Li, "Solving a nonlinear fractional differential equation using Chebyshev wavelets," *Communications in Nonlinear Science and Numerical Simulation*, vol. 15, no. 9, pp. 2284–2292, 2010.
- [21] M. H. Heydari, M. R. Hooshmandasl, F. M. M. Ghaini, and F. Mohammadi, "Wavelet collocation method for solving multi order fractional differential equations," *Journal of Applied Mathematics*, vol. 2012, Article ID 542401, 19 pages, 2012.
- [22] M. H. Heydari, M. R. Hooshmandasl, F. Mohammadi, and C. Cattani, "Wavelets method for solving systems of nonlinear singular fractional volterra integro-differential equations," *Communications in Nonlinear Science and Numerical Simulation*, vol. 19, no. 1, pp. 37–48, 2014.
- [23] M. R. Hooshmandasl, M. H. Heydari, and F. M. M. Ghaini, "Numerical solution of the one-dimensional heat equation by using chebyshev wavelets method," *Applied and Computational Mathematics*, vol. 1, no. 6, Article ID 42401, 19 pages, 2012.
- [24] Y. Wang and Q. Fan, "The second kind Chebyshev wavelet method for solving fractional differential equations," *Applied*

- Mathematics and Computation*, vol. 218, no. 17, pp. 8592–8601, 2012.
- [25] C. Cattani, “Fractional calculus and Shannon wavelet,” *Mathematical Problems in Engineering*, vol. 2012, Article ID 502812, 26 pages, 2012.
 - [26] C. Cattani, “Shannon wavelets for the solution of integrodifferential equations,” *Mathematical Problems in Engineering*, vol. 2010, Article ID 408418, 22 pages, 2010.
 - [27] C. Cattani and A. Kudreyko, “Harmonic wavelet method towards solution of the Fredholm type integral equations of the second kind,” *Applied Mathematics and Computation*, vol. 215, no. 12, pp. 4164–4171, 2010.
 - [28] C. Cattani, “Shannon wavelets theory,” *Mathematical Problems in Engineering*, vol. 2008, Article ID 164808, 24 pages, 2008.
 - [29] J. Biazar and H. Ebrahimi, “Chebyshev wavelets approach for nonlinear systems of Volterra integral equations,” *Computers & Mathematics with Applications*, vol. 63, no. 3, pp. 608–616, 2012.
 - [30] I. Podlubny, *Fractional Differential Equations*, vol. 198, Academic Press, San Diego, Calif, USA, 1999.
 - [31] Y. Shen and W. Lin, “Collocation method for the natural boundary integral equation,” *Applied Mathematics Letters*, vol. 19, no. 11, pp. 1278–1285, 2006.
 - [32] C. A. Micchelli and Y. Xu, “Reconstruction and decomposition algorithms for biorthogonal multiwavelets,” *Multidimensional Systems and Signal Processing*, vol. 8, no. 1-2, pp. 31–69, 1997.
 - [33] C. A. Micchelli and Y. Xu, “Using the matrix refinement equation for the construction of wavelets on invariant sets,” *Applied and Computational Harmonic Analysis*, vol. 1, no. 4, pp. 391–401, 1994.
 - [34] A. Kilicman, A. Zhour, and Z. A. Aziz, “Kronecker operational matrices for fractional calculus and some applications,” *Applied Mathematics and Computation*, vol. 187, no. 1, pp. 250–265, 2007.
 - [35] M. H. Heydari, M. R. Hooshmandasl, and F. M. M. Ghaini, “A good approximate solution for lienard equation in a large interval using block pulse functions,” *Journal of Mathematical Extension*, vol. 7, no. 1, pp. 17–32, 2013.
 - [36] H. Xu, “Analytical approximations for a population growth model with fractional order,” *Communications in Nonlinear Science and Numerical Simulation*, vol. 14, no. 5, pp. 1978–1983, 2009.
 - [37] K. G. TeBeest, “Numerical and analytical solutions of Volterra’s population model,” *SIAM Review*, vol. 39, no. 3, pp. 484–493, 1997.
 - [38] F. M. Scudo, “Vito Volterra and theoretical ecology,” *Theoretical Population Biology*, vol. 2, pp. 1–23, 1971.
 - [39] K. Parand, A. R. Rezaei, and A. Taghavi, “Numerical approximations for population growth model by rational chebyshev and hermite functions collocation approach: a comparison,” *Mathematical Methods in the Applied Sciences*, vol. 33, no. 17, pp. 2076–2086, 2010.
 - [40] A.-M. Wazwaz, “Analytical approximations and Padé approximants for Volterra’s population model,” *Applied Mathematics and Computation*, vol. 100, no. 1, pp. 13–25, 1999.
 - [41] K. Al-Khaled, “Numerical approximations for population growth models,” *Applied Mathematics and Computation*, vol. 160, no. 3, pp. 865–873, 2005.
 - [42] K. Al-Khaled, “Analytical approximations for a population growth model with fractional order,” *Communications in Nonlinear Science and Numerical Simulation*, vol. 14, pp. 1978–1983.
 - [43] K. Krishnaveni and S. B. K. Kannan, “Approximate analytical solution for fractional population growth model,” *International Journal of Engineering and Technology*, vol. 5, no. 3, pp. 2832–2836, 2013.

Research Article

An Efficient Patch Dissemination Strategy for Mobile Networks

Dawei Zhao,^{1,2} Haipeng Peng,^{1,2} Lixiang Li,^{1,2} Yixian Yang,^{1,2} and Shudong Li³

¹ Information Security Center, State Key Laboratory of Networking and Switching Technology,
Beijing University of Posts and Telecommunications, Beijing 100876, China

² National Engineering Laboratory for Disaster Backup and Recovery, Beijing University of Posts and Telecommunications,
Beijing 100876, China

³ College of Mathematics and Information Science, Shandong Institute of Business and Technology, Shandong, Yantai 264005, China

Correspondence should be addressed to Haipeng Peng; penghaipeng@bupt.edu.cn

Received 8 June 2013; Accepted 5 July 2013

Academic Editor: Ming Li

Copyright © 2013 Dawei Zhao et al. This is an open access article distributed under the Creative Commons Attribution License, which permits unrestricted use, distribution, and reproduction in any medium, provided the original work is properly cited.

Mobile phones and personal digital assistants are becoming increasingly important in our daily life since they enable us to access a large variety of ubiquitous services. Mobile networks, formed by the connection of mobile devices following some relationships among mobile users, provide good platforms for mobile virus spread. Quick and efficient security patch dissemination strategy is necessary for the update of antivirus software so that it can detect mobile virus, especially the new virus under the wireless mobile network environment with limited bandwidth which is also large scale, decentralized, dynamically evolving, and of unknown network topology. In this paper, we propose an efficient semi autonomy-oriented computing (SAOC) based patch dissemination strategy to restrain the mobile virus. In this strategy, some entities are deployed in a mobile network to search for mobile devices according to some specific rules and with the assistance of a center. Through experiments involving both real-world networks and dynamically evolving networks, we demonstrate that the proposed strategy can effectively send security patches to as many mobile devices as possible at a considerable speed and lower cost in the mobile network. It is a reasonable, effective, and secure method to reduce the damages mobile viruses may cause.

1. Introduction

The last decade has witnessed a surge of wireless mobile devices such as mobile phones, PocketPCs, netbooks, and tablet PCs. With the appearance and development of intelligent operating system, mobile devices are getting smarter and more functional. For example, they can connect to the Internet, receive and send emails and short messages (SMS)/multimedia messages (MMS), and connect to other devices for exchanging information and activating various applications. Meanwhile, these mobile devices also become the ideal targets of mobile virus because they are popular, designed to be open, programmable, and general of purpose, and highly dependent on common software platforms such as Android, Symbian, Windows Mobile, and Linux.

Mobile networks, formed by the connection of mobile devices following some relationships among mobile users, provide good platforms for mobile virus spread. For

example, an MMS-based worm named “Commwarrior” (<http://www.f-secure.com/v-descs/commwarrior.shtml>) can spread in MMS network which is formed based on the social relationships among mobile users. And a Bluetooth-based worm named “Cabir” (<http://www.f-secure.com/v-descs/cabir.shtml>) can spread in Bluetooth network which is formed according to the geographical positions of mobile devices. There have been extensive studies on modeling the virus/epidemic propagation [1–6] in complex networks which can be used to estimate the scale of a virus/epidemic outbreak before it actually occurs and evaluate the effect of new or improved countermeasures in restraining virus/epidemic propagation. And based on these studies, many network immunization strategies [7–10] have been proposed for restraining virus propagation by selectively immunizing some nodes based on the measurements of degree or betweenness. But it would be difficult for these strategies to deal with large-scale, decentralized, and dynamic

mobile networks. Intrusion detection technology [11] is another straight and effective means for the containment of mobile virus. However, the detection capabilities of most antivirus software are depend on the existence of an updated virus signature repository. Antivirus users are not protected whenever an attacker spreads a previously never encountered virus. In order to protect the mobile phones from the damage of new virus, service providers or security companies need to quickly identify the new virus, generate a signature, and disseminate patches to smart phones. Currently, most researches have been done on intrusion detection [11–13] and patch generation [14–16], while this paper aims to study the dissemination [17–20] of security patch in the wireless mobile network environment.

Due to the limited bandwidth of wireless networks, it is difficult to disseminate the security patches to all phones simultaneously and timely. And since the mobile network is always large-scale, decentralized, dynamically, and of unknown network topology, good patch dissemination strategy is necessary. Some strategies attempt to forward security notifications or patches based on the short-range communication capabilities of intermittently connected phones [17, 18]. These strategies select some important phones that can divide a Bluetooth-based network into different communities based on the contact time and frequency. Thereafter, they send security signatures to all communities based on the local detection. However, this method cannot ensure that users acquire patches in time. References [20, 21] presented a quick and efficient autonomy-oriented computing (AOC) [22, 23] based patch dissemination strategy, based on SMS that can be used in multiple forms of mobile network. But, this strategy still has the following deficiencies: (1) the number of patches disseminated is not determined at a time step. Especially, there may be many patches disseminated at the initial stage which can potentially cause network congestion [24, 25]; (2) a phone may receive the same patch from different neighbors more than once which may lead to network congestion and the waste of network resource. Therefore, it is still in high demand to develop a new strategy that can efficiently and quickly send security patches to as many phones as possible in the mobile network.

In this paper, we propose a patch dissemination strategy based on semi autonomy-oriented computing (SAOC) to restrain the mobile virus. For the AOC-based strategy, certain entities reside in some phones in the mobile network. They autonomously work with each other and move in the network based on their own autonomous behaviors. But in our SAOC-based strategy, a center is added to the AOC-based strategy to combine and analyze the information received from the entities. At each time step, each entity moves to the next location according to its own autonomous behavior and the information feedbacked from the center. Through many experiments involving both synthetic and real-world networks, we find that the proposed SAOC-based strategy can quickly send security patches to as many phones as possible in the mobile network with limited bandwidth which is also large-scale, decentralized, dynamically, and of unknown network topology. Besides, it can control the number of patches disseminated at each time step and make adjustment

according to the network conditions. The selected phones, which receive the patches, are always the most important ones of the phones found by the entities at each time step for the virus propagation, and thus the virus propagation can be effectively restrained. The network congestion and the waste of the network resources can also be avoided because each phone receives the patch only once.

2. SAOC-Based Patch Dissemination Strategy

SMS/MMS messages and Bluetooth are becoming the two major propagation routes of mobile virus. Since SMS-based viruses are found more dangerous than Bluetooth-based viruses in terms of propagation speed and scope [20], we propose a semi autonomy-oriented computing (SAOC) based patch dissemination strategy to restrain the SMS-based virus propagation in this paper. For the autonomy-oriented computing (AOC) approach [20, 26], a group of computational entities are dispatched into a mobile network. They reside in some phones, autonomously work with each other, move from one phone to another, and update their local environment based on their own autonomous behaviors. However, in our SAOC-based approach, the entities no longer work full autonomously and a center is added to help the entities finish their tasks. At each time step, the center is responsible for combining and analyzing the information received from the entities, and each entity moves from its present position to a new one according to some rules, the information feedbacked from the center and the cooperation with other entities. We use a graph G to denote the mobile phones network formed according to the address books of mobile phones. Some definitions which are used to formulate the SAOC-based dissemination strategy are as follows.

Definition 1. A graph $G = \langle V, L \rangle$ is a mobile network formed according to the address books of mobile phones, where $V = \{v_1, v_2, \dots, v_N\}$ is a set of phones and $L = \{\langle v_i, v_j \rangle | 1 \leq i, j \leq N, i \neq j\}$ is a set of undirected links (if v_i is in the address book of v_j , then there is a link between v_i and v_j , and v_i is called a friend of v_j). $N = |V|$ represents the total number of phones in the network.

Each phone v_i in G has two states $\langle phoneId, all friendIds \rangle$, where *phoneId* denotes the identifier of v_i and *friendId* is the identifier of the friend of v_i .

Definition 2. The center, denoted by C , contains two states $\langle id, task \rangle$, where *id* denotes its identifier and *task* stores a series of its tasks.

Definition 3. Let e be an entity in a network G . Entity e is represented by a tuple $\langle id, phoneId, all friendIds, lifecycle, rule \rangle$, where *id* denotes the identifier of the entity; *phoneId* represents the identifier of the phone resided by e ; *friendId* is the identifier of the friend of the resided phone; *lifecycle* is the maximum time steps for an entity to reside on a phone; and *rule* is a set which stores four local behaviors of an entity, including rational-move, rational-jump, random-jump, and wait.

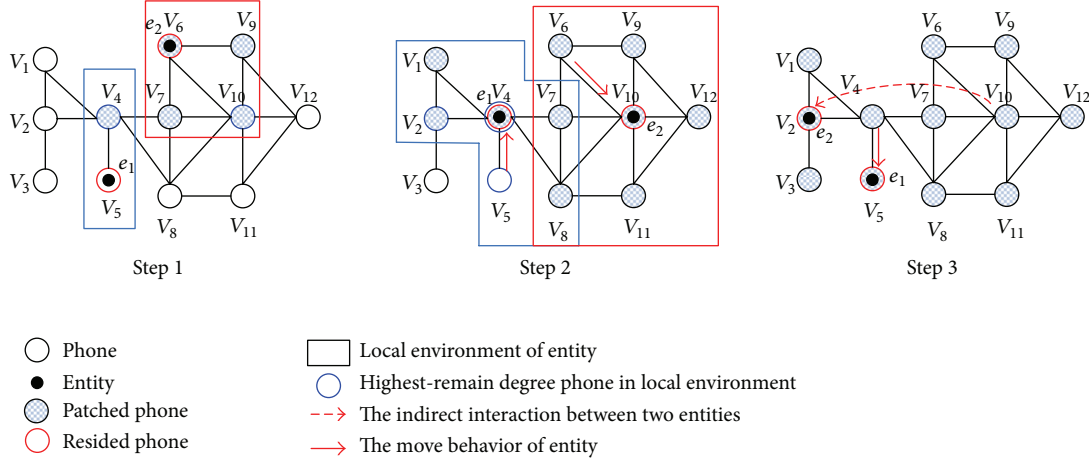


FIGURE 1: An example of the SAOC-based patch dissemination strategy.

Definition 4. The local environment and prelocal information of an entity are denoted by E_l and $preI_l$, respectively. If an entity e resides on phone v_i , its local environment and prelocal information are defined as $E_l(e) = \{v_i; \{v_j\}\}$ and $preI_l(e) = \{v_i's\ id \& v_i's\ all\ friendIds; \{v_j's\ id \& v_j's\ all\ friendIds\}$ respectively, where $\{v_j\}$ is the set of friends of v_i .

Definition 5. Remain degree of a phone denotes the number of friends who have not received the patches of a phone. A phone is regarded as its own friend.

At each time step, each entity sends its prelocal information searched in its local environment to the center. The center combines and analyzes the information received from all entities according to its *task*, and shares the analysis results which are called the postlocal information $postI_l(e)$ with each entity e , where $postI_l(e) = \{v_i's\ id \& v_i's\ remain\ degree; \{v_j's\ id \& v_j's\ remain\ degree\}$, $\{v_j\}$ is the set of friends of v_i resided by e . If two phones resided by two entities are friends or they have at least a same friend, we assume that these two entities can share their postlocal information. Each entity then moves to the next location (*targetId*) according to its *rule*. Algorithm 1 shows the detailed process of SAOC-based patch dissemination strategy.

The *task* of the center includes the following.

- (1) Delete the *friendIds* who have received the patches from each phone's *all friendIds* in all the prelocal information.
- (2) Compute each phone's remain degree and send the security patches to the first m phones with the highest-remain degree. (Therefore, the number of patches disseminated at each time step is controllable that can be adjusted according to the network conditions.) And record the *ids* of the phones who just received the patches.

- (3) Delete the new patched *friendIds* from each phone's *all friendIds* and compute each phone's new remain degree.
- (4) Send the postlocal information to the entity.

The main behaviors of each entity are as follows.

- (1) Rational move: An entity moves to a phone with the highest-remain degree in its postlocal information or the shared postlocal information if it exists. If there exists more than one highest-remain degree phone, the entity will randomly choose one for residing in.
- (2) Rational jump: the entity requests from the center a phone for residing in, if such phone exists.
- (3) Random jump: an entity moves along the edges with a randomly-determined number of steps in order to avoid getting stuck in local optima.
- (4) Wait: If an entity does not find any available phone for residing in, it will stay at its current position.

For example, as shown in Figure 1, two entities e_1 and e_2 reside in phones v_5 and v_6 at the initial phase of step 1, respectively. e_1 and e_2 begin to search their local environments and obtain the prelocal information as:

$$\begin{aligned} preI_l(e_1) &= \{v_5 \& v_5, v_4; \{v_4 \& v_4, v_1, v_2, v_5, v_7, v_8\}\}, \\ preI_l(e_2) &= \{v_6 \& v_6, v_7, v_9, v_{10}; \\ &\quad \{v_7 \& v_7, v_4, v_6, v_8, v_{10}; v_9 \& v_9, v_6, v_{10}, v_{12}; \\ &\quad v_{10} \& v_{10}, v_6, v_7, v_8, v_9, v_{11}, v_{12}\}\}. \end{aligned} \quad (1)$$

When receiving $preI_l(e_1)$ and $preI_l(e_2)$, the center firstly deletes the phones' *id* that has been immunized from each phone's *friendIds* and computes the remain degree of each phone. Since there are no phones have been immunized, the remain degree of each phone will be $\{v_4 \& 6; v_5 \& 2; v_6 \& 4; v_7 \& 5; v_9 \& 4; v_{10} \& 7\}$. In this

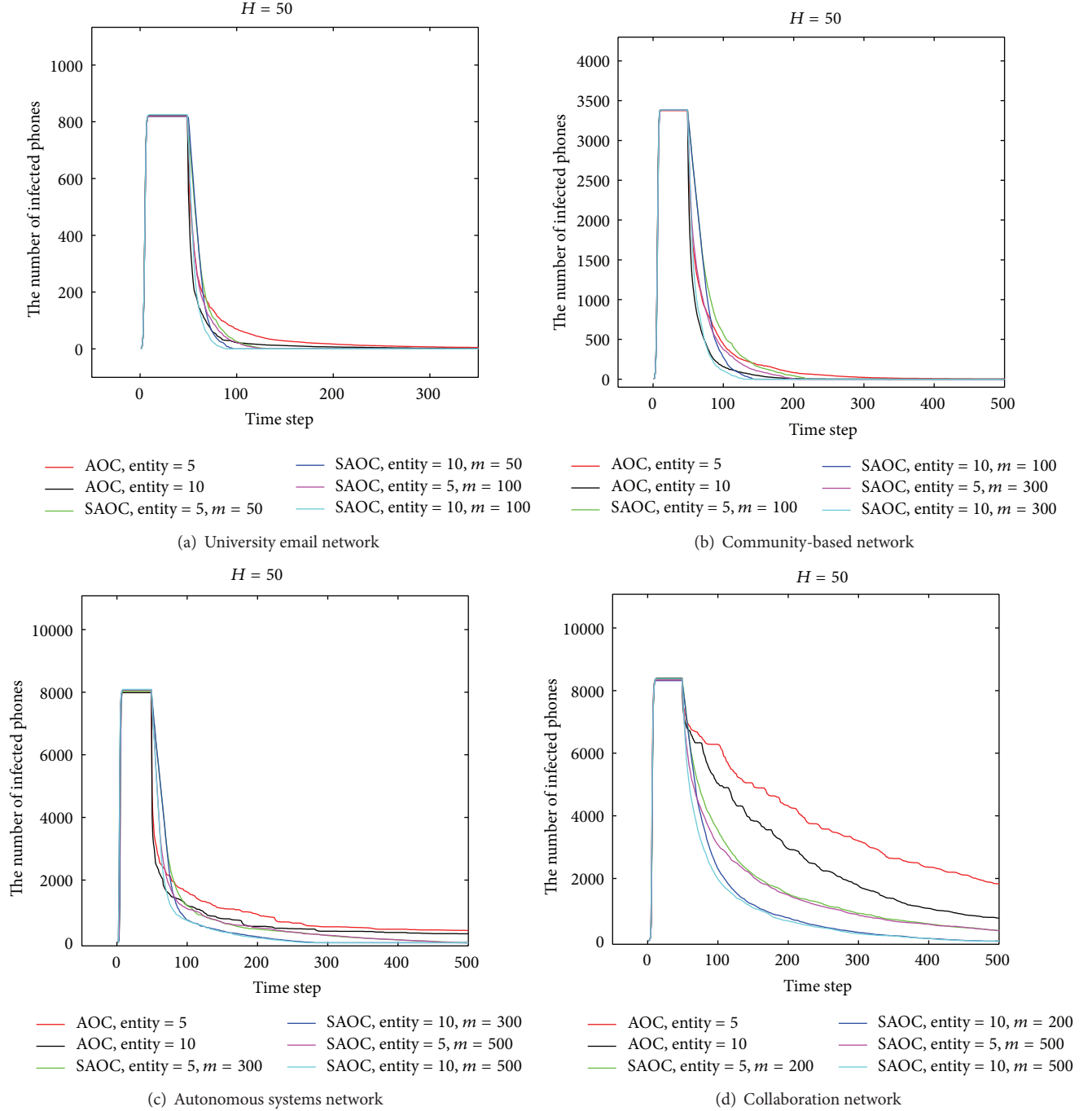
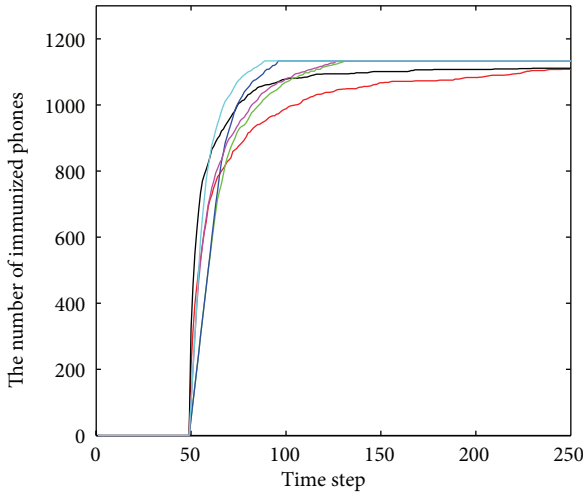


FIGURE 2: The number of infected phones over time.

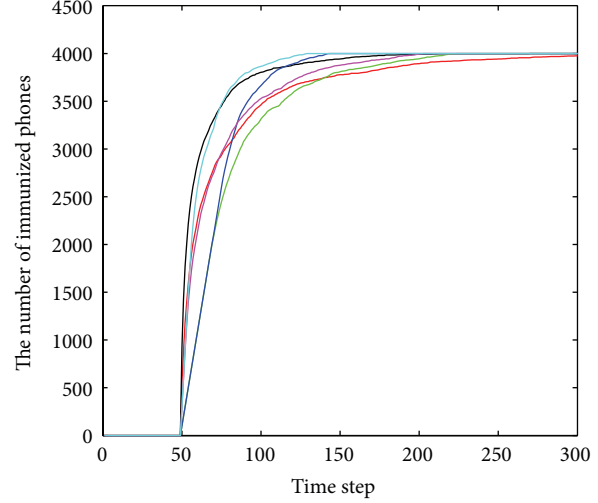
moment, the center sends the security patches to the first 5 unimmunized phones (in this example, we assume that no more than $m = 5$ phones are immunized at each time step) with highest-remain degree, that is, $\{v_4, v_6, v_7, v_9, v_{10}\}$, and deletes these phones' *id* from each phones' *friendIds* and computes the new remain degree of each phone. The new remain degree will be sent to entities as their postlocal information, that is, $postI_l(e_1) = \{v_5 \& 1; \{v_4 \& 4\}\}$ and $postI_l(e_2) = \{v_6 \& 0; \{v_7 \& 1; v_9 \& 1; v_{10} \& 3\}\}$. When

receiving the postlocal information, each entity will move to the phone which has the highest-remain degree in its postlocal information. Therefore, e_1 and e_2 move from v_5 to v_4 and from v_6 to v_{10} , respectively. In this step, these two entities perform the rational move relying on their own postlocal information. Step 2 will show the case of the movement of the entities relying on the shared postlocal information. In step 2, when e_1 and e_2 receive $postI_l(e_1)$ and $postI_l(e_2)$ from the center, they can share their postlocal



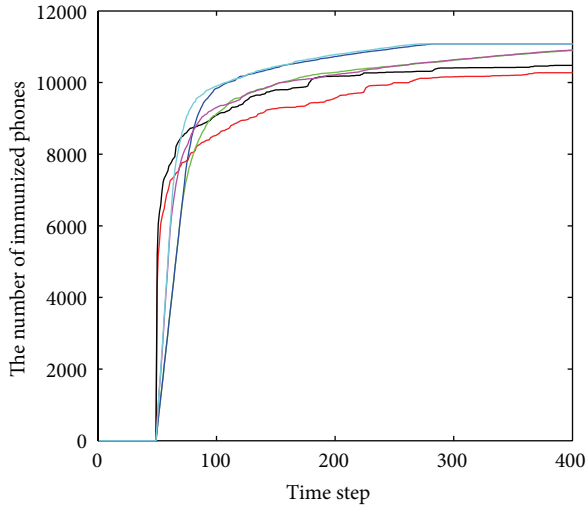
— AOC, entity = 5 — SAOC, entity = 10, $m = 100$
 — AOC, entity = 10 — SAOC, entity = 5, $m = 200$
 — SAOC, entity = 5, $m = 100$ — SAOC, entity = 10, $m = 200$

(a) University email network



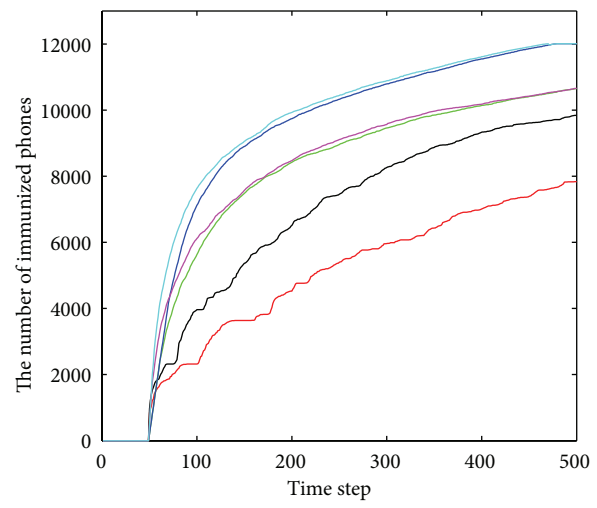
— AOC, entity = 5 — SAOC, entity = 10, $m = 200$
 — AOC, entity = 10 — SAOC, entity = 5, $m = 300$
 — SAOC, entity = 5, $m = 200$ — SAOC, entity = 10, $m = 300$

(b) Community-based network



— AOC, entity = 5 — SAOC, entity = 10, $m = 300$
 — AOC, entity = 10 — SAOC, entity = 5, $m = 500$
 — SAOC, entity = 5, $m = 300$ — SAOC, entity = 10, $m = 500$

(c) Autonomous systems network



— AOC, entity = 5 — SAOC, entity = 10, $m = 200$
 — AOC, entity = 10 — SAOC, entity = 5, $m = 500$
 — SAOC, entity = 5, $m = 200$ — SAOC, entity = 10, $m = 500$

(d) Collaboration network

FIGURE 3: The number of immunized phones over time.

information with each other since they have the mutual friends v_7 and v_8 . $postI_l(e_1)$, $postI_l(e_2)$ and the shared postlocal information are as follows:

$$postI_l(e_1) = \{v_4 \& 1; \{v_1 \& 0; v_2 \& 1; v_5 \& 1; v_7 \& 0; v_8 \& 0\}\},$$

$$postI_l(e_2) = \{v_{10} \& 0;$$

$$\{v_6 \& 0; v_7 \& 0; v_8 \& 0;$$

$$v_9 \& 0; v_{11} \& 0; v_{12} \& 0\}\},$$

$$postI_l(e_1) \cup postI_l(e_2)$$

$$= \{v_1 \& 0; v_2 \& 1; v_4 \& 1; v_5 \& 1; v_6 \& 0;$$

$$v_7 \& 0; v_8 \& 0; v_9 \& 0; v_{10} \& 0; v_{11} \& 0; v_{12} \& 0\}.$$

(2)

e_1 and e_2 will choose the first two phones with the highest-remain degree in the shared postlocal information as their target locations. Note that there are three phones can be resided and e_1 is residing in one of the highest-remain degree phone. In this case, we let e_1 continue from

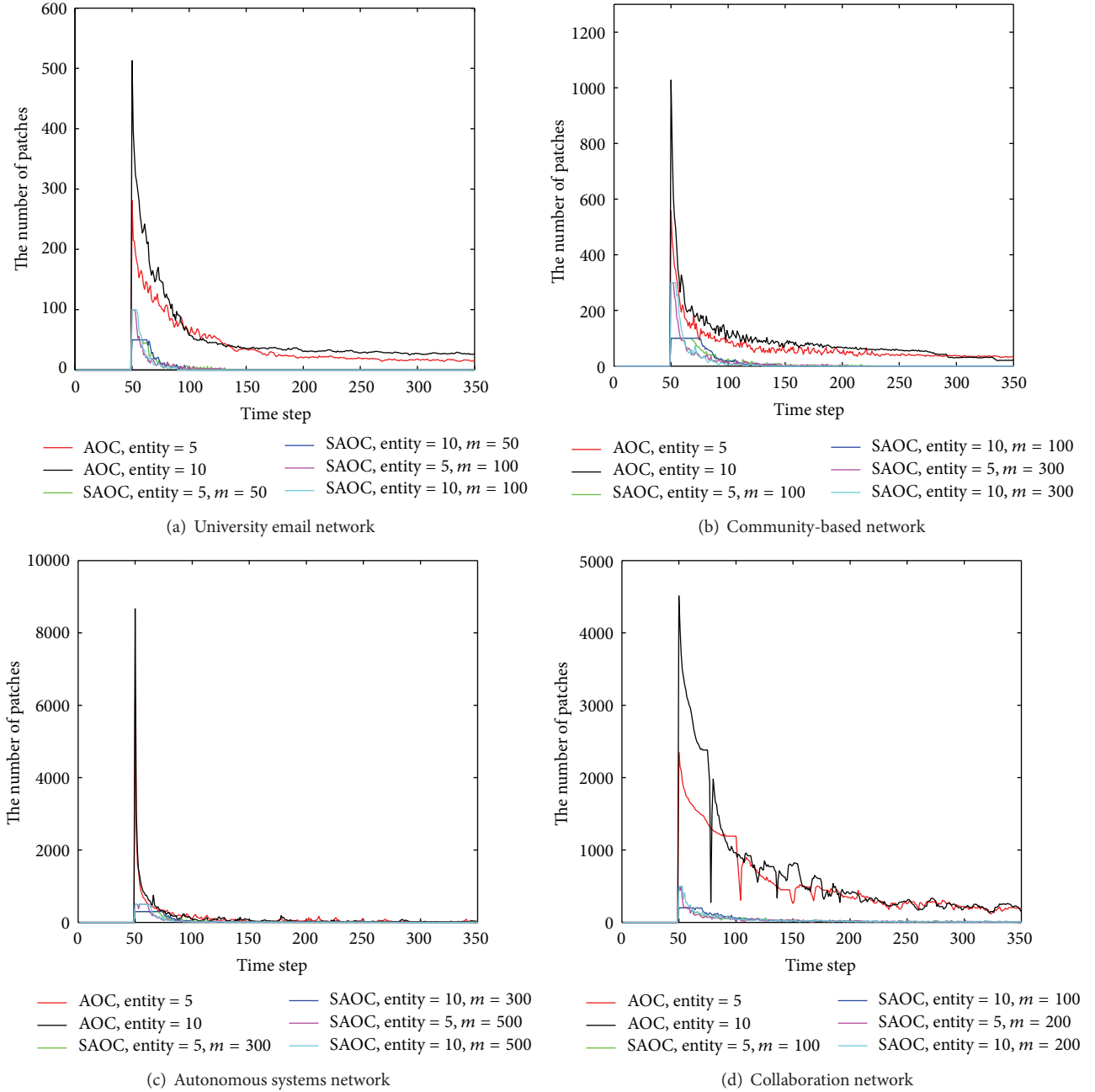


FIGURE 4: The number of patches over time.

moving. Therefore, e_1 and e_2 move from v_4 to v_5 and v_{10} to v_2 , respectively. Table 1 presents the detailed patch dissemination process of Figure 1 based on our SAOC-based patch dissemination strategy.

3. Experimentation and Validation

3.1. Static Networks. A mobile network is constructed based on the address books of smart phones, which reflects the social relationship among mobile users in real world situations. Here, we use some benchmark networks

(university email network, autonomous systems network, and collaboration network) to reflect the relationship structures in the real world. Table 2 shows the structure and degree of four networks. University email network [27], autonomous systems network [28], and collaboration network of Arxiv High Energy Physics category [29] are real-world networks. Community-based network is a synthetic network with four communities based on the GLP algorithm [30].

We use the four networks shown in Table 2 to evaluate the efficiency of the proposed SAOC-based patch dissemination strategy in restraining the SMS-based virus. For the SMS-based virus propagation model, we assume the following.

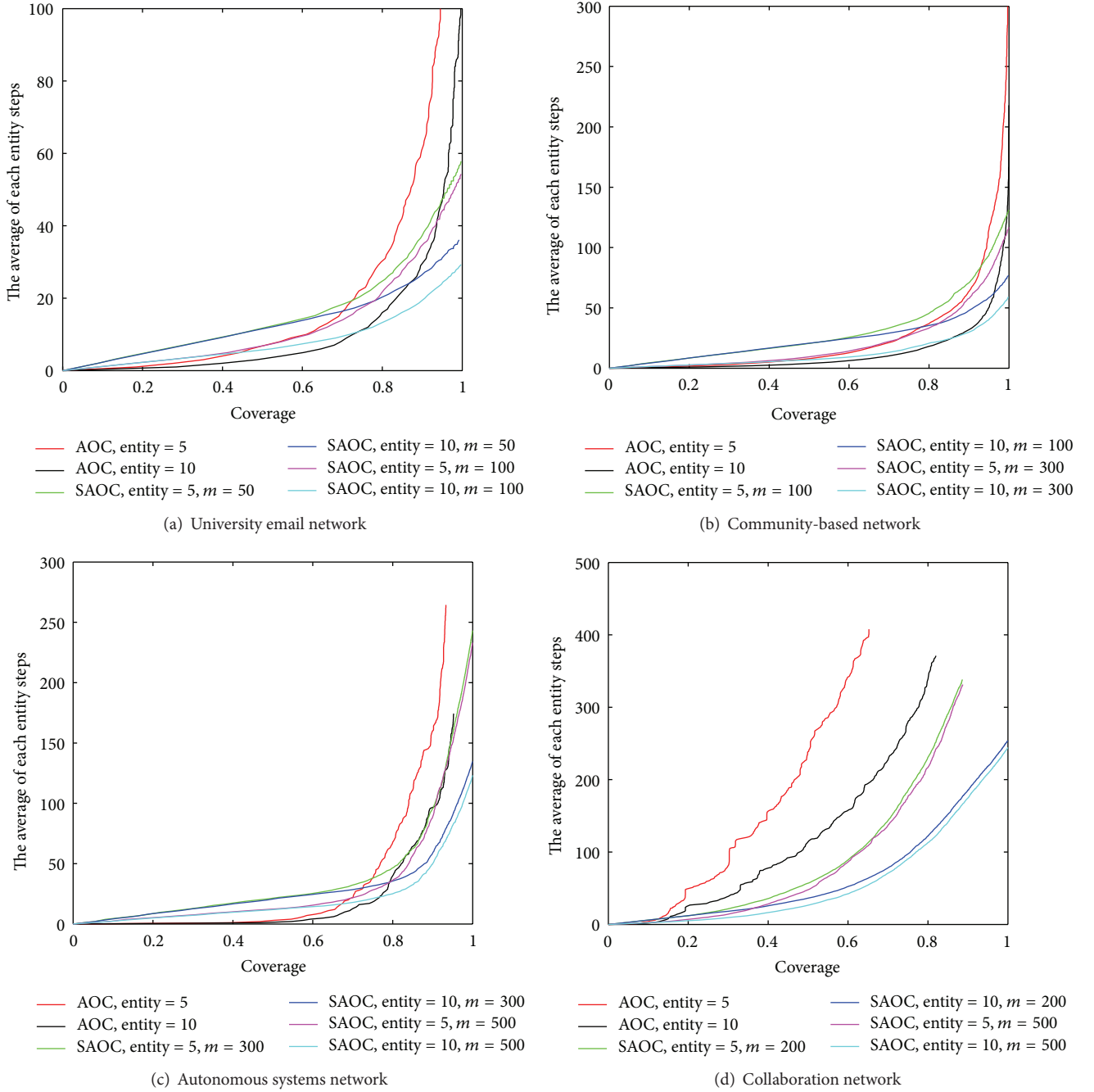


FIGURE 5: The average of each entity steps with respect to coverage rate.

- (1) If a user receives a message from his friend, he may open or delete this message determined by his security awareness [20, 31, 32]. The security awareness of different users in this paper is consistent with that used by [20] and follows a normal distribution, $N(0.5, 0.3^2)$.
- (2) If a user opens a virus message, he is infected and will automatically send the virus message to all his friends.

- (3) An infected phone sends the virus to his friends only once, after which the infected phone will not send out virus any more.
- (4) If a phone has received the patch, it will not send out virus even if the user opens an infected message again.

At some point, we deploy a few entities into a mobile network. These entities reside in the phones with the highest degree which are found by the AOC-based immunization strategy [26]. Each entity then moves according to

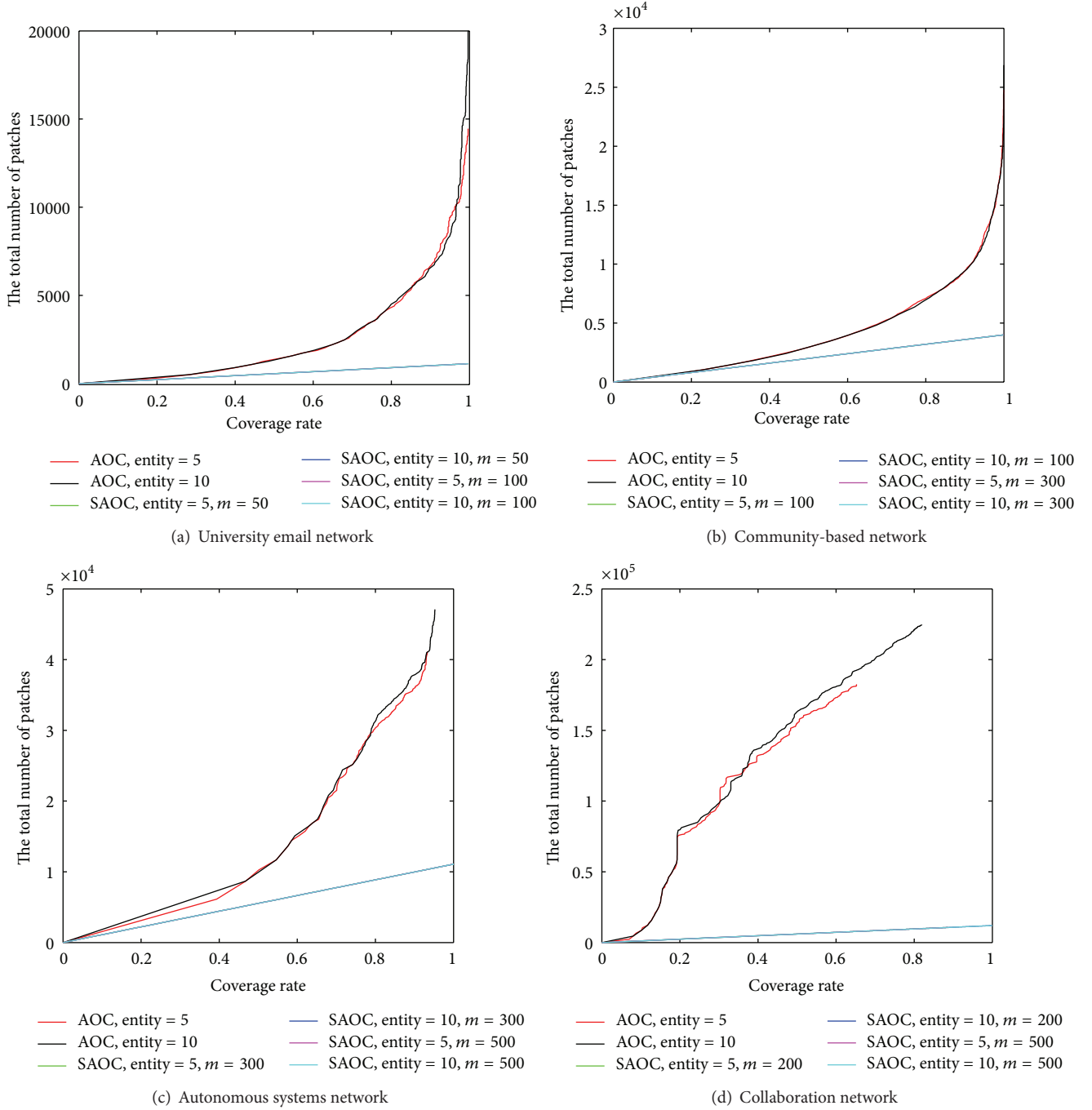


FIGURE 6: The number of patches with respect to coverage rate.

Algorithm 1. We compare the efficiency of our SAOC-based dissemination strategy with the AOC-based dissemination strategy [20] by different indexes in the above static benchmark networks.

Figure 2 shows the average numbers of infected phones over time when 5 and 10 entities are deployed into the networks from the time step of 50. At each time step, no more than m patches can be sent in SAOC-based strategy that is, up to m phones can be immunized at each time step in

SAOC-based strategy. Obviously, the earlier and the more the patch is disseminated, the shorter the propagation duration will be. Figure 3 shows the average number of immunized phones over time when the entities are deployed into the networks from 50. Since we set a limit on the size of m to avoid the network congestion, the effect of SAOC-based strategy is inferior to the AOC-based one at the initial phase after the deploying of the entities when m is small. But simulation results show that the SAOC-based strategy can recover all the

```

(1) For each entity  $e$ 
    search the local environment  $E_l(e)$  and obtain pre-local information  $preI_l(e)$ ;
    send  $preI_l(e)$  to the center;
End
(2) For center  $C$ 
    perform a series of task according to its task;
End
(3) For each entity  $e$ 
    compute  $targetId$  based on the post-local information or the shared post-local information;
    If  $targetId$  is not null Then
        Rational move to  $targetId$ ;
    Else if  $e.lifecycle < 1$  Then
        request the center a  $targetId$ ;
        If receive a  $targetId$  Then
            Rational jump to  $targetId$ ;
        Else if not receive a  $targetId$  Then
            Random jump to  $targetId$ ;
    Else
        Wait;
    End
End

```

ALGORITHM 1: The process of SAOC-based patch dissemination strategy.

infected phones and immune all the phones faster than the AOC-based one even if m is relatively small. Figure 4 shows the number of the patches disseminated at each time step. We find that the number of the patches disseminated at each time step in AOC-based strategy is much more than that of the SAOC-based one. Figure 4 also shows the main inadequacies of AOC-based strategy; that is, too many patches are sent at certain times which may lead to network congestion and a phone may receive the patch from different neighbors more than once which causes the waste of network resources. However, in our SAOC-based strategy, the number of patches disseminated at each time step is controllable that can be adjusted according to the network conditions, and a phone receives the patch only once.

Figures 5 and 6 show the average number of steps of each entity and the total number of patches disseminated corresponding to the coverage rate, respectively. The coverage rate is defined as $N_{\text{immunized}}/N$, where $N_{\text{immunized}}$ represents the total number of immunized phones that are patched by the center and N represents the total number of phones in the network. In Figure 5, each entity in SAOC-based strategy needs to move a bit more steps than that in the AOC-based strategy when the coverage rate is small due to the limitation on m . But in the case of achieving a significant amount of coverage rate, the number of steps of each entity needed to move is much smaller in SAOC-based strategy than that in AOC-based strategy. In Figure 6, we can see that the total number of patches disseminated is much smaller in SAOC-based strategy than in AOC-based strategy to attain the same coverage rate.

From the simulations performed above, we can see that the SAOC-based dissemination strategy can efficiently send security patches to as many phones as possible with considerable speed and relatively lower cost in the static networks.

3.2. Dynamically Evolving Networks. In this section, we evaluate the efficiency of SAOC-based dissemination strategy in dynamically evolving networks since the structure of a network is changing in the real world. We assume that the initial network contains 1000 phones with $\langle k \rangle = 8$. Three different patterns of network evolving are considered as follows: (1) the network scale will grow to 4000; (2) 50 or 100 phones are added into the network at each step from the time step of 20; (3) the network degree, $\langle k \rangle$, will remain unchanged or change from 8 to 18, respectively. We use the SIR [33–35] model to characterize the SMS-based virus propagation in dynamically evolving networks. SIR is the most basic and well-studied epidemic spreading model. In the SIR model, the elements of a network are divided into three compartments, including susceptibles (S, those who can contract the infection), infectious (I, those who have contracted the infection and are contagious), and recovered (R, those who have recovered from the disease). At each time step, we assume that a susceptible phone becomes infected with a probability λ if it is directly connected to an infected phone. Meanwhile, if an infected phone receives the patch, it will become to be recovered from the infected state.

Simulation results shown in Figure 7 indicate that when selecting the appropriate number of patches disseminated at each time step, our SAOC-based strategy can send security patches to as many phones as possible and reduce the damages of mobile virus in the dynamically evolving networks with various complex evolving patterns.

4. Conclusion

In this paper, we propose an efficient SAOC-based patch dissemination strategy to restrain the SMS-based mobile

TABLE 1: The detailed process of Figure 1 based on SAOC-based patch dissemination strategy.

Entity	Center	Entity	
Pre-local information	Analytical information	Post-local information	Movement
Step 1:			
Entity e_1: V_5 & V_5, V_4 V_4 & $V_4, V_1, V_2, V_5, V_7, V_8$	V_4 & $V_4, V_1, V_2, V_5, V_7, V_8$ & 6 & 4 V_5 & V_5, V_4 & 2 & 1 V_6 & V_6, V_7, V_9, V_{10} & 4 & 0 V_7 & $V_7, V_4, V_6, V_8, V_{10}$ & 5 & 1 V_9 & V_9, V_6, V_{10}, V_{12} & 4 & 1 V_{10} & $V_{10}, V_6, V_7, V_8, V_9, V_{11}, V_{12}$ & 7 & 3 Store immune phones: $V_4, V_6, V_7, V_9, V_{10}$	Entity e_1: V_5 & 1 V_4 & 4 Entity e_2: V_6 & 0 V_7 & 1 V_9 & 1 V_{10} & 3	$e_1: V_5 \rightarrow V_4$ $e_2: V_6 \rightarrow V_{10}$
Step 2:			
Entity e_1: V_4 & $V_4, V_1, V_2, V_5, V_7, V_8$ V_1 & V_2, V_1, V_4 V_2 & V_1, V_2, V_3, V_4 V_5 & V_5, V_4 V_7 & $V_7, V_4, V_6, V_8, V_{10}$ V_8 & $V_8, V_4, V_7, V_{10}, V_{11}$	V_1 & V_1, V_2, V_4 & 2 & 0 V_2 & V_2, V_1, V_3, V_4 & 3 & 1 V_4 & $V_4, V_1, V_2, V_5, V_7, V_8$ & 4 & 1 V_5 & V_5, V_4 & 1 & 1 V_6 & V_6, V_7, V_9, V_{10} & 0 & 0 V_7 & $V_7, V_4, V_6, V_8, V_{10}$ & 1 & 0 V_8 & $V_8, V_4, V_7, V_{10}, V_{11}$ & 2 & 0 V_9 & V_9, V_6, V_{10}, V_{12} & 1 & 0 V_{10} & $V_{10}, V_6, V_7, V_8, V_9, V_{11}, V_{12}$ & 3 & 0 V_{11} & $V_{11}, V_8, V_{10}, V_{12}$ & 3 & 0 V_{12} & $V_{12}, V_9, V_{10}, V_{11}$ & 2 & 0 Store immune phones: $V_1, V_2, V_4, V_6, V_7, V_8, V_9, V_{10}, V_{11}, V_{12}$	Entity e_1: V_4 & 1 V_1 & 0 V_2 & 1 V_5 & 1 V_7 & 0 V_8 & 0 Entity e_2: V_{10} & 0 V_6 & 0 V_7 & 0 V_8 & 0 V_9 & 0 V_{11} & 0 V_{12} & 0	e_1 and e_2 share their post-local informations, then $e_1: V_4 \rightarrow V_5$ $e_2: V_{10} \rightarrow V_2$
Step 3:			
Entity e_1: V_2 & V_2, V_1, V_3, V_4 V_1 & V_2, V_1, V_4 V_3 & V_3, V_2 V_4 & $V_4, V_1, V_2, V_5, V_7, V_8$	V_1 & V_2, V_1, V_4 & 0 & 0 V_2 & V_2, V_1, V_3, V_4 & 1 & 0 V_3 & V_3, V_2 & 1 & 0 V_4 & $V_4, V_1, V_2, V_5, V_7, V_8$ & 1 & 0 V_5 & V_5, V_4 & 1 & 0 Store immune phones: $V_1, V_2, V_3, V_4, V_5, V_6, V_7, V_8, V_9, V_{10}, V_{11}, V_{12}$	Entity e_1: V_2 & 0 V_1 & 0 V_3 & 0 V_4 & 0 Entity e_2: V_5 & 0 V_4 & 0	end

In the analytical information v_i & v_{j1}, \dots, v_{jk} & n_1 & n_2 of the center, v_i is the identifier of a phone, v_{j1}, \dots, v_{jk} the friends of v_i , n_1 the first computed remain degree of v_i , and n_2 the second computed remain degree of v_i . The identifiers in red indicate the phones that have received the patches in the previous steps. The identifiers in blue indicate the phones that will receive the patches in the current step. The no more than 5 red numbers in each step refers to the unimmunized phones with the highest-first computed remain degree.

virus. The advantages of our SAOC-based strategy could be described as follows:

network with limited bandwidth which is also large-scale, decentralized, dynamically evolving, and of unknown network topology;

- (1) it sends security patches to as many phones as possible at a considerable speed and lower cost in the mobile

- (2) it can control the number of patches disseminated at each time step and make adjustment according to the

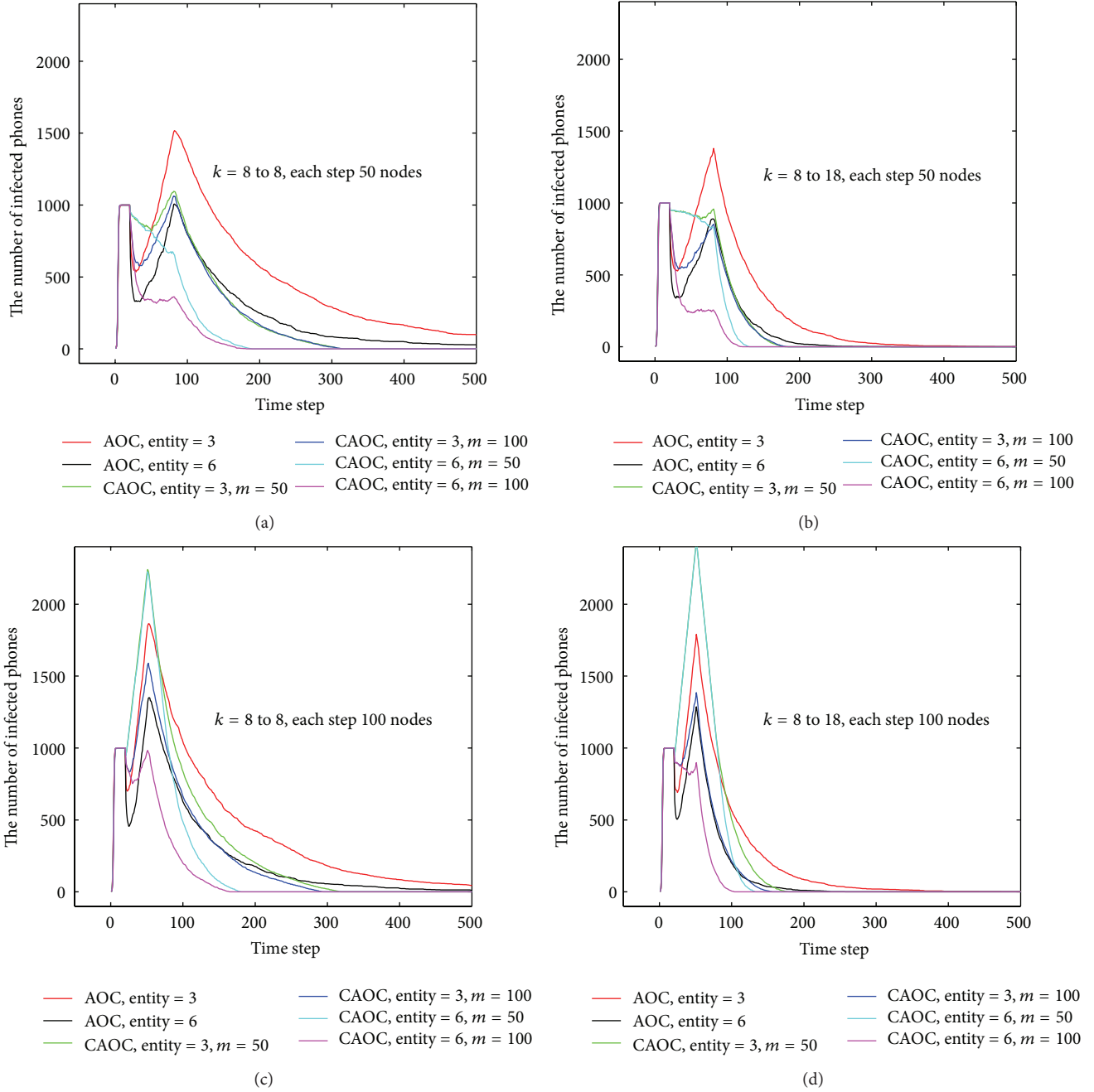


FIGURE 7: The number of infected phones over time in different dynamicin-evolving networks. (a) 50 phones are added into the network at each step, and the average degree $\langle k \rangle$ maintains 8; (b) 50 phones are added into the network at each step, and the average degree $\langle k \rangle$ increases from 8 to 18; (c) 100 phones are added into the network at each step, and the average degree $\langle k \rangle$ maintains 8; (d) 100 phones are added into the network at each step, and the average degree $\langle k \rangle$ increases from 8 to 18.

network conditions. Thus the network congestion can be avoided;

- (3) the selected phones which receive the patches are always the most important ones of the phones found by the entities at each time step for the virus propagation, and thus the virus propagation can be effectively restrained;

- (4) each phone receives the patch only once, which is beneficial to avoiding the network congestion and the waste of network resource.

In summary, the SAOC-based patch dissemination strategy is a reasonable, effective, and secure method to send security patches in mobile networks and reduce the damages mobile viruses cause.

TABLE 2: The structures of networks.

	Nodes	Edges	$\langle k \rangle$
University email network	1133	5451	9.62
Community-based network	4000	16855	8.42
Autonomous systems network	11080	31538	5.69
Collaboration network	12008	237010	39.47

Acknowledgments

This paper was supported by the National Natural Science Foundation of China (Grant nos. 61202362, 61070209, 61121061, and 61272402), the Asia Foresight Program under NSFC Grant (Grant no. 61161140320), and the Specialized Research Fund for the Doctoral Program of Higher Education (Grant no. 20120005110017).

References

- [1] P. Wang, M. C. González, C. A. Hidalgo, and A.-L. Barabasi, "Understanding the spreading patterns of mobile phone viruses," *Science*, vol. 324, no. 5930, pp. 1071–1076, 2009.
- [2] S.-M. Cheng, W. C. Ao, P.-Y. Chen, and K.-C. Chen, "On modeling malware propagation in generalized social networks," *IEEE Communications Letters*, vol. 15, no. 1, pp. 25–27, 2011.
- [3] G. Yan and S. Eidenbenz, "Modeling propagation dynamics of bluetooth worms (Extended version)," *IEEE Transactions on Mobile Computing*, vol. 8, no. 3, pp. 353–367, 2009.
- [4] P. De, Y. Liu, and S. K. Das, "An epidemic theoretic framework for vulnerability analysis of broadcast protocols in wireless sensor networks," *IEEE Transactions on Mobile Computing*, vol. 8, no. 3, pp. 413–425, 2009.
- [5] C. Toma, "Advanced signal processing and command synthesis for memory-limited complex systems," *Mathematical Problems in Engineering*, vol. 2012, Article ID 927821, 13 pages, 2012.
- [6] E. G. Bakhoun and C. Toma, "Specific mathematical aspects of dynamics generated by coherence functions," *Mathematical Problems in Engineering*, vol. 2011, Article ID 436198, 10 pages, 2011.
- [7] Y. Chen, G. Paul, S. Havlin, F. Liljeros, and H. E. Stanley, "Finding a better immunization strategy," *Physical Review Letters*, vol. 101, no. 5, Article ID 058701, 2008.
- [8] W.-J. Bai, T. Zhou, and B.-H. Wang, "Immunization of susceptible-infected model on scale-free networks," *Physica A*, vol. 384, no. 2, pp. 656–662, 2007.
- [9] R. Cohen, S. Havlin, and D. Ben-Avraham, "Efficient immunization strategies for computer networks and populations," *Physical Review Letters*, vol. 91, no. 24, Article ID 247901, 4 pages, 2003.
- [10] P. Holme, B. J. Kim, C. N. Yoon, and S. K. Han, "Attack vulnerability of complex networks," *Physical Review E*, vol. 65, no. 5, Article ID 056109, 14 pages, 2002.
- [11] D. Samfat and R. Molva, "IDAMN: an intrusion detection architecture for mobile networks," *IEEE Journal on Selected Areas in Communications*, vol. 15, no. 7, pp. 1373–1380, 1997.
- [12] T. S. Yap and H. T. Ewe, "A mobile phone malicious software detection model with behavior checker," in *Web and Communication Technologies and Internet-Related Social Issues—HSI 2005*, vol. 3597 of *Lecture Notes in Computer Science*, pp. 57–65, 2005.
- [13] J. Cheng, S. H. Y. Wong, H. Yang, and S. Lu, "SmartSiren: Virus detection and alert for smartphones," in *Proceedings of the 5th International Conference on Mobile Systems, Applications and Services (MobiSys '07)*, pp. 258–271, June 2007.
- [14] A. Smirnov and T.-C. Chiueh, "Automatic patch generation for buffer overflow attacks," in *Proceedings of the 3rd International Symposium on Information Assurance and Security (IAS '07)*, pp. 165–170, August 2007.
- [15] S. Sidiroglou and A. D. Keromytis, "Countering network worms through automatic patch generation," *IEEE Security and Privacy*, vol. 3, no. 6, pp. 41–49, 2005.
- [16] W. Cui, M. Peinado, H. J. Wang, and M. E. Locasto, "ShieldGen: automatic data patch generation for unknown vulnerabilities with informed probing," in *Proceedings of the IEEE Symposium on Security and Privacy (SP '07)*, pp. 252–266, May 2007.
- [17] F. Li, Y. Yang, and J. Wu, "CPMC: an efficient proximity malware coping scheme in smartphone-based mobile networks," in *Proceedings of the IEEE Conference on Computer Communications (INFOCOM '10)*, pp. 1–9, March 2010.
- [18] G. Zyba, G. M. Voelker, M. Liljenstam, A. Méhes, and P. Johansson, "Defending mobile phones from proximity malware," in *Proceedings of the 28th Conference on Computer Communications (INFOCOM '09)*, pp. 1503–1511, April 2009.
- [19] M. H. R. Khouzani, S. Sarkar, and E. Altman, "Dispatch then stop: optimal dissemination of security patches in mobile wireless networks," in *Proceedings of the 49th IEEE Conference on Decision and Control (CDC '10)*, pp. 2354–2359, December 2010.
- [20] C. Gao and J. Liu, "Modeling and restraining mobile virus propagation," *IEEE Transactions on Mobile Computing*, vol. 12, no. 3, pp. 529–541, 2013.
- [21] C. Gao and J. Liu, "Modeling and restraining mobile virus propagation," *IEEE Transactions on Mobile Computing*, 2013.
- [22] J. Liu, "Autonomy-Oriented Computing (AOC): the nature and implications of a paradigm for self-organized computing," in *Proceedings of the 4th International Conference on Natural Computation (ICNC '08)*, pp. 3–11, October 2008.
- [23] J. Liu, X. Jin, and K. C. Tsui, *Autonomy Oriented Computing (AOC): From Problem Solving to Complex Systems Modeling*, Springer, New York, NY, USA, 2005.
- [24] M. Li and W. Zhao, "Asymptotic identity in min-plus algebra: a report on CPNS," *Computational and Mathematical Methods in Medicine*, vol. 2012, Article ID 154038, 11 pages, 2012.
- [25] M. Li and W. Zhao, "Representation of a stochastic traffic bound," *IEEE Transactions on Parallel and Distributed Systems*, vol. 21, no. 9, pp. 1368–1372, 2010.
- [26] C. Gao, J. Liu, and N. Zhong, "Network immunization with distributed autonomy-oriented entities," *IEEE Transactions on Parallel and Distributed Systems*, vol. 22, no. 7, pp. 1222–1229, 2011.
- [27] R. Guimerà, L. Danon, A. Díaz-Guilera, F. Giralt, and A. Arenas, "Self-similar community structure in a network of human interactions," *Physical Review E*, vol. 68, no. 6, Article ID 065103, pp. 651031–651034, 2003.
- [28] J. Leskovec, J. Kleinberg, and C. Faloutsos, "Graphs over time: densification laws, shrinking diameters and possible explanations," in *Proceedings of the 11th ACM SIGKDD International Conference on Knowledge Discovery and Data Mining*, pp. 177–187, ACM, August 2005.
- [29] J. Leskovec, J. Kleinberg, and C. Faloutsos, "Graph evolution: densification and shrinking diameters," *ACM Transactions on Knowledge Discovery from Data*, vol. 1, no. 1, pp. 1–41, 2007.

- [30] T. Bu and D. Towsley, "On distinguishing between internet power law topology generators," in *Proceedings of the 21st IEEE International Conference on Computer and Communications (INFOCOM '02)*, pp. 638–647, 2002.
- [31] C. C. Zou, D. F. Towsley, and W. Gong, "Modeling and simulation study of the propagation and defense of internet e-mail worms," *IEEE Transactions on Dependable and Secure Computing*, vol. 4, no. 2, pp. 106–118, 2007.
- [32] C. Gao, J. Liu, and N. Zhong, "Network immunization and virus propagation in email networks: experimental evaluation and analysis," *Knowledge and Information Systems*, vol. 27, no. 2, pp. 253–279, 2011.
- [33] T. J. Norman Bailey, *The Mathematical Theory of Infectious Diseases and Its Applications*, Griffin, London, UK, 2nd edition, 1975.
- [34] D. J. Daley and J. Gani, *Epidemic Modelling: An Introduction*, Cambridge University Press, Cambridge, UK, 2000.
- [35] O. Diekmann and J. A. P. Heesterbeek, *Mathematical Epidemiology of Infectious Diseases*, John Wiley & Sons, New York, NY, USA, 2000.

Research Article

Content-Based Image Retrieval Based on Hadoop

DongSheng Yin and DeBo Liu

School of Information Science and Technology, Sun Yat-sen University, Guangzhou 510000, China

Correspondence should be addressed to DongSheng Yin; yindsh@mail.sysu.edu.cn

Received 9 July 2013; Accepted 22 August 2013

Academic Editor: Ming Li

Copyright © 2013 D. Yin and D. Liu. This is an open access article distributed under the Creative Commons Attribution License, which permits unrestricted use, distribution, and reproduction in any medium, provided the original work is properly cited.

Generally, time complexity of algorithms for content-based image retrieval is extremely high. In order to retrieve images on large-scale databases efficiently, a new way for retrieving based on Hadoop distributed framework is proposed. Firstly, a database of images features is built by using Speeded Up Robust Features algorithm and Locality-Sensitive Hashing and then perform the search on Hadoop platform in a parallel way specially designed. Considerable experimental results show that it is able to retrieve images based on content on large-scale cluster and image sets effectively.

1. Introduction

Content-based image retrieval (CBIR) is a long-term hotspot in computer vision and information retrieval and there are many mature theories on this topic. For example, an algorithm proposed in early time by using multiresolution wavelet decompositions [1] had achieved favorable results in searching images that are similar in content or structure. And scale invariant feature transform (SIFT) [2], published in 1999, was able to be stable with light, noise, and small perspective change in a sense. But SIFT was so complex that it cost too much time and this led to several other improvements, such as principle component analysis SIFT (PAC-SIFT) [3] which speed up feature matching by reducing the dimension of image features and fast approximated SIFT [4, 5] which speed up by using an integral image and an integral orientation histogram. Another considerable algorithm on CBIR is speededup robust features (SURF) [6] and it is stable and fast enough to gain excellent results on region of computer vision such as object recognition and 3D reconstruction. SURF is also involved from SIFT but faster and announced to be more robust than SIFT when coming to image transformation.

Normally, CBIR has two steps, the feature extraction which mainly affects the quality of searching, and the feature matching, which mainly affects the efficiency. Usually, features are in high dimension, so matching features means

searching in high-dimension. There are many ways to search high dimension space such as linear scanning, tree searching, vector quantization, and hashing. Among these methods, hashing is the easiest way to keep time complexity $O(1)$ as well as designing as a fuzzy search method. Details about hashing will be discussed later.

Even features matching is optimized via hashing; due to the huge amount of information of CBIR, time complexity is still too high, preventing it from being widely used. Particularly in the age of explosive expansion in information, the stand-alone method for CBIR is becoming harder and harder to fulfill the load of storage and computing brought by data explosion. Hadoop [7] is an open-source software framework for reliable, scalable, distributed computing. It enables large datasets processing distributedly across clusters using simple programming models. It is widely used by IT companies like Yahoo!.

In this paper, image features extraction and matching are combined with three techniques, SURF, LSH, and Hadoop distributed platform, intending to migrate computing to cluster with multiple nodes and improve the efficiency of CBIR significantly. The rest of the paper is organized as follows. Section 2 discusses related algorithms and techniques. Architecture of implementation of such method is discussed in Section 3. Section 4 presents our experimental results and analysis. Finally, the conclusions are drawn in Section 5, with a brief description of future work.

2. CBIR Algorithms and Hadoop Introduction

2.1. Speeded-Up Robust Features. The SURF algorithm is divided into two stages: the interest points' detection and feature description. In the first stage, integral images and fast Hessian matrix is used for detection of image features. In the second stage, a reproducible orientation of each interest point is fixed first, then constructing a square region aligned with the selected orientation and extracting the SURF descriptor with 64 dimensions from this region. Steps are as follow [6].

- (1) *Scale Spaces Analysis.* Image pyramids are built by repeatedly Gaussian blur and subsampling.
- (2) *Interest Points Locating.* The maximum of the determinant of the Hessian matrix is calculated first. Then, nonmaximum suppression in a $3 \times 3 \times 3$ neighborhood to the image is applied, scale and image space interpolation are taken.
- (3) *Orientation Assignment.* Haar-wavelet responses in x and y direction in a circular neighborhood around the interest point is calculated. A dominant orientation is estimated and it is now invariant to rotation.
- (4) *Descriptor Extraction.* A square region centered around the interest point is constructed and oriented along the orientation selected. Then, the region is split into 4×4 square subregions and the sum of wavelet response in horizontal and vertical direction of each subregion is calculated. After normalization, a descriptor in 64 dimensions is obtained.

SURF is improved from SIFT both are based on robust points (or interest points) which are not sensitive to transformation, brightness, and noise but is less complex and more efficient than SIFT due to the smaller number and lower dimension of descriptors. An open-source library OpenSURF (<http://www.mathworks.com/matlabcentral/fileexchange/2-8300>) written by Dirk-Jan Kroom for SURF descriptor extraction is used in this paper.

2.2. Locality Sensitive Hashing. It is mentioned previously that SURF descriptors are in 64 dimensions and matching features means searching in high dimension. Among the four regularly searching methods, locality sensitive hashing (LSH) [8] is the fastest way for indexing and could be faster than other three methods for several orders of magnitude in huge-scale searching. In addition, LSH is based on probability and is more suitable for nonprecise searching. LSH was first introduced by Indyk and Motwani for nearest neighbor search [9]. The main idea is to hash vectors using several hash functions and make sure that for each hashing, the vectors with smaller distances between each other are more likely to collide in probability than that with longer distances. Different hash functions could be designed for different metrics such as Euler distance.

A family of functions can be defined as follows [10].

A family $\mathcal{H} = \{h : s \rightarrow U\}$ is said to be locality sensitive if, for any q , function $p(t) = \Pr_{\mathcal{H}}[h(q) = h(v) : q - v = t]$ decreases strictly as t increases. That is, the probability of the

collision of q and v decreases as the distance between them increases.

Stable distribution is one of the most important methods for LSH function implementation. And Gaussian distribution, one kind of famous stable distribution, is used for LSH function design frequently.

Given k, L, w , suppose that A is an $k \times d$ Gaussian matrix, A_i represents the i row of A , $b \in \mathcal{R}^k$ is a random vector, and $b_i \in [w]$, $x \in \mathcal{R}^d$; then the hash code of x can be represented as

$$g(x) = (h_1(x), \dots, h_k(x)), \quad (1)$$

$$h_i(x) = \frac{A_i x + b_i}{w}, \quad i \in [k], \quad (2)$$

$g(x)$ is the concatenation of k hash codes, and it is regularly designed as normal hash function to obtain the final scalar index, such as the following one recommended by Andoni and Indyk in one of his LSH library [10]:

$$\begin{aligned} g(x) &= f(a_1, \dots, a_k) \\ &= \left(\left(\sum_{i=1}^k r'_i a_i \right) \bmod \text{prime} \right) \bmod \text{tableSize}, \end{aligned} \quad (3)$$

in which r'_i is a random integer, prime equals $(2^{32} - 5)$, tableSize represents the size of hash table, usually equals to $|P|$, the size of searching space.

b_i in (2) is a random factor, and because it can be noticed that A itself is random already, so just set $b_i = 0$. Denominator w in (2) represents a segment mapping such that the similar values in numerator can be hashed into the same code for the purpose of neighbor searching and its value represents the segment size. In this paper, we chose $w = 0.125$.

There are two more parameters that should be determined; k for the number of hash codes should be calculated by each hash function and L for the number of hash functions. From the fact that two similar vectors will collide with the probability greater than or equal to $(1 - \delta)$ when applying LSH, we get some conditions that k and L should satisfy.

Suppose that the distance of a query q and its neighbor v is less than a constant R , and let $p_R = p(R)$; then

$$\Pr_{g \in \mathcal{G}} [g(q) = g(v)] \geq p_R^k. \quad (4)$$

And for all L hash tables, the probability that q and v does not collide is no more than $(1 - p_R^k)^L$; that is

$$1 - (1 - p_R^k)^L \geq 1 - \delta. \quad (5)$$

We get better performance if there are less hash tables. So let L be the minimum possible integer and there is

$$L = \text{floor} \frac{\log \delta}{\log (1 - p_R^k)}. \quad (6)$$

Now L is a function of k .

According to Andoni and Indyk [10], the best value of k or L should be tested by sampling. Experimental results of Corel1K image set testing show that k prefer 5, and let the value of L be 7 from (6).

2.3. Hadoop. Hadoop is mainly composed of Hadoop distributed file system (HDFS), MapReduce, and HBase. HDFS is a distributed file system using by Hadoop while HBase is a distributed NoSQL database. And MapReduce is a kind of simple but powerful programming model for parallelly processing large dataset. The operation of MapReduce contains two steps: the map step that outputting $\langle \text{key}, \text{value} \rangle$ pairs after processing the input data and the reduce step that collecting and processing the $\langle \text{key}, \text{value} \rangle$ pairs coming from the map step with the same key. Figure 1 shows how MapReduce works.

3. System Design

3.1. Overall Design. The overall design of this system is as in Figure 2. Among all the modules, Feature Extraction and Feature Matching are the most time consuming. And Matlab is used as auxiliary because there are too many image processing and matrix operations. The workflows are as follow.

- (1) *Image preprocessing*, including image scaling and graying (notice that SURF is based on gray images and is nonsensitive with image scaling).
- (2) *SURF extraction*: multiple vectors in 64 dimensions are obtained.
- (3) *Hashing*: hashing each feature from last step using (2) and (3), and 7 hash codes are obtained.
- (4) *Feature matching*: for each hash codes from last step, search corresponding hash table for match features using MapReduce then results are collected and sorted.
- (5) Output results.

3.2. Parallelization Design for Feature Matching. In this module, candidate matching features for each feature of input image are searched and candidate similar images are selected according to matching counts. For simplicity, two features are considered to be similar if their hash codes collide. In this step, the input is the feature set and several hash codes for each feature, and the output is the list of candidate similar images. This is the most time-consuming part of the whole system and is implemented by MapReduce.

Suppose $\langle K, V \rangle$ represents Key-Value pair in MapReduce; then workflow of query in parallel is shown as Figure 3.

The feasibility of this parallelization is based on two facts.

- (1) All splits are pairwise independent. That is, there are no relationships between any two splits. The format of features description is the same as the value of mapper input. Each line contains information about a feature's hash codes and image id to which it belongs and features are independent. So splits based on line break can be processed independently and concurrently.
- (2) Results from all mappers will be collected by reducer. In addition, the number of reducers is set to one; thus, all parallel processing output will be counted

and sorted in single reducer. Eventually, retrieval results are unrelated to the way the descriptions split.

Suppose that N represents set of n job servers, N_i represents the i th job server, and t_i equals to the time N_i finishes its task; then the total time for the whole cluster to finish its searching assignment is

$$T = \max \{t_1, \dots, t_n\}. \quad (7)$$

As the cluster is designed to be isomorphic, so in the case of overall task remains constant, the minimum of total time should be

$$T_{\min} = t_1 = \dots = t_n; \quad (8)$$

that is, it will take the cluster the least time as long as the sizes of all splits are the same. What should be pointed out here is that, due to the independence of each split, actually t_i is related to N_i and its real task. So, only the elements that could be controlled are discussed here.

If the size of description file before splitting is Size (MB), the split size is seg (MB), then

$$\text{seg} = \frac{\text{Size}}{n} > 64?64 : \frac{\text{Size}}{n}. \quad (9)$$

Meaning that the task is averagely split first, and every job server gets a split with the size of $\text{seg} = \text{Size}/n$. At this time, the task is balanced in all nodes, and T will get its minimum value. If seg is larger than 64 (MB), which is HDFS default block size, it may cost extra effort due to cross block accessing. At this time

$$\text{Size} = k * 64 + \text{tail}, \quad (10)$$

where k is integer and tail is less than 64 MB. That is, a description file with size Size is split into $k + 1$ parts, with k parts size 64 MB, one part size tail. These $k + 1$ parts then will be assigned to job servers by Hadoop job tracker. In later section, it can be seen that such segmentation strategy which combines all compute resource and features of Hadoop framework into thinking is simple and highly efficient.

3.3. Data Structure. There are three kinds of data in the system: the image set, the features, and the hash tables. The image set is stored in the OS file system and the other two are stored in HBase built on HDFS, the Hadoop file system. HBase does not support SQL query, so primary keys or range of primary keys are needed. Details are as follow.

- (1) *Image Set*. Images are stored as normal image files such as bmp files in the local file system, named start from 1 incrementally.
- (2) *SURF Features Table*. Normally, there are hundreds of features for each image, so invert index is better for features storage. The pattern is in this form:

$$(\text{ImageId}, i_{\text{key}}, \text{Float}, \text{Float}, \dots) \quad (11)$$

ImageId represents the identifier of an image in the local file system while i represents the i th features of image *ImageId*. Followings are 64 floats, representing a vector in 64 dimensions.

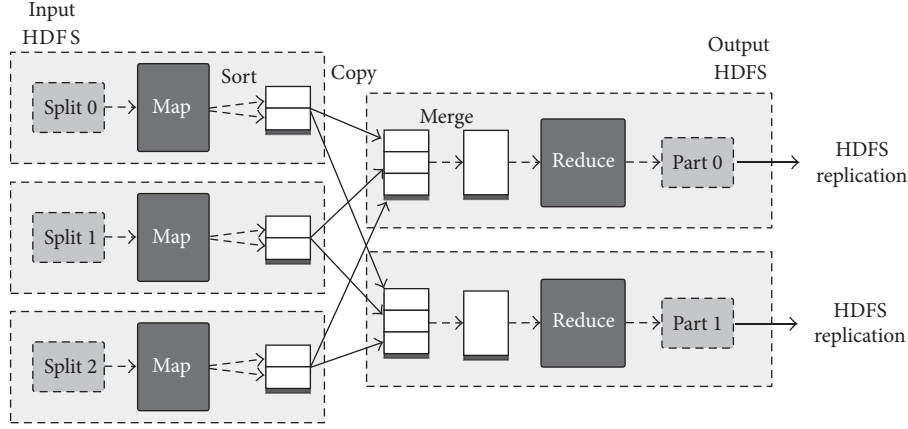


FIGURE 1: The MapReduce programming model.

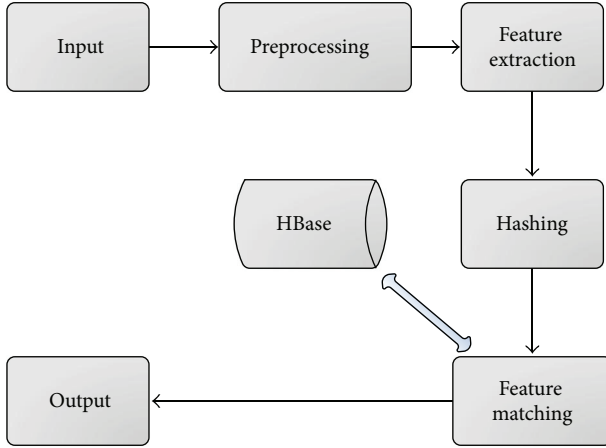


FIGURE 2: Overall design. Preprocessing, Feature Extraction and Hashing are mainly matrix operations and are implemented as Matlab scripts for the purpose of speeding up and convenience.

- (3) *Hash Table*. The hash table is used for neighbor searching. That is, select a hash code of a specific feature as key and query the corresponding value. There are 7 hash tables according to LSH in this paper, so the storage form is similar to SURF features table for the purpose of reducing database connections. That is,

$$(\text{Hashcode}_{i_{\text{key}}}, \text{ImageId}_{j_1}, \dots, \text{ImageId}_{j_k}) \quad (12)$$

Hashcode represents a hash value while *i* represents the *i*th hash function and $i = 1, \dots, 7$; for example, 55555_3 represents that the hash value of the third hash function is 55555. And *ImageId*_{*j_k*} is a key in SURF features table.

4. Experiment and Analysis

4.1. *Accuracy*. Precision and recall are the main criteria for evaluating content-based image retrieval algorithms. Because

TABLE 1: Example for feature matching.

Input	Outputs	Matches	Feature number	Percentage
118	118	256	267	99.25
	159	86	267	32.21
	472	79	267	29.59
	127	70	267	26.22
	199	70	267	26.22

the primary focus of this system is the design and implementation of distributed computing and for fuzzy searching in large-scale image database, recall is less meaningful, so only the precision is selected and tested.

As mentioned previously, SURF is robust to revolution and small change of perspective, so Corel image database is used for fully testing the precision of the system. Corel image database contains 10 kinds of images, each of 100 images, a total of 1000 images, including human, landscape, and architecture.

Results show that the percentage of the 6 returning results that are similar to the input image is 60.4%, as shown in Figure 4.

Here, two images are considered similar to each other if at least 30 pairs of features are matched, and the more they match, the more similar those two images are. As in Table 1, there are 5 outputs for image with ID “118.” Among them, the most similar one is “159” except “118” itself, with 86 matches in total 267 features.

In addition, CBIR algorithms are related to specific image database in a considerable sense, so the result in the paper is just for reference.

4.2. *Experimental Environment*. The topology of the system deploying environment is as in Figure 5. The physical machines are listed in Table 2. The configurations of virtual machines are listed in Table 3 and the software environments are listed in Table 4. As shown, there are 11 physical machines, containing 1 master and 30 slaves and HBase Region Servers which are all virtual machines.

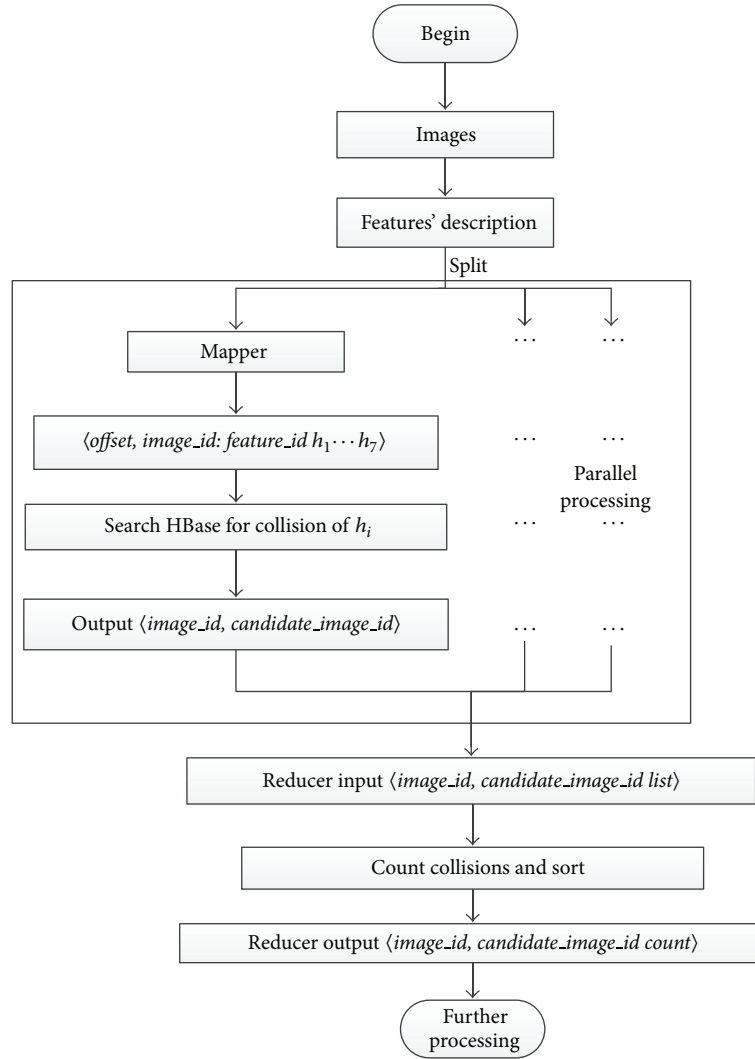


FIGURE 3: Parallel processing model.



FIGURE 4: Typically, 6 images that are most similar to the input one will be shown.

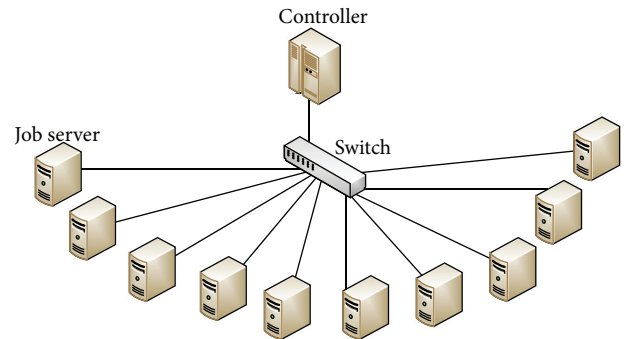


FIGURE 5: Topology of system deploying environment. 11 servers are connect with a switch.

4.3. Results and Analysis. In the system, 30 million features of 159955 images are recorded. The size of data, including scaled images, features, and hash codes, is up to 9.93 GB.

Efficiency testing is divided into two parts: the feature extraction and feature matching. Feature extraction is tested in single node as its algorithm is not distributed and feature

TABLE 2: Physical machines configurations.

Type	CPU	Memory	Number
Controller	Intel Core i7 2600 4 × 3.4 GHZ	16 GB	1
Job Server	Intel Xeon E3-1235 4 × 3.2 GHZ	32 GB	10

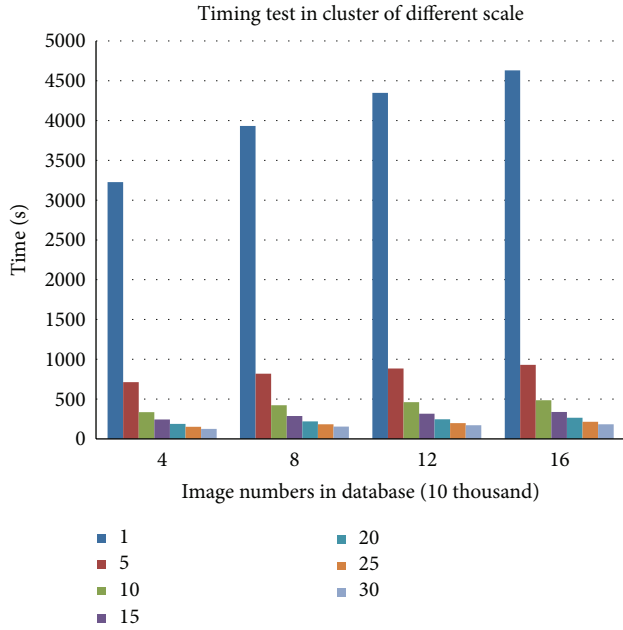


FIGURE 6: Time spent for feature matching. Legends from 1 to 30 indicate the number of nodes in a cluster.

matching is tested in cluster of different scale (single node, five nodes to thirty nodes increasing by 5 nodes a time), respectively.

Extracting the features of all the 159955 JPEG images with the resolution less than or equal to 256×256 in the Controller takes about 180 minutes, in speed of about 14.8 images per second. Extracted features will be written into database, so this extraction operation only has to be done for one time.

Results of feature matching of 31993 input images whose features have been extracted are shown in Table 5 and Figure 6.

Table 5 shows that, when there are 40 thousand images in the database, it costs 3227 seconds for single node to accomplish the job while only 125 seconds for thirty nodes and the ratio is almost 25.8. Other scales of database are similar. In addition, with 160 thousand images in database, the system can match features as fast as 0.006 second per image.

Figure 6 shows that, in a specific database, consuming time is reducing linearly as the number of nodes increases. That is, the performance of the system is increasing linearly as the number of nodes increases.

Another view of the results shown in Table 5 is in Figure 7. The abscissa represents the nodes of a cluster, and the ordinate is the ratio of cost time in single node and in corresponding

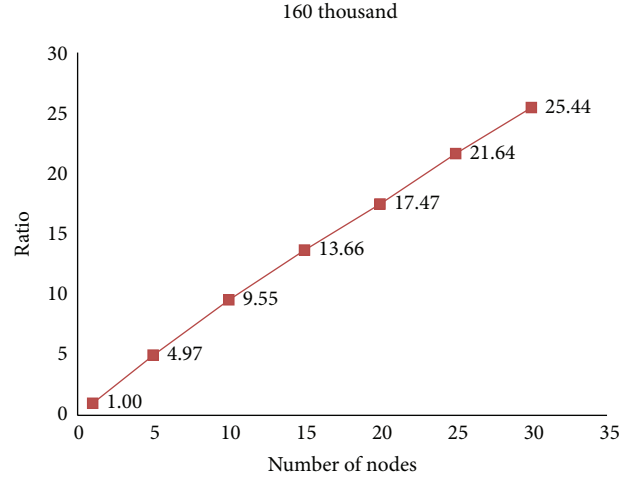


FIGURE 7: Ratio of performance improvement with 160 thousand images in database.

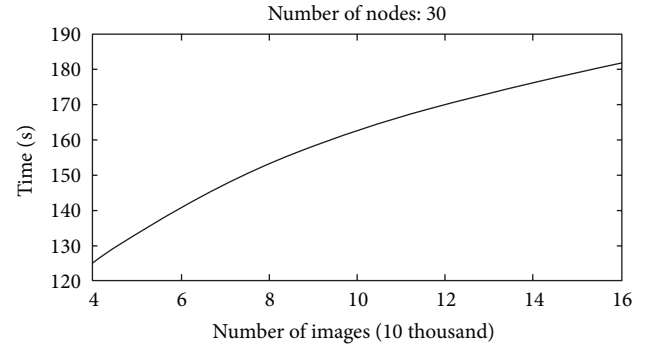


FIGURE 8: Time spent increases logarithmically as data in database grows when there are 30 nodes running in a cluster.

scale of cluster. For example, 9.55 means that the time cost in single node is 9.55 times of that in cluster of 10 nodes. From Figure 7, it can be confirmed that, in a specific database, the performance of the system increases almost linearly as the number of nodes increases which indicates that the system is able to accomplish the jobs distributedly by calling all the nodes in the cluster efficiently and fully prove the system's availability and excellent expansibility in distributed environment. Other cases are similar.

Time consumed for different databases in cluster of 30 nodes is shown in Figure 8. It can be seen that the time cost is increased logarithmically as database grows, indicating that the system has strong suitability and advantage in performance for large-scale database. Other cases are similar.

To conclude, especially from the analysis of Figures 6–8, it can be seen that the system has two major advantages.

- (1) It can be expanded quite easily as the performance of the system is increasing linearly with the increasing in the number of nodes. Adding nodes means speeding up.

TABLE 3: Virtual machines configurations.

Role	Belongs to	Frequency	Memory	Number	Network
Master	Controller	5.0 GHz	8 GB	1	1 Gbps Switch
Slave	Job Server	3.0 GHz	4 GB	3×10	

TABLE 4: Virtual machines software environment.

OS	Hadoop	HBase	JDK
Centos 6.3	Hadoop-1.0.1	HBase-0.92.1	1.6.0_22

TABLE 5: Time (second) spent for feature matching.

Nodes	10 thousand				Average
	4	8	12	16	
1	3227	3933	4347	4630	4034.25
5	713	819	883	931	836.5
10	335	423	461	485	426
15	243	287	317	339	296.5
20	188	220	247	265	230
25	152	183	198	214	186.75
30	125	153	171	182	157.75
1:30	25.82	25.71	25.42	25.44	25.60

- (2) Time cost is increased logarithmically as database grows. So, it will perform better against larger database.

The system designed is able to take full advantage of distributed architecture, making the searching rate increased almost linearly as the number of nodes grows to achieve the goal of fast content-based image retrieval.

5. Conclusion

In this paper, a method for content-based image retrieval under distributed framework is proposed and discussed from theory and implementation. Experimental results show that it is able to retrieve images based on content on large-scale image sets effectively. Distributed framework and large scale of data are the main focus of the system. It is rather significant to solve the severe problems of huge amount of computing and storage by combining the traditional CBIR with distributed computing to gain higher efficiency. In addition, the system is remaining to be improved such as the following:

- (1) *Make Improvement on CBIR Algorithms.* CBIR is a complexity technique. So, in the context of getting an acceptable result, only one algorithm is used to simplify. Other image processing techniques could be applied to improve both the precision and performance. Techniques such as the affine invariant features extraction method in [11, 12] which can be used for object classification both in database building and parallel searching stages may speed up the whole process by indexing images to different category.

- (2) *System Optimization and Real-Time Enhancement.* Optimization can be done by optimizing Hadoop and HBase. But as it takes a long time for Hadoop jobs to start up and be scheduled, it is not suitable for real-time processing. Other distributed computing model such as Twitter Storm (<http://storm-project.net/>) stream computing can be considered.

References

- [1] W. Niblack, R. Barber, W. Equitz et al., "QBIC project: querying images by content, using color, texture, and shape," in *Storage and Retrieval for Image and Video Databases*, pp. 173–187, February 1993.
- [2] D. G. Lowe, "Distinctive image features from scale-invariant keypoints," *International Journal of Computer Vision*, vol. 60, no. 2, pp. 91–110, 2004.
- [3] Y. Ke and R. Sukthankar, "PCA-SIFT: a more distinctive representation for local image descriptors," in *Proceedings of the IEEE Computer Society Conference on Computer Vision and Pattern Recognition (CVPR '04)*, pp. II506–II513, July 2004.
- [4] M. Grabner, H. Grabner, and H. Bischof, "Fast Approximated SIFT," in *Proceedings of the Asian Conference on Computer Vision*, pp. 918–927, Hyderabad, India, 2006.
- [5] B. Smith, "An approach to graphs of linear forms," unpublished.
- [6] H. Bay, A. Ess, T. Tuytelaars, and L. Van Gool, "Speeded-Up Robust Features (SURF)," *Computer Vision and Image Understanding*, vol. 110, no. 3, pp. 346–359, 2008.
- [7] T. White, *Hadoop: The Definitive Guide*, O'Reilly Media, 2009.
- [8] A. Gionis, P. Indyk, and R. Motwani, "Similarity search in high dimension via hashing," in *Proceedings of the International Conference on Very Large Databases*, 1999.
- [9] P. Indyk and R. Motwani, "Approximate nearest neighbors: towards removing the curse of dimensionality," in *Proceedings of the 30th Annual ACM Symposium on Theory of Computing*, pp. 604–613, Dallas, Tex, USA, May 1998.
- [10] A. Andoni and P. Indyk, "E2LSH.0.1 User Manual," June 2005.
- [11] J. Yang, M. Li, Z. Chen, and Y. Chen, "Cutting affine moment invariants," *Mathematical Problems in Engineering*, vol. 2012, Article ID 928161, 12 pages, 2012.
- [12] J. Yang, G. Chen, and M. Li, "Extraction of affine invariant features using fractal," *Advances in Mathematical Physics*, vol. 2013, Article ID 950289, 8 pages, 2013.

Research Article

Attractor Transformation by Impulsive Control in Boolean Control Network

Bo Gao,^{1,2,3} Haipeng Peng,² Dawei Zhao,² Wenguang Zhang,⁴ and Yixian Yang^{1,2}

¹ School of Computer and Information Technology, Beijing Jiaotong University, Beijing 100044, China

² Information Security Center, Beijing University of Posts and Telecommunications, P.O. Box 145, Beijing 100876, China

³ School of Computer Information Management, Inner Mongolia University of Finance and Economics, Hohhot 010051, China

⁴ College of Animal Science, Inner Mongolia Agricultural University, Hohhot 010018, China

Correspondence should be addressed to Bo Gao; gaobonmghht@gmail.com

Received 11 June 2013; Accepted 9 July 2013

Academic Editor: Ming Li

Copyright © 2013 Bo Gao et al. This is an open access article distributed under the Creative Commons Attribution License, which permits unrestricted use, distribution, and reproduction in any medium, provided the original work is properly cited.

Boolean control networks have recently been attracting considerable interests as computational models for genetic regulatory networks. In this paper, we present an approach of impulsive control for attractor transitions in Boolean control networks based on the recent developed matrix semitensor product theory. The reachability of attractors is estimated, and the controller is also obtained. The general derivation proposed here is exemplified with a kind of gene model, which is the protein-nucleic acid interactions network, on numerical simulations.

1. Introduction

Gene regulatory networks (GRNs) have been offering plenty of holistic approaches to biological processes. They can explicitly represent the causality of developmental processes and exactly describe the state set of biological systems [1]. Waddington and Kacser proposed a metaphor that the developmental process of GRNs can be represented by a ball rolling down along a landscape with peaks and valleys, and the steady states, which were called attractors, were found at the bottom of the basins [2]. In cell model, there is a one-to-one relationship between the attractors and the observed phenotypes. This means that different cell types can be characterized by different attractors [3]. The states of a GRN will stay in an attractor, unless it is perturbed by an outside impact [4].

In several studies on GRNs such as genetic organogenesis and diseases, researchers have considered to make the states of GRN transit from one attractor to another one by using control methods [5–7]. It was found that repression of a single RNA binding polypyrimidine tract-binding protein was sufficient to induce transdifferentiation of fibroblasts into functional neurons in [8]. An approach was presented to evaluate drug targets of GRN inference to ovarian cancer in [9].

The previous studies mainly focused on intervening the system to help it transit to the desirable attractors by controlling a (or some) valid genetic locus. Since most of the existing achievements in related fields were obtained based on the experiments, the actual impact of control on the same GRN is uncertain [10]. In brief, to estimate the effectiveness of the controller for the transformation of GRNs from one attractor to another one, still remains an open crucial theoretical problem [11–15].

A Boolean network (BN) is often used as a model for gene regulation which treats genes as binary nodes that are either expressed or unexpressed [4]. In order to manipulate networks, the control of BNs is an important topic. A Boolean control network (BCN) can be considered as a BN with additional binary inputs. BCNs are attracting considerable interests as computational models for GRNs which use the exogenous inputs. BCN has been widely used in yeast cell-cycle [16], *Drosophila melanogaster* [17], and other kinds of cells.

In this paper, we propose a theoretical method to estimate the effects of a certain impulsive controller in a BCN and solve the appropriate controller by using semitensor product. Compared with the existing methods, based on the results of the experiments, our mathematics-based approach is more accurate and simpler.

The rest of this paper is organized as follows. Section 2 reviews STP and the model of BN. In Section 3, the reachability of an attractor is realized and the controller is also obtained. Section 4 gives our main results of an example. Section 5 is the conclusion.

2. Preliminaries

2.1. Semitensor Product. Semitensor product (STP) of matrices was firstly proposed by Cheng and Dong. It is the algebraic form and the coordinate transformation of BN and BCN. Based on STP, BNs and BCNs can be converted into equivalent algebraic form of some standard discrete-time system [18]. In this paper, STP is denoted by “ \ltimes ”.

Definition 1. Assuming there are two matrices $A \in \mathbb{R}^{m \times n}$ and $B \in \mathbb{R}^{p \times q}$, the STP of A and B is $A \ltimes B = (A \otimes I_{\alpha/n})(B \otimes I_{\alpha/p})$, where α is the least common multiple of n and p , “ \otimes ” is the Kronecker product, and I_k is the identity matrix.

The STP of matrices makes all the fundamental properties of the conventional matrix product remain true [19]. With STP, Boolean operation can be converted into matrix product. These two logical values, “true” and “false,” are expressed in vector forms as δ_2^1 and δ_2^2 , where δ_n^r denotes the r th column of the identity matrix I_n . Some fundamental logical functions are identified as $M = [\delta_n^{i_1}, \delta_n^{i_2}, \dots, \delta_n^{i_s}]$, which is also briefly expressed as $M = \delta_n[i_1, i_2, \dots, i_s]$. And the logic relationships are

- (1) negation: $M_n = \delta_2[2, 1]$;
- (2) disjunction: $M_d = \delta_2[1, 1, 1, 2]$;
- (3) conjunction: $M_c = \delta_2[1, 2, 2, 2]$;
- (4) XOR: $M_p = \delta_2[2, 1, 1, 2]$.

The above matrices are called the structure matrices.

2.2. Attractor. A BN, which is typically formulated as a directed graph, composed of n nodes, whose state indicates whether the gene is switched 1 (on) or 0 (off). The state of each node at time $t + 1$ is determined by the state of its spatial neighbors at time t . The system can be described by

$$\begin{aligned} x_1(t+1) &= f_1(x_1(t), x_2(t), \dots, x_n(t)), \\ x_2(t+1) &= f_2(x_1(t), x_2(t), \dots, x_n(t)), \\ &\vdots \\ x_n(t+1) &= f_n(x_1(t), x_2(t), \dots, x_n(t)), \end{aligned} \quad (1)$$

where f_i ($i = 1, 2, \dots, n$) is an n -ary logical function.

The BN is a globally convergence system. An attractor, called the stable state of system, is in the form of either a single state (fixed point) or a repeating set of states (cycle) [20]. Here, we consider how to find the attractors of (1). According to STP, we define

$$A(t) = \ltimes_{i=1}^n x_n(t). \quad (2)$$

Then

$$A(t+1) = \ltimes_{i=1}^n M_i A(t), \quad (3)$$

where M_i ($i = 1 \dots n$) is the structure matrix. Using the properties of STP, (3) can be converted into an algebraic form as

$$A(t+1) = LA(t), \quad (4)$$

where $L \in \Delta_{2^n \times 2^n}$ is called the transition matrix. The state of (1) is uniquely determined by the transition matrix. Each column of L , which is called state number, represents a state of the BN. The attractor has the following definitions:

- (1) a state $x(t) \in \Delta_{2^n}$ is called a fixed point if $Lx(t) = x(t)$;
- (2) $\{x(t), Lx(t), \dots, L^k x(t)\}$ is called a cycle with length k if $L^k x(t) = x(t)$ and the elements in the set $\{x(t), Lx(t), \dots, L^{k-1} x(t)\}$ are distinct.

Theorem 2. In system (1), the number of length s cycles, N_s , is inductively determined by

$$\begin{aligned} N_1 &= \text{Trace}(L), \\ N_k &= \frac{(\text{Trace}(L^k) - \sum_{s \in \mathcal{P}(k)} s N_s)}{k}, \quad 2 \leq k \leq 2^n, \end{aligned} \quad (5)$$

where $\mathcal{P}(k)$ is the set of proper factors of k . According to (5), one can find all the attractors in the state space of BN (1) [21].

3. Main Results

In GRNs, much attention focuses on making the whole system transit from one attractor to another by control methods [22, 23]. Since the impulsive controller could destroy the cycle structure of the biological system, it is widely used in GRNs [24]. First, we will judge the reachability of an attractor.

Assume $\mathcal{A}_1 = \{x_h \mid h = 1 \dots l_1\}$ and $\mathcal{A}_2 = \{y_r \mid r = 1 \dots l_2\}$ are two attractors in system (1). l_1 and l_2 are the lengths of \mathcal{A}_1 and \mathcal{A}_2 , respectively. We will determine the reachability from \mathcal{A}_1 to \mathcal{A}_2 .

Here, we consider a BCN with m impulsive inputs at time t , and it is defined as

$$\begin{aligned} \tilde{x}_1(t+1) &= \tilde{f}_1(x_1(t), \dots, x_n(t), u_1(t), \dots, u_m(t)), \\ &\vdots \\ \tilde{x}_n(t+1) &= \tilde{f}_n(x_1(t), \dots, x_n(t), u_1(t), \dots, u_m(t)), \end{aligned} \quad (6)$$

where f_i ($i = 1, 2, \dots, n$) is an n -ary logical function and u_j ($j = 1 \dots m$) is the impulsive input. u_j is described as

$$u_j(t) = \begin{cases} \text{input}, & t = t_k, \\ \text{no input}, & t \neq t_k, \end{cases} \quad (7)$$

where input is 0 or 1. When system (6) is at time $t = t_k$, according to STP, we define

$$\tilde{A}(t) = (\ltimes_{i=1}^n x_i(t)) \ltimes (\ltimes_{j=1}^m u_j(t)), \quad (8)$$

then

$$\tilde{A}(t+1) = \times_{i=1}^n M_i \tilde{A}(t), \quad (9)$$

where M_i ($i = 1 \cdots n$) is the structure matrix. So (9) can be converted into an algebraic form as follows:

$$\tilde{A}(t+1) = \tilde{L}\tilde{A}(t), \quad (10)$$

where $\tilde{L} \in \Delta_{2^n \times 2^{n+m}}$ is called the state transition matrix of system (6).

Theorem 3. Consider (6). The transformation from attractor \mathcal{A}_1 to attractor \mathcal{A}_2 is reachable with controllers $u_1(t) \cdots u_m(t)$ if and only if

$$\tilde{L}\mathcal{A}_1 \cap \mathcal{A}_2 \neq \phi, \quad (11)$$

where ϕ is the null set.

Proof. Since \tilde{L} is the linear representation of matrix L with the inputs $u_1(t) \cdots u_m(t)$, $\tilde{L}\mathcal{A}_1$ is the reachable state set of \mathcal{A}_1 . The intersection set of $\tilde{L}\mathcal{A}_1$ and \mathcal{A}_2 is the destination states from \mathcal{A}_1 to \mathcal{A}_2 with controllers $u_1(t) \cdots u_m(t)$. \square

Definition 4. Assume y_r is the destination state for the transition from \mathcal{A}_1 to \mathcal{A}_2 if and only if

$$y_r \in \tilde{L}\mathcal{A}_1 \cap \mathcal{A}_2, \quad (12)$$

then x_h is the source state if and only if

$$y_r = \tilde{L}x_h, \quad (13)$$

where $x_h \in \mathcal{A}_1$ and $y_r \in \mathcal{A}_2$.

Next, we will find the existence of the controller for attractor transition.

Theorem 5. Consider system (6). Assume $\tilde{L}x_h = \{e_k \mid k = 1 \cdots 2^m\}$; if $y_r = e_k$, we have $\delta_{2^m}^k$. The impulsive controllers are obtained by

$$\delta_{2^m}^k = u_1(t) \times u_2(t) \times \cdots \times u_m(t), \quad (14)$$

where $u_j(t)$ ($j = 1 \cdots m$) is the impulsive input at time t .

Proof. Since $\tilde{L}x_h$ is the destination state from x_h with impulsive inputs $u_1(t) \cdots u_m(t)$, each e_k represents each state which is from x_h by inputs $u_1(t) \cdots u_m(t)$. Equation (14) is based on the properties of STP.

We can solve the input values for a deterministic target by using (14). \square

4. Example

In order to illustrate our approach, an example is given in this section. It is an idealized protein-nucleic acid interaction

involved in gene regulation model in cells [25]. The type of unit component which we will study is shown as follows:

$$\begin{aligned} x_1(t+1) &= 1 + x_3(t) + x_6(t) + x_3(t)x_6(t), \\ x_2(t+1) &= x_1(t), \\ x_3(t+1) &= x_2(t), \\ x_4(t+1) &= 1 + x_3(t) + x_6(t) + x_3(t)x_6(t), \\ x_5(t+1) &= x_4(t), \\ x_6(t+1) &= x_5(t), \end{aligned} \quad (15)$$

where $A \cdot B$ represents A Conjunction B and $A + B$ represents the XOR operation between A and B . Based on (2)–(4), the L matrix of system (15) is $L = \delta_{64}[37 \ 37 \ 38 \ 38 \ 39 \ 39 \ 40 \ 40 \ 37 \ 1 \ 38 \ 2 \ 39 \ 3 \ 40 \ 4 \ 45 \ 45 \ 46 \ 46 \ 47 \ 47 \ 48 \ 48 \ 45 \ 9 \ 46 \ 10 \ 47 \ 11 \ 48 \ 12 \ 53 \ 53 \ 54 \ 54 \ 55 \ 55 \ 56 \ 56 \ 53 \ 17 \ 54 \ 18 \ 55 \ 19 \ 56 \ 20 \ 61 \ 61 \ 62 \ 62 \ 63 \ 63 \ 64 \ 64 \ 61 \ 25 \ 62 \ 26 \ 63 \ 27 \ 64 \ 28]$.

Using (5), we obtain that there are the following two attractors in the state space:

$$\begin{aligned} \mathcal{A}_1 &= (19) \longrightarrow (46) \longrightarrow (19), \\ \mathcal{A}_2 &= (1) \longrightarrow (37) \longrightarrow (55) \longrightarrow (64) \longrightarrow (28) \\ &\longrightarrow (10) \longrightarrow (1). \end{aligned} \quad (16)$$

The attractors of this system represent different quantities of the generation of a metabolic species.

Next, assume the system is already in attractor \mathcal{A}_1 ; we want to transit the whole system from \mathcal{A}_1 to \mathcal{A}_2 with some impulsive controllers.

The BCN is expressed as

$$\begin{aligned} x_1(t+1) &= 1 + x_3(t) + x_6(t) + x_3(t)x_6(t), \\ x_2(t+1) &= x_1(t) + u_1(t), \\ x_3(t+1) &= x_2(t), \\ x_4(t+1) &= 1 + x_3(t) + x_6(t) + x_3(t)x_6(t), \\ x_5(t+1) &= x_4(t) + u_2(t), \\ x_6(t+1) &= x_5(t), \end{aligned} \quad (17)$$

where u_1, u_2 are controllers.

Step 1. Using (8)–(10), we obtain the matrix \tilde{L} . Based on the computing of \tilde{L} , we obtain $\tilde{L}\mathcal{A}_1 = \delta_{64}[64 \ 62 \ 48 \ 46 \ 1 \ 3 \ 17 \ 19]$. According to (11), the intersection of two sets is $\tilde{L}\mathcal{A}_1 \cap \mathcal{A}_2 = \delta_{64}[64 \ 1] \neq \phi$. So, the transformation from \mathcal{A}_1 to \mathcal{A}_2 is reachable, and $y_{r1} = \delta_{64}[64]$ and $y_{r2} = \delta_{64}[1]$ are the destination states.

Step 2. Since \mathcal{A}_1 is made up of two states, which are $\mathcal{A}_{11} = \delta_{64}[19]$ and $\mathcal{A}_{12} = \delta_{64}[46]$, we have

$$\begin{aligned} \tilde{L}\mathcal{A}_{11} &= \delta_{64}[64 \ 62 \ 48 \ 46], \\ \tilde{L}\mathcal{A}_{12} &= \delta_{64}[1 \ 3 \ 17 \ 19], \end{aligned} \quad (18)$$

then $\tilde{L}\mathcal{A}_{11} \cap y_{r1} \neq \phi$ and $\tilde{L}\mathcal{A}_{12} \cap y_{r2} \neq \phi$.

So $x_{h1} = \mathcal{A}_{11} = \delta_{64}$ [19] and $x_{h2} = \mathcal{A}_{12} = \delta_{64}$ [46] are source states.

Step 3. Letting $\tilde{\mathcal{L}}\mathcal{A}_{11} = \{e_k \mid k = 1, \dots, 4\}$, $y_{r1} = e_1$, we have δ_4^1 . Based on Theorem 5, the impulsive controllers are described as

$$\begin{aligned} u_1(t) &= \begin{cases} 1, & t = t_k, \\ \text{no input}, & t \neq t_k, \end{cases} \\ u_2(t) &= \begin{cases} 1, & t = t_k, \\ \text{no input}, & t \neq t_k. \end{cases} \end{aligned} \quad (19)$$

Similarly, we can obtain other impulsive controllers which are described as

$$\begin{aligned} u_1(t) &= \begin{cases} 1, & t = t_k, \\ \text{no input}, & t \neq t_k, \end{cases} \\ u_2(t) &= \begin{cases} 1, & t = t_k, \\ \text{no input}, & t \neq t_k, \end{cases} \end{aligned} \quad (20)$$

whose source state is $\mathcal{A}_{12} = \delta_{64}$ [46].

The conclusion of this example is that there are two kinds of controllers which can transform the state of system (17) from attractor \mathcal{A}_1 to attractor \mathcal{A}_2 . They can be described as follows.

The First. The source state number is 19, the destination state number is 64, and the impulsive controllers are

$$\begin{aligned} u_1(t) &= \begin{cases} 1, & t = t_k, \\ \text{no input}, & t \neq t_k, \end{cases} \\ u_2(t) &= \begin{cases} 1, & t = t_k, \\ \text{no input}, & t \neq t_k. \end{cases} \end{aligned} \quad (21)$$

The Second. The source state number is 46, destination state number is 1, and the impulsive controllers are

$$\begin{aligned} u_1(t) &= \begin{cases} 1, & t = t_k, \\ \text{no input}, & t \neq t_k, \end{cases} \\ u_2(t) &= \begin{cases} 1, & t = t_k, \\ \text{no input}, & t \neq t_k. \end{cases} \end{aligned} \quad (22)$$

5. Conclusion

This paper explores the problem of attractor transformation by impulsive control in BCN. We propose an effective algorithm which allows us to realize the transformation among different attractors of the BCN. Although the protein-nucleic acid gene network has relatively simple structure compared with those exhibited by metazoans, the attractors transformation by impulsive control is impressively significant. Our findings open a new perspective in the attractor transformation by impulsive control which is of utmost importance in areas as diverse as drug target and gene regulation and so forth. Developing more effective algorithms or approximate techniques for the present approaches will be the future work.

Acknowledgments

This paper is supported by the National Natural Science Foundation of China (Grant nos. 61100204, 61070209, 61121061, and 61272402), the Asia Foresight Program under NSFC Grant (Grant no. 61161140320), and Inner Mongolia Colleges and Universities Scientific and Technological Research Projects (Grant no. NJZY12176).

References

- [1] E. Davidson and M. Levine, "Gene regulatory networks," *Proceedings of the National Academy of Sciences of the United States of America*, vol. 102, no. 14, p. 4935, 2005.
- [2] C. H. Waddington and H. Kacser, *The Strategy of Genes*, George Allen Unwin, Bristol, UK, 1957.
- [3] S. Huang, "Regulation of cellular states in mammalian cells from a genomewide view," in *Gene Regulation and Metabolism*, pp. 181–220, MIT Press, Cambridge, Mass, USA, 2002.
- [4] S. A. Kauffman, "Metabolic stability and epigenesis in randomly constructed genetic nets," *Journal of Theoretical Biology*, vol. 22, no. 3, pp. 437–467, 1969.
- [5] F. H. Willeboordse and K. Kaneko, "Externally controlled attractor selection in a high-dimensional system," *Physical Review E*, vol. 72, no. 2, Article ID 026207, 2005.
- [6] A. Sakata, K. Hukushima, and K. Kaneko, "Funnel landscape and mutational robustness as a result of evolution under thermal noise," *Physical Review Letters*, vol. 102, no. 14, Article ID 148101, 2009.
- [7] C. Cattani, G. Pierro, and G. Altieri, "Entropy and multifractality for the myeloma multiple TET 2 gene," *Mathematical Problems in Engineering*, vol. 2012, Article ID 193761, 14 pages, 2012.
- [8] Y. Xue, K. Ouyang, J. Huang et al., "Direct conversion of fibroblasts to neurons by reprogramming PTB-regulated MicroRNA circuits," *Cell*, vol. 152, pp. 82–96, 2013.
- [9] P. B. Madhamshettiwar, S. R. Maetschke, M. J. Davis, A. Reverter, and M. A. Ragan, "Gene regulatory network inference: evaluation and application to ovarian cancer allows the prioritization of drug targets," *Genome Medicine*, vol. 4, no. 5, article 41, 2012.
- [10] L. T. MacNeil and A. J. M. Walhout, "Gene regulatory networks and the role of robustness and stochasticity in the control of gene expression," *Genome Research*, vol. 21, no. 5, pp. 645–657, 2011.
- [11] C. Toma, "Advanced signal processing and command synthesis for memory-limited complex systems," *Mathematical Problems in Engineering*, vol. 2012, Article ID 927821, 13 pages, 2012.
- [12] E. G. Bakhoun and C. Toma, "Specific mathematical aspects of dynamics generated by coherence functions," *Mathematical Problems in Engineering*, vol. 2011, Article ID 436198, 10 pages, 2011.
- [13] M. Li, "Approximating ideal filters by systems of fractional order," *Computational and Mathematical Methods in Medicine*, vol. 2012, Article ID 365054, 6 pages, 2012.
- [14] M. Li and W. Zhao, "Visiting power laws in cyber-physical networking systems," *Mathematical Problems in Engineering*, vol. 2012, Article ID 302786, 13 pages, 2012.
- [15] M. Li, S. C. Lim, and S. Chen, "Exact solution of impulse response to a class of fractional oscillators and its stability," *Mathematical Problems in Engineering*, vol. 2011, Article ID 657839, 9 pages, 2011.

- [16] A. Fauré, A. Naldi, C. Chaouiya, and D. Thieffry, "Dynamical analysis of a generic Boolean model for the control of the mammalian cell cycle," *Bioinformatics*, vol. 22, no. 14, pp. e124–e131, 2006.
- [17] R. Albert and H. G. Othmer, "The topology of the regulatory interactions predicts the expression pattern of the segment polarity genes in *drosophila melanogaster*," *Journal of Theoretical Biology*, vol. 223, no. 1, pp. 1–18, 2003.
- [18] D. Cheng and Y. Dong, "Semi-tensor product of matrices and its some applications to physics," *Methods and Applications of Analysis*, vol. 10, no. 4, pp. 565–588, 2003.
- [19] D. Cheng and H. Qi, "A linear representation of dynamics of Boolean networks," *IEEE Transactions on Automatic Control*, vol. 55, no. 10, pp. 2251–2258, 2010.
- [20] L. Li, H. Peng, Y. Yang, and X. Wang, "On the chaotic synchronization of Lorenz systems with time-varying lags," *Chaos, Solitons and Fractals*, vol. 41, no. 2, pp. 783–794, 2009.
- [21] D. Cheng and H. Qi, "Controllability and observability of Boolean control networks," *Automatica*, vol. 45, no. 7, pp. 1659–1667, 2009.
- [22] L. Li, Y. Yang, H. Peng, and X. Wang, "An optimization method inspired by "chaotic" ant behavior," *International Journal of Bifurcation and Chaos in Applied Sciences and Engineering*, vol. 16, no. 8, pp. 2351–2364, 2006.
- [23] H. Peng, L. Li, Y. Yang, and F. Sun, "Conditions of parameter identification from time series," *Physical Review E*, vol. 83, no. 3, Article ID 036202, 2011.
- [24] C. Villarreal, P. Padilla-Longoria, and E. R. Alvarez-Buylla, "General theory of genotype to phenotype mapping: derivation of epigenetic landscapes for N-node complex gene regulatory networks," *Physical Review Letters*, vol. 109, no. 11, Article ID 118102, 5 pages, 2012.
- [25] B. C. Goodwin, *Temporal Organization in Cells: A Dynamic Theory of Cellular Control Process*, chapter 4, Academic Press, New York, NY, USA, 1963.

Research Article

Transient Aspects of Wave Propagation Connected with Spatial Coherence

Ezzat G. Bakhoun¹ and Cristian Toma²

¹ Department of Electrical and Computer Engineering, University of West Florida, 11000 University Parkway, Pensacola, FL 32514, USA

² Faculty of Applied Sciences, Politechnica University, 315 Spl. Independentei, Bucharest, Romania

Correspondence should be addressed to Cristian Toma; cgtoma@physics.pub.ro

Received 30 June 2013; Accepted 10 July 2013

Academic Editor: Carlo Cattani

Copyright © 2013 E. G. Bakhoun and C. Toma. This is an open access article distributed under the Creative Commons Attribution License, which permits unrestricted use, distribution, and reproduction in any medium, provided the original work is properly cited.

This study presents transient aspects of light wave propagation connected with spatial coherence. It is shown that reflection and refraction phenomena involve spatial patterns which are created within a certain transient time interval. After this transient time interval, these patterns act like a memory, determining the wave vector for subsequent sets of reflected/refracted waves. The validity of this model is based on intuitive aspects regarding phase conservation of energy for waves reflected/refracted by multiple centers in a certain material medium.

1. Introduction

As it is known, the study of light wave propagation phenomena as reflection and refraction at the interface between two different media is based on wavefronts generated by multiple centers of reflection/refraction situated on this interface. These wavefronts correspond to surfaces over which the light wave has a constant phase. Usually, a wavefront is represented by the surface over which the wave has a maximum value (the crest of a wave).

The direction of propagation for the wave (which is also the direction of the wave vector, usually denoted by \mathbf{k}) is always perpendicular to the surface of the wavefront at each point. Thus, the wavefronts of a point source (emitting in all spatial directions) are spheres, and the wave propagates radially outward the radius of a sphere being perpendicular to the circumference at each point.

According to Huygens' principle for propagation of light, each point on a certain wavefront acts as a point source that emits spherical wavelets. These wavelets propagate with the speed of light in the medium and generate the total wavefront at a later time as the envelope that encloses all of these wavelets. This corresponds to the tangent line that joins the front surface for each of them.

However, we must take into account the fact that each center of reflection/refraction (usually represented by an

infinitely small spatial area of the interface) should be considered also as emitting spherical energy waves in all directions. For an oblique incidence of a plane wave, a certain center of reflection/refraction will be the first one which emits wavelets with the speed of light specific to that material medium. Until it interacts with the wavefront generated by another center of reflection/refraction, we should consider that the energy received from the incident wave is radiated along all spatial directions. After these first two wavelets interact, it can be considered that they create a wavefront with a greater radius of curvature along the main direction of reflection/refraction, resulting a lower-divergence beam. However, a significant amount of energy will still be radiated in all spatial directions. The same aspect can be noticed by analyzing the interaction of each newly created wavefront with previously reflected/refracted wavelets. The radius of curvature is lowered, but supplementary amounts of energy are still radiated in all spatial directions (not just along the main axis of reflection/refraction) by these new wavefronts. If the lowering of beam divergence is not a prevailing phenomenon, the reflected/refracted wave would vanish very quickly.

Moreover, the assumption regarding the constant phase shift (π for electric field \mathbf{E} , e.g.) for reflected/refracted wave in surface point is also questionable, since the interface is

far from being perfectly smooth and perfectly conductive. A certain transient time interval for creating the electrostatic equilibrium is always required. As a consequence, local phase shifts for reflected/refracted wave cannot be avoided within this local mathematical model. According to the standard propagation theory of waves, these could generate multiple local waves propagating in all spatial directions. Thus, the energy of reflected/refracted wave would be dissipated in a large solid angle (corresponding to a high divergence of the light beam) and directionality would be lost within a very short length interval.

For this reason, a complete analysis of phenomena on such transient time intervals should be based on a global analysis of interface and wavefront aspects. Spatial coherence should be taken into consideration.

As a consequence, a certain amount of energy is lost during this transient time interval. A deeper analysis of this model (for the stationary regime) requires a certain memory of previous interaction and a certain spatial coherence to be taken into account, as will be shown in the next paragraphs.

2. Periodical Effect of Momentum Space Patterns

As it is known, quantum theory uses either position or momentum space for representing states and evolution of particles and their associated fields. A preliminary analysis of reflection/refraction phenomena is based on classical electromagnetic field, which corresponds in fact to the wave function associated to a photon (the electric field \mathbf{E} , magnetic field \mathbf{B} , vector potential \mathbf{A} , and scalar potential \mathbf{V} being the main quantities used). This wave function can explain basic aspects in wave theory of light as reflection/refraction working within position space.

However (as it has been shown in the introduction), this theory working within position representation is suitable just for idealized cases (such as a perfectly smooth interface). It can be argued that light consists of photons which are packets of energy that primarily interact with interface atoms. Through this interaction, the energy of the photon is absorbed by collectivised electrons of the solid crystalline lattice, and the photon ceases to exist. Usually, the electron will quickly return to a lower energy state by emitting a photon. Since the photons are reemitted, not reflected or refracted, each photon behaves more like a point source—as if the light was originating right there. At a later time, these emitted spherical waves generate the total wavefront as the envelope that encloses all these point-source waves. The effect of interface nonuniformities could be considered as vanishing by drawing a tangent line as a global approximation through the front surface for each point-source wave. Yet there is no valid argument regarding a minimum value for the radii of curvature of this tangent line. Theoretically, it could be very small, and thus the global tangent line could consist of a lot of local curves with significant curvatures which are joined together. This way a lot of divergent light beams could be created along the reflected/refracted trajectory, and the energy would disappear very quickly.

A better argument regarding the perfectly smooth approximation for reflection/refraction theory could consist in the fact that photons usually interact with collectivised electrons of the solid crystalline lattice before being reemitted. These electrons could be considered as moving tangents to the interface since sudden changes of trajectory could generate significant electromagnetic field (accelerations being involved). This picture is supported also by quantum physics, since the associated wave function for the collectivised electrons is represented in position for large space intervals, the influence of local nonuniformities being decreased. Thus, a tangent line local radii of curvature greater than a certain value can be drawn, and a better directionality for reflected/refracted wave can be obtained.

However, this explanation does not take into account the phase shift between the incident and the reemitted wave for different points of the interface. A complete analysis based on quantum theory should consider that waves reemitted from different points of the interface are part of the wave-train corresponding to a certain photon; the probability of detecting a reflected/refracted photon is determined by the coherent plane-wave compounding method (it is well known that a particle interferes just with itself). There is no valid argument for the assumption regarding the constant phase shift between the local incident wave and the corresponding local reemitted wave in each interface point. The wave function for collectivised electrons of the crystal lattice is far from being constant in space-time along this interface. For this reason, space correlations for the incident wave-train and the reemitted wave-train should be taken into account.

It is useful to mention that a certain kind of spatial coherence can be noticed within classical electromagnetic theory, since the reflection on a perfectly conductive (metallic) interface requires the electric field \mathbf{E} to vanish on this surface. For this, a certain transient time interval necessary for creating the electrostatic equilibrium is required.

As a consequence, local phase shifts for reflected/refracted wave cannot be avoided within any local mathematical model. According to the standard propagation theory of waves, these could generate multiple local waves propagating along spatial directions which differ from the main reflection/refraction axis. Thus, the energy of reflected/refracted wave would be dissipated in a large solid angle (corresponding to a high divergence of the light beam) and directionality would be lost within a very short length interval. Thus the use of spatial coherence (based on nonlocal aspects) is justified. A harder task is to add some transient time considerations into a model based mainly on spatial correlations.

Analyzing the hypothesis of constant wave shift for the reflected/refracted wave in any point of the interface, we can observe that incident waves (parts of the associated wave corresponding to a certain photon—according to quantum mechanics) for first time interact with spatially extended functions/patterns defined on the interface material medium (crystal lattice with specific quantum functions for collectivised electrons and for phonons—quanta corresponding to spatially extended vibrations). This could suggest that lattice quantum functions interact in a global manner with parts of the incident wave on a large spatial area of the interface,

a certain correlation between phase of reflected/refracted wave being noticed even for surface points separated by possible crystal defects. This implies that a kind of support wave is generated on this interface, which acts upon reflecting/refracting points and correlates the phase of reemitted waves by interface points situated at great distance.

This aspect regarding space correlations achieved within a very short time interval for nonadjacent spatial intervals which interact with wavefronts (part of the reflected/refracted wave) becomes a key issue if we consider that reflected/refracted wave can undergo diffraction at a later time. The requirement of constant phase shift for parts of the associated wave generated by points or edges of a diffraction grating is still valid—yet the points or edges of such a diffraction grating are nonadjacent and cannot be correlated by any surface quantum wave functions. So, the support waves previously mentioned should propagate with high speed in space in order to regroup the wavefronts into a light beams with certain directionality, so as the diffracted wave does not vanish within a short time interval after interaction with the diffraction grating.

For connecting nonadjacent spatial areas, the position space representation for associated wave function is no more recommended. However, the associated wave corresponds to the same photon (defined on a certain wavelength interval and on a certain three-dimensional wave vector interval). This implies that the use of momentum space representation is suitable for interconnecting these nonadjacent space intervals where a certain material medium interacts with parts of the same incident or reflected/refracted wave-train (an example being the case of a later diffraction when a limited number of high-intensity directions are created). With a certain periodicity, this momentum representation becomes active and generates momentum (wave vector) values. For nonadjacent space intervals, the phase correlation within this momentum representation should be achieved through high-speed propagating support waves. The momentum values generated when this representation is active represents the base for wave propagation on subsequent time intervals, when the position representation becomes active.

We must check whether such high speed support waves can be considered using the standard wave equation. As it is known, the homogeneous wave equation in free space (in a space-time point without any sources) in one dimension (when movement is restricted along the Ox -axis) is represented by

$$\frac{\partial^2 \phi}{\partial x^2} = \frac{1}{v^2} \frac{\partial^2 \phi}{\partial t^2}, \quad (1)$$

where v corresponds to the wave velocity. The standard mathematical solution is represented by

$$\phi(x, t) = \phi_f(x - vt) + \phi_r(x + vt), \quad (2)$$

where $\phi_f(x - vt)$ corresponds to the forward wave (which moves towards $x = +\infty$ as time t increases) and $\phi_r(x + vt)$ corresponds to the reverse wave (which moves towards $x = -\infty$ as time t increases).

The three-dimensional homogeneous wave equation in free space (in a space-time point without any sources) is represented by

$$\frac{\partial^2 \phi}{\partial x^2} + \frac{\partial^2 \phi}{\partial y^2} + \frac{\partial^2 \phi}{\partial z^2} = \frac{1}{v^2} \frac{\partial^2 \phi}{\partial t^2}. \quad (3)$$

For spherical coordinates, considering that the wave function ϕ is invariant under rotations (the case when spherical waves are emitted from a certain point in space or are convergent towards a central point), the wave equation for ϕ (depending only on distance r to this central point and time) can be written as

$$\frac{\partial^2 \phi}{\partial r^2} + \frac{2}{r} \frac{\partial \phi}{\partial r} = \frac{1}{v^2} \frac{\partial^2 \phi}{\partial t^2}. \quad (4)$$

The standard mathematical solutions for this case are

$$\phi(r, t) = \frac{1}{r} \phi_d(r - vt) + \frac{1}{r} \phi_c(r + vt), \quad (5)$$

where $\phi_d(r - vt)$ corresponds to a divergent wave (which moves from a certain point outwards along all radial directions as time t increases) and $\phi_c(r + vt)$ corresponds to a convergent wave (which moves from all radial directions towards a certain point as time t increases).

However, these standard solutions are not suitable for our purpose. Their velocity is limited by the v parameter of the wave equation. Yet we can notice that the three-dimensional homogeneous wave equation admits solutions under the following form:

$$\phi(x, y, z, t) = ax + by + cx + dt + e, \quad (6)$$

where quantities a, b, c, d, e are constant values. This corresponds to a time-dependent plane equation—a plane which moves in the three-dimensional space. Let us suppose that ϕ equals e in the origin, at the zero moment of time (this means $x = y = z = t = 0$). At this zero moment of time, this value corresponds also (according to standard analytical geometry) to a spatial plane defined by the following:

$$ax + by + cx + 0d + e = e, \quad (7)$$

which means that

$$ax + by + cx = 0 \quad (8)$$

(the spatial origin being included in this plane). At a later time t , the same value e could be noticed for ϕ in a plane defined by the following:

$$e = ax + by + cx + dt + e, \quad (9)$$

which means

$$ax + by + cx + dt = 0. \quad (10)$$

At this time moment t , the distance from spatial origin to this plane (parallel to the plane defined at zero moment, since

quantities a, b, c corresponding to a vector normal to the plane do not vary in time) equals

$$D = \left| \frac{0a + 0b + 0c + (dt)}{\sqrt{a^2 + b^2 + c^2}} \right| = \left| \frac{dt}{\sqrt{a^2 + b^2 + c^2}} \right|. \quad (11)$$

This can be also written as

$$\frac{D}{t} = \left| \frac{d}{\sqrt{a^2 + b^2 + c^2}} \right|, \quad (12)$$

which means that the plane on which ϕ equals e passing through origin at zero time moment which moves with velocity

$$w = \frac{D}{t} = \left| \frac{d}{\sqrt{a^2 + b^2 + c^2}} \right| \quad (13)$$

in space. The propagation velocity depends only on a, b, c, d constants. Since there is no restriction regarding the choice for these constant values, it results that (unlike standard solutions of wave equation) these polynomials can be represented as constant values propagating in space-time with any velocity (this physical quantity being no more correlated to the wave equation). Since the velocity has no more an upper limit, these polynomials can be put in correspondence with the high-speed support wave requested for performing practically an instant correlation between different non-adjointing space intervals interacting with the same associated wave (the values in momentum space representation being the same).

3. Conclusions

This study has presented transient aspects of light wave propagation connected with spatial coherence. It has been shown that reflection and refraction phenomena involve spatial patterns which are created within a certain transient time interval. After this transient time interval, these patterns (connected to spatial coherence) act like a certain memory, determining the wave vector for subsequent sets of reflected/refracted waves. The validity of this model is based on the study of wavefronts generated by multiple centers of reflection/refraction situated on the interface—the total wavefront at a later time being the envelope that encloses all of these wavelets. Analyzing the hypothesis of constant wave shift for the reflected/refracted wave in any point of the interface, it is shown that this should be connected with a nonlocal mathematical model which takes into account

- (i) that incident waves (parts of the associated wave corresponding to a certain photon—according to Quantum Mechanics) the first time interaction with spatially extended functions/patterns defined on the interface material medium (crystal lattice with specific quantum functions for collectivised electrons and for phonons—quanta corresponding to spatially extended vibrations);
- (ii) that these kinds of spatially extended functions are generated also for nonadjacent spatial intervals which interact with wavefronts (part of the reflected/refracted wave) at a later time.

The first aspect is not surprising (since a spatially extended wave function for the interface can be easily be defined using quantum considerations). However, the second is a novel aspect which implies the use of momentum space representation for defining the same values for parts of the same reflected/refracted associated wave-train in nonadjacent space intervals (an example being the case of a later diffraction).

This extended spatial model can explain why minor different local shifts do not appear, since (according to standard wave propagation theory) these could lead to multiple local waves propagating along spatial directions which differ to the main reflection/refraction axis. Thus, the entire reflected/refracted wave would be dissipated in a large solid angle (corresponding to a high divergence of the light beam) and directionality would be lost within a very short length interval.

The mathematical aspects are based on first order polynomials satisfying the wave equation. Unlike standard solutions of wave equation, these polynomials can be represented as constant values propagating in space-time with any velocity (this physical quantity being no more correlated to the wave equation). Since the velocity has no more upper limit, these polynomials can be put in correspondence with certain support waves able to perform practically an instant phase correlation between different non-adjointing space intervals interacting with the same associated wave. This correlation should be achieved within momentum space representation for the associated wave, since within this representation all values corresponding to the same wave-train are the same in nonadjacent space intervals.

These linear functions differ from time dynamics based on temporal coherence (as presented in [1]). Being constant values propagating in space time, they can be put in correspondence with traveling wavelets inside a certain material medium as in [2, 3]. The difference consists in the fact that these functions correspond to linear space-time functions which are active with a certain periodicity. Phase aspects of quantum interactions were also presented in [4], without any spatial correlations to be mentioned. A nonlinear model for creating spatial patterns (using nonlinear equations) has been presented in [5]. Scale spatial aspects were also presented in [6], in opposition to temporal noise aspects generating uncorrelation presented in [7, 8] by the same group of researchers.

References

- [1] E. G. Bakhoun and C. Toma, "Dynamical aspects of macroscopic and quantum transitions due to coherence function and time series events," *Mathematical Problems in Engineering*, vol. 2010, Article ID 428903, 13 pages, 2010.
- [2] J. J. Rushchitsky, C. Cattani, and E. V. Terletskaia, "Wavelet analysis of the evolution of a solitary wave in a composite material," *International Applied Mechanics*, vol. 40, no. 3, pp. 311–318, 2004.
- [3] C. Cattani, "Multiscale analysis of wave propagation in composite materials," *Mathematical Modelling and Analysis*, vol. 8, no. 4, pp. 267–282, 2003.

- [4] E. G. Bakhoun and C. Toma, "Mathematical transform of traveling-wave equations and phase aspects of quantum interaction," *Mathematical Problems in Engineering*, vol. 2012, Article ID 695208, 15 pages, 2010.
- [5] F. Doboga, "Different structural patterns created by short range variations of internal parameters," in *Computational Science—ICCS 2007*, vol. 4488 of *Lecture Notes in Computer Science*, pp. 1060–1066, 2007.
- [6] M. Li, Y. Q. Chen, J. Y. Li, and W. Zhao, "Holder scales of sea level," *Mathematical Problems in Engineering*, vol. 2012, Article ID 863707, 22 pages, 2012.
- [7] M. Li and W. Zhao, "On bandlimitedness and lag-limitedness of fractional Gaussian noise," *Physica A*, vol. 392, no. 9, pp. 1955–1961, 2013.
- [8] M. Li and W. Zhao, "On $1/f$ noise," *Mathematical Problems in Engineering*, vol. 2012, Article ID 673648, 23 pages, 2012.

Research Article

Smoothing the Sample Autocorrelation of Long-Range-Dependent Traffic

Ming Li¹ and Wei Zhao²

¹ School of Information Science & Technology, East China Normal University, No. 500 Dongchuan Road, Shanghai 200241, China

² Department of Computer and Information Science, University of Macau, Avenida Padre Tomas Pereira, Taipa 1356, Macau, China

Correspondence should be addressed to Ming Li; ming_lihk@yahoo.com

Received 15 May 2013; Accepted 4 June 2013

Academic Editor: Ezzat G. Bakhoum

Copyright © 2013 M. Li and W. Zhao. This is an open access article distributed under the Creative Commons Attribution License, which permits unrestricted use, distribution, and reproduction in any medium, provided the original work is properly cited.

This paper depicts our work in smoothing the sample autocorrelation function (ACF) of traffic. The experimental results exhibit that the sample ACF of traffic may be smoothed by the way of average. In addition, the results imply that the sum of sample ACFs of traffic convergences. Considering that the traffic data used in this research is long-range dependent (LRD), the latter may be meaningful for the theoretical research of LRD traffic.

1. Introduction

Let $x(t(i))$ be a sample record of teletraffic time series (traffic for short), where $t(i)$ for $i \in \mathbf{N}$ (the set of natural numbers) is the series of timestamps, indicating the timestamp of the i th packet arriving at a server. Thus, $x(t(i))$ represents the packet size of the i th packet recorded at time $t(i)$ on a packet-by-packet basis. We use a real-traffic trace named BC-Aug89 recorded on an Ethernet at the Bellcore Morristown Research and Engineering facility, which contains 1,000,000 packets [1]. It was used in the pioneering work for revealing some statistical properties of traffic in fractals, such as self-similarity and long-range dependence (LRD) [2, 3].

Note 1. The statistical properties described in the early literature, for example, [2, 3], turn to be ubiquitous in today's traffic, according to the research stated in [4, 5]. Thus, the trace measured in 1989 keeps its value in the research of general patterns of traffic.

The word traffic is a collective noun. In addition to the traffic on a packet-by-packet basis as previously described, it may imply the time series called interarrival times, which is in the form (see [6, 7])

$$s(i) = t(i+1) - t(i). \quad (1)$$

The term traffic may also imply the time series named accumulated traffic, denoted by $y(n)$, on an interval-by-interval basis, which is given by

$$y(n) = \sum_{i=nT}^{(n+1)T} x(i), \quad (2)$$

where T is the interval width. It stands for the accumulated bytes of arrival traffic in the n th interval.

Note 2. The statistical properties of $x(t(i))$, $s(i)$, and $y(n)$ may be identical [5].

Note 3. The attributes of traffic are application dependent. More other meanings of traffic are available. It may mean the packet count [2]. In some applications, one may be interested in the number of connections within a given time interval [4], the packet size or the number of packets on a flow-by-flow basis [8], envelopes of traffic [9], or traffic bounds [10].

This paper relates to the aggregated traffic $x(t(i))$. Figure 1 illustrates four types of the series of BC-Aug89. Let the interval width be $T = 1024$. Then, we obtain $y(n)$ of BC-Aug89 according to (2), as shown in Figure 2. Note that the pattern of $x(t(i))$ is consistent with that of $x(i)$ that represents the size of the i th packet. Besides, the statistics of $x(i)$ and $y(n)$ may generally be identical [5]. Therefore, in what follows,

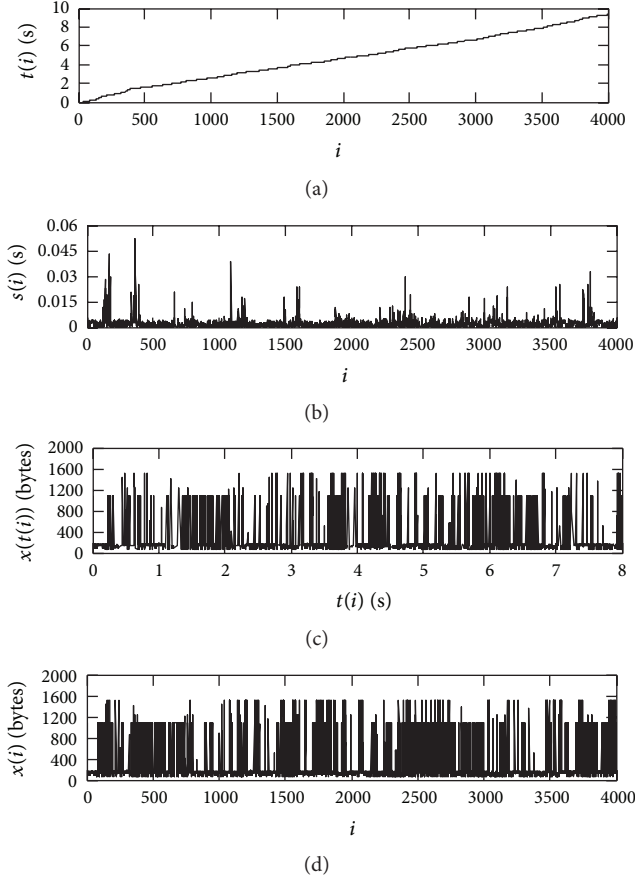


FIGURE 1: Illustrations of real-traffic trace BC-Aug89. (a) Timestamp series $t(i)$. (b) Interarrival times $s(i)$. (c) Traffic in packet size $x(t(i))$. (d) Traffic in packet size $x(i)$.

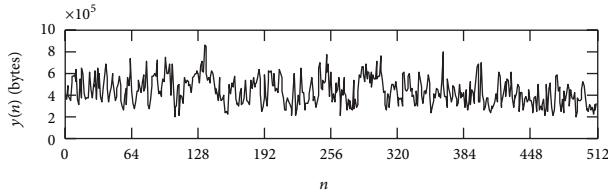


FIGURE 2: Accumulated traffic of BC-Aug89 with the interval width $T = 1024$.

we will use $x(i)$ for the discussions instead of $x(t(i))$ for the purpose of simplicity.

Remark 1 (burstiness). Without considering the Ethernet preamble, header, or CRC, the Ethernet protocol forces all packets to have at least a minimum size of 64 bytes and at most the maximum size of 1518 bytes. The fixed limit of 1518 bytes is specified by IEEE standard without technical reason. Thus, it is often the case that the packet size of traffic may take the same value within a short period of time as Figure 1(c) shows. In addition, traffic has the behavior of “burstiness.” By burstiness, one implies that there would be no packets transmitted for a while, then flurry of transmission,

no transmission for another long time, and so forth if one observes traffic over a long period of time [11, 12]. This phenomenon, indicated in Figures 1(b)–1(d), was described as intermittency by Tobagi et al. [13].

Note 4. The intermittency of a random function is conventionally discussed in the field of turbulence [14], but we note that it is also a phenomenon of traffic.

The traffic series $x(i)$ is LRD. Denote its autocorrelation function (ACF) by $r(k)$ in the stationarity case. Then,

$$r(k) = E[x(i)x(i+k)], \quad (3)$$

where E is the mean operator and k is lag. Its power spectrum density (PSD) denoted by $S(\omega)$ is the Fourier transform of $r(k)$:

$$S(\omega) = F[r(k)], \quad (4)$$

where F is the operator of the Fourier transform, $\omega = 2\pi f$, where f is the frequency. Note that the PSD of $x(i)$ belongs to $1/f$ noise [15]. Thus, even from a view of data processing, $r(k)$ is preferred [16], because $S(\omega)$ is divergent at $\omega = 0$. In addition, the correlation model of traffic is desired in networking; see the statement of Paxson and Floyd [17, p. 5] as follows. The issue of “how to go from the pure correlational structure, expressed in terms of a time series of packet arrivals per unit time, to the details of exactly when within each unit of time each individual packet arrives” has not been solved. For this reason, we discuss the issue of ACF estimation of LRD traffic.

The remainder of this paper is as follows. In Section 2, we shall brief the preliminaries. Smoothing the sample ACF of traffic is discussed in Section 3. A case study is shown in Section 4. Discussions and future work are in Section 5, which is followed by conclusions.

2. Brief of Time Series

Denote by $\{x_l(t)\}$ a set of sample functions for $l \in \mathbf{N}$ and $0 < t < \infty$, and $x_l(t) \in \mathbf{R}$ (set of real numbers) is the l th sample function. A process consists of a set of sample functions [18, 19].

Note 5. In the case of traffic, requiring a set of sample functions $\{x_l(t)\}$ for $l \in \mathbf{N}$ at a specific point in networks may be unrealistic since one can only measure a single history of traffic trace at that specific point. One may never achieve a set of sample records of real traffic in the sense of repeated experiments under the exactly same conditions for $0 < t < \infty$. Therefore, in traffic engineering, we are interested in a sample function $x(t)$ instead of a process.

Note 6. We consider a time series $x(t)$ that is a random function. In this research, the terms of random function, time series, or process are interchangeable if there are no confusions.

2.1. Moment. Denote by $p(x, t)$ the probability density function (PDF) of a random function $x(t)$, which is usually

written as $p(x)$ in short. Then, the following is called its moment of order n :

$$m_n(t) = E[x^n(t)] = \int_{-\infty}^{\infty} x^n p(x, t) dx. \quad (5)$$

The moment of a random function is consistent with the moment of a force in physics as well as mechanics in expression [20]. It serves as a useful tool to represent certain important characteristics of a random function.

2.1.1. Mean and Mean Square. Using the concept of the moment, one may conveniently represent the mean of $x(t)$ as its first-order moment given by

$$m_1(t) = \mu(t) = E[x(t)] = \int_{-\infty}^{\infty} xp(x, t) dx. \quad (6)$$

The second moment of $x(t)$ may be its mean square value denoted by

$$m_2(t) = \Psi(t) = E[x^2(t)] = \int_{-\infty}^{\infty} x^2 p(x, t) dx. \quad (7)$$

Note 7. The mean of $x(t)$ represents its average value around which $x(t)$ fluctuates.

Note 8. The mean square of $x(t)$ stands for its strength or average power. To explain this, we assume that $x(t)$ is a voltage exerting on a resistor of one Ohm. In this case, $x^2(t)$ is the power the resistor consumes at time t . Therefore, (7) implies the average power. Hence, the strength of $x(t)$.

2.1.2. ACF. Now, we consider the product of $x(t)$ at two points, say $x(t_1)x(t_2)$ for $t_1 \neq t_2$. Since both $x(t_1)$ and $x(t_2)$ are random variables, we denote by $p(x_1, t_1; x_2, t_2)$ the joint PDF of $x(t_1)$ and $x(t_2)$. With the help of the concept of moment, $E[x(t_1)x(t_2)]$ may be expressed in the form

$$\begin{aligned} r(t_1, t_2) &= E[x(t_1)x(t_2)] \\ &= \iint_{-\infty}^{\infty} x(t_1)x(t_2)p(x_1, t_1; x_2, t_2)dx_1dx_2. \end{aligned} \quad (8)$$

The function $r(t_1, t_2)$ in (8) is called the ACF of $x(t)$. It represents how one random variable $x(t_1)$ at time t_1 correlates with the other $x(t_2)$ at another time t_2 . In other words, it represents the correlation of $x(t)$ at two different points t_1 and t_2 .

Note 9. In the case of $t_1 = t_2 = t$, the ACF of $x(t)$ reduces to its mean square:

$$r(t_1, t_2)|_{t_1=t_2} = E[x(t)x(t)] = \int_{-\infty}^{\infty} x^2(t)p(x, t)dx. \quad (9)$$

Note 10. The term of the second-order moment of $x(t)$ may imply the moments of order 2, which in the wide sense or in general include mean square (7) and ACF (8).

Note 11. If we consider the moments of $x(t)$ up to 2, $x(t)$ is called 2-order random function, which plays a role in engineering. The moments of orders higher than 2 correspond to the case of higher order statistics, which we do not discuss in this paper.

2.1.3. PSD. The Fourier transform of the ACF $r(t, s)$ is given by

$$S(\omega, t) = \int_{-\infty}^{\infty} r(t, s)e^{-j\omega s}ds, \quad j = \sqrt{-1}. \quad (10)$$

It represents the energy distribution of $x(t)$.

Note 12. In general, $m_n(t)$ is time dependent. Therefore, the mean, mean square, ACF, and PSD may generally be time dependent. In the stationary case, they are independent of time.

2.1.4. Weak Stationarity. If all moments of $x(t)$ do not vary with time, $x(t)$ has the property of strong stationarity. If the moments up to 2 are independent of time, irrelevant of the moments of order higher than 2, we say that $x(t)$ is of weak stationarity or stationary in the wide sense.

Note 13. In the case of weak stationarity, $\mu(t)$ and $\Psi(t)$ are constants. The ACF only replies on the time lag $\tau = |t - s|$. Hence, $r(t, s) = r(\tau)$. Consequently, $S(\omega, t) = S(\omega)$.

2.2. Central Moment. Often, one may be interested in a random function with mean zero. For random functions with mean zero, the previous expression regarding the moment (5) is extended to the central moment expressed by

$$\begin{aligned} mc_n(t) &= E\{[x(t) - \mu(t)]^n\} \\ &= \int_{-\infty}^{\infty} [x(t) - \mu(t)]^n p(x, t) dx. \end{aligned} \quad (11)$$

2.2.1. Variance and Standard Deviation. The central moment of order 2 given by

$$\begin{aligned} mc_2(t) &= E\{[x(t) - \mu(t)]^2\} \\ &= \int_{-\infty}^{\infty} [x(t) - \mu(t)]^2 p(x, t) dx \end{aligned} \quad (12)$$

is usually denoted by $\sigma^2(t)$ called the variance of $x(t)$. The standard deviation, denoted by $\text{stdev}(t)$, is given by

$$\text{stdev}(t) = \sqrt{\sigma^2(t)} = \sigma(t). \quad (13)$$

Note 14. How much the variation of $x(t)$ away from its mean $\mu(t)$ is characterized by its variance or standard deviation.

Remark 2. Analysis of variance (ANOVA) is a branch of statistics, which plays a role in many aspects of techniques, especially in the fields of statistics tests and experimental design [21–23].

2.2.2. Autocovariance. In the case of mean zero, one uses the autocovariance function denoted by $C(t_1, t_2)$ (ACF for short

again) to characterize the correlation property of $[x(t) - \mu(t)]$. It may be given by

$$\begin{aligned} C(t_1, t_2) &= E \{ [x(t_1) - \mu(t_1)] [x(t_2) - \mu(t_2)] \} \\ &= \iint_{-\infty}^{\infty} [x(t_1) - \mu(t_1)] [x(t_2) - \mu(t_2)] \\ &\quad \times p(x_1, t_1; x_2, t_2) dx_1 dx_2. \end{aligned} \quad (14)$$

Note 15. When $t_1 = t_2 = t$, $C(t_1, t_2)$ reduces to $\sigma^2(t)$:

$$C(t, t) = E \{ [x(t) - \mu(t)]^2 \} = \sigma^2(t). \quad (15)$$

Remark 3. ACF analysis is an important branch in statistics; see, for example, [19, 23–28].

Remark 4. A Gaussian random function is uniquely determined by its ACF [29, 30].

As a matter of fact, the PDF of a Gaussian random function is given by

$$p(x) = \frac{1}{\sqrt{2\pi}\sigma} \exp \left[-\frac{(x - \mu)^2}{2\sigma^2} \right], \quad -\infty < x < \infty. \quad (16)$$

In (16), σ can be determined by (15) while μ can be obtained from the following:

$$C(t, t) = r(t, t) - \mu^2(t). \quad (17)$$

Hence, Remark 4 results.

Note 16. If $x(t)$ is weak stationary, its $\mu(t)$ and $\sigma(t)$ are constants. Its ACF depends only on lag:

$$C(t_1, t_2) = C(|t_1 - t_2|) = C(\tau), \quad \tau = |t_1 - t_2|. \quad (18)$$

We list two properties of ACF below.

P1: ACF is an even function: $r(\tau) = r(-\tau)$, $C(\tau) = C(-\tau)$.

P2: $r(0) \geq r(\tau)$, $C(0) \geq C(\tau)$.

Note 17. P1 is obvious because the correlation between $x(t_1)$ and $x(t_2)$ is always equal to that between $x(t_2)$ and $x(t_1)$. P2 is natural because the correlation between the same point $x(t_1)$ and $x(t_1)$ always reaches its maximum.

Without loss of generality for the statistical analysis of random functions, one may adopt the concept of normalized random functions. By normalized, we mean $r(0) = 1$ or $C(0) = 1$. Therefore, a normalized random function may be obtained by $x(t)/\sqrt{C(t, t)}$.

2.3. Computational Methods. Previous expressions in (5)~(15) regarding the mean, variance, and ACF of a random function $x(t)$ are associated with its PDF. That implies that they can be determined under the condition that the PDF is known. However, that may usually be too restrictive in practical applications in engineering. Fortunately, Wiener et al. proposed a computation approach using time average without relating to its PDF if $x(t)$ is ergodic [18, 31, 32].

Note 18. It may be very difficult if not impossible for one to test the ergodicity by a sample function of a traffic trace. In practice, one may simply assume that a traffic trace $x(t)$ is ergodic.

In what follows, we suppose that $x(t)$ is causal. By causal, we mean that $x(t)$ is defined for $0 \leq t < \infty$ and $x(t) = 0$ for $t < 0$. In addition, we only consider $x(t)$ in the weak stationary sense. By using the time average, therefore, the mean of $x(t)$ is given by

$$\mu = E[x(t)] = \lim_{T \rightarrow \infty} \frac{1}{T} \int_0^T x(t) dt. \quad (19)$$

Its mean square is written by

$$\Psi = E[x^2(t)] = \lim_{T \rightarrow \infty} \frac{1}{T} \int_0^T x^2(t) dt. \quad (20)$$

Its ACF is expressed by

$$r(\tau) = E[x(t)x(t+\tau)] = \lim_{T \rightarrow \infty} \frac{1}{T} \int_0^T x(t)x(t+\tau) dt. \quad (21)$$

Its variance is given by

$$\sigma^2 = E\{[x(t) - \mu]^2\} = \lim_{T \rightarrow \infty} \frac{1}{T} \int_0^T [x(t) - \mu]^2 dt. \quad (22)$$

Similarly, its autocovariance is given by

$$\begin{aligned} C(\tau) &= E\{[x(t) - \mu][x(t+\tau) - \mu]\} \\ &= \lim_{T \rightarrow \infty} \frac{1}{T} \int_0^T [x(t) - \mu][x(t+\tau) - \mu] dt. \end{aligned} \quad (23)$$

In what follows, we only consider random functions with mean zero. Accordingly, $r(\tau)$ is equal to $C(\tau)$, and $\Psi = \sigma^2$ unless otherwise stated.

We write the PSD of $x(t)$ by

$$S(\omega) = \int_{-\infty}^{\infty} r(\tau) e^{-j\omega\tau} d\tau. \quad (24)$$

Alternatively, $r(\tau)$ can be expressed by

$$r(\tau) = \frac{1}{2\pi} \int_{-\infty}^{\infty} S(\omega) e^{j\omega\tau} d\omega. \quad (25)$$

2.4. Defaulted Assumptions in Conventional Time Series. In the field of conventional time series, the following assumptions are usually defaulted [18, 21–37].

- (i) The mean of $x(t)$ exists.
- (ii) The variance of $x(t)$ exists.
- (iii) $S(0) = \int_{-\infty}^{\infty} r(\tau) d\tau$ is convergent.

However, the above may be untrue for LRD traffic; see, for example, [16, 38, 39], which we shall not discuss more in this paper.

3. Smoothing Sample ACF of Traffic

Previous discussions require that $-\infty < t < \infty$. Even in the case of $x(t)$ being causal, $0 < t < \infty$ is always required. However, that requirement may not be satisfied in practice in general since traffic $x(t)$ can be measured only in a finite time interval.

3.1. Sample ACF. Suppose that one records traffic $x(t)$ in $[0, T]$. Then, he or she attains a sample ACF of $x(t)$, which may be estimated by $r_1(\tau)$:

$$r_1(\tau) = \frac{1}{T} \int_0^T x(t) x(t + \tau) dt. \quad (26)$$

Note 19. The sample ACF $r_1(\tau)$ may yet be a representative of the true ACF $r(\tau)$ in a way. Mathematically, $r_1(\tau) = r(\tau)$ under the condition of $T \rightarrow \infty$. Unfortunately, the condition $T \rightarrow \infty$ may be physically unrealizable.

Now, assume that there is another person who measures the traffic at the same point in networks, but he does the measurement in the time interval $[T, 2T]$. Then, the sample ACF is obtained by

$$r_2(\tau) = \frac{1}{T} \int_T^{2T} x(t) x(t + \tau) dt. \quad (27)$$

Due to the randomness of $x(t)$, errors in numerical computations, and errors in the measurement of traffic data, though the width of $[T, 2T]$ is equal to that of $[0, T]$, one has, in general,

$$r_2(\tau) \neq r_1(\tau). \quad (28)$$

Denote by $r_n(\tau)$ the sample ACF of $x(t)$ in the interval $[(n-1)T, nT]$ for $n = 1, 2, \dots, N$. Then,

$$r_n(\tau) = \frac{1}{T} \int_{(n-1)T}^{nT} x(t) x(t + \tau) dt. \quad (29)$$

For the similar reasons we explained in (28), one generally has

$$r_m(\tau) \neq r_n(\tau) \quad \text{for } m \neq n. \quad (30)$$

Note 20. It may be quite reasonable to consider each sample ACF $r_n(\tau)$ as an estimate of the true ACF of $x(t)$, but neither may be so appropriate unless T is large enough. In fact, $r_n(\tau)$ is a random variable [32].

3.2. Smoothed Sample ACF. Denote by $\hat{r}(\tau)$ the ACF estimate of $x(t)$. The estimate $\hat{r}(\tau)$ is a random variable again. It has its distribution in the general form of (31). The issue studying the concrete form of (31) is interesting, but it is beyond the scope of this paper:

$$\text{Prob}[\hat{r}(\tau)]. \quad (31)$$

In this research, we are interested in good estimate of $r(\tau)$. By good estimate, we mean that both its bias and variance are small. Since

$$E[r_n(\tau)] = \frac{1}{T} \int_{(n-1)T}^{nT} E[x(t) x(t + \tau)] dt = r(\tau), \quad (32)$$

the sample ACF $r_n(\tau)$ is unbiased. Therefore, what one is interested in is to find a way such that $\text{Var}[\hat{r}(\tau)]$ is small. The literature about this is relatively rich; see, for example, [31] and references therein. A simple way to reduce $\text{Var}[\hat{r}(\tau)]$ is average. That is, one may compute $\hat{r}(\tau)$ by the average of the sample ACFs as follows assuming that both $\lim_{T \rightarrow \infty} r_n(\tau)$ and $\lim_{N \rightarrow \infty} \hat{r}(\tau)$ exist:

$$\hat{r}(\tau) = \frac{1}{N} \sum_{n=1}^N r_n(\tau). \quad (33)$$

In that case, $\text{Var}[\hat{r}(\tau)]$ is inversely proportional to N [31]:

$$\text{Var}[\hat{r}(\tau)] \text{ is proportional to } \frac{1}{N}. \quad (34)$$

The above implies the assumptions that both $\lim_{T \rightarrow \infty} r_n(\tau)$ and $\lim_{N \rightarrow \infty} \hat{r}(\tau)$ exist. The research of whether $\lim_{T \rightarrow \infty} r_n(\tau)$ or $\lim_{N \rightarrow \infty} \hat{r}(\tau)$ exists is attractive, but it is out of the scope of the paper. In the experimental research discussed in this paper, we assume that both exist.

Note 21. The previous expression needs, for the purpose of ACF estimation of real-traffic $x(t)$, purposely sectioning the sample record of a traffic trace $x(t)$ into a set of blocks such that the number of blocks, that is, the average count N , is large enough for the desired level of $\text{Var}[\hat{r}(\tau)]$.

Note 22. ACF estimate $\hat{r}(\tau)$ is the average of the sample ACFs or the sum of the sample ACFs divided by N . Other smoothing methods are available; see, for example, [40].

The previous discussions take the usage of integral. In numerical computations, the integral above should be replaced by summation. In the discrete case, we replace T by I for $i = 1, 2, \dots, I$. In addition, $r_n(\tau)$ is replaced by $r_n(k)$ and $x(t)$ by $x(i)$. Thus, we have

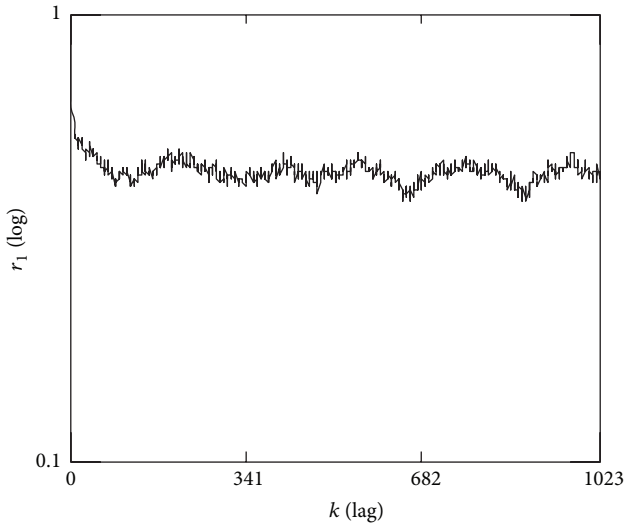
$$r_n(k) = \frac{1}{I} \sum_{(n-1)I}^{nI} x(i) x(i + k). \quad (35)$$

The above computation does not follow (35) directly. In practice, the fast Fourier transform (FFT) and its inverse (IFFT) are suggested. More precisely, in the interval $[(n-1)I, nI]$, according to the Wiener theorem [18–20, 23, 31, 32, 34, 35], we have

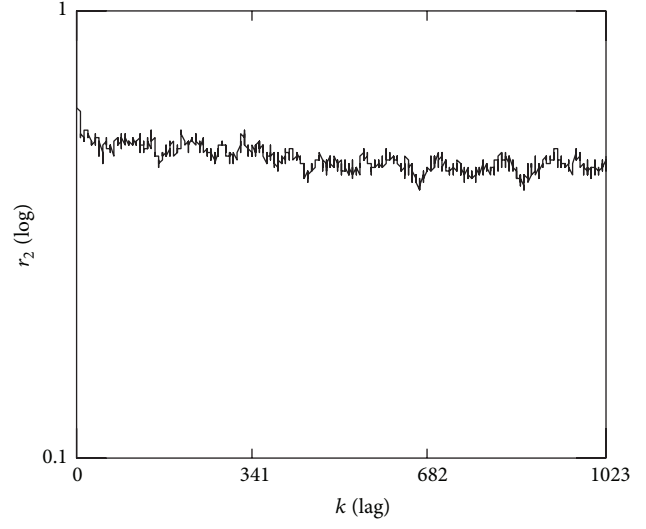
$$r_n(k) = \text{IFFT} \left\{ \left| \text{FFT}[x(i)] \right|^2 \right\} \quad \text{for } (n-1)I \leq i \leq nI. \quad (36)$$

Then,

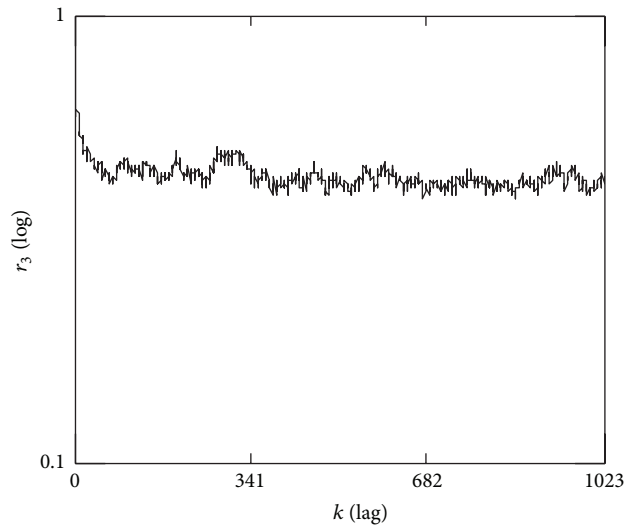
$$\hat{r}(k) = \frac{1}{N} \sum_{n=1}^N r_n(k). \quad (37)$$



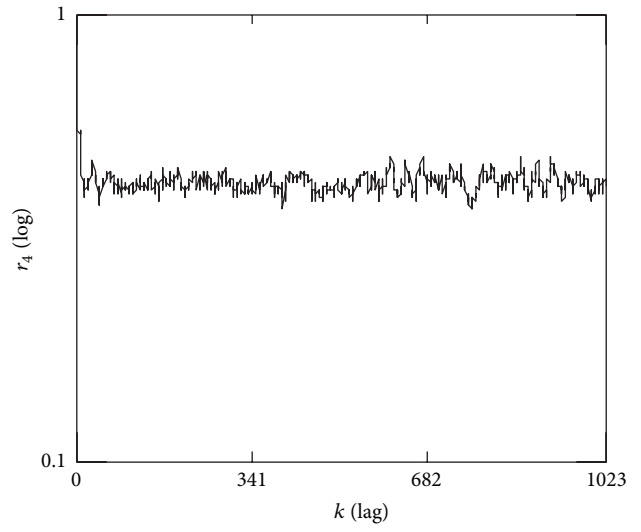
(a)



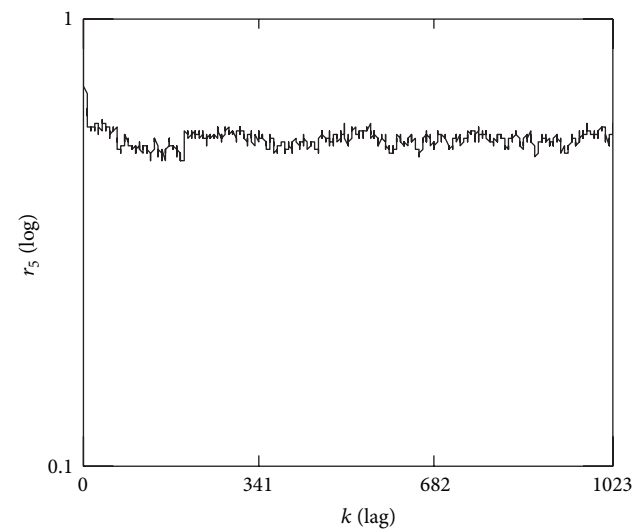
(b)



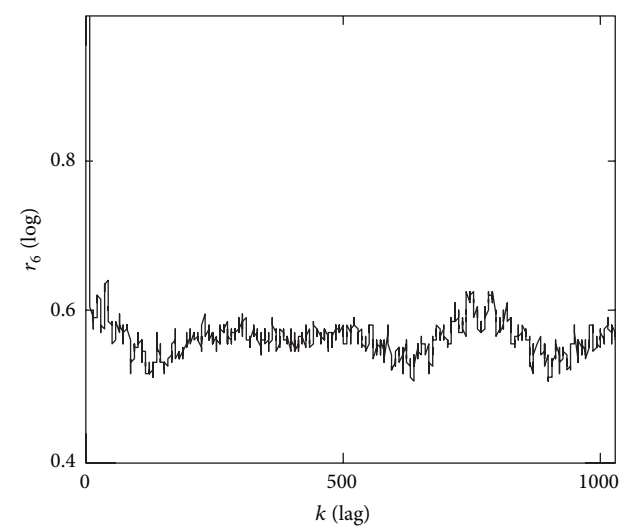
(c)



(d)



(e)



(f)

FIGURE 3: Continued.

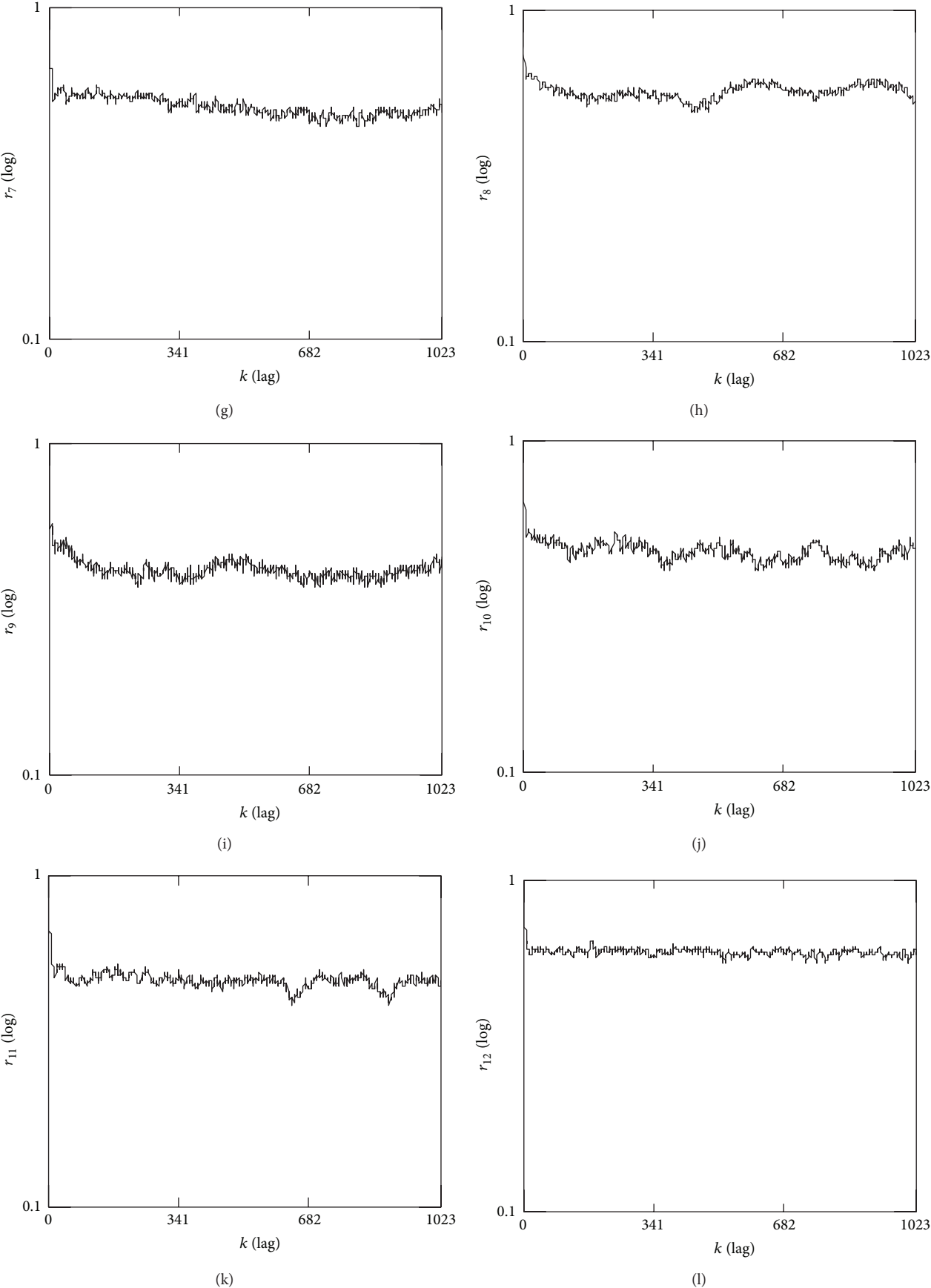


FIGURE 3: Continued.

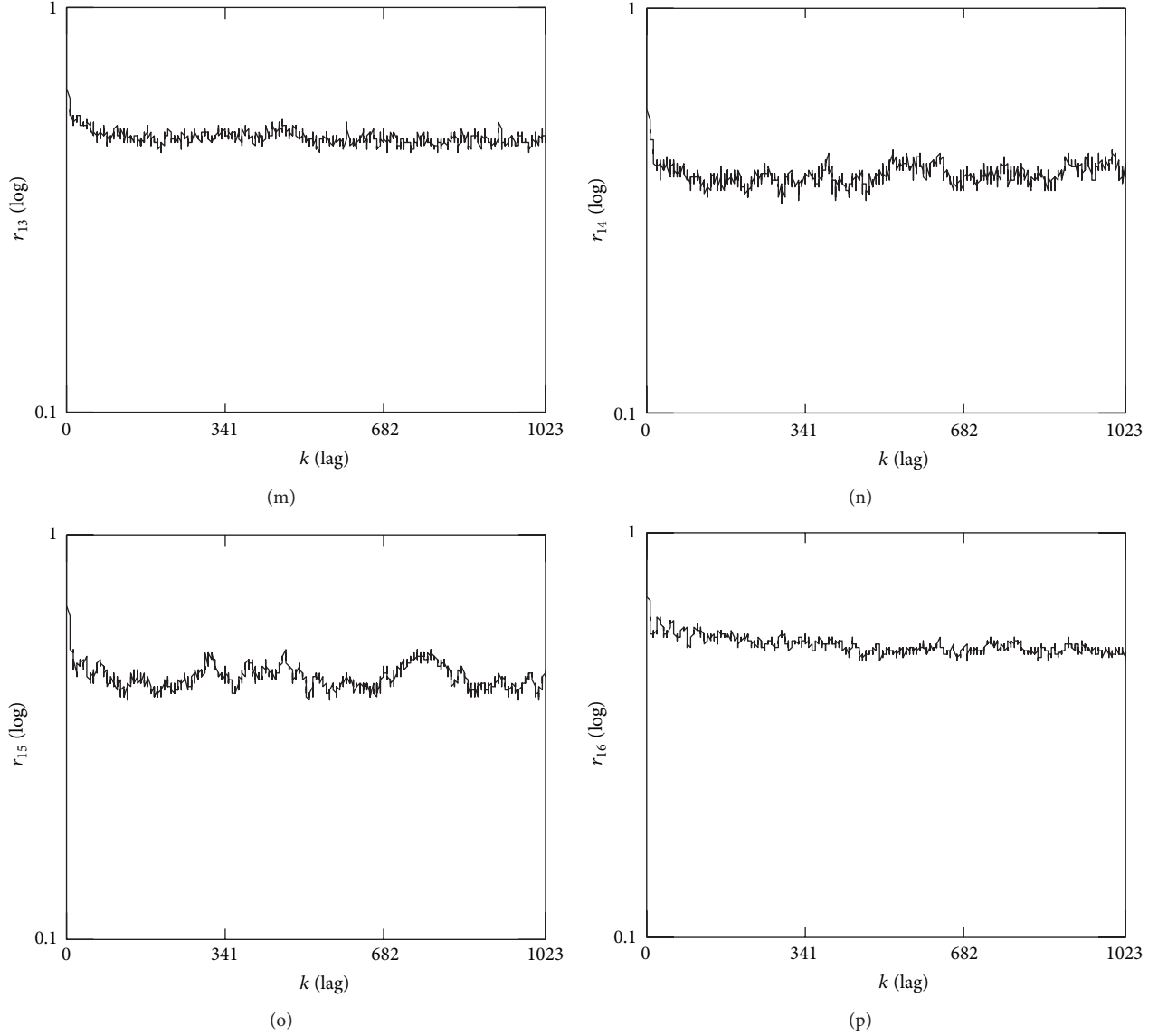


FIGURE 3: Illustrations of sample ACFs. (a) $r_1(k)$. (b) $r_2(k)$. (c) $r_3(k)$. (d) $r_4(k)$. (e) $r_5(k)$. (f) $r_6(k)$. (g) $r_7(k)$. (h) $r_8(k)$. (i) $r_9(k)$. (j) $r_{10}(k)$. (k) $r_{11}(k)$. (l) $r_{12}(k)$. (m) $r_{13}(k)$. (n) $r_{14}(k)$. (o) $r_{15}(k)$. (p) $r_{16}(k)$.

Note 23. Usually, I as well as N take the form of 2^M , where M is a positive integer.

Note 24. If $x(i)$ is for $i = 0, 1, \dots, I-1$, the part of $r_n(k)$ for $k = 0, 1, \dots, (I-1)/2$ is enough for the analysis purpose because $r_n(k) = r_n(-k)$. For example, when one sets $I = 1024$, $r_n(k)$ is for $k = 0, 1, \dots, 511$.

4. A Case Study

Using the real-traffic trace BC-Aug89 in this case study, we set $I = 2048$. Figure 2 illustrates the 16 sample ACFs for $i \in [(n-1)2048, n2048]$ with $n = 1, \dots, 16$. The ordinate is in log. From Figure 3, we see that sample ACFs $r_n(k)$ differ from each other. Each sample ACF consists of a certain amount of fluctuations.

Using the technique of average may reduce the variance of the sample ACF. Denote by $R16(k)$ the average of $r_n(k)$ for $n = 1, \dots, 16$. Denote by $R32(k)$ the average of $r_n(k)$ for $n = 1, \dots, 32$. Denote by $R64(k)$ the average of $r_n(k)$ for $n = 1, \dots, 64$. Figures 4, 5, and 6, respectively, indicate the smoothed sample ACFs $R16(k)$, $R32(k)$, and $R64(k)$. It can be seen that the fluctuations in Figure 3 are considerably reduced in $R16(k)$. As a result, the larger the average count, the smoother the curve of the sample ACF estimate; see Figures 5 and 6.

Note 25. Though $\text{Var}[\hat{r}(\tau)]$ is inversely proportional to the averages count N , over-large N may be unnecessary for improving an estimate. For instance, by eye, one may see that the one in Figure 6 does not show much improvement as that in Figure 5.

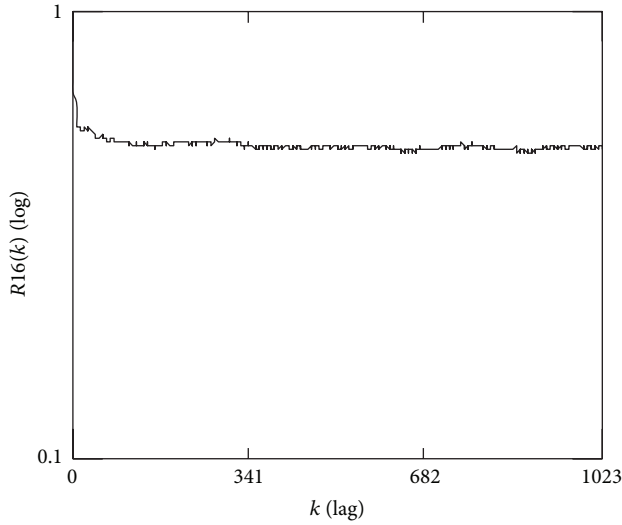


FIGURE 4: Smoothed sample ACF with average count 16.

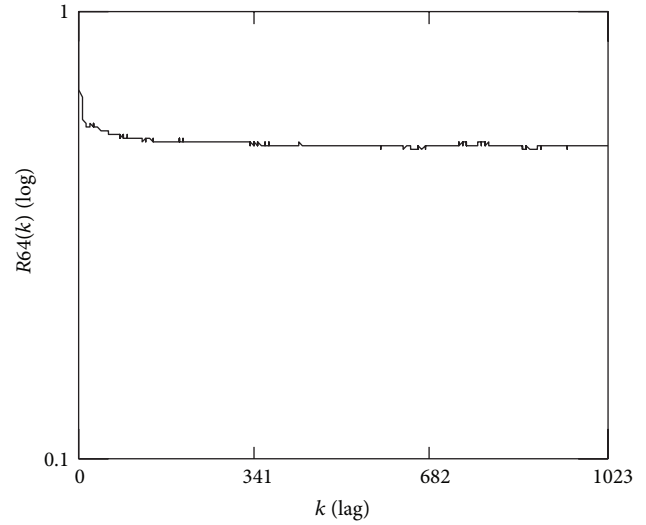


FIGURE 6: Smoothed sample ACF with average count 64.

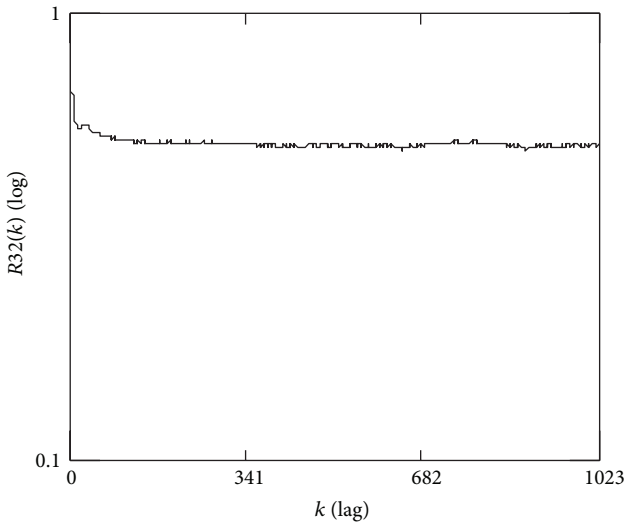


FIGURE 5: Smoothed sample ACF with average count 32.

5. Discussions and Future Work

The previous exhibits the obvious effects of smoothing sample ACFs by average. However, there are critical points that need discussions regarding the smoothing of sample ACFs of traffic.

Traffic is LRD [1–5]. According to Taqqu's law, it is heavy tailed [41]. Resnick et al. [42] explained an important result in the aspect of sample ACF of heavy-tailed time series. It was stated in [42] that the sample ACF of heavy-tailed series may be random when the sample size approaches infinity if the series is with infinite variance. The case study in Section 4 demonstrates that the sum of sample ACFs is convergent. Consequently, the sample ACF is convergent too. Thus, may we infer that traffic, at least the data used there, is with finite variance? The answer to that question may be desired in traffic theory. We shall work on it in the future.

Finally, it is noted that the relationship between the sample size and the variance of the sample ACF refers to [43]. In addition, the relationship between the sample size and the variance bound of the sample ACF of fractional Gaussian noise with LRD is described in [44].

6. Conclusions

We have discussed the smooth effect of sample ACFs of traffic by average. Future research whether traffic is with finite variance or infinite one has been noted.

Acknowledgments

This work was supported in part by the 973 plan under the Project Grant no. 2011CB302800 and by the National Natural Science Foundation of China under the Projects Grants nos. 61272402, 61070214, and 60873264.

References

- [1] <http://ita.ee.lbl.gov/html/contrib/BC.html>.
- [2] W. E. Leland, M. S. Taqqu, W. Willinger, and D. V. Wilson, "On the self-similar nature of Ethernet traffic (extended version)," *IEEE/ACM Transactions on Networking*, vol. 2, no. 1, pp. 1–15, 1994.
- [3] V. Paxson and S. Floyd, "Wide area traffic: the failure of Poisson modeling," *IEEE/ACM Transactions on Networking*, vol. 3, no. 3, pp. 226–244, 1995.
- [4] A. Feldmann, A. C. Gilbert, W. Willinger, and T. G. Kurtz, "The changing nature of network traffic: scaling phenomena," *ACM SIGCOMM Computer Communication Review*, vol. 28, no. 2, pp. 5–29, 1998.
- [5] P. Borgnat, G. Dewaele, K. Fukuda, P. Abry, and K. Cho, "Seven years and one day: sketching the evolution of internet traffic," in *Proceedings of the 28th Conference on Computer Communications (IEEE INFOCOM '09)*, pp. 711–719, Rio de Janeiro, Brazil, April 2009.

- [6] J. M. Pitts and J. A. Schormans, *Introduction to IP and ATM Design and Performance: With Applications and Analysis Software*, John Wiley, 2000.
- [7] M. Li, W. Jia, and W. Zhao, "Correlation form of timestamp increment sequences of self-similar traffic on Ethernet," *Electronics Letters*, vol. 36, no. 19, pp. 1668–1669, 2000.
- [8] S. Wang, D. Xuan, R. Bettati, and W. Zhao, "Providing absolute differentiated services for real-time applications in static-priority scheduling networks," *IEEE/ACM Transactions on Networking*, vol. 12, no. 2, pp. 326–339, 2004.
- [9] C. A. V. Melo and N. L. S. Da Fonseca, "An envelope process for multifractal traffic modeling," in *Proceedings of the IEEE International Conference on Communications*, pp. 2168–2173, June 2004.
- [10] R. L. Cruz, "A calculus for network delay—I: network elements in isolation," *IEEE Transactions on Information Theory*, vol. 37, no. 1, pp. 114–131, 1991.
- [11] D. McDysan, *QoS & Traffic Management in IP & ATM Networks*, McGraw-Hill, 2000.
- [12] H. Jiang and C. Dovrolis, "Why is the internet traffic bursty in short time scales?" in *Proceedings of the International Conference on Measurement and Modeling of Computer Systems (SIGMETRICS '05)*, pp. 241–252, June 2005.
- [13] F. A. Tobagi, R. W. Peebles, and E. G. Manning, "Modeling and measurement techniques in packet communication networks," *Proceedings of the IEEE*, vol. 66, no. 11, pp. 1423–1447, 1978.
- [14] B. B. Mandelbrot, *Gaussian Self-Affinity and Fractals*, Springer, 2001.
- [15] M. Li, "Fractal time series—a tutorial review," *Mathematical Problems in Engineering*, vol. 2010, Article ID 157264, 26 pages, 2010.
- [16] M. Li, "Generation of teletraffic of generalized Cauchy type," *Physica Scripta*, vol. 81, no. 2, Article ID 025007, 2010.
- [17] V. Paxson and S. Floyd, "Why we don't know how to simulate the Internet," in *Proceedings of the Winter Simulation Conference*, pp. 1037–1044, December 1997.
- [18] A. Papoulis and S. U. Pillai, *Probability, Random Variables and Stochastic Processes*, McGraw-Hill, 1997.
- [19] A. M. Yaglom, *Correlation Theory of Stationary and Related Random Functions*, vol. 1, Springer, 1987.
- [20] K. H. Grote and E. K. Antonsson, Eds., *Springer Handbook of Mechanical Engineering*, Springer, 2009.
- [21] D. A. Freedman, *Statistical Models: Theory and Practice*, Cambridge University Press, 2005.
- [22] A. Gelman, T. Tjor, P. McCullagh, J. Hox, H. Hoijtink, and A. M. Zaslavsky, "Discussion paper analysis of variance—why it is more important than ever," *Annals of Statistics*, vol. 33, no. 1, pp. 1–53, 2005.
- [23] J. S. Bendat and A. G. Piersol, *Engineering Application of Correlations and Spectral Analysis*, Wiley, 2nd edition, 1993.
- [24] J. L. Rodgers and W. A. Nicewander, "Thirteen ways to look at the correlation coefficient," *The American Statistician*, vol. 42, no. 1, pp. 59–66, 1988.
- [25] G. J. Székely, M. L. Rizzo, and N. K. Bakirov, "Measuring and testing dependence by correlation of distances," *Annals of Statistics*, vol. 35, no. 6, pp. 2769–2794, 2007.
- [26] E. G. Bakhoun and C. Toma, "Specific mathematical aspects of dynamics generated by coherence functions," *Mathematical Problems in Engineering*, vol. 2011, Article ID 436198, 10 pages, 2011.
- [27] D. Nikolić, R. C. Mureşan, W. Feng, and W. Singer, "Scaled correlation analysis: a better way to compute a cross-correlogram," *European Journal of Neuroscience*, vol. 35, no. 5, pp. 742–762, 2012.
- [28] J. Aldrich, "Correlations genuine and spurious in Pearson and Yule," *Statistical Science*, vol. 10, no. 4, pp. 364–376, 1995.
- [29] J. L. Doob, "The elementary Gaussian processes," *The Annals of Mathematical Statistics*, vol. 15, no. 3, pp. 229–281, 1944.
- [30] B. W. Lindgren and G. W. McElrath, *Introduction to Probability and Statistics*, The Macmillan Company, New York, NY, USA, 1959.
- [31] S. K. Mitra and J. F. Kaiser, *Handbook for Digital Signal Processing*, John Wiley & Sons, 1993.
- [32] J. S. Bendat and A. G. Piersol, *Random Data: Analysis and Measurement Procedure*, John Wiley & Sons, 3rd edition, 2000.
- [33] R. A. Bailey, *Design of Comparative Experiments*, Cambridge University Press, 2008.
- [34] W. A. Fuller, *Introduction to Statistical Time Series*, Wiley, 2nd edition, 1996.
- [35] C. Toma, "Advanced signal processing and command synthesis for memory-limited complex systems," *Mathematical Problems in Engineering*, vol. 2012, Article ID 927821, 2012.
- [36] C. Cattani, M. Scalia, E. Laserra, I. Bochicchio, and K. K. Nandi, "Correct light deflection in Weyl conformal gravity," *Physical Review D*, vol. 87, Article ID 47503, 2013.
- [37] C. Cattani, "Shannon wavelets theory," *Mathematical Problems in Engineering*, vol. 2008, Article ID 164808, 2008.
- [38] W. Willinger, V. Paxson, R. H. Riedi, and M. S. Taqqu, "Long-Range Dependence and Data Network Traffic," in *Long-Range Dependence: Theory and Applications*, P. Doukhan, G. Oppenheim, and M. S. Taqqu, Eds., Birkhäuser, 2002.
- [39] R. J. Adler, R. E. Feldman, and M. S. Taqqu, Eds., *A Practical Guide to Heavy Tails: Statistical Techniques and Applications*, Birkhäuser, Boston, Mass, USA, 1998.
- [40] M. Li, "Representing smoothed spectrum estimate with the Cauchy integral," *Mathematical Problems in Engineering*, vol. 2012, Article ID 673049, 5 pages, 2012.
- [41] P. Doukhan, G. Oppenheim, and M. S. Taqqu, Eds., *Long-Range Dependence: Theory and Applications*, Birkhäuser, 2002.
- [42] S. Resnick, G. Samorodnitsky, and F. Xue, "How misleading can sample ACFs of stable MAs be? (very!)," *Annals of Applied Probability*, vol. 9, no. 3, pp. 797–817, 1999.
- [43] J. R. M. Hosking, "Asymptotic distributions of the sample mean, autocovariances, and autocorrelations of long-memory time series," *Journal of Econometrics*, vol. 73, no. 1, pp. 261–284, 1996.
- [44] M. Li and W. Zhao, "Variance bound of ACF estimation of one block of fGn with LRD," *Mathematical Problems in Engineering*, vol. 2010, Article ID 560429, 14 pages, 2010.

Research Article

Essay on Fractional Riemann-Liouville Integral Operator versus Mikusinski's

Ming Li¹ and Wei Zhao²

¹ School of Information Science & Technology, East China Normal University, No. 500 Dongchuan Road, Shanghai 200241, China

² Department of Computer and Information Science, University of Macau, Avenue Padre Tomas Pereira, Taipa, Macau

Correspondence should be addressed to Ming Li; ming_lihk@yahoo.com

Received 23 April 2013; Accepted 7 May 2013

Academic Editor: Ezzat G. Bakhoun

Copyright © 2013 M. Li and W. Zhao. This is an open access article distributed under the Creative Commons Attribution License, which permits unrestricted use, distribution, and reproduction in any medium, provided the original work is properly cited.

This paper presents the representation of the fractional Riemann-Liouville integral by using the Mikusinski operators. The Mikusinski operators discussed in the paper may yet provide a new view to describe and study the fractional Riemann-Liouville integral operator. The present result may be useful for applying the Mikusinski operational calculus to the study of fractional calculus in mathematics and to the theory of filters of fractional order in engineering.

1. Introduction

Fractional calculus gains increase interests in processing biomedical signals; see, for example, [1–16]. The fractional integral of the Riemann-Liouville type is widely used in the field; see, for example, [17–22].

Denote by $C(0, \infty)$ the set of piecewise continuous functions on $(0, \infty)$. Let $\nu > 0$ and $f(t) \in C(0, \infty)$. Assume that $f(t)$ is integrable on any finite subinterval of $[0, \infty)$. For $t > 0$, denote by ${}_0D_t^{-\nu}$ the fractional Riemann-Liouville integral operator of order ν [19]. Then, the fractional Riemann-Liouville integral of order ν of $f(t)$ is given by

$${}_0D_t^{-\nu} f(t) = \frac{1}{\Gamma(\nu)} \int_0^t (t-u)^{\nu-1} f(u) du, \quad (1)$$

where $\Gamma(\cdot)$ is the gamma function. As early as 1919, O'Shaughnessy and Post studied the problem indexed by 433 [23]. The desired solution to Problem 433 is the solution to the differential equation of order $1/2$ expressed by

$$\frac{d^{1/2} f(t)}{dt^{1/2}} - \frac{f(t)}{t} = 0. \quad (2)$$

The above needs the differential of order $1/2$. They gave the following solution to (2) based on the fractional Riemann-Liouville integral [24]:

$$f(t) = Ct^{-1/2} \exp\left(-\frac{1}{t}\right), \quad (3)$$

where C is a constant.

This short paper aims at exhibiting that ${}_0D_t^{-\nu}$ is equivalent to the Mikusinski operator I^ν . The significance of our analysis is as follows. Since the algebra properties of the Mikusinski operators are satisfactorily studied and well known, see, for example, [25–28], one may immediately infer that the algebra properties of ${}_0D_t^{-\nu}$ are consistent with the Mikusinski operators. Moreover, the present result suggests that the Mikusinski operators may be used for studying differential equations or filters of fractional order in signal processing.

The remainder of this paper is organized as follows. We will derive (1) from the point of view of the Mikusinski operators in Section 2. Discussions are given in Section 3, which is followed by conclusions.

2. Derivation

In this section, we will first brief the Mikusinski operators. Then, the derivation of (1) is given based on the Mikusinski operators.

The Mikusinski operators are described by convolution [28–30]. Let $a(t)$ and $b(t)$ belong to $C(0, \infty)$. Following the usage of Mikusinski's, we rewrite $a(t)$ and $b(t)$ by

$$a = \{a(t)\}, \quad b = \{b(t)\}. \quad (4)$$

The convolution described by Mikusinski is then given by

$$ab = \{a(t)\} \{b(t)\} = \left\{ \int_0^t a(t-\tau) b(\tau) d\tau \right\}. \quad (5)$$

The deconvolution, therefore, is expressed by

$$\frac{a}{b} = \frac{\{a(t)\}}{\{b(t)\}}. \quad (6)$$

Define $l = \{1\}$ such that

$$\{1\} \{a(t)\} = \left\{ \int_0^t a(\tau) d\tau \right\}. \quad (7)$$

The representations (5) and (6) may be convenient to study the operations of the convolution and its inverse from a view of algebra. For instance, that $C(0, \infty)$ is a commutative ring is obvious.

Let $a = \{1\}$ in (7). Then,

$$l^2 = \{1\} \{1\} = \left\{ \int_0^t d\tau \right\} = \left\{ \frac{t}{1} \right\}. \quad (8)$$

In the general case of $n = 1, \dots$, one has

$$l^n = \left\{ \frac{t^{n-1}}{(n-1)!} \right\}, \quad (9)$$

where $0! = 1$. The above l^n may be termed as a Mikusinski operator.

When one exerts l^n on $f(t) \in C(0, \infty)$, that is, $l^n \{f(t)\}$, the following Cauchy formula results:

$$l^n \{f(t)\} = \left\{ \int_0^t \frac{(t-\tau)^{n-1}}{(n-1)!} f(\tau) d\tau \right\}. \quad (10)$$

Considering the generalization of l^n in (9) for $\nu > 0$ yields another Mikusinski operator given by

$$l^\nu = \left\{ \frac{t^{\nu-1}}{(\nu-1)!} \right\} = \left\{ \frac{t^{\nu-1}}{\Gamma(\nu)} \right\}. \quad (11)$$

Further, by taking into account $l^\nu \{f(t)\}$, we have

$$l^\nu \{f(t)\} = \left\{ \int_0^t \frac{(t-\tau)^{\nu-1}}{\Gamma(\nu)} f(\tau) d\tau \right\}. \quad (12)$$

Releasing the usage of Mikusinski in $\{\cdot\}$ for the purpose of his operational calculus, we have

$$l^\nu f(t) = \int_0^t \frac{(t-\tau)^{\nu-1}}{\Gamma(\nu)} f(\tau) d\tau. \quad (13)$$

This completes the derivation because (13) is the definition of the fractional Riemann-Liouville integral of order ν .

3. Discussions

From (1) and (13), one sees that the fractional Riemann-Liouville integral operator of order ν , that is, ${}_0D_t^{-\nu}$, is equivalent to the Mikusinski operator l^ν though the originality of Mikusinski's by introducing l^ν may be for the purpose of his theory of operational calculus.

On the one hand, we recall that the Mikusinski operational calculus is a useful tool for studying differential equations. On the other hand, l^ν may yet be an alternative of ${}_0D_t^{-\nu}$, so that the Mikusinski operational calculus may be expanded into the field of differential equations and signal processing of fractional order, which attracts interest in biomedical engineering; see, for example, [31].

We note that $f(t) \in C(0, \infty)$ is not necessary in (1). In fact, (1) exists if $f(t)$ is a generalized function [32]. In addition, $f(t)$ may be a random function such as the Brownian motion [33]. Due to the consistence of ${}_0D_t^{-\nu}$ with l^ν , one sees that a generalized function $f(t)$ in (13) may also be allowed. Finally, we should remember that the fractional Riemann-Liouville integral operator may be extended to its corresponding, more precisely, the fractional Riemann-Liouville differential operator if $\nu < 0$. This may correspond to the deconvolution in the Mikusinski's operational calculus, which we will work on in the future. Finally, we mention that possible applications of the Mikusinski's operational calculus to other issues, for example, in [34–36], may be interesting.

4. Conclusions

We have exhibited that the fractional Riemann-Liouville integral operator may be expressed by using the Mikusinski operators, giving another outlook of the fractional Riemann-Liouville integral operator. Thus, we have noticed that the Mikusinski operational calculus may yet be a tool for studying differential equations or systems of fractional order.

Acknowledgments

This work was supported in part by the 973 plan under the project Grant no. 2011CB302800 and by the National Natural Science Foundation of China under the project Grant nos. 61272402, 61070214, and 60873264.

References

- [1] F. Liu and K. Burrage, "Novel techniques in parameter estimation for fractional dynamical models arising from biological systems," *Computers and Mathematics with Applications*, vol. 62, no. 3, pp. 822–833, 2011.
- [2] R. L. Magin, "Fractional calculus models of complex dynamics in biological tissues," *Computers and Mathematics with Applications*, vol. 59, no. 5, pp. 1586–1593, 2010.
- [3] W. G. Glöckle and T. F. Nonnenmacher, "A fractional calculus approach to self-similar protein dynamics," *Biophysical Journal*, vol. 68, no. 1, pp. 46–53, 1995.
- [4] B. J. West, "Fractal physiology and the fractional calculus: a perspective," *Frontiers in Fractal Physiology*, vol. 1, article 12, 2010.

- [5] E. G. Bakhoun and C. Toma, "Specific mathematical aspects of dynamics generated by coherence functions," *Mathematical Problems in Engineering*, vol. 2011, Article ID 436198, 10 pages, 2011.
- [6] C. A. Monje, Y. Q. Chen, B. M. Vinagre, D. Xue, and V. Feliu, *Fractional Order Systems and Controls—Fundamentals and Applications*, Springer, 2010.
- [7] H. Sun, Y. Chen, and W. Chen, "Random-order fractional differential equation models," *Signal Processing*, vol. 91, no. 3, pp. 525–530, 2011.
- [8] C. Toma, "Advanced signal processing and command synthesis for memory-limited complex systems," *Mathematical Problems in Engineering*, vol. 2012, Article ID 927821, 13 pages, 2012.
- [9] S. V. Muniandy, W. X. Chew, and C. S. Wong, "Fractional dynamics in the light scattering intensity fluctuation in dusty plasma," *Physics of Plasmas*, vol. 18, no. 1, Article ID 013701, 2011.
- [10] J. Yang, Z. Chen, W. S. Chen, and Y. Chen, "Robust affine invariant descriptors," *Mathematical Problems in Engineering*, vol. 2011, Article ID 185303, 15 pages, 2011.
- [11] H. M. Srivastava and Ž. Tomovski, "Fractional calculus with an integral operator containing a generalized Mittag-Leffler function in the kernel," *Applied Mathematics and Computation*, vol. 211, no. 1, pp. 198–210, 2009.
- [12] C. Cattani, G. Pierro, and G. Altieri, "Entropy and multifractality for the myeloma multiple TET 2 gene," *Mathematical Problems in Engineering*, vol. 2012, Article ID 193761, 14 pages, 2012.
- [13] I. S. Jesus and J. A. Tenreiro Machado, "Application of integer and fractional models in electrochemical systems," *Mathematical Problems in Engineering*, vol. 2012, Article ID 248175, 17 pages, 2012.
- [14] J. A. Tenreiro MacHado, M. F. Silva, R. S. Barbosa et al., "Some applications of fractional calculus in engineering," *Mathematical Problems in Engineering*, vol. 2010, Article ID 639801, 34 pages, 2010.
- [15] C. Cattani, M. Scalia, E. Laserra, I. Bochicchio, and K. K. Nandi, "Correct light deflection in Weyl conformal gravity," *Physical Review D*, vol. 87, no. 4, Article ID 47503, 4 pages, 2013.
- [16] C. H. Eab and S. C. Lim, "Fractional Langevin equations of distributed order," *Physical Review E*, vol. 83, no. 3, Article ID 031136, 2011.
- [17] C. Cattani, "Fractional calculus and shannon wavelet," *Mathematical Problems in Engineering*, vol. 2012, Article ID 502812, 26 pages, 2012.
- [18] S. Castellucci and M. Carlini, "Modelling and simulation for energy production parametric dependence in greenhouses," *Mathematical Problems in Engineering*, vol. 2010, Article ID 590943, 28 pages, 2010.
- [19] K. S. Miller and B. Ross, *An Introduction to the Fractional Calculus and Fractional Differential Equations*, John Wiley & Sons, 1993.
- [20] S. V. Muniandy and S. C. Lim, "Modeling of locally self-similar processes using multifractional Brownian motion of Riemann-Liouville type," *Physical Review E*, vol. 63, no. 4, pp. 461041–461047, 2001.
- [21] S. C. Lim and S. V. Muniandy, "On some possible generalizations of fractional Brownian motion," *Physics Letters A*, vol. 266, no. 2-3, pp. 140–145, 2000.
- [22] J. Klafter, S. C. Lim, and R. Metzler, *Fractional Dynamics: Recent Advances*, World Scientific, 2012.
- [23] L. O'Shaughnessy and E. L. Post, "Problem 433," *The American Mathematical Monthly*, vol. 25, no. 4, pp. 172–173, 1918.
- [24] L. O'Shaughnessy and E. L. Post, "Discussion of problem 433," *The American Mathematical Monthly*, vol. 26, no. 1, pp. 37–39, 1919.
- [25] R. A. Struble, "Analytical and algebraic aspects of the operational calculus," *SIAM Review*, vol. 19, no. 3, pp. 403–436, 1977.
- [26] R. G. Buschman, "The algebraic derivative of Mikusinski," *The American Mathematical Monthly*, vol. 74, no. 6, pp. 717–718, 1967.
- [27] D. A. Klarner, "Algebraic theory for difference and differential equations," *The American Mathematical Monthly*, vol. 76, no. 4, pp. 366–373, 1969.
- [28] J. Mikusinski, *Operational Calculus*, Pergamon Press, 1959.
- [29] T. K. Boehme, "The Convolution integral," *SIAM Review*, vol. 10, no. 4, pp. 407–416, 1968.
- [30] G. Bengochea and L. Verde-Star, "Linear algebraic foundations of the operational calculi," *Advances in Applied Mathematics*, vol. 47, no. 2, pp. 330–351, 2011.
- [31] H. Sheng, Y. Q. Chen, and T. S. Qiu, *Fractional Processes and Fractional Order Signal Processing*, Springer, 2012.
- [32] I. M. Gelfand and K. Vilenkin, *Generalized Functions*, vol. 1, Academic Press, New York, NY, USA, 1964.
- [33] B. B. Mandelbrot and J. W. van Ness, "Fractional Brownian motions, fractional noises and applications," *SIAM Review*, vol. 10, no. 4, pp. 422–437, 1968.
- [34] M. Carlini, T. Honorati, and S. Castellucci, "Photovoltaic greenhouses: comparison of optical and thermal behaviour for energy savings," *Mathematical Problems in Engineering*, vol. 2012, Article ID 743764, 10 pages, 2012.
- [35] E. G. Bakhoun and C. Toma, "Mathematical transform of traveling-wave equations and phase aspects of quantum interaction," *Mathematical Problems in Engineering*, vol. 2010, Article ID 695208, 15 pages, 2010.
- [36] J. W. Yang, Y. J. Chen, and M. Scalia, "Construction of affine invariant functions in spatial domain," *Mathematical Problems in Engineering*, vol. 2012, Article ID 690262, 11 pages, 2012.

Research Article

A Class of Solutions for the Hybrid Kinetic Model in the Tumor-Immune System Competition

Carlo Cattani¹ and Armando Ciancio²

¹ Department of Mathematics, University of Salerno, Via Ponte Don Melillo, 84084 Fisciano, Italy

² Department of Mathematics and Computer Science, University of Messina, Viale Ferdinando d'Alcontres 31, 98166 Messina, Italy

Correspondence should be addressed to Armando Ciancio; aciancio@unime.it

Received 6 March 2013; Accepted 7 April 2013

Academic Editor: Ezzat G. Bakhoun

Copyright © 2013 C. Cattani and A. Ciancio. This is an open access article distributed under the Creative Commons Attribution License, which permits unrestricted use, distribution, and reproduction in any medium, provided the original work is properly cited.

In this paper, the hybrid kinetic models of tumor-immune system competition are studied under the assumption of pure competition. The solution of the coupled hybrid system depends on the symmetry of the state transition density which characterizes the probability of successful occurrences. Thus by defining a proper transition density function, the solutions of the hybrid system are explicitly computed and applied to a classical (realistic) model of competing populations.

1. Introduction

In this paper, the two-scale tumor immune-system competition hybrid model [1–6] is studied under the assumption that the transition density function is a symmetric and separable function. The competition between tumor and immune-system can be modeled at different scales. Cells of different populations are characterized by biological functions heterogeneously distributed, and they are represented by some probability distributions. The interacting system is characterized at a macroscopic scale by a density distribution function which describes the cells activity during the interaction proliferation. At this level, the distribution of cells fulfills some partial differential equations taken from the classical kinetic theory. In this case, the more general model consists in a nonlinear system of partial differential equations. From the solution of this system, one can define a parameter which defines the time evolving distance between the two distributions, and this parameter is the characterizing coefficient of the microscopic equations, typically an ordinary differential system for the competition of two populations.

This parameter has been considered [4, 5] as a random coefficient whose probability density distribution is modeled by the hiding-learning dynamics referred to biological events where tumor cells attempt to escape from immune cells which, conversely, attempt to learn about their presence.

Therefore, when the coupling parameter is obtained by solving the kinetic equations for the distribution functions, then it will be included in the classical Lotka-Volterra competition equations. We will analyze on a concrete example the influence of this stochastic parameter on the evolution. This method can be easily extended to more realistic competition models (see, e.g., [7–20]).

2. The Hybrid Model for the Tumor-Immune System Competition

Let us consider a physical system of two interacting populations, each one constituted by a large number of active particles with sizes:

$$n_i = n_i(t), \quad (n_i(t) : [0, T] \longrightarrow \mathbb{R}_+) \quad (1)$$

for $i = 1, 2$ and $\mathbb{R}_+ \stackrel{\text{def}}{=} [0, +\infty)$.

Particles are homogeneously distributed in space, while each population is characterized by a microscopic state, called *activity*, denoted by the variable u . The physical meaning of the microscopic state may differ for each population. We assume that the competition model depends on the activity through a function of the overall distribution:

$$\mu = \mu[f_i(t, u)], \quad (\mu[f_i(t, u)] : \mathbb{R}_+ \longrightarrow \mathbb{R}_+). \quad (2)$$

The description of the overall distribution over the microscopic state within each population is given by the probability density function:

$$f_i = f_i(t, u), \quad (f_i(t, u) : [0, T] \times D_u \longrightarrow \mathbb{R}_+, D_u \subseteq \mathbb{R}) \quad (3)$$

for $i = 1, 2$, such that $f_i(t, u)du$ denotes the probability that the activity u of particles of the i th population, at the time t , is in the interval $[u, u + du]$:

$$d\mu = f_i(t, u) du. \quad (4)$$

Moreover, it is

$$\forall i, \forall t \geq 0 : 0 \leq f_i(t, u) \leq 1, \quad \int_{D_u} f_i(t, u) du = 1. \quad (5)$$

We consider, in this section, the competition between two cell populations. The first one with uncontrolled proliferating ability and with hiding ability; the second one with higher destructive ability, but with the need of learning about the presence of the first population. The analysis developed in what follows refers to a specific case where the second population attempts to learn about the first population which escapes by modifying its appearance. The hybrid evolution equations specifically can be formally written as follows [4, 5]:

$$\begin{aligned} \frac{dn_i}{dt} &= G_i(n_1, n_2; \mu[f]), \\ \frac{\partial f_i}{\partial t} &= \mathcal{A}_i[f], \end{aligned} \quad (6)$$

where G_i , for $i = 1, 2$, is a function of $n = \{n_1, n_2\}$ and μ acts over $f = \{f_1, f_2\}$, while \mathcal{A}_i , for $i = 1, 2$, is a nonlinear operator acting on f and $\mu[f]$ is a functional ($0 \leq \mu \leq 1$) which describes the ability of the second population to identify the first one. Then, (6) denotes a hybrid system of a deterministic system coupled with a microscopic system statistically described by a kinetic theory approach. In the following the evolution of density distribution will be taken within the kinetic theory.

The derivation of (6)₂ can be obtained starting from a detailed analysis of microscopic interactions. Consider *binary interactions* specifically between a *test*, or *candidate*, particle with state u_* belonging to the i th population and *field particle* with state u^* belonging to the j th population. The modelling of microscopic interactions is supposed to lead to the following quantities.

- (i) *The encounter rate*, which depends for each pair of interacting populations on a suitable average of the relative velocity η_{ij} , with $i, j = 1, 2$.
- (ii) *The transition density function* $\varphi_{ij}(u_*, u^*, u)$, which is such that $\varphi_{ij}(\cdot; u)$ denotes the probability density that a candidate particle with activity u_* belonging to the i th population falls into the state $u \in D_u$, of the test particle, after an interaction with a field entity,

belonging to the j th population, with state u^* . The transition density $\varphi_{ij}(u_*, u^*, u)$ fulfills the condition

$$\begin{aligned} \forall i, j, \forall u_*, u^* : \int_{D_u} \varphi_{ij}(u_*, u^*, u) du &= 1, \\ \varphi_{ij}(u_*, u^*, u) &> 0, \end{aligned} \quad (7)$$

when $\varphi_{ij}(u_*, u^*, u) \neq 0$ and

$$\forall u_*, u^* : \int_{D_u} \varphi_{ij}(u_*, u^*, u) du = 0 \iff \varphi_{ij}(u_*, u^*, u) = 0. \quad (8)$$

The state transition

$$u_* \xrightarrow{u^*} u \quad (9)$$

follows from the mutual action of the field particle (F) of the i th population on the test particle (T) of the j th population and vice versa so that

$$u_*(F) \xrightarrow{u^*(T)} u \iff u^*(T) \xrightarrow{u_*(F)} u. \quad (10)$$

With respect to this mutual action, we can assume that this function depends on the biological model, as follows.

- (1) Competition within the first group and with others: particles of the i th population interact with any other particle both from its own i th population and from the j th population so that

$$\varphi_{ij}(u_*, u^*, u) \neq 0, \quad (i \text{ fixed}, \forall j). \quad (11)$$

In this case, each particle of the i th population can change its state not only due to the competition with the j th population but also by interacting with particles of its own population. Instead, the individuals of the j th population change their state only due to the interaction with the other i th populations. They do not interfere with each other within their i th group.

- (2) Competition within the second group and with others: particles of the j th population interact with any other particles both from its own j th population and from the i th population so that

$$\varphi_{ij}(u_*, u^*, u) \neq 0, \quad (j \text{ fixed}, \forall i). \quad (12)$$

- (3) Full competition within a group and with others: particles of each population interact with any other particles both from its own population and from the other population so that

$$\varphi_{ij}(u_*, u^*, u) \neq 0, \quad (\forall i, \forall j). \quad (13)$$

- (4) Competition of two groups: particles of each population interact only with particles from the other population so that

$$\varphi_{ij}(u_*, u^*, u) = 0, \quad (i = j). \quad (14)$$

We can assume that this kind of competition arises when the dynamics in each population are stable and each population behaves as a unique individual.

Then, by using the mathematical approach, developed in [1, 2], it yields the following class of evolution equations:

$$\begin{aligned} \frac{\partial f_i}{\partial t}(t, u) = & \sum_{j=1}^2 \int_{D_u \times D_u} \eta_{ij} \varphi_{ij}(u_*, u^*, u) f_i(t, u_*) \\ & \times f_j(t, u^*) du_* du^* \\ & - f_i(t, u) \sum_{j=1}^2 \int_{D_u} \eta_{ij} f_j(t, u^*) du^*, \end{aligned} \quad (15)$$

($i = 1, 2$)

which can be formally written as (6)₂.

3. Transition Density Function Based on Separable Functions

In this section, we give the solution of (15) under some simple assumptions on the form of the transition density (7).

3.1. On the Symmetries of the State Transition Density. We assume that the integrability condition on φ_{ij} ,

$$\frac{\partial^2}{\partial u_* \partial u^*} \varphi_{ij}(u^*, u_*, u) = 0, \quad (16)$$

holds true. As a consequence, if we write the transition density as a linear combination of separable functions, this definition implies some symmetries which will be useful for the following computations, in particular.

Theorem 1. *If one defines the transition density as*

$$\begin{aligned} \varphi_{ij}(u^*, u_*, u) & \stackrel{\text{def}}{=} \frac{1}{2} [a_i \psi_j(u_*, u) + a_j \psi_i(u^*, u)], \\ & (a_i, a_j \geq 0; i, j = 1, 2) \end{aligned} \quad (17)$$

with $\psi_i(u^*, u), \psi_j(u_*, u) > 0$ ($i, j = 1, 2$), the following symmetry holds true:

$$\int_{D_u} \varphi_{ij}(u_*, u^*, u) du = \int_{D_u} \varphi_{ji}(u^*, u_*, u) du. \quad (18)$$

Proof. From (7), (17), we have

$$\int_{D_u} [a_i \psi_j(u_*, u) + a_j \psi_i(u^*, u)] du = 2. \quad (19)$$

There follows, with $i = 1, j = 2$ and $i = 2, j = 1$,

$$\begin{aligned} \int_{D_u} [a_1 \psi_2(u_*, u) + a_2 \psi_1(u^*, u)] du &= 2, \\ \int_{D_u} [a_2 \psi_1(u_*, u) + a_1 \psi_2(u^*, u)] du &= 2 \end{aligned} \quad (20)$$

so that by a comparison of

$$\begin{aligned} \int_{D_u} \{a_1 [\psi_2(u_*, u) - \psi_2(u^*, u)] \\ + a_2 [\psi_1(u^*, u) - \psi_1(u_*, u)]\} du &= 0 \end{aligned} \quad (21)$$

to be valid for all a_1, a_2 , that is, as a consequence of the definition (17),

$$\begin{aligned} \int_{D_u} \psi_2(u_*, u) du &= \int_{D_u} \psi_2(u^*, u) du, \\ \int_{D_u} \psi_1(u^*, u) du &= \int_{D_u} \psi_1(u_*, u) du. \end{aligned} \quad (22)$$

In particular, to fulfill (20), we can assume

$$\begin{aligned} \int_{D_u} a_1 \psi_2(u_*, u) du &= 1, & \int_{D_u} a_2 \psi_1(u^*, u) du &= 1, \\ \int_{D_u} a_2 \psi_1(u_*, u) du &= 1, & \int_{D_u} a_1 \psi_2(u^*, u) du &= 1, \end{aligned} \quad (23)$$

from which, by taking into account (22), we get

$$\begin{aligned} \int_{D_u} a_2 \psi_1(u_*, u) du &= \int_{D_u} a_2 \psi_1(u^*, u) du \\ &= 1 \implies \int_{D_u} \psi_1(w, u) du = \frac{1}{a_2}, \\ \int_{D_u} a_1 \psi_2(u_*, u) du &= \int_{D_u} a_1 \psi_2(u^*, u) du \\ &= 1 \implies \int_{D_u} \psi_2(w, u) du = \frac{1}{a_1} \end{aligned} \quad (24)$$

so that, by a difference,

$$\begin{aligned} \int_{D_u} [a_i \psi_j(v, u) - a_j \psi_i(w, u)] du &= 0, \\ (v, w = u_*, u^*; i, j = 1, 2). \end{aligned} \quad (25)$$

Thus, according to (25), the mutual action of the state transition given by the definition (7) can be summarized by (18). \square

Equations (17), (18) imply that the functions ψ_i have to be carefully chosen so that (22), (24), and (18) are fulfilled.

In the following, we will consider a special choice for the transition density (17) as

$$\begin{aligned} \varphi_{ij}(u^*, u_*, u) & \stackrel{\text{def}}{=} \frac{1}{2} a_{ij} [\psi(u_*, u) + \psi(u^*, u)], \\ & (a_{ij} \geq 0; i, j = 1, 2) \end{aligned} \quad (26)$$

so that (18) is fulfilled.

3.2. Preliminary Theorems. The special choice of $\varphi_{ij}(u_*, u^*, u)$, as defined in (26), enables us to explicitly solve (15); however, prior to computing the analytical solutions of (15), we need to show these preliminary theorems.

Theorem 2. *Let $X(t, u)$ be a function satisfying*

$$\int_{D_u} X(t, u) du = K \quad (|f(t, u)| < M < \infty; K \geq 0) \quad (27)$$

and $\psi(w, u)$ a given function for which

$$\int_{D_u} \psi(w, u) dw = \frac{b}{a} \quad (0 \leq \psi(w, u) \leq 1; a \neq 0) \quad (28)$$

holds, then the equation

$$\frac{\partial X}{\partial t}(t, u) = a \int_{D_u} \psi(w, u) X(t, w) dw - bf(t, u) \quad (29)$$

$$(a \geq 0, b \geq 0)$$

is solved by

$$X(t, u) = F(u) e^{-(b-a/\lambda)t} + KG(u) \quad (K \geq 0), \quad (30)$$

where $F(u)$ is the solution of the second kind homogeneous Fredholm integral equation

$$F(u) = \lambda \int_{D_u} \psi(w, u) F(w) dw, \quad \int_{D_u} F(u) du = 0, \quad (31)$$

with λ being the eigenvalue of the integral equation, and

$$G(u) = \frac{a}{b} \int_{D_u} \psi(w, u) G(w) dw, \quad (32)$$

$$\int_{D_u} G(u) du = 1 \quad (b \neq 0),$$

when $b = 0$, $G(u)$ is any arbitrary function fulfilling (32)₂.

Proof. Let us first notice that in the trivial case of $a = 0$, there is no dependence on the function ψ

$$\frac{\partial X}{\partial t}(t, u) = -bX(t, u) \quad (b \geq 0), \quad (33)$$

but this equation is also solved by (30) being

$$X(t, u) = F(u) e^{-bt} + KG(u). \quad (34)$$

In the more general case, (31)₂, (32)₂ are direct consequence of the condition (5).

By a simple computation, (29) can be transformed into the Fredholm integral equations (31), (32).

In fact, by deriving (30), we have

$$\frac{\partial X}{\partial t} \stackrel{(30)}{=} -\left(b - \frac{a}{\lambda}\right) F(u) e^{-(b-a/\lambda)t} \quad (35)$$

so that (29), taking into account (30), becomes

$$-\left(b - \frac{a}{\lambda}\right) F(u) e^{-(b-a/\lambda)t}$$

$$= a \int_{D_u} \psi(w, u) \left[F(w) e^{-(b-a/\lambda)t} + KG(w) \right] dw \quad (36)$$

$$- b \left[F(u) e^{-(b-a/\lambda)t} + KG(u) \right],$$

that is,

$$\left[\left(\frac{a}{\lambda} \right) F(u) - a \int_{D_u} \psi(w, u) F(w) dw \right] e^{-(b-a/\lambda)t}$$

$$= K \left[a \int_{D_u} \psi(w, u) G(w) dw - bG(u) \right], \quad (37)$$

from which (31), (32) and (30) hold true.

When $b = 0$, from the r.h.s, we have

$$\int_{D_u} \psi(w, u) dw = 0, \quad \int_{D_u} G(w) dw = 1 \quad (38)$$

so that $G(u)$ cannot be univocally determined. \square

When the initial conditions are given, we have the following corollary.

Corollary 3. Let $X(t, u)$ be a function satisfying (27) that is

$$\int_{D_u} X(t, u) du = K, \quad (|f(t, u)| < M < \infty; K \geq 0) \quad (39)$$

and $\psi(w, u)$ a given function for which

$$\int_{D_u} \psi(w, u) dw = \frac{b}{a} \quad (0 \leq \psi(w, u); a > 0, b \geq 0) \quad (40)$$

holds, then the solution of the initial value problem

$$\frac{\partial X}{\partial t}(t, u) = a \int_{D_u} \psi(w, u) X(t, w) dw - bf(t, u), \quad (41)$$

$$X(t, u)|_{t=0} = X(0, u)$$

$$(a \geq 0, b \geq 0)$$

is as follows:

$$(1) a > 0, b > 0, K > 0$$

$X(t, u)$

$$= \frac{\lambda b/a}{\lambda b/a - 1} \left[X(0, u) \right.$$

$$\left. - \frac{a}{b} \int_{D_u} \psi(w, u) f(0, w) dw \right] e^{-(b-a/\lambda)t}$$

$$+ \frac{1}{1 - \lambda b/a} \left[X(0, u) - \lambda \int_{D_u} \psi(w, u) X(0, w) dw \right],$$

$$\lambda \neq 1, \quad (42)$$

$$X(t, u) = 0, \quad \lambda = 1, \quad (43)$$

$$(2) a > 0, b > 0, K = 0.$$

The solution

$$X(t, u) = X(0, u) e^{-(b-a/\lambda)t} \quad (44)$$

exists only for $X(0, u) = \lambda \int_{D_u} \psi(w, u) X(0, w) dw$,

(3) $a > 0, b \geq 0$. The solution

$$X(t, u) = X(0, u) e^{a/\lambda t} \quad (45)$$

exists only for $X(0, u) = \lambda \int_{D_u} \psi(w, u) X(0, w) dw$,

(4) $a = 0, b \geq 0$. For $K > 0$, the solution of (41) does not exist. When $K = 0$, the solution is

$$X(t, u) = X(0, u) e^{-bt}. \quad (46)$$

Proof. According to Theorem 2, the solution of (41)₁ is (30) with derivative (35). In the more general case, these two equations, at the initial time, give

$$X(0, u) = F(u) + KG(u),$$

$$-\left(b - \frac{a}{\lambda}\right) F(u) = a \int_{D_u} \psi(w, u) X(0, w) dw - bX(0, u) \quad (47)$$

having taken into account (41)₁.

The proof of all cases above is followed by solving these two equations in $F(u)$, $G(u)$ with respect to the initial condition $X(0, u)$.

For instance, for the first case (1), there follows

$$\begin{aligned} KG(u) &= X(0, u) - F(u), \\ F(u) &= -\frac{1}{b/a - 1/\lambda} \int_{D_u} \psi(w, u) X(0, w) dw \\ &\quad + \frac{b/a}{b/a - 1/\lambda} X(0, u), \end{aligned} \quad (48)$$

that is

$$\begin{aligned} KG(u) &= \frac{1}{1 - \lambda b/a} \left[X(0, u) - \lambda \int_{D_u} \psi(w, u) X(0, w) dw \right], \\ F(u) &= \frac{\lambda b/a}{\lambda b/a - 1} \left[X(0, u) - \frac{a}{b} \int_{D_u} \psi(w, u) X(0, w) dw \right] \end{aligned} \quad (49)$$

so that (42) holds true.

When

$$X(0, u) = \frac{a}{b} \int_{D_u} \psi(w, u) X(0, w) dw \quad (50)$$

which implies $\lambda = 1$, from (49), we get a trivial solution of (29), (31), (32) and (47); that is,

$$F(u) = 0, \quad G(u) = 0. \quad (51)$$

Analogously, for the case (2) system (47) becomes

$$\begin{aligned} X(0, u) &= F(u) + KG(u), \\ -F(u) &= \lambda \int_{D_u} \psi(w, u) X(0, w) dw. \end{aligned} \quad (52)$$

However, if $K \neq 0$, the integral of the right side of the second equation is K , while the integral of the first side must be zero.

With similar reasonings, we get the proof of the remaining cases. \square

4. Solution of the System (15)

In this section, we will give the explicit solution of the system (15) under some suitable hypotheses on both the encounter rate η_{ij} and the transition density $\varphi_{ij}(u_*, u^*, u)$. Let us assume the symmetry of η_{ij} so that

$$\eta_1 \stackrel{\text{def}}{=} \eta_{11}, \quad \eta_2 \stackrel{\text{def}}{=} \eta_{22}, \quad \eta_0 \stackrel{\text{def}}{=} \eta_{12} = \eta_{21}. \quad (53)$$

Thanks to the previous theorems, and the symmetry of $\varphi_{ij}(u_*, u^*, u)$ as given by (18), system (15) simplifies, the following.

Theorem 4. Let the transition density $\varphi_{ij}(u_*, u^*, u)$ be defined as

$$\begin{aligned} \varphi_{ij}(u_*, u^*, u) &= \frac{1}{2} a_{ij} [\psi(u_*, u) + \psi(u^*, u)], \quad (i, j = 1, 2) \\ a_1 &\stackrel{\text{def}}{=} a_{11}, \quad a_2 \stackrel{\text{def}}{=} a_{22}, \quad a_0 \stackrel{\text{def}}{=} a_{12} = a_{21}, \end{aligned} \quad (54)$$

which fulfills (7) and the symmetries conditions (18), and the density function $\psi(w, u)$ such that

$$\frac{1}{2} a_{ij} \int_{D_u} [\psi(u_*, u) + \psi(u^*, u)] du \stackrel{(7)}{=} 1 \quad (55)$$

holds. Equation (15) can be simplified into

$$\begin{aligned} \frac{\partial f_1}{\partial t}(t, u) &= \eta_1 a_1 \int_{D_u} \psi(w, u) f_1(t, w) dw \\ &\quad + \frac{1}{2} \eta_0 a_0 \int_{D_u} \psi(w, u) [f_1(t, w) + f_2(t, w)] dw \\ &\quad - f_1(t, u) [\eta_1 + \eta_0], \\ \frac{\partial f_2}{\partial t}(t, u) &= \frac{1}{2} \eta_0 a_0 \int_{D_u} \psi(w, u) [f_2(t, w) + f_1(t, w)] dw \\ &\quad + \eta_2 a_2 \int_{D_u} \psi(w, u) f_2(t, w) dw \\ &\quad - f_2(t, u) [\eta_0 + \eta_2]. \end{aligned} \quad (56)$$

Proof. By a substitution of (54) into (15), we get

$$\begin{aligned} \frac{\partial f_1}{\partial t}(t, u) &= \sum_{j=1}^2 \int_{D_u \times D_u} \eta_{1j} a_{1j} [\psi(u_*, u) + \psi(u^*, u)] \\ &\quad \times f_1(t, u_*) f_j(t, u^*) du_* du^* \\ &\quad - f_1(t, u) \sum_{j=1}^2 \int_{D_u} \eta_{1j} f_j(t, u^*) du^*, \\ \frac{\partial f_2}{\partial t}(t, u) &= \sum_{j=1}^2 \int_{D_u \times D_u} \eta_{2j} a_{2j} [\psi(u_*, u) + \psi(u^*, u)] \\ &\quad \times f_2(t, u_*) f_j(t, u^*) du_* du^* \\ &\quad - f_2(t, u) \sum_{j=1}^2 \int_{D_u} \eta_{2j} f_j(t, u^*) du^*, \end{aligned} \quad (57)$$

that is,

$$\begin{aligned} \frac{\partial f_1}{\partial t}(t, u) &= \frac{1}{2} \left[\int_{D_u \times D_u} \eta_{11} a_{11} [\psi(u_*, u) + \psi(u^*, u)] \right. \\ &\quad \times f_1(t, u_*) f_1(t, u^*) du_* du^* \\ &\quad + \int_{D_u \times D_u} \eta_{12} a_{12} [\psi(u_*, u) + \psi(u^*, u)] \\ &\quad \times f_1(t, u_*) f_2(t, u^*) du_* du^* \left. \right] \\ &\quad - f_1(t, u) \left[\int_{D_u} \eta_{11} f_1(t, u^*) du^* \right. \\ &\quad \left. + \int_{D_u} \eta_{12} f_2(t, u^*) du^* \right], \\ \frac{\partial f_2}{\partial t}(t, u) &= \frac{1}{2} \left[\int_{D_u \times D_u} \eta_{21} a_{21} [\psi(u_*, u) + \psi(u^*, u)] \right. \\ &\quad \times f_2(t, u_*) f_1(t, u^*) du_* du^* \\ &\quad + \int_{D_u \times D_u} \eta_{22} a_{22} [\psi(u_*, u) + \psi(u^*, u)] \\ &\quad \times f_2(t, u_*) f_2(t, u^*) du_* du^* \left. \right] \\ &\quad - f_2(t, u) \left[\int_{D_u} \eta_{21} f_1(t, u^*) du^* \right. \\ &\quad \left. + \int_{D_u} \eta_{22} f_2(t, u^*) du^* \right], \end{aligned} \quad (58)$$

from which,

$$\begin{aligned} \frac{\partial f_1}{\partial t}(t, u) &= \frac{1}{2} \eta_{11} a_{11} \left[\int_{D_u \times D_u} \psi(u_*, u) f_1(t, u_*) \right. \\ &\quad \times f_1(t, u^*) du_* du^* \\ &\quad + \int_{D_u \times D_u} \psi(u^*, u) f_1(t, u_*) \\ &\quad \times f_1(t, u^*) du_* du^* \left. \right] \\ &\quad + \frac{1}{2} \eta_{12} a_{12} \left[\int_{D_u \times D_u} \psi(u_*, u) f_1(t, u_*) \right. \\ &\quad \times f_2(t, u^*) du_* du^* \\ &\quad + \int_{D_u \times D_u} \psi(u^*, u) f_1(t, u_*) \\ &\quad \times f_2(t, u^*) du_* du^* \left. \right] \\ &\quad - f_1(t, u) \left[\eta_{11} \int_{D_u} f_1(t, u^*) du^* \right. \\ &\quad \left. + \eta_{12} \int_{D_u} f_2(t, u^*) du^* \right], \\ \frac{\partial f_2}{\partial t}(t, u) &= \frac{1}{2} \eta_{21} a_{21} \left[\int_{D_u \times D_u} \psi(u_*, u) f_2(t, u_*) \right. \\ &\quad \times f_1(t, u^*) du_* du^* \\ &\quad + \int_{D_u \times D_u} \psi(u^*, u) f_2(t, u_*) \\ &\quad \times f_1(t, u^*) du_* du^* \left. \right] \\ &\quad + \frac{1}{2} \eta_{22} a_{22} \left[\int_{D_u \times D_u} \psi(u_*, u) f_2(t, u_*) \right. \\ &\quad \times f_2(t, u^*) du_* du^* \\ &\quad + \int_{D_u \times D_u} \psi(u^*, u) f_2(t, u_*) \\ &\quad \times f_2(t, u^*) du_* du^* \left. \right] \\ &\quad - f_2(t, u) \left[\int_{D_u} \eta_{21} f_1(t, u^*) du^* \right. \\ &\quad \left. + \int_{D_u} \eta_{22} f_2(t, u^*) du^* \right]. \end{aligned} \quad (59)$$

There follows

$$\begin{aligned}
 & \frac{\partial f_1}{\partial t}(t, u) \\
 &= \frac{1}{2} \eta_{11} a_{11} \left[\int_{D_u} \psi(u_*, u) f_1(t, u_*) du_* \right. \\
 & \quad \times \int_{D_u} f_1(t, u^*) du^* \\
 & \quad + \int_{D_u} \psi(u^*, u) f_1(t, u^*) du^* \\
 & \quad \times \left. \int_{D_u} f_1(t, u_*) du_* \right] \\
 &+ \frac{1}{2} \eta_{12} a_{12} \left[\int_{D_u} \psi(u_*, u) f_1(t, u_*) du_* \right. \\
 & \quad \times \int_{D_u} f_2(t, u^*) du^* \\
 & \quad + \int_{D_u} \psi(u^*, u) f_2(t, u^*) du^* \\
 & \quad \times \left. \int_{D_u} f_1(t, u_*) du_* \right] \\
 &- f_1(t, u) \left[\eta_{11} \int_{D_u} f_1(t, u^*) du^* \right. \\
 & \quad \left. + \eta_{12} \int_{D_u} f_2(t, u^*) du^* \right], \\
 & \frac{\partial f_2}{\partial t}(t, u) \\
 &= \frac{1}{2} \eta_{21} a_{21} \left[\int_{D_u} \psi(u_*, u) f_2(t, u_*) du_* \right. \\
 & \quad \times \int_{D_u} f_1(t, u^*) du^* \\
 & \quad + \int_{D_u} \psi(u^*, u) f_1(t, u^*) du^* \\
 & \quad \times \left. \int_{D_u} f_2(t, u_*) du_* \right] \\
 &+ \frac{1}{2} \eta_{22} a_{22} \left[\int_{D_u} \psi(u_*, u) f_2(t, u_*) du_* \right. \\
 & \quad \times \int_{D_u} f_2(t, u^*) du^* \\
 & \quad + \int_{D_u} \psi(u^*, u) f_2(t, u^*) du^* \\
 & \quad \times \left. \int_{D_u} f_2(t, u_*) du_* \right]
 \end{aligned}$$

$$\begin{aligned}
 & - f_2(t, u) \left[\eta_{21} \int_{D_u} f_1(t, u^*) du^* \right. \\
 & \quad \left. + \eta_{22} \int_{D_u} f_2(t, u^*) du^* \right].
 \end{aligned} \tag{60}$$

According to (5), we get

$$\begin{aligned}
 & \frac{\partial f_1}{\partial t}(t, u) \\
 &= \frac{1}{2} \eta_{11} a_{11} \left[\int_{D_u} \psi(u_*, u) f_1(t, u_*) du_* \right. \\
 & \quad \left. + \int_{D_u} \psi(u^*, u) f_1(t, u^*) du^* \right] \\
 &+ \frac{1}{2} \eta_{12} a_{12} \left[\int_{D_u} \psi(u_*, u) f_1(t, u_*) du_* \right. \\
 & \quad \left. + \int_{D_u} \psi(u^*, u) f_2(t, u^*) du^* \right] \\
 &- f_1(t, u) [\eta_{11} + \eta_{12}], \\
 & \frac{\partial f_2}{\partial t}(t, u) \\
 &= \frac{1}{2} \eta_{21} a_{21} \left[\int_{D_u} \psi(u_*, u) f_2(t, u_*) du_* \right. \\
 & \quad \left. + \int_{D_u} \psi(u^*, u) f_1(t, u^*) du^* \right] \\
 &+ \frac{1}{2} \eta_{22} a_{22} \left[\int_{D_u} \psi(u_*, u) f_2(t, u_*) du_* \right. \\
 & \quad \left. + \int_{D_u} \psi(u^*, u) f_2(t, u^*) du^* \right] \\
 &- f_2(t, u) [\eta_{21} + \eta_{22}].
 \end{aligned} \tag{61}$$

Thus, we obtain, by a variable change,

$$\begin{aligned}
 & \frac{\partial f_1}{\partial t}(t, u) = \eta_{11} a_{11} \int_{D_u} \psi(w, u) f_1(t, w) dw \\
 & \quad + \frac{1}{2} \eta_{12} a_{12} \int_{D_u} \psi(w, u) [f_1(t, w) + f_2(t, w)] dw \\
 & \quad - f_1(t, u) [\eta_{11} + \eta_{12}], \\
 & \frac{\partial f_2}{\partial t}(t, u) = \frac{1}{2} \eta_{21} a_{21} \left[\int_{D_u} \psi(w, u) [f_2(t, w) + f_1(t, w)] dw \right] \\
 & \quad + \eta_{22} a_{22} \int_{D_u} \psi(w, u) f_2(t, w) dw \\
 & \quad - f_2(t, u) [\eta_{21} + \eta_{22}]
 \end{aligned} \tag{62}$$

so that (56) follows. \square

4.1. Pure Competition Model. We will consider the solution of (56) when, together with the hypotheses (53), (54)₂, some more conditions are given on the parameters.

According to (26), let us assume

$$\varphi_{ij}(u^*, u_*, u) \stackrel{\text{def}}{=} \frac{1}{2} a_{ij} [\psi(u_*, u) + \psi(u^*, u)], \quad (63)$$

$$(a_{ij} \geq 0; i, j = 1, 2)$$

together with the symmetries conditions (18).

If we define

$$\begin{aligned} \eta_1 &\stackrel{\text{def}}{=} \eta_{11}, & \eta_2 &\stackrel{\text{def}}{=} \eta_{22}, & \eta_0 &\stackrel{\text{def}}{=} \eta_{12} = \eta_{21}, \\ a_1 &\stackrel{\text{def}}{=} a_{11}, & a_2 &\stackrel{\text{def}}{=} a_{22}, & a_0 &\stackrel{\text{def}}{=} a_{12} = a_{21}, \end{aligned} \quad (64)$$

we will discuss only the following hypotheses:

$$a \stackrel{\text{def}}{=} a_1 = a_2 = 0, \quad (65)$$

$$\eta_1 = \eta_2 = \eta \neq 0, \quad \eta_0 a_0 \neq 0, \quad (66)$$

which seem to have some biological interpretations, being the pure encounter-competition model. This happens when the transition of state arises only when particles of one population interact only with an individual of the other population. In this case, individuals of one population do not interact with individuals of the same population.

Theorem 5. Let the transition density $\varphi_{ij}(u_*, u^*, u)$ be defined as

$$\varphi_{ij}(u_*, u^*, u) = \frac{1}{2} a_{ij} [\psi(u_*, u) + \psi(u^*, u)], \quad (i, j = 1, 2) \quad (67)$$

with a_{ij} as given by (64), (65). This definition of the transition density fulfills (7) and the symmetries conditions (18). The density function $\psi(w, u)$ is such that

$$\int_{D_u} \psi(w, u) du = \frac{1}{a}. \quad (68)$$

By assuming

$$a_1 = a_2 = 0, \quad \eta_1 = \eta_2 = \eta \neq 0 \quad (69)$$

and for a_0, η_0 , the condition

$$\eta_0 a_0 \neq 0 \quad (70)$$

system (56) becomes

$$\begin{aligned} \frac{\partial f_1}{\partial t}(t, u) &= \frac{1}{2} \eta_0 a_0 \int_{D_u} \psi(w, u) [f_1(t, w) + f_2(t, w)] dw \\ &\quad - f_1(t, u) [\eta + \eta_0], \\ \frac{\partial f_2}{\partial t}(t, u) &= \frac{1}{2} \eta_0 a_0 \int_{D_u} \psi(w, u) [f_2(t, w) + f_1(t, w)] dw \\ &\quad - f_2(t, u) [\eta + \eta_0], \end{aligned} \quad (71)$$

and its solution is given by

$$\begin{aligned} f_1(t, u) &= e^{-[\eta + \eta_0]t} [F(u) e^{[\eta_0 a_0 / \lambda]t} + H(u)] + G(u), \\ f_2(t, u) &= e^{-[\eta + \eta_0]t} [F(u) e^{[\eta_0 a_0 / \lambda]t} - H(u)] + G(u), \\ F(u) &= \lambda \frac{\eta + \eta_0}{\eta_0 a_0} \int_{D_u} \psi(w, u) F(w) dw, \quad \int_{D_u} F(u) du = 0, \\ G(u) &= \frac{\eta_0}{\eta + \eta_0} a_0 \int_{D_u} \psi(w, u) G(w) dw, \quad \int_{D_u} G(u) du = 1, \\ \int_{D_u} \psi(w, u) dw &= \frac{\eta + \eta_0}{\eta_0 a_0}, \\ \int_{D_u} H(w) dw &= 0. \end{aligned} \quad (72)$$

Proof. From (56), we have

$$\begin{aligned} \frac{\partial f_1}{\partial t}(t, u) &= \frac{1}{2} \eta_0 a_0 \int_{D_u} \psi(w, u) [f_1(t, w) + f_2(t, w)] dw \\ &\quad - f_1(t, u) [\eta + \eta_0], \\ \frac{\partial f_2}{\partial t}(t, u) &= \frac{1}{2} \eta_0 a_0 \int_{D_u} \psi(w, u) [f_2(t, w) + f_1(t, w)] dw \\ &\quad - f_2(t, u) [\eta + \eta_0], \end{aligned} \quad (73)$$

from which by linear combination, we get

$$\begin{aligned} \frac{\partial}{\partial t} [f_1(t, u) + f_2(t, u)] &= \eta_0 a_0 \int_{D_u} \psi(w, u) [f_1(t, w) + f_2(t, w)] dw \\ &\quad - [f_1(t, u) + f_2(t, u)] [\eta + \eta_0], \\ \frac{\partial}{\partial t} [f_1(t, u) - f_2(t, u)] &= -[f_1(t, u) - f_2(t, u)] [\eta + \eta_0]. \end{aligned} \quad (74)$$

With the above positions, we have

$$\begin{aligned} \frac{\partial}{\partial t} X(t, u) &= \eta_0 a_0 \int_{D_u} \psi(w, u) X(t, w) dw - X(t, u) [\eta + \eta_0], \\ \frac{\partial}{\partial t} Y(t, u) &= -Y(t, u) [\eta + \eta_0] \end{aligned} \quad (75)$$

so that, by taking into account Theorem 2, it is

$$\begin{aligned}
 X(t, u) &= F(u) e^{-[\eta + \eta_0 - \eta_0 a_0 / \lambda]t} + G(u), \\
 F(u) &= \lambda \frac{\eta + \eta_0}{\eta_0 a_0} \int_{D_u} \psi(w, u) F(w) dw, \\
 \int_{D_u} F(u) du &= 0, \\
 G(u) &= \frac{\eta_0}{\eta + \eta_0} a_0 \int_{D_u} \psi(w, u) G(w) dw, \\
 \int_{D_u} G(u) du &= 1, \\
 \int_{D_u} \psi(w, u) dw &= \frac{\eta + \eta_0}{\eta_0 a_0}, \\
 Y(t, u) &= H(u) e^{-[\eta + \eta_0]t}, \\
 \int_{D_u} H(w) dw &= 0
 \end{aligned} \tag{76}$$

from which (72) follows. \square

Example 6. A transition density, which is compatible with this case, is the following:

$$\varphi_{ij}(u_*, u^*, u) = \frac{a_0}{2} (1 - \delta_{ij}) [\psi(u_*, u) + \psi(u^*, u)], \tag{77}$$

($i, j = 1, 2$)

with δ_{ij} , Kronecker symbol.

5. Application to Lotka-Volterra Model

In this section, we will study a coupled system (6) where the macroscopic equations are the Lotka-Volterra equations (6)₁. Concerning the coupling stochastic parameter $\mu[f]$, we have to define the functional μ in (2), (6) depending on the “distance” between distributions; that is,

$$\mu[f_i, f_j](t) = \mu(|f_i - f_j|)(t) \tag{78}$$

with

$$\begin{aligned}
 0 &\leq \mu[f_i, f_j](t) \leq 1, \quad \forall u \in D_u \wedge t \in T, \\
 \mu[f_i, f_j](t) &= 1 \iff f_i = f_j, \\
 \mu[f_i, f_j](t) &= 0 \iff f_i = 0 \vee f_j = 0,
 \end{aligned} \tag{79}$$

where the maximum learning result is obtained when the second population is able to reproduce the distribution of the first one: $f_1 = f_2$, while the minimum learning is achieved when one distribution is vanishing.

In some recent papers; it has been assumed [4, 5] that

$$\begin{aligned}
 \mu[f_i, f_j](t) &= \mu(|f_i - f_j|)(t) \\
 &= 1 - \int_{D_u} |f_1(t, u) - f_2(t, u)| du.
 \end{aligned} \tag{80}$$

In this case, it is $\mu = 1$, when $f_1 = f_2$; otherwise $\mu \neq 1$ with $\mu \downarrow 0$, depending on the time evolution of the distance between f_1 and f_2 .

Let us notice that μ is the coupling term which links the macroscopic model (6)₁ to the microscopic model (6)₂. There follows that the solution of the hybrid system (6) depends on the coupling parameter μ (80) which follows from the solution of (15). System (15) is a system of two nonlinear integrodifferential equations constrained by the conditions (7), (5). Moreover, its solution depends also the constant encounter rate η_{ij} , on the transition density function φ_{ij} , and the initial conditions $f_i(0, u)$. In the following section, we will study the solution of (6), under some suitable, but not restrictive, hypotheses on φ_{ij} .

Under the hypotheses of Theorem 5 and the solution (72), we have

$$f_1(t, u) - f_2(t, u) = \begin{cases} 2e^{-(\eta + \eta_0)t} H(u), & H(u) \neq 0, \\ 0, & H(u) = 0. \end{cases} \tag{81}$$

Let us take

$$D_u = [0, 1], \quad \eta + \eta_0 = p > 0, \quad H(u) = \sin 2\pi u \tag{82}$$

so that (72) are fulfilled. We have

$$\mu[f](t) = 1 - 2e^{-pt} \left[\int_0^{1/2} \sin 2\pi u du - \int_{1/2}^1 \sin 2\pi u du \right], \tag{83}$$

that is

$$\mu[f](t) = \begin{cases} 1 - \frac{1}{\pi} e^{-pt}, & \sin 2\pi u \neq 0, \quad u \in [0, 1], \\ 1, & u \in \left\{0, \frac{1}{2}, 1\right\}. \end{cases} \tag{84}$$

In the last case we have the usual Lotka-Volterra system, therefore, we will investigate the first case. Thus, according to (6), we have the system

$$\begin{aligned}
 \frac{dn_1}{dt} &= \alpha n_1 - \left(1 - \frac{1}{\pi} e^{-pt}\right) n_1 n_2, \\
 \frac{dn_2}{dt} &= -\beta n_2 + \gamma n_1 n_2
 \end{aligned} \tag{85}$$

with

$$\alpha \geq 0, \quad \beta \geq 0, \quad \gamma \geq 0. \tag{86}$$

The numerical solution of this system depends on both the parameters α, β, γ, p and on the initial conditions $n_1(0), n_2(0)$. We can see from Figures 1 and 2 that albeit the initial aggressive population n_2 is greater than n_1 , the first population can increase and keep nearly always over n_2 in the quasilinear case in Figure 1(a) or always under n_2 in presence of a strong nonlinearity in Figure 1(b).

If we invert the initial conditions so that the initial population of n_1 is greater than n_2 , we can see that in case of quasilinear conditions (see Figure 2(a)) the population n_1 after some short time becomes lower than n_2 . For a strong nonlinearity, instead after an initial growth n_1 , it

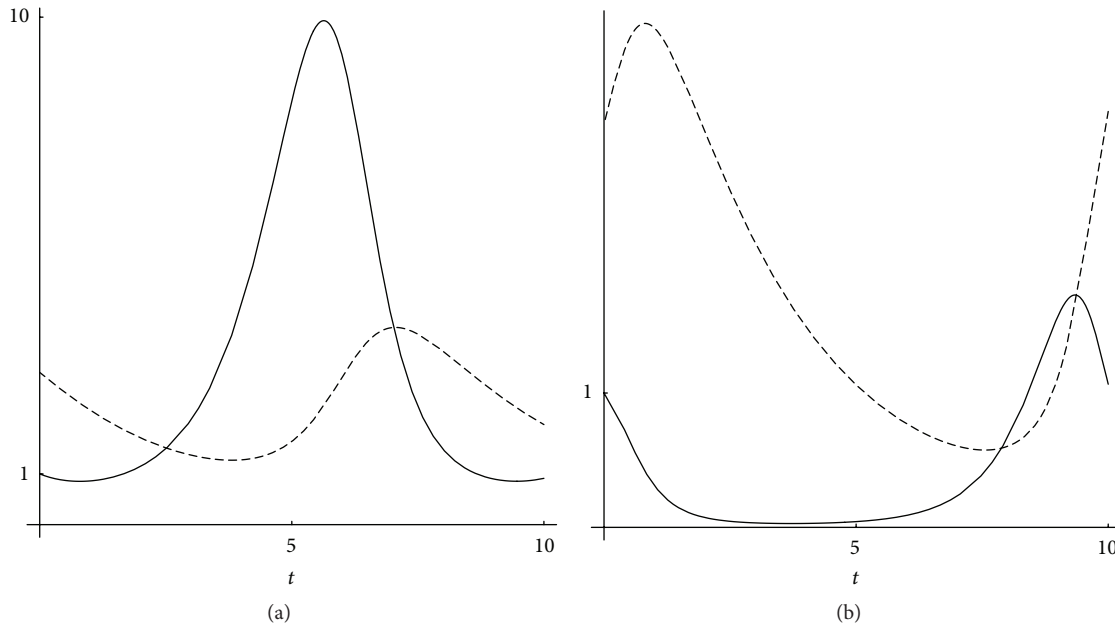


FIGURE 1: Numerical solution of $n_1(t)$ (plain) and $n_2(t)$ (dashed) of the system (85) with initial conditions $n_1(0) = 1$, $n_2(0) = 3$, for $t \leq 10$, and parameters $\alpha = 1.636$, $\beta = 0.3743$ ((a) with parameters $\gamma = 0.1$, $p = 0.01$) and ((b) with parameters $\gamma = 0.9$, $p = 0.9$).

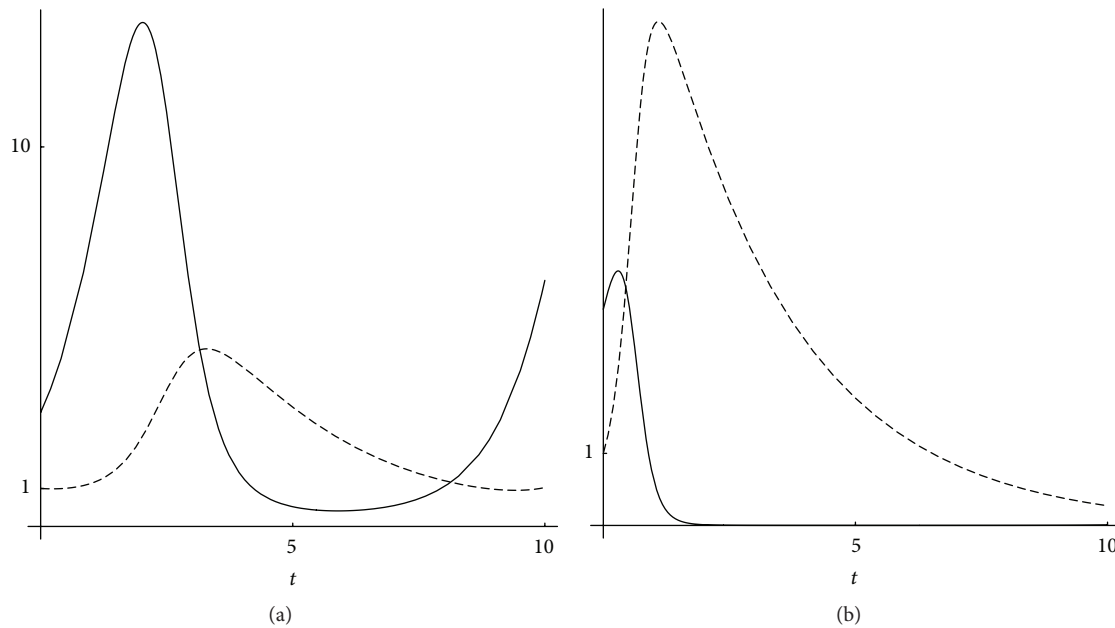


FIGURE 2: Numerical solution of $n_1(t)$ (plain) and $n_2(t)$ (dashed) of the system (85) with initial conditions $n_1(0) = 3$, $n_2(0) = 1$, for $t \leq 10$ and parameters $\alpha = 1.636$, $\beta = 0.3743$ ((a) with parameters $\gamma = 0.1$, $p = 0.01$) and ((b) with parameters $\gamma = 0.9$, $p = 0.9$).

tends to zero in a short time, while the second population grows very fast and becomes the prevalent population in Figure 2(b).

6. Conclusion

In this paper, the hybrid competition model has been solved under some assumptions on the transition density. In the simple case of Lotka-Volterra, the numerical solution gives

some significant and realistic insights on the evolution of competing populations.

References

- [1] N. Bellomo, *Modeling Complex Living Systems—Kinetic Theory and Stochastic Game Approach*, Springer, Boston, Mass, USA, 2008.

- [2] A. Bellouquid and M. Delitala, *Mathematical Modeling of Complex Biological Systems. A Kinetic Theory Approach*, Springer, Boston, Mass, USA, 2006.
- [3] C. Bianca and N. Bellomo, *Towards a Mathematical Theory of Multiscale Complex Biological Systems*, World Scientific, Singapore, 2010.
- [4] C. Cattani and A. Ciancio, "Qualitative analysis of second-order models of tumor-immune system competition," *Mathematical and Computer Modelling*, vol. 47, no. 11-12, pp. 1339–1355, 2008.
- [5] C. Cattani and A. Ciancio, "Hybrid two scales mathematical tools for active particles modelling complex systems with learning hiding dynamics," *Mathematical Models and Methods in Applied Sciences*, vol. 17, no. 2, pp. 171–187, 2007.
- [6] C. Cattani and A. Ciancio, "Separable transition density in the hybrid model for tumor-immune system competition," *Computational and Mathematical Methods in Medicine*, vol. 2012, Article ID 610124, 6 pages, 2012.
- [7] D. Abrams, "The evolution of predator-prey systems: theory and evidence," *Annual Review of Ecology, Evolution, and Systematics*, vol. 31, Article ID 79105, 2000.
- [8] H. P. de Vladar and J. A. González, "Dynamic response of cancer under the influence of immunological activity and therapy," *Journal of Theoretical Biology*, vol. 227, no. 3, pp. 335–348, 2004.
- [9] A. d'Onofrio, "A general framework for modeling tumor-immune system competition and immunotherapy: mathematical analysis and biomedical inferences," *Physica D*, vol. 208, no. 3-4, pp. 220–235, 2005.
- [10] A. d'Onofrio, "Metamodeling tumor-immune system interaction, tumor evasion and immunotherapy," *Mathematical and Computer Modelling*, vol. 47, no. 5-6, pp. 614–637, 2008.
- [11] U. Forys, "Marchuk's model of immune system dynamics with application to tumor growth," *Journal of Theoretical Medicine*, vol. 4, no. 1, pp. 85–93, 2002.
- [12] M. Galach, "Dynamics of the tumor-immune system competition—the effect of time delay," *International Journal of Applied Mathematics and Computer Science*, vol. 13, no. 3, pp. 395–406, 2003.
- [13] R. A. Gatenby, T. L. Vincent, and R. J. Gillies, "Evolutionary dynamics in carcinogenesis," *Mathematical Models & Methods in Applied Sciences*, vol. 15, no. 11, pp. 1619–1638, 2005.
- [14] S. A. Gourley and Y. Kuang, "A stage structured predator-prey model and its dependence on maturation delay and death rate," *Journal of Mathematical Biology*, vol. 49, no. 2, pp. 188–200, 2004.
- [15] M. Kolev, "A mathematical model of cellular immune response to leukemia," *Mathematical and Computer Modelling*, vol. 41, no. 10, pp. 1071–1081, 2005.
- [16] V. A. Kuznetsov, I. A. Makalkin, M. A. Taylor, and A. S. Perelson, "Nonlinear dynamics of immunogenic tumors: parameter estimation and global bifurcation analysis," *Bulletin of Mathematical Biology*, vol. 56, no. 2, pp. 295–321, 1994.
- [17] N. V. Stepanova, "Course of the immune reaction during the development of a malignant tumour," *Biophysics*, vol. 24, no. 5, pp. 917–923, 1979.
- [18] O. Sotolongo-Costa, L. Morales Molina, D. Rodríguez Perez, J. C. Antoranz, and M. Chacón Reyes, "Behavior of tumors under nonstationary therapy," *Physica D*, vol. 178, no. 3-4, pp. 242–253, 2003.
- [19] T. E. Wheldon, *Mathematical Models in Cancer Research*, Hilger, Boston, Mass, USA, 1988.
- [20] H. R. Thieme, *Mathematics in Population Biology*, Princeton, NJ, USA, 2003.